MONASH University

Molecular basis of the human leukocyte antigen (HLA) recognition by inhibitory killer cell immunoglobulin-like receptors (KIRs)

Shoeib Moradi
(MSc)

Department of Biochemistry and Molecular Biology
Faculty of Medicine, Nursing and Health Sciences

Monash University

Submitted in fulfilment of the requirements for the degree of
Doctor of Philosophy

Copyright notice

Abstract

Natural killer (NK) cells are the main components of the innate immune system, and their function is tightly regulated by a variety of receptors on their cell surface. Among which, killer cell immunoglobulin-like receptors (KIR) fine-tune the activity of NK cells by interacting with specific human leukocyte antigen (HLA) class I molecules. KIRs are transmembrane glycoproteins with two (D1-D2) or three (D0-D1-D2) extracellular immunoglobulin (Ig) domains. KIR2DL2 and KIR2DL3 are inhibitory KIRs with two extracellular Ig domains. They are allelic variants segregated from each other during evolution that share more than 90% sequence identity with each other. However, despite the high degree of similarity, clinical studies suggest that they are associated with different disease outcomes. That is, KIR2DL3 is more protective than KIR2DL2 in the development of viral infections such as Hepatitis. Furthermore, they possess different avidity of binding against a panel of HLA-C molecules. It has been reported that KIR2DL2 binds to a broader range of HLA-C molecules compared to KIR2DL3.

The second chapter of this thesis aims to understand the principles governing the structural basis of dissimilarities between KIR2DL2 and KIR2DL3. Using X-ray crystallography, I determined the crystal structures of the extra-membrane domains of KIR2DL2 and KIR2DL3 in complex with HLA-C*07:02 to 3.1 Å and 2.5 Å resolutions, bound to the RL9 peptide, respectively. Structural comparison of these complexes indicated the existence of the same inter-domain hinge-angle for KIR2DL2 and KIR2DL3 but notable differences in the “twist” of the receptor in docking to HLA-C*07:02, leading to a wide binding footprint for KIR2DL2 to the α1 helix of HLA-C. Collectively, my findings suggest that this differential binding to the α1 helix facilitates the broader recognition of HLA-C molecules by the KIR2DL2 receptor.

The third chapter of this thesis underpins the structural characteristics of KIR2DL4. KIR2DL4 belongs to KIR2DL subgroup, but instead of sharing a D0-D2 domain arrangement, it contains a D1-D2 domain arrangement. Unlike other KIRs, KIR2DL4

exhibits both activating and inhibitory domains, and the question about its exact ligand(s) remains unknown to the best of my knowledge to the date of writing my thesis. Crystal structure of the extracellular domains of KIR2DL4 was determined to a resolution of 2.8 Å and further characterized by small angle x-ray scattering (SAXS), multi angle light scattering (MALS) and analytical ultracentrifugation techniques.

I found that unlike other members of KIR2DL family, KIR2DL4 oligomerizes and is present in an equilibrium between dimeric and tetrameric states. Although the monomeric structure of KIR2DL4 resembles other members of the KIR2D family, I revealed that KIR2DL4 oligomerizes in a concentration-dependent manner. SAXS data revealed that D0 domain served as the oligomerization site of KIR2DL4. This unique feature of KIR2DL4 indicates that in solution, its structure is significantly different from other members of KIRs family and it does not follow the conventional pattern of KIRs binding to HLA class I molecules. Collectively, these findings could provide better insight into ligand discovery of KIR2DL4.

Declaration

This thesis contains no material which has been accepted for the award of any other degree or diploma at any university or equivalent institution and that, to the best of my knowledge and belief, this thesis contains no material previously published or written by another person, except where due reference is made in the text of the thesis.

Signature: 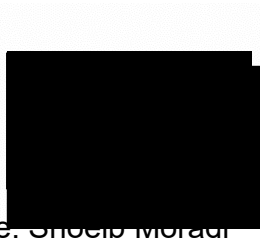

Print Name: Shoeib Moradi

Date: 08 August 2017

Thesis including published works declaration

I hereby declare that this thesis contains no material which has been accepted for the award of any other degree or diploma at any university or equivalent institution and that, to the best of my knowledge and belief, this thesis contains no material previously published or written by another person, except where due reference is made in the text of the thesis.

This thesis includes one original paper published in peer reviewed journals and one submitted publications. The core theme of the thesis is the structural characterization of Killer immunoglobulin-like receptors. The ideas, development and writing up of all the papers in the thesis were the principal responsibility of myself, the student, working within the Department of Biochemistry and Molecular Biology, Faculty of Medicine, Nursing and Health Sciences under the supervision of Professor Jamie Rossjohn.

The inclusion of co-authors reflects the fact that the work came from an active collaboration between researchers and acknowledges input into team-based research.

In the case of Chapter 3, my contribution to the work involved the following:

- Expression and purification of KIR2DL4, 100%
- SAXS experiment, 80%
- SAXS data analysis, 20%
- MALS experiment, 80%
- MALS data analysis, 20%
- Analytical gel filtration, 100%
- Data interpretation, 50%

Thesis Chapter	Publication Title	Status	Nature of student contribution	Co-author name(s) Nature and Co-author's contribution	Co-author(s), Monash student
3	The Structure of the Atypical Killer Cell Immunoglobulin-like Receptor, KIR2DL4	Published	Concept, Collecting data	1) Richard Berry, SAXS SAXS experiment 2) Philip Pymm, input into manuscript 3) Corinne Hitchen, Material preparation, 4) Simone Beckham, MALS 5) Matthew Wilce, MALS 6) Nicholas Walpole Cloning 7) Craig Clements AUC 8) Hugh Reid, KIR2DL4 construct 9) Matthew Perugini AUC 10) Andrew Brooks Project leader 11) Jamie Rossjohn Project leader 12) Julian Vivian, Manuscript preparation, Structural analysis	Only Number 6

I have renumbered sections of submitted or published papers in order to generate a consistent presentation within the thesis.

Student signature [redacted] **Date: 08 August 2017**

The undersigned h[redacted]e above declaration correctly reflects the nature and extent of the student's and co-authors' contributions to this work. In instances where I am not the responsible author, I have consulted with the responsible author to agree on the respective contributions of the authors.

Main Supervisor signature: [redacted] **Date: 08 August 2017**

Acknowledgements

I would firstly like to thank my supervisor, Professor Jamie Rossjohn who let me join his group and accomplish a Ph.D. in his laboratory. I did brush up my scientific understanding by his broad knowledge, guidance, and encouragements and indeed his kind supervision, which I am always grateful for all his kind advice. Being is his laboratory helped me significantly to understand and chose what I want to be in my personal life and scientific career.

I would like to extremely thank my co-supervisor, Dr. Julian Vivian, for a great person he is and his kind nature. His kind patience and guidance during my Ph.D. significantly helped me to move forward. I would not be able to accomplish my Ph.D. without his great supervision and leadership. I would also like to thank him for my thesis corrections. Whenever I faced experimental failures, he always tried to encourage me by saying: “Never give up, tomorrow is another day.”

I would also like to thank my co-supervisor and collaborator, Professor Andrew Brooks, from Melbourne University for his great advice and guidance mainly during supervisory meetings that I always found his recommendations greatly helpful to improve my thesis approaches. I would like to thank Dr. Philipa Saunders, Dr. Lucy Sullivan, and Dr. Geraldine O'Connor from Prof. Brooks’s laboratory for their contribution in my thesis and assistance for running cell assay experiments.

I would like to thank the entire Professor Rossjohn’s laboratory members, in particular, Dr. Richard Berry for his great contribution in chapter 3 of my thesis and assisting me with SAXS experiment. Dr. Phillip Pymm for his entire kind support in the lab and his involvement in chapter 2 experiments, namely LUMINXES and FACS analysis.

In the end, I would like to thank my family for their entire kind supports during years of being away from them.

Table of contents

List of Figures

List of Tables

Abbreviations

APC, Antigen presenting cells
AS, Ankylosing spondylitis
AIDS, Acquired immune deficiency syndrome
AICL, Activation-induced C-type lectin
AUC, Analytical ultracentrifugation
BCRs, B cell receptors
CCL5, Chemokine ligand 5
CD, Crohn's disease
CD+, Cluster of differentiation
CMV, Cytomegalovirus
CSF, Colony stimulating factor
CTL, Cytotoxic T cells
DCs, Dendritic cells
EAE, Experimental auto-immune encephalomyelitis
ECTV, Ectromelia virus
ER, Endoplasmic reticulum
FasL, Fas ligand
GM-CSF, Granulocyte macrophage colony stimulating factor
HA, Hemagglutinin
HCT, Hematopoietic cell transplantation
HCV, Hepatitis C virus
HIV, Human immunodeficiency virus
HLA, Human leukocyte antigen
HN, Hemagglutinin-neuraminidase
HSCT, Hematopoietic stem cell transplantation
HSPG, Heparan sulfate proteoglycan
HTLV-1, Human T lymphotropic virus type 1
IFN-γ, Interferon gamma
Ig, Immunoglobulin
IKDCs, Interferon-producing killer dendritic cells
ILC, Innate lymphocytes
IL, Interleukin
ITAM, Immunoreceptor tyrosine-based activation motif
ITIM, Immunoreceptor tyrosine-based inhibitory motif
IV, Influenza virus
KACL, Keratinocyte-associated C-type lectin
KIR, Killer immunoglobulin-like receptor
KIR2D, Killer immunoglobulin-like receptor with two domains
KIR2DL, Inhibitory killer immunoglobulin-like receptor with two domains
KIR2DS, Activating Killer immunoglobulin-like receptor with two domains
KIR3D, Killer immunoglobulin-like receptor with three domains
KIR3DL, Inhibitory killer immunoglobulin-like receptor with three domains
KIR3DS, Activating Killer immunoglobulin-like receptor with three domains
LILR, Leukocyte Immunoglobulin-Like Receptor

LPS, Lipopolysaccharides
LRC, Leukocyte receptor complex
LTA, Lipoteichoic Acid
MALS, Multi angle light scattering
MASP, Mannose-binding protein-associated serine protease
MCMV, Maize chlorotic mottle virus
MFI, Mean fluorescent intensity
MHC, Major histocompatibility complex
MS, Multiple sclerosis
NDV, Newcastle disease virus
NK, Natural Killer
NKC, Natural killer complex
PAMPs, Pathogen associated molecular patterns
PDB, Protein data bank
Pf, Plasmodium falciparum
PRRs, Pattern-recognition receptors
RAG, Recombination-activating gene
r.m.s.d., Root mean square deviation
SAXS, Small-angle X-ray scattering
SET, Reticulum-associated complex
SEM, Standard error of the mean
SeV, Sendai virus
SFK, SRC family kinase
SPR, Surface Plasmon Resonance
TAP, Transporter associated with antigen processing
TCM, Central memory T cells
TCR, T-cell receptor
Terg, Regulatory T cells
TEFF, Effector T cells
TEM, Effector memory cells
T_{FH}, Follicular T_H cells
TGFβ, Transforming growth factor β
T_H, T helper
TLRs, Toll-like receptors
TN, Naïve T cells
TNFα, Tumour necrosis factor α
TSCM, Stem cell memory T cells
TRAIL, Tumour necrosis factor-related apoptosis-inducing ligand
VM, Vimentin
VV, Vaccinia virus
WT, Wild type

1. Chapter 1: Introduction

1.1 Infection and immunity

Multi-cellular organisms are equipped with complex immune systems to identify and directly eliminate pathogens and to remove cells that are infected. The counter-balancing pressures of infection and immunity drive the evolution of both the immune system and, by corollary, the foreign pathogens like viruses, bacteria, and parasites that the immune system is designed to counter (Mortellaro and Ricciardi-Castagnoli, 2011). In humans, the immune system can be broadly sub-divided into two distinctive and specific arms. Namely, the innate immune system and the adaptive immune system (Figure 1.1). The innate immune system builds the first line of defence against pathogens and is characterized by rapid response to infections, typically activated minutes after exposure to the pathogen. During the inflammatory response cells within the innate immune system (shown in Figure 1.1) become activated and differentiate into short-lived effector cells (Janeway and Medzhitov, 2002). By comparison, the adaptive immune system has a slower response to pathogens. The differentiation of naïve adaptive lymphocytes into effector cells requires ~ three to five days upon exposure to pathogen and activation (Janeway, 2001, Janeway and Medzhitov, 2002). The life-span of effector cells is limited by apoptotic pathways that are initiated following antigen removal (Janeway, 2001). Table 1.1 highlights the properties and differences of the innate and adaptive immune systems.

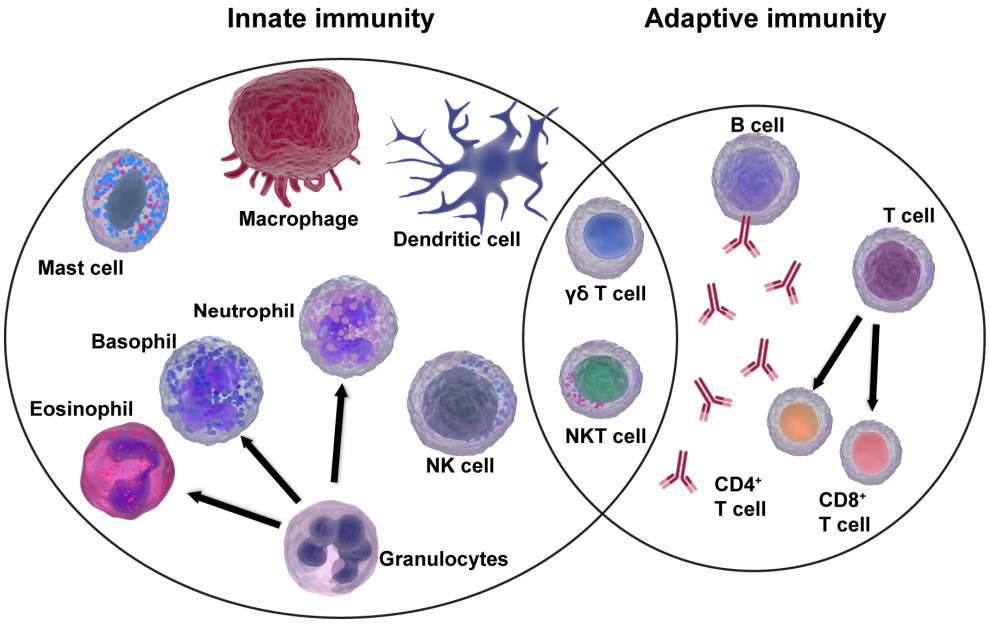

Figure 1.1. Innate and adaptive immunity.

The innate immune system is the first line of protection against pathogens and is composed of macrophages, dendritic cells, mast cells, basophils, eosinophils, neutrophils and NK cells. The innate immune system is recognized for its rapid response to infection and its mediation of the inflammatory response. The adaptive immune system is characterized by a slower response and the generation of memory against infection and includes B cells, antibodies, $CD4^+$ and $CD8^+$ T cells. The figure is adapted from (Dranoff, 2004).

Table 1.1 Properties of innate and adaptive immune systems.

Property	Innate immune system	Adaptive immune system
Receptors	Fixed in genome and rearrangement is not necessary	Encoded in gene segments and rearrangement is necessary
Recognition	Conserved molecular patterns (LPS, LTA, mannans, glycans)	Molecular structure (proteins, peptides, carbohydrates)
Distribution	Non-clonal All cells of a class identical	Clonal All cells of a class distinct
Self and Non-self discrimination	Selected over evolutionary time	Selected in individual somatic cells
Response	Co-stimulatory molecules Cytokines (IL-1β, IL-6) Chemokines (IL-8)	Clonal expansion IL-2 Effector cytokines: (IL-4, IFN-γ)
Action time	Immediate activation of effectors	Delayed activation of effectors

* The table is adapted from (Janeway and Medzhitov, 2002).

** Lipoteichoic Acid (LTA), Lipopolysaccharides (LPS), Interleukin (IL), Interferon gamma (IFN-γ).

*** LTA, LPS and peptidoglycan are part of pathogen-associated molecular patterns (PAMPs) which can activate innate immune receptors such as Toll-like receptors (TLRs), expressed at the surface of macrophages and dendritic cells.

1.2 Human immune system

1.2 1 Evolution of the adaptive immune system

Approximately 3.5 billion years ago, single cell micro-organisms emerged on our planet. The appearance of other organisms such as eubacteria, archaebacteria, and eukaryotes followed. Multicellular organisms known as metazoans started to shape and develop about 600 million years ago and then vertebrates and diverse metazoan lineages as we know them today were created 500 million years ago (Figure 1.2) (Cooper and Alder, 2006).

The evolution of the adaptive immune arm coincided with the appearance of vertebrates ~500 million years ago. The development of lymphocytes of the adaptive immune system provides protection from re-infection by the same pathogens and also helped overcome the limitations of the innate immune system (Boehm et al., 2012, Cooper and Alder, 2006, Hirano, 2015, Hirano et al., 2011, Janeway, 2001). Although it was thought for a long time that the aspects of the adaptive immune arm were limited to jawed vertebrates, the recent discovery of adaptive immune systems in

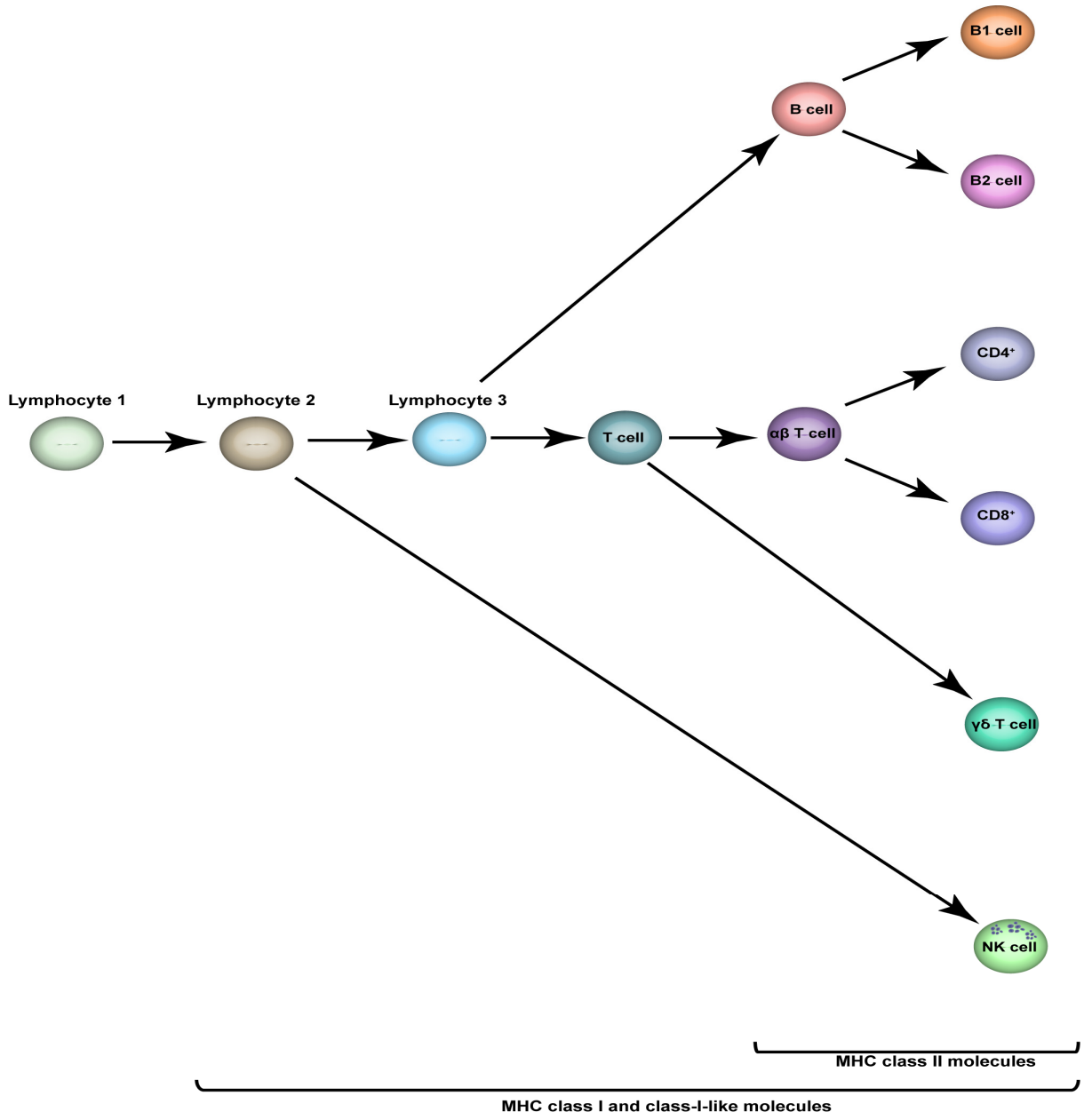

Figure 1.2 Hypothetical evolution of lymphocytes involved in immunity.
Recently evolved forms of lymphocytes are shown on the right side. Lymphocyte 1 is characterized as the primary lymphocyte ancestor. NK cells are originated from lymphocyte 2 which is the common ancestor for other modern lymphocytes. T-cell and immunoglobulin receptor genes are developed from lymphocyte 3. The appearance of MHC-class I, class I-like and class-II molecules during the evolution of lymphocytes is also highlighted at the bottom of the figure. The figure is adapted from (Parham, 2005).

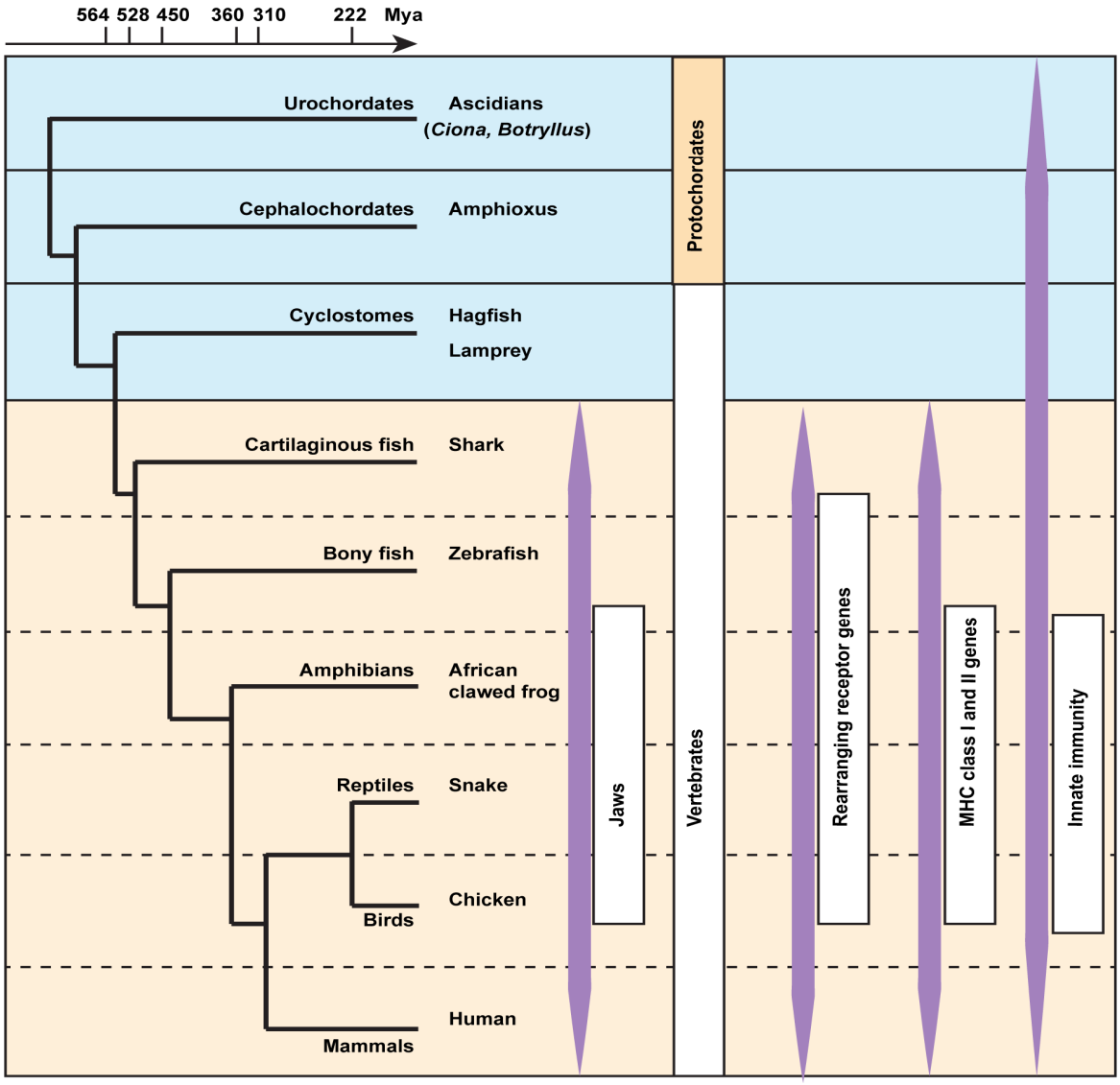

Figure 1.3 Evolution of the adaptive immune system.
Chordates are categorized into two groups of vertebrates and protochordates. Urochordates and cephalochordates belong to protochordates. Vertebrates can further be subdivided into two main groups: jawless vertebrates and jawed vertebrates. Lampreys and hagfish are characterized as vertebrates without jaws. They are also known as cyclostomes. The time scale at the top represents million years ago from the present (Mya). The absence of the adaptive immune system during evolution is highlighted with light-blue background while the emergence of the adaptive immune system is shown in the light-brown background. The figure is adapted from (Kasahara et al., 2004).

1.2.1.1 Antigen recognition of T-cell receptors and B-cell receptors

One of the main features of the adaptive immune system is that of “immunological memory” or the ability to respond more quickly and efficiently to a subsequent challenge by a pathogen (Linehan and Fitzgerald, 2015, Janeway, 2001). Antigen recognition by the adaptive immune system is mediated by immunoglobulin B cell receptors (BCRs) and also T cell antigen receptors (TCRs) (shown in Figure 1.4), which are able to interact with antigen presenting cells (APC), and are expressed at the surface of lymphocytes (van den Berg et al., 2004). The thymus and the bone marrow are responsible for the creation of T and B lymphocytes, respectively (Cooper et al., 1966, Greaves et al., 1968). Upon exposure to antigens, activation and clonal expansion of T cells is triggered which consequently results in the generation of a large population of effector T cells. Upon subsequent encounters with the same antigen again, a very fast and potent response is generated by memory T cells (Godfrey et al., 2015, Burnet, 1959).

T and B lymphocytes can reposition different gene fragments known as joining (J), variable (V) and diversity (D) to produce antigen binding sites for T and B cell receptors by somatic recombination and assistance from the recombination-activating gene (RAG). T and B cell receptors are structurally related members of the immunoglobulin super-family (Flajnik, 2002, Litman et al., 2010, van den Berg et al., 2004). TCRs identify short fragments of peptides displayed by major histocompatibility complexes (MHC) class I and II molecules (Brownlie and Zamoyska, 2013) and BCRs recognize antigens such as soluble molecules within the extracellular fluid (Janeway, 2001). Recently it has also been shown that TCRs are able to interact with Vitamin B derivatives and lipids, presented by MHC class I like molecules (Gras et al., 2016, Keller et al., 2017, Birkinshaw et al., 2015). As a result of the re-positioning of different gene fragments, each recombined BCRs and TCRs has a distinctive antigen specificity, thereby generating ~ 1-2x10^5 and ~ 1x10^8 permutations of BCRs (Yang and Reth, 2016) and TCRs (Wooldridge et al., 2012), respectively, for providing immunity against diverse types of antigens.

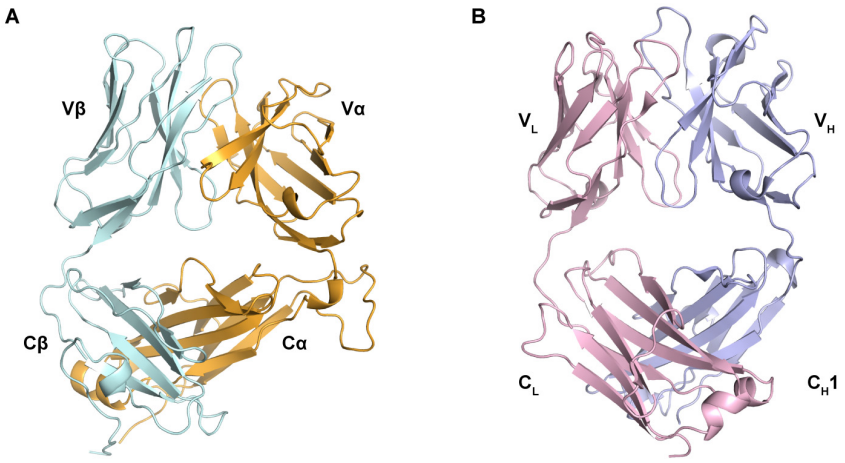

Figure 1.4 Structures of TCR and BCR.

Crystal structure of a α/β T cell receptor comprising variable (V) and a constant I region domains outside the cell surface (PDB ID: 1TCR). **B**. Crystal structure of the antigen binding (Fab) fragment. Fab fragments are regions of an antibody that can bind to antigens. The secondary structure of the antibody light chain (L) and heavy chain (H) are shown (PDB ID: 3I9G).

1.2.1.2 T-cell subtypes

T cells are classified into different subtypes including cytotoxic T cells, T helper (T_H) cells, memory and effector T cells, and regulatory T cells (Treg) (Figure 1.5). Within the thymus, T cells mature and express either CD8 or CD4 glycoproteins at their cell surface, known at $CD8^+$ and $CD4^+$, respectively (Golubovskaya and Wu, 2016). T_H and Treg are recognised by expression of $CD4^+$ at their cell surface, but cytotoxic T cells are recognized by expression of $CD8^+$ at their cell surface. $CD8^+$ T cells are able to lyse infected cells, but $CD4^+$ T_H cells can produce a variety of cytokines, which consequently results in downstream activations and responses of other compartments of the immune system (Linehan and Fitzgerald, 2015). T_H1, T_H2, T_H17, T_{FH} (follicular T_H cells), T_H9 and T_H22 are different types of T_H cells which are able to generate diverse cytokines profiles and each subset has a crucial role in immune and effector response task of T cells (Russ et al., 2013, Golubovskaya and Wu, 2016, Raphael et al., 2015).

Naïve T cells become activated when they encounter APC which results in the elevation of T cell quantity and also their differentiation into effector T cells and leads to their migration to the place of infection. Whereas effector T cells have a very short life-span, the subsets of memory T cells possess a long-standing life-span and can be placed in the newly infected organs or the secondary lymphoid tissues. Upon re-infection, the establishment of a second immune response occurs rapidly and to a larger extent than the primary response via memory T cells (Golubovskaya and Wu, 2016). The common characteristics of memory T cells include their persistence even if the antigen is absent, the existence of former development and activation and elevation of their function once re-exposed to the same antigen (Golubovskaya and Wu, 2016, Rosenblum et al., 2016).

TCRs are involved in responding to antigens that are presented to them by MHC molecules. MHC molecules present peptides that are fragments of endogenous self-proteins or exogenous molecules (Carson et al., 1997). TCRs become activated upon interaction with MHC peptide-bound complexes, followed by a series of reactions which are mediated by specific adaptor proteins, enzymes and co receptors (Brownlie and Zamoyska, 2013, Russ et al., 2013). Briefly, this includes the secretion of pro-inflammatory cytokines like tumor necrosis factor (TNF-α) and IFN-γ (La Gruta et al., 2004), expression of granule enzymes (granzymes) A, B and K (Jenkins et al., 2007, Moffat et al., 2009, Peixoto et al., 2007) and perforin (Kagi et al., 1994), co-receptors such as CD4 and CD8 (Veillette et al., 1988), association of CD3 (Artyomov et al., 2010, Brownlie and Zamoyska, 2013), as well as recruitment and activation of the SRC family kinase (SFK) members including LCK and FYN (Brownlie and Zamoyska, 2013, Palacios and Weiss, 2004, Parsons and Parsons, 2004, Salmond et al., 2009). However, the adaptive immune system differs from the innate immune system in its response to pathogens. These two systems indeed overlap and work in collaboration to generate a potent and effective immune response (Linehan and Fitzgerald, 2015). For instance, dendritic cells (DCs) that are components of the innate immune system are crucial for the activation of T cells, *in vitro* and *in vivo* (Boog et al., 1985, den Haan et al., 2014, Jung et al., 2002, Lechler and Batchelor, 1982).

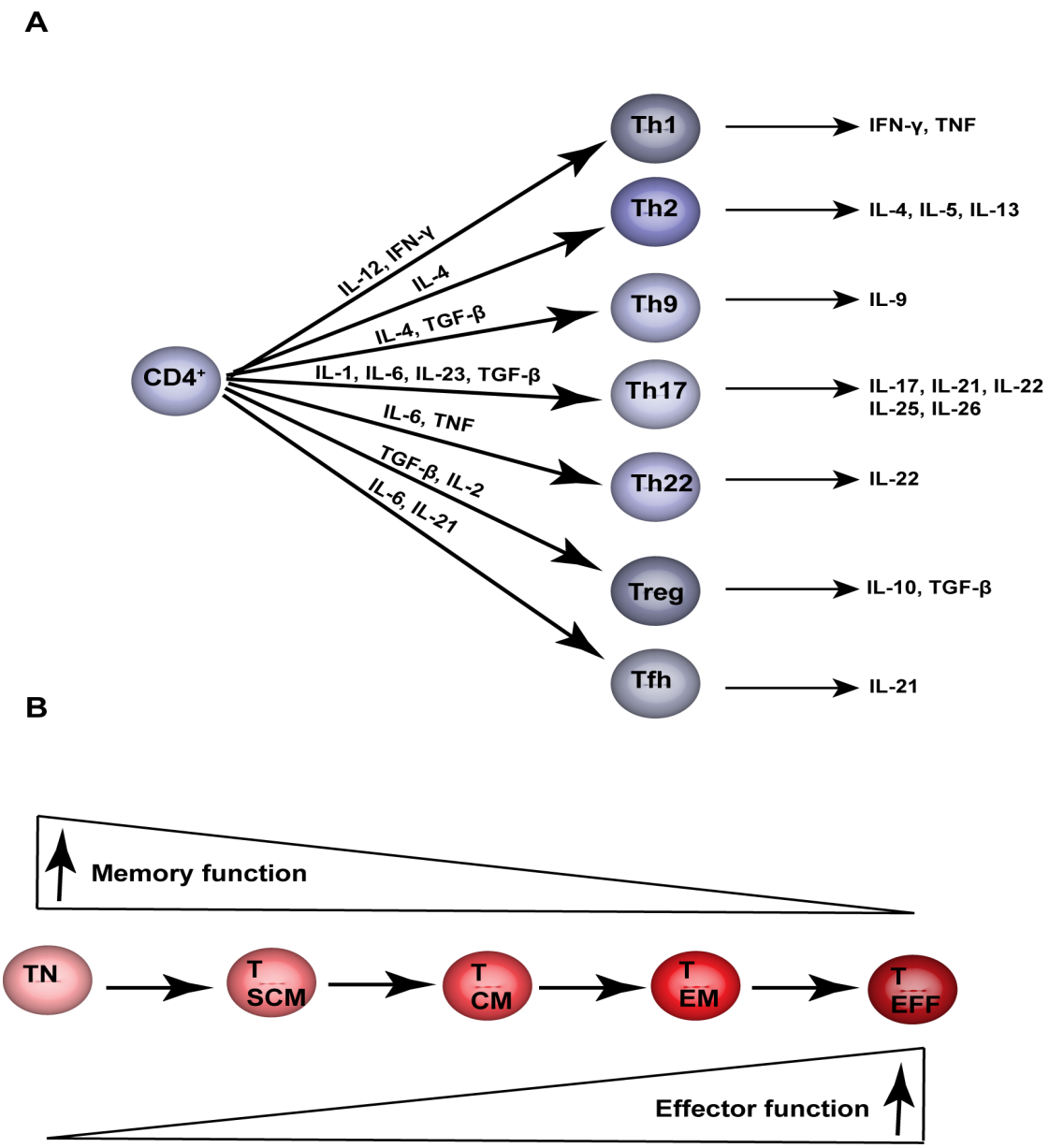

Figure 1.5 Subsets of T cells.

Different subsets of CD4⁺ T cells generated from naïve T cells are shown. Each subset is developed by the effect of certain types of different cytokines, and each subset of CD4⁺ T cells is involved in the production of different types of cytokines. **B**. A linear model for differentiation of CD8+ T cells. Different types of CD8⁺ T cell subsets upon activation of Naïve T cells (TN) include Stem cell memory T cells (T SCM), central memory T cells (T CM), effector T cells (T EFF), and effector memory cells (T EM). Naïve, T SCM and T CM cells can circulate and relocate into lymphoid tissue, while TEM and TEFF can migrate to peripheral tissues. The figure is adapted from (Golubovskaya and Wu, 2016, Sharpe and Mount, 2015).

1.2.2 Innate immune system

There are two major components that form the innate immune system, the humoral and cellular elements (Figure 1.6). Humoral components include complement and cytokines, whereas cellular components contain specialized cells such as natural killer (NK) cells, macrophages, and DCs (Mortellaro and Ricciardi-Castagnoli, 2011). The cellular elements of the innate immune system in vertebrates are of myeloid origin. Myeloid cells can be sub-divided into mono-nuclear and poly-morphonuclear phagocytes. Macrophages, which are originated from blood monocytes, are members of the mono-nuclear phagocyte class, as are dendritic cells, which are derived from monocytes (Figure 1.6) (Beutler, 2004). On the other hand, eosinophils, basophils, and neutrophils belong to the polymorpho-nuclear phagocyte class, and their presence is very crucial for inhibition of the infection (Figure 1.6). Upon severe infection, the quantity of neutrophils increases up to 10-fold compared to the normal state of the cells. However, their life-span is very short, and regardless of pathogenic challenge, they go through apoptosis every six hours. Mast cells are other cellular components of the innate immune system and share a similar role and are considered the main mediators of allergic responses similar to eosinophils (Figure 1.6) (Beutler, 2004).

Early suggestions were that unlike the adaptive immune system, the innate immune system was completely non-specific (Akira et al., 2006). However, currently, it is accepted that the innate immune system is not entirely non-specific and can indeed distinguish between “self” and different types of “non-self” pathogens and micro-organisms by utilising pattern-recognition receptors (PRRs). Pathogens express a variety of markers or unique “molecular signatures” by which they can be identified. These markers, known as pathogen associated molecular patterns (PAMPs), can be sensed by PRRs. PRRs are independent of immunological memory, and are able to detect micro-organisms irrespective of the life-stage and can repeatedly be expressed in the cell (Akira et al., 2006). The basic mechanism of pathogen detection by the apparatus of the innate immune system is significantly conserved between different species from mammals to plants. Various classes of PRRs exist in the ancient

branches of the immune system such as Toll receptors and cytoplasmic receptors. In some species lacking the adaptive immune system, such as *Drosophila*, Toll receptors are the major components of the immune system and have been shown to play important roles in antifungal defence (Hoffmann, 2003, Lemaitre et al., 1996). Toll receptors are evolutionarily conserved among species ranging from flies and worms to mammals, including humans (Akira and Takeda, 2004, Akira et al., 2006, Beutler, 2004, Hoffmann, 2003, Janeway and Medzhitov, 2002).

Other examples of pattern recognition include the terminal mannosyl residues located on the surface of a variety of microbes that can be detected by the mannose-binding proteins in mammals. This recognition results in initiation of the complement cascade using the mannose-binding protein-associated serine protease (MASP) pathway (Matsushita et al., 1998, Matsushita and Fujita, 1992, Matsushita and Fujita, 1995, Terai et al., 1997, Thiel et al., 1997). CD14, Lipopolysaccharide binding protein, C-reactive protein and other members of the pentraxin family, are other examples of molecules that can sense other microbial markers and alert infection (Beutler, 2004).

There are sets of proteolytic enzymes recognized as “complement” which can be triggered once they sense the presence of pathogens via three different pathways, classical, properdin, and MASP (Beutler, 2004). Whereas the classical pathway is stimulated by antibodies, the properdin pathway relies on the presence of properdin which is a plasma glycoprotein and can directly bind to the microbial surface via the assistance of co-factors such as factors B, D, H, and I of also a series of thrombospondin-like repeats (Beutler, 2004). The existence of a complicated innate immune system inside multi-cellular organisms highlights the fundamental need to constitutively produce receptors to detect specific markers on a wide range of potential pathogens (Akira et al., 2006, Cooper and Alder, 2006, Hoffmann, 2003, Janeway and Medzhitov, 2002).

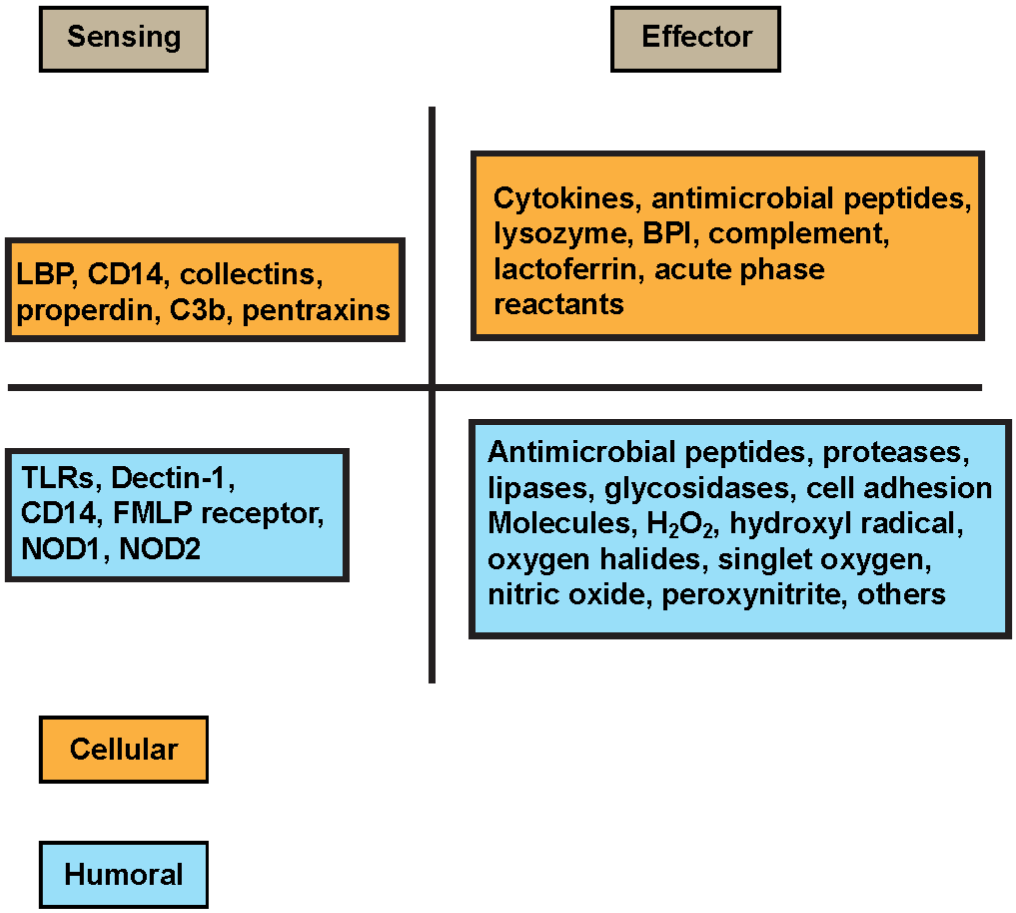

Figure 1.6 Cellular and humoral elements of the innate immune system.
The sensing and effector arms of the innate immune system for each part of the cellular and humoral components are shown. Cellular components of the innate immune system are shown in boxes with an orange background, and humoral components are shown in boxes with the light-blue background. The figure is adapted from (Beutler, 2004).

1.2.3 Other means of pathogen removal

Not only multi-cellular organisms but also single-cell organisms are equipped with different devices for protection against pathogens, devices like RNA interference, restriction endonucleases, and antimicrobial peptides (Danilova, 2006, Judice et al., 2016). Antimicrobial peptides also play a role in pathogen elimination by disrupting the biological membrane of microbes. In *Drosophila*, there are seven different families of antimicrobial peptide genes and in mammals; there are cathelicidins and defensins that enable pathogen removal (Ganz and Lehrer, 1998, Lehrer and Ganz, 2002).

1.2.4 Innate immune system and NK cells

NK cells are the major machinery of the innate immune system. They are equipped with a variety of receptors at the cell surface for binding to markers of both healthy and stressed cells expressed at the cell surface of target cells. The participation of NK cells in the first line of defence against pathogenic invasion or malignancies via non-Toll like receptor system is well established (Di Santo, 2008, Moretta et al., 2002). The interaction of NK cells with dendritic cells is a prerequisite for escalating the innate immune responses (Andrews et al., 2003, Vivier et al., 2008, Akira et al., 2006). Of interest to this study, NK cells express killer cell immunoglobulin-like receptors (KIRs) at their cell surface to monitor the presence of MHC molecules at the surface of target cells. The engagement of inhibitory and activating KIRs receptors with MHC molecules is crucial for the NK cell to discriminate between “self” and “non-self” and thus for the final fate of the target cell.

1.3 Major histocompatibility complexes

In all jawed vertebrates, the MHC is a large gene complex playing an essential role in the immune system (Mosaad, 2015). A large part of their genome contains genes encoding MHC molecules that can be categorized into three groups: class I, class II and class III. The high polymorphic class I and also low polymorphic non-classical MHC molecules are encoded by genes located in class I regions (Gunther and Walter, 2000). Class I MHCs are expressed on all nucleated cells and function by presenting peptide fragments at the cell surface for antigen recognition by NK cells and $CD8^+$ T cells (Dohring and Colonna, 1997, Yewdell et al., 2003). In this way, they provide a snapshot of the protein content of the cell that can be interrogated by the innate or the adaptive arms of the immune system. In other words, MHC class I molecules provide a link between the two arms of the immune system. Classical MHC class I molecules possess a higher level of expression compared to non-classical MHC class I molecules. Non-classical MHC class I molecules present a more limited peptide antigen repertoire to NK cells, NKT cells, as well as αβ and $\gamma\delta$ T cells (Rodgers and Cook, 2005).

APCs express the high polymorphic MHC molecules which are encoded by the class II region that display exogenous peptide antigens to $CD4^+$ T cells (Blum et al., 2013). Furthermore, there are genes located in class II region that are necessary for processing of antigens like *TAP1* and *TAP2* which form two sub-units of the transporter associated with antigen processing (Gunther and Walter, 2000). The importance of MHC molecules in transplantation and also their key role in reacting with malignancies highlights their critical function in the regulation of immune responses (Archbold et al., 2008).

1.3.1 Classical MHC class I molecules

Classical MHC class I molecules are expressed on the surface of all nucleated cells. Their major function is the presentation of short peptides to $CD8^+$ T cell and NK cell receptors of the adaptive and innate immune systems, respectively. The molecular architecture of classical class I molecules consists of three components: a heavy chain, a light chain and small peptide (typically 8-10 residues in length) (Figure 1.7). The heavy chain is a transmembrane protein encoded by the HLA-, -B, -C loci and it associates non-covalently with the light chain, also known as β_2-microglobulin (β_2m), encoded on chromosome 7. Finally, a short peptide associates with the heavy chain to form stable and properly folded MHC class I molecules that can be transported to the cell surface. The heavy chain is composed of three extracellular domains named, α1, α2, and α3. The peptide-binding pocket is formed by two anti-parallel α-helical walls and a β-pleated sheet floor derived from the α1 and α2 domains. The α1 and α2 domains are where the majority of polymorphisms in MHC class I molecules are located. The existence of polymorphisms in the peptide-binding pocket results in restrictions selecting appropriate peptide sequences for accommodation and permits only a range of peptides during complex formation within the endoplasmic reticulum (ER). The peptide is tethered at both the N and C termini and also at “anchor” sites in the cavities inside the peptide-binding pocket (Matsumura et al., 1992, Ruppert et al., 1993, Rock et al., 1994, Saper et al., 1991).

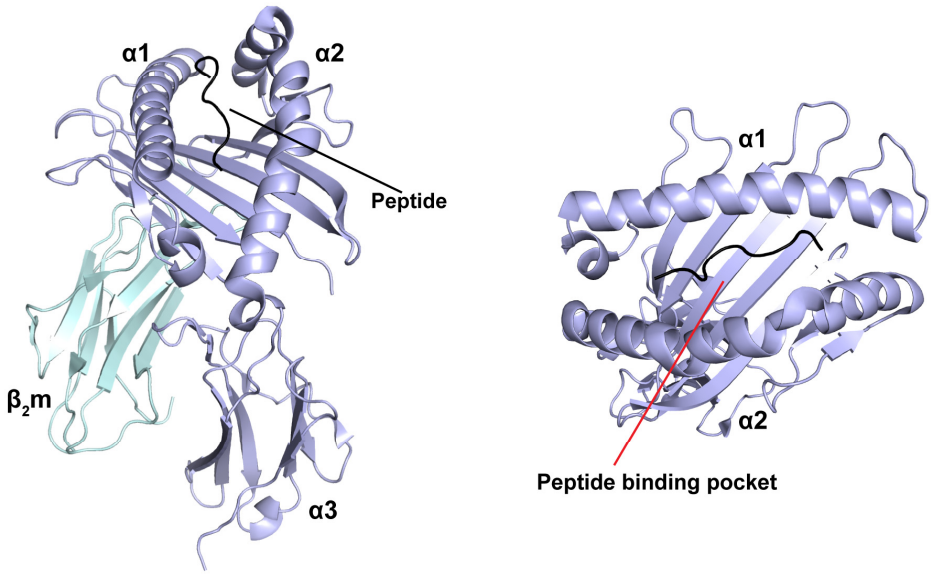

Figure 1.7 Structure of MHC class I molecule.

The crystal structure of an MHC class I molecule that is comprised of three components: polymorphic heavy chain (α1, α2, and α3), a light chain β_2-microglobulin (β_2M) and a peptide epitope. PDB ID: 1EFX.

The peptides that are loaded into the peptide-binding pocket of MHC class I molecules, originate from endogenous or exogenous proteins (Figure 1.8.1). The first step of antigen presentation begins with the degradation of proteins into peptides by the proteasome following labelling by ubiquitin. (Figure 1.8.2) (Rock et al., 1994, Rock et al., 2002). The newly generated fragments of peptides (Figure 1.8.3) then migrate into the lumen of the ER with the assistance of TAP (Figure 1.8.4) (Parcej and Tampe, 2010). In the ER, peptides are either completely degraded or applied to the formation of MHC complexes and antigen presentation (Figure 1.8.5) (Blanchard et al., 2010, Hearn et al., 2009, Shen et al., 2011, van Endert, 2011). In the lumen of the ER, the transport of newly produced heavy chain is assisted via chaperones such as calreticulin and calnexin, as well as help from the oxidoreductase Erp57 in order to

assess its proper folding and help with the correct formation of its disulfide bonds. β_2m then forms a heterodimer with the heavy chain and together they assemble with the peptide loading complex (PLC) including Erp57, TAP, calreticulin and tapasin. This complex assists loading of the peptide into the peptide-binding groove while retaining the conformation of heterodimer (Androlewicz et al., 1993, Cresswell et al., 1999, Ortmann et al., 1994, Ortmann et al., 1997, Shastri et al., 2002, Vigneron et al., 2009). After loading of an appropriate peptide into the MHC complex, it stabilizes and leaves the ER and migrates towards cell surface via the Golgi (Figure 1.8.6).

Depending on conditions within the cell, the accessibility of a diverse range of peptides for loading onto MHC class I molecules may vary. For example, when the cell is in its normal condition, self-peptides are bound to MHC class I molecule, and retain the steady-state of MHC class I expression. However, exposure of cells to stresses such as carcinogenic transformation or viral infection results in changes to the steady-state with the presentation of fragments of either a tumour or viral products at the cell surface or to alterations of the peptide loading apparatus (Lu et al., 2012, Mohammed et al., 2008).

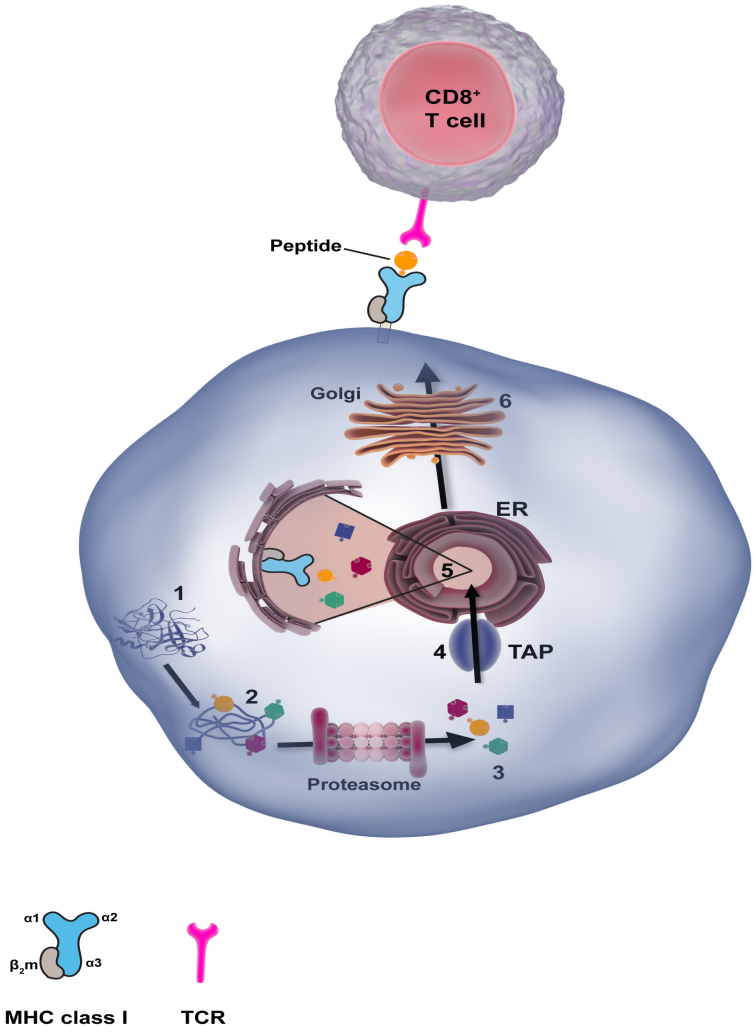

Figure 1.8 MHC class I antigen presentation pathway.
The presentation of endogenous peptides by MHC class I molecules results from a series of events. At the start, proteins are ubiquitinated and unfolded for degradation (**1**, **2**) by the proteasome. Then, newly generated fragments of peptides (**3**) are translocated into the lumen of the ER via TAP (**4**) and the inside the lumen of ER, peptides with sufficient affinity are selected for complex formation and loading on peptide-binding pocket of MHC class I molecules (**5**). This complex then leaves the ER and is transported through the Golgi (**6**) to the surface of the cell for antigen presentation to $CD8^+$ T cells. The figure is adapted from (Neefjes et al., 2011).

1.3.1.1. Human leukocyte antigen class I molecules

The human leukocyte antigen (HLA) system, is a gene complex encoding for MHC proteins in human. HLA class I molecules belong to the immunoglobulin super-family of glycoproteins encoded on chromosome 6. HLA proteins are grouped into classical and non-classical. The classical HLA glycoproteins include HLA-A, -B and -C, which are known to be highly polymorphic. In contrast, the non-classical HLA glycoproteins are less polymorphic and include HLA-E, -F and -G. HLA-C ranks as the least polymorphic among classical HLA molecules (Kulpa and Collins, 2011, Mosaad, 2015, Neefjes et al., 2011). In addition to the existence of different polymorphic states between HLA molecules, they also display variation with regards to their levels of expression. For instance, the level of expression for HLA-C is lower compared to other HLA class I molecules (Apps et al., 2015, Zemmour and Parham, 1992).

1.4 Natural killer cells

NK cells were first discovered in the late 1970s when their involvement in targeting infected cells and their ability to quickly lyse specific tumour cells in mice was observed (Herberman et al., 1975, Kiessling et al., 1975, West et al., 1977). NK cells are characterized as a population of lymphocytes that eliminate infected target cells with no need for former priming (Caligiuri, 2008, Schenk et al., 2016, Kiessling et al., 1975). More recently, this population has been allocated to a newly defined family of innate lymphocytes (ILC) (Dulphy et al., 2016, Spits et al., 2013), which are further categorized into three distinct groups with different functions. ILC group 1 (ILC1), comprises NK cells as a major population, ILC2, and ILC3 (Killig et al., 2014). Parallels exist between subsets of innate lymphocytes and subsets of T-lymphocytes according to their cytokine secretion patterns (Dulphy et al., 2016). That is, T_H1, T_H2 and T_H17 secreting IFN-γ, interleukin (IL) 17 and/or IL22, IL-5 and IL-13 and are similarly produced by ILC1 (IFN-γ), ILC2 (IL-5 and IL-13), and ILC3 (IL17 and/or IL22) subsets of ILC family. Thus, the ILCs contribute and assist the progress of the local immune response (Dulphy et al., 2016).

The phenotype of NK cells is characterized by expression of cell surface markers and is traditionally identified as CD56 positive and CD3 negative ($CD3^-$ $CD56^+$) (Caligiuri, 2008, Dulphy et al., 2016, Schenk et al., 2016). There are two main sub-types of NK cells within secondary lymphoid organs and blood, characterised by CD56 expression as $CD56^{bright}$ or $CD56^{dim}$ (Cooper et al., 2001). $CD56^{dim}$ $CD16^+$ subset of NK cells are highly cytotoxic and represent the main population of NK cells (around 90%-95%) in blood (Cooper et al., 2001, Dulphy et al., 2016, Schenk et al., 2016, Walzer et al., 2007), and after being triggered by a sensitive target, this subset generates IFN-γ and TFN-α (Fauriat et al., 2010b). On the other hand, the $CD56^{dim}$ $CD16^{low/-}$ subset which are located in secondary lymphoid organs display lower levels of cytokine production and represent around 10% of the NK cell population in blood (Caligiuri, 2008, Cooper et al., 2001, Dulphy et al., 2016, Schenk et al., 2016, Walzer et al., 2007, Fehniger et al., 2003). Figure 1.9 highlights some of the major functions of NK cells.

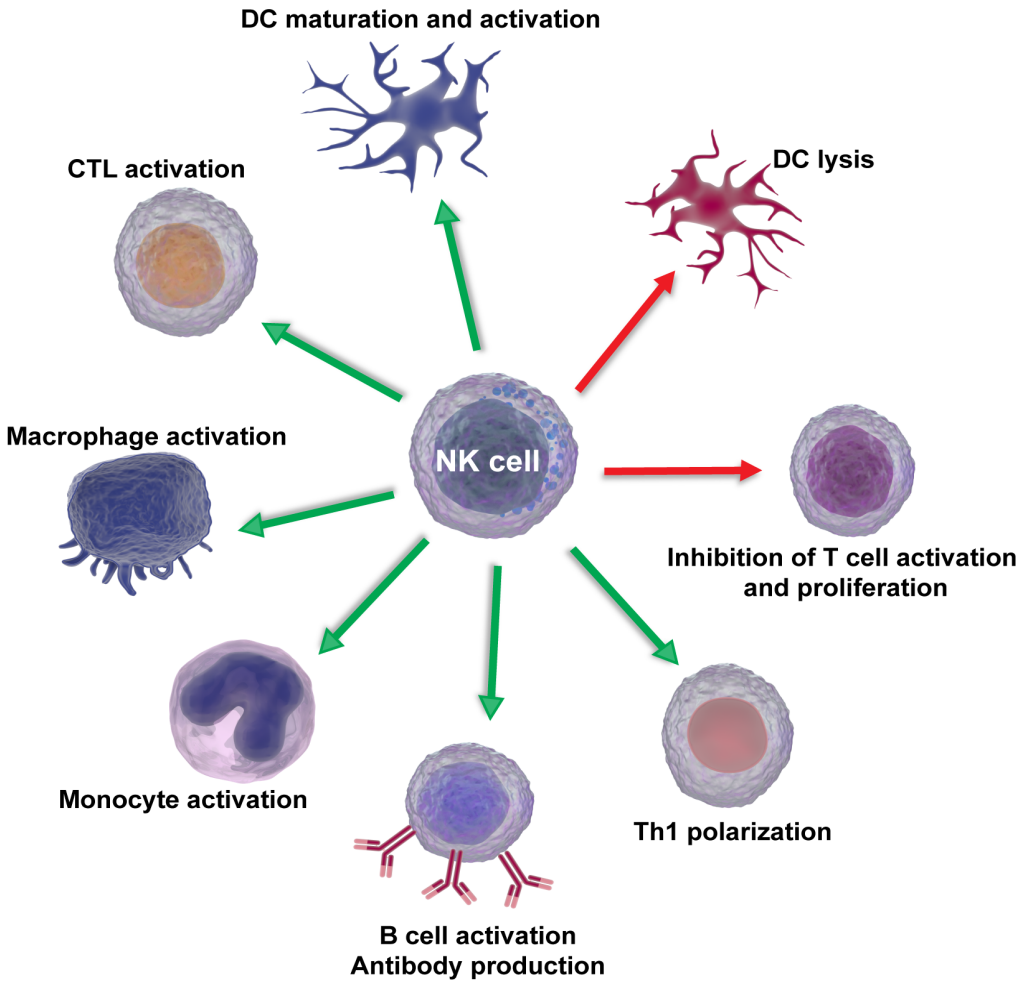

Figure 1.9 Functions of NK cells.
NK cells are involved in promoting the activation and maturation of DCs, triggering the activation of cytotoxic T cells (CTL), activation of monocytes and macrophages, improving the creation of immunoglobulin antibodies and consequently promoting the activation of B cells, secretion of cytokines such as IFN-γ which consequently effects TH cell polarization, and also regulation of T-cell activation and proliferation and also elimination of immature DCs. The figure is adapted from (Deniz et al., 2013, Tian et al., 2012).

1.4.1 NK cells and their cytolytic activity

As effectors, NK cells use different mechanisms to defend the host, and their function depends on the integration of activating and inhibitory signals through receptors expressed at the cell surface (Seaman, 2000). The main mechanisms are through direct killing of infected or malignant cells and through the secretion of cytokines. During direct cytotoxicity of target cells, NK cells can kill by the degranulation or

activation of death receptors. During degranulation, NK cells release endogenous granules containing perforin and granzymes that mediate target cell membrane disruption and apoptosis. In addition, NK cells can directly kill target cells via pathways induced by the engagement of the death receptors including tumour necrosis factor-related apoptosis-inducing ligand (TRAIL) and Fas ligand (FasL) that recognize their cognate receptor on target cells (Podack, 1995, Seaman, 2000, Voskoboinik et al., 2015).

Degranulation involves the secretion of cargos carrying perforin, a pore-forming protein, and assistance of serine protease granzymes including granzymes A and B (Voskoboinik et al., 2015). In the extracellular environment, the presence of high-calcium flux enables perforin to introduce granzymes into infected target cells by binding to target cells and creating membrane pores. Granzyme A induces caspase-independent cell death. On the other hand, human granzyme B is able to induce apoptosis through the mitochondrial pathway after it selectively cleaves Bid, an anti-apoptotic Bcl-2 family member (Lieberman and Fan, 2003, Orange, 2008, Sutton and Trapani, 2010, Voskoboinik et al., 2015). Granzymes A and B can trigger DNA damage via two dissimilar pathways with the assistance of a DNAase. Granzyme A cleaves protein members of the reticulum-associated complex (SET), consequently leading to single stranded DNA damage, whereas granzyme B causes double strand cleavage (Lieberman and Fan, 2003, Orange, 2008, Sutton and Trapani, 2010, Voskoboinik et al., 2015). Interestingly, NK cells that are missing granzymes A and B are still able to lyse the target cells suggesting that they have additional uncharacterized pathways for lysing the target cells (Simon et al., 1997, Voskoboinik et al., 2015).

In addition to direct cytotoxicity, NK cell effector function includes the secretion of cytokines. For instance, NK cells can produce and secrete tumour necrosis factor α (TNFα) (Cuturi et al., 1989, Degliantoni et al., 1985), transforming growth factor β (TGFβ) (Gray et al., 1994), interferon-γ (IFN-γ) (Handa et al., 1983), interleukins such as IL-3 (Cuturi et al., 1989), IL-5 (Warren et al., 1995), IL-10 (Mehrotra et al., 1998),

IL-13 (Hoshino et al., 1999), granulocyte macrophage colony stimulating factor (GM-CSF) (Cuturi et al., 1989) and CSF-1 (Cuturi et al., 1989). Cytokines produced by NK cells are highly important in the development of the immune response. For example, TNF-α is involved in initiation of pro-inflammatory cytokine cascades (O'Shea et al., 2002), and IFN-γ is responsible for different events such as stimulation of Th1 differentiation (Szabo et al., 2003). In addition, both cytokines are able to increase level of the expression of HLA class I molecules (Rock et al., 2002).

1.4.2 NK cells development

Generally, the population of human NK cells comprises around 5% to 15% of peripheral blood and splenic lymphocytes. They are predominantly produced in the bone marrow, with a limited number of NK cells produced in the thymus, fetal liver, spleen, and lymph nodes (Freud and Caligiuri, 2006, Huntington et al., 2007, Luci and Tomasello, 2008). Investigations into NK cells using human and mouse cell lines, demonstrated that *in vitro*, NK cells originate from hematopoietic cells, and can be cultured from fetal liver progenitor cells and bone marrow progenitor cells, in the presence of stem cell factors and interleukins such as IL-7 and IL-15 (Di Santo, 2006, Muench et al., 2000, Williams et al., 1999, Yu et al., 1998). In the late 1970s, it was reported that modification and alteration in the integral micro-environment of bone marrow obstructs the activity and development of NK cells (Kumar et al., 1979, Seaman et al., 1978). Earlier studies showed that NK cell development does not require the thymus, and their quantities can remain at standard levels in athymic *nude* mice (Herberman et al., 1975, Kiessling et al., 1975, Su et al., 1993). However, recent findings have shown that the thymus is involved in the origination of a small and limited population of NK cells expressing CD127 (Vosshenrich et al., 2006). Although it is currently accepted that the bone marrow is the primary site for development of NK cells, further investigation is required to better understand whether the limited number of NK cells derived from the thymus, liver and lymph node represent divergent and diverse linages of NK cells or whether they represent immature NK cells that are originally derived from bone marrow (Sun and Lanier, 2011)

1.4.2.1 NK cells trafficking

Mature NK cells are located in different organs including the spleen, liver, lung and circulating in the body through blood (Shi et al., 2011, Sun and Lanier, 2011). The presence of NK cells in the muscle, skin, and brain is rare or absent. However, upon inflammation or infection, NK cells are recruited to peripheral organs (Di Santo, 2006). Unlike mice, in humans, in the steady-state NK cells reside in the uterine tissue, yet the number of NK cells elevates markedly in both species during pregnancy (Moffett-King, 2002). A variety of chemokines play crucial roles in the localization and circulation of NK cells including chemokine ligand 5 (CCL5) and CCL19, and expression of chemokine receptors such as CCR5 and CCR2 (Di Santo, 2008, Gregoire et al., 2007, Maghazachi, 2003, Maghazachi, 2010, Robertson, 2002, Sun and Lanier, 2011).

1.4.3 NK cells and their role in immunity

The involvement of NK cells in protection against viral infection was discovered in 1989 when a patient suffering from severe life threating infection was observed to present a rare disorder linked to the complete loss of NK cells (Biron et al., 1989, Ballas et al., 1990, Joncas et al., 1989). This resulted in uncontrolled infection caused by DNA viruses including the herpes viruses varicella and cytomegalovirus (CMV). In order to further understand the critical role of NK cells in fighting against CMV, other groups used mice deficient in NK cells and found that infected mice were likewise not protected from CMV (Salazar-Mather et al., 1998, Welsh et al., 1991). NK cells have similarly been found to be protective against bacterial infections including *malaria* (Doolan and Hoffman, 1999), *Leishmania* (Laskay et al., 1993), *Toxoplasma gondii* (Denkers et al., 1993, Sher et al., 1993) and *Listeria monocytogenes* (Bancroft et al., 1987, Unanue, 1997, Wherry et al., 1991).

By monitoring the level of HLA class I molecules, NK cells can perform a significant duty in recognition and removal of infected tumour cells. Target cells need to express the appropriate amount of self HLA class I molecules to be considered as healthy

cells. In the absence of the expression of HLA class I molecules that most likely happens due to viral infection or in tumour cells, NK cells can be activated. Consequently, removal of NK cells can result in increased tumour burdens. For example, Seaman et al. found that, *in vivo*, the progression of several implanted tumour cells were elevated upon removal and deletion of NK cells (Seaman et al., 1987). By triggering the activity of NK cells, others have shown that malignancy can be eliminated, *in vitro* and *in vivo* (Lotze et al., 1990, Roberts et al., 1987), highlighting the importance of NK cells in tumours removal.

Several studies have shown that NK cells are also able to lyse hematopoietic blasts (George et al., 1997, Kiessling et al., 1977, Rolstad et al., 1985). Similarly, NK cells control the growth of hematopoietic blast cells through the release of TNFα, CSF-1, and GM-CSF. The recognition of hematopoietic cells is clinically important, as NK cells can result in rejection of the transplantation of bone marrow grafts due to the activation of NK cells and release of chemokines and cytokines (George et al., 1997, Kiessling et al., 1977, Neipp et al., 1999, Benichou et al., 2011).

1.4.3.1 NK cells and auto-immunity

NK cells are important in the regulation of auto-immunity and have the ability to display both protective and non-protective roles in auto-immune diseases. The pathology of auto-immune diseases varies and can affect specific organs like in type 1 diabetes, or can be systemic and target several organs and tissues as seen for lupus erythematosus. NK cells participate in all stages of auto-immunity, and numerous studies have documented their involvement (Flodstrom-Tullberg et al., 2009, Peng and Tian, 2014, Seaman, 2000, Tian et al., 2012) (Table 1.2).

Table 1.2 NK cell subsets and their role in auto-immune diseases

NK subset	Cytokine secretion	Role in autoimmune diseases	Reference
$CD56^{bright}$ NK	Abundant immunoregulatory cytokines	Protection against MS	(Jiang et al., 2011)
NK2 (ILC2)*	IL-4, IL-5, and IL-13	Protective role	(Wei et al., 2005)
NK3	IL-10	Protection from type 1 diabetes	(Wei et al., 2005)
NKr1	TGF-β	Protective role	(Saito et al., 2008, Yu et al., 2006)
$CD127^{+}$ NK	High cytokine production	Protective role	(Vosshenrich et al., 2006)
IKDCs	High level of IFN-γ	Protection against EAE	(Huarte et al., 2011)
$NKp44^{+}$NK (ILC3)*	IL-22	Protective role in gut of AS	(Ciccia et al., 2012)
$NKp46^{+}$NK	IFN-γ	Mediate the pathogenesis of CD	(Takayama et al., 2010)

Experimental auto-immune encephalomyelitis (EAE), Interferon-producing killer dendritic cells (IKDCs), Multiple sclerosis (MS), Crohn's disease (CD), Ankylosing spondylitis (AS).
The table is adapted from (Tian et al., 2012). *These NK sub-sets share NK cell surface markers but are not classical ILC1/NK cells (Killig et al., 2014, Poggi and Zocchi, 2014).

1.4.3.2 NK cells and pregnancy

NK cells also play a crucial role during pregnancy. Normally, the uterine decidua is rich in NK cells that reside predominantly in the endometrium. However, during pregnancy, the number of NK cells increases markedly to the point that they are the dominant hematopoietic cell population during first 12 weeks of pregnancy. Following this, the quantity of NK cells returns to baseline levels (King et al., 1998, Seaman, 2000).

The maternal immune system faces excessive challenges during early pregnancy, and there is a requirement for tolerogenic mechanisms to avoid rejection of the fetus by the maternal immune system. In terms of phenotype, the uterine NK cells are predominantly $CD56^{superbright}$, $CD16^{-}$ (as opposed to 90 % of $CD56^{dim}$, $CD16^{+}$ in circulating blood) and are also significantly different in functional tests and other relative phenotypic indicators and properties (King et al., 1991, Koopman et al., 2003, Starkey, 1991).

It has been proposed that during decidualisation, changes in the shape and configuration of arteries is mediated by different types of angiogenic elements, which are released by NK cells (Hanna et al., 2006). Further investigations showed that mice lacking NK cells suffered from having atypical decidua, and also by weight loss of the fetus leading to the suggestion that decidualisation is also affected by NK cells (Ashkar et al., 2000, Barber and Pollard, 2003). Others have proposed that NK cells located in the uterus play a significant role in the management of placentation (Moffett and Colucci, 2014). More recently, Brosens and colleagues reported that NK cells residing in the uterus are in charge of keeping the defective placentation and excessive trophoblast intrusion in equilibrium, potentially through direct impact on the arteries. Disturbing such a precise balance results in elevating the possibility of miscarriage and disorders such as Great Obstetric Syndromes (Brosens et al., 2011).

1.4.4 NK cells and the missing-self hypothesis

Extensive studies on NK cells by Karre and his group led to the discovery that NK cells kill targets missing the expression of MHC molecules at their cell surface in a selective manner (Karre et al., 1986, Piontek et al., 1985). In many cases, when cells are infected by pathogens such as microbes or viruses, or even due to tumour transformation, the level of expression of self-HLA class I molecules is affected and may reduce. The molecular mechanism of missing-self detection was specified once the inhibitory receptors of NK cells that are specific for binding to HLA class I molecules were determined (Joncker and Raulet, 2008). This proposal was supported by other groups that reported that B lymphoblastoid cell lines lacking MHC class I molecules and infected by EBV were detected and removed by human NK cells, but, upon transfection of genes of specific types of MHC class I molecules into these cell lines, the lytic activity of NK cells was eliminated (Shimizu and DeMars, 1989, Storkus et al., 1989).

1.4.5 NK cells: To kill or not to kill?

It has been hypothesized that the cytotoxic activity of NK cells occurs when the markers of the target cell (such as MHC class I molecules) are missing (Karre et al., 1986). This hypothesis points at two final fates for target cells based on availability and the absence of self-markers on their cell surface. If the target cell expresses appropriate self-marker molecules for presentation on its cell surface, it will survive from NK cell cytolytic activity, due to the engagement of markers with inhibitory receptors located on the surface of NK cell. However, if target cell fails to express and present any of these markers on its cell surface, then the NK cell kills the target cell because there is no ligand for inhibitory receptor engagement (Figure 1.10). It is likely that at least one inhibitory receptor must be expressed and exist on the surface of NK cell to provide self-tolerance for cells.

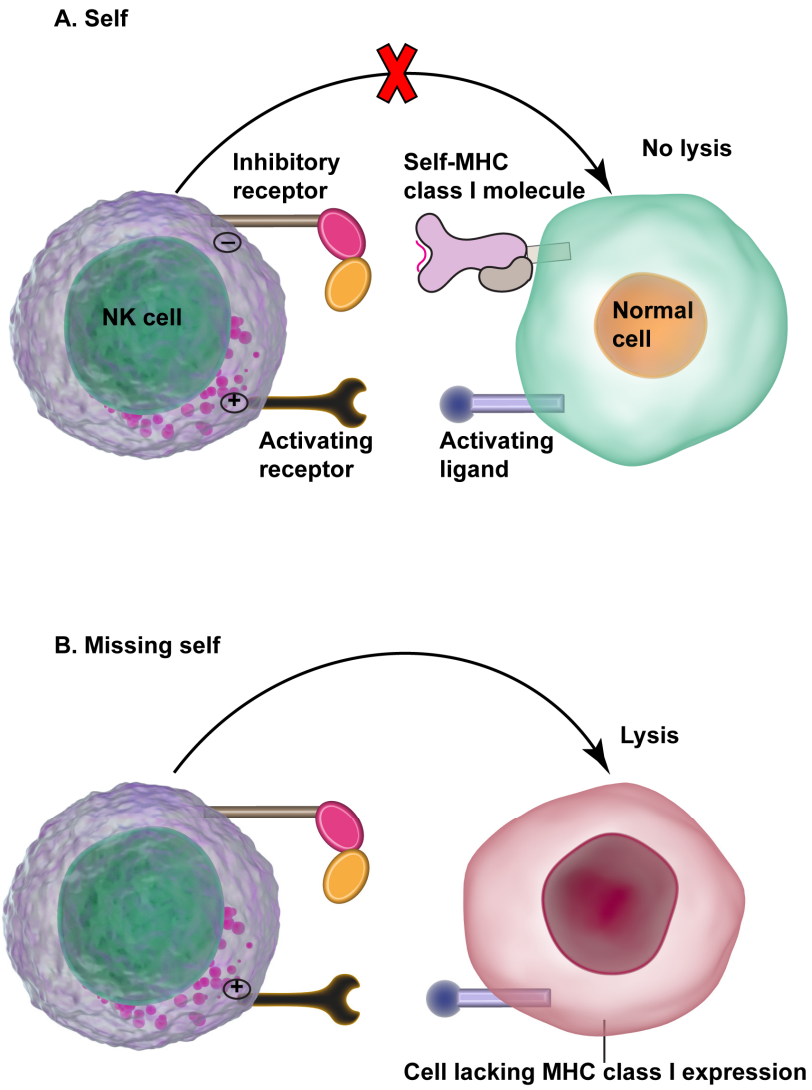

Figure 1.10 NK cell self-tolerance and the 'missing-self' hypothesis.
Upon interaction with healthy cells activation signals delivered to NK cells are overridden by engagement of inhibitory receptors and the transmission of inhibitory signals. **B.** In the absence of MHC class I molecules (as can occur during viral infection and tumour pathogenesis) there is a reduction in the engagement of NK cell inhibitory receptors. As a result, the NK cell is "disinhibited", and the activation signal is dominant leading to the NK cell killing of the target cell. The figure is adapted from (Kumar and McNerney, 2005).

1.4.6 NK cells and their receptors

Extensive research on mouse NK cells led to the discovery of a family of genes by Yokoyama and colleagues named as *Ly49-1A* that express Ly49 receptors on the surface of NK cells in mice (Karlhofer et al., 1992, Smith et al., 1994, Yokoyama et al., 1989). In the cytoplasmic tail of these receptors are immuno-receptor tyrosine-based inhibitory motifs (ITIM) that are responsible for recruiting cytoplasmic tyrosine phosphatase (SHP-1 and SHP-2) via their phosphorylated tyrosine residues which finally leads to the inhibition of cytolytic activity of NK cells (Nakamura et al., 1997, Olcese et al., 1996).

Primates lack *Ly49* and instead utilize the functionally orthologous *KIR* genes (Fan et al., 1996, Rojo et al., 1997, Wagtmann et al., 1995b). However, the KIR and the Ly49 family of receptors have orthologous functions in NK cells. They are encoded on different chromosomes and are structurally dissimilar (Cooper and Alder, 2006, Flajnik and Kasahara, 2010, Hirano, 2015), indicating that these receptors appeared on the surface of NK cells by the time primates and rodents were segregated from each other, ~ 65 million years ago (Hirano, 2015, Paust and von Andrian, 2011).

Numerous studies have demonstrated that some of the activating and inhibitory KIRs that exist on the surface of NK cells, are able to interact specifically with MHC class I molecules located on the surface of target cells (Chan et al., 2014, Middleton et al., 2002, Vivian et al., 2011). However, the surface of NK cells also includes other receptors that interact with non-MHC class I molecules (Chan et al., 2014, Colucci et al., 2002, Vivier et al., 2008). Therefore, the activity of NK cells is tightly controlled through a dynamic between activating and inhibitory signals upon engagement of their cell surface receptors with target cells. Table 1.3 summarizes the variety of receptors expressed on the NK cells cell surface.

Table 1.3 Main NK cell receptors and their non-MHC ligands

Receptor	Ligand(s)
KLRG1	E-, N-, and R-cadherin
NKR-P1A (CD161)	LLT1
NKp46 (CD335)	HSPG, heparin, VM, PfEMP-1, VM, HA (IV, VV, ECTV), HN (SeV, NDV),
NKp30 (CD337)	B7-H6, BAT3, HSPG, HA (VV, ECTV), pp65 (HCMV), PfEMP-1
FcγRIIIA (CD16)	Fc of IgG immune complexes
NKG2D (CD314)	ULBP: ULBP1, ULBP2, ULBP3, ULBP4, ULBP5, ULBP6, MICA, MICB
NKp65 (KLRF2)	KACL
NKp80 (KLRF1)	AICL
DNAM-1 (CD226)	Nectin-2, PVR, CD112, CD155
2B4 (CD244)	CD48
NKp44 (CD336)	PCNA, HSPG, heparin, E-protein (DV, WNV), HA (IV, SeV), HN (NDV),
CD2	CD58
LFA-1 (CD11a/CD18)	ICAM
LAIR-1 (CD305)	Collagen
Siglec-7 (CD328)	Sialic acid
Siglec-9 (CD329)	Sialic acid

(Plasmodium falciparum), (keratinocyte-associated C-type lectin), (activation-induced C-type lectin), ECTV, Ectromelia virus; HA, Hemagglutinin; HN, Hemagglutinin-neuraminidase; HSPG, Heparan sulfate proteoglycan; IV, Influenza virus; NDV, Newcastle disease virus; SeV, Sendai virus; VM, Vimentin; VV, Vaccinia virus. The table is adapted from (Campbell and Hasegawa, 2013, Deniz et al., 2013, Flodstrom-Tullberg et al., 2009).

Human NK cells have two structurally different families of inhibitory receptors on their cell surface; the lectin-like and immunoglobulin-like (Ig) receptors (Colonna and Samaridis, 1995, Ryan and Seaman, 1997, Wagtmann et al., 1995a). There are two major gene complexes that contain the genes responsible for encoding of NK cell receptors, one complex is responsible for genes encoding Ig like-receptors known as the leukocyte receptor complex (LRC), and the other one, C-type lectin like molecules are encoded by natural killer complex (NKC) (Trowsdale, 2001). Members of C-type lectin like receptors include CD94:NKG2 which are located on chromosome 12q1.3–13.4. On the other hand, members of Ig-like super-family include leucocyte immunoglobulin-like receptors, the leucocyte-associated immunoglobulin-like receptors, and KIRs, located on chromosome 19q13.4 (Liu et al., 2000, Middleton and Gonzelez, 2010, Trowsdale et al., 2001, Wende et al., 1999).

1.4.7 NK cells and memory

Although NK cells are part of the innate immune system, they also display memory-like responses that are long-lived. For example, studies on mice lacking T and B cells indicate that subsets of hepatic NK cells are involved in gaining of immunological memory in an antigen-specific manner to hapten-inducted contact sensitizers (O'Leary et al., 2006, Paust et al., 2010). Further investigations demonstrated that NK cells are able to have long-lived memory against a variety of viruses. For example, in response to MCMV infection, it was revealed that Ly49H$^+$ NK cells acquire definite development and function matching the response of CD4$^+$ T cells to infection caused by MCMV (Sun et al., 2009). Interestingly, signaling of Ly49H$^+$ NK cells was long-lived and continued after infection with features of memory T cell phenotypes (Sun et al., 2009). Similarly, in humans, infection with human CMV was linked to the development of CD94/NKG2C$^+$ cells, whose antiviral activity was increased markedly upon relocation into infected transplant organ tissue (Foley et al., 2012). Others have shown that after being slightly pre-activated via cytokines such as IL-12, IL-15, and IL-18, human NK cells reproduced potent memory-like responses upon reactivation, and markedly elevated levels of IFN-γ production (Cooper et al., 2009, Romee et al., 2012). These memory NK cells are believed to be distinct from the CMV-driven memory cells and cytokine-driven memory cells. CMV-driven memory-like NK cells have more recently been defined as “adaptive NK cells” (Malone et al., 2017, Tschan-Plessl et al., 2016), whereas this unique subset of memory NK cells are not prevalent in the peripheral blood and indeed uniquely located in the liver and express CXCR6 (Deniz et al., 2013, Paust and von Andrian, 2011, Paust et al., 2010).

1.4.8 Signaling of NK cells

Unlike T and B cells, the function of NK cells is dependent on a combination of a variety of receptors located on their cell surface. Based on observations by Long and colleagues, a term called ‘co-activating receptor’ (Bryceson et al., 2006) has been coined to explain the collaboration and communication between inhibitory and activating receptors at the surface of NK cells. Long et al. showed that none of the

activating receptors of human NK cells alone were able to exhibit any cytokine production or even cytolytic activity, using agonist antibodies cross-linked to activating receptors (Bryceson et al., 2006). However, upon cross-linking of combinations of different sets of receptors to agonist antibodies, the effective function of NK cells was observed, as well as stimulation and synergistic activities in some cases (Bryceson et al., 2006).

Although NK cells receptors differ in their extracellular domains, they share similar activating or inhibitory signaling motifs in their cytoplasmic region. NK receptors send activating signals via immune-receptor tyrosine-based activation motif (ITAM) domains or inhibitory signals via ITIM domains. These motifs have conserved tyrosine residues that become phosphorylated after engagement of NK receptors with their cognate ligand (Blery et al., 2000, Isakov, 1997). Others have shown that mutation of the N-terminal tyrosine within the ITIM to phenylalanine results in loss of the KIR inhibitory signal (Burshtyn et al., 1999).

Receptors comprising ITIMs are not limited to NK cells and are expressed in a variety of different cell types and are required for the regulation of the inhibitory activity of different cell pathways (Long, 2008). *In vitro* and *in vivo* experiments have indicated that after phosphorylation of tyrosine, the association of protein tyrosine phosphatases SHP-1 and SHP-2 with the ITIMs occurs (Bruhns et al., 1999, Burshtyn et al., 1996, Campbell et al., 1996, Olcese et al., 1996). This allows the association of the tyrosine phosphatases SHP-1 or SHP-2 or the lipid phosphatase SHIP with the ITIM domain (Ravetch and Lanier, 2000), which consequently leads to inhibition of NK cell's function and elimination of calcium flux, cytokine production, proliferation and degranulation of NK cells (Ravetch and Lanier, 2000).

Activating NK receptors often couple adaptor proteins containing ITAM sequences in their subunits such as DAP12 and Fcγ. In order to initiate this process, they require the presence of Src and Syk family kinases, as well as calcium fluxes and alteration in the cytoskeleton to prompt degranulation (Kirwan and Burshtyn, 2007). In general,

receptors containing ITAM in their cytoplasmic subunit have an aspartate amino acid residue in their transmembrane domain and can assemble via charged interactions with amino acid residues with opposite charges, such as lysine and arginine in the transmembrane domains of the receptors (Lanier, 2008).

1.4.8.1 NK cells and education

To avoid auto-immunity, it has been proposed that NK cells undergo developmental "education" during maturation to discriminate between self and non-self. NK self-tolerance is highly regulated, and so far, there is no report of auto-immunity caused by NK cell dysfunction. The engagement of MHC class I molecules by both activating and inhibitory receptors is an important step in "education" (Kumar and McNerney, 2005) (Luci and Tomasello, 2008).

It's been shown that the process of "education" is dynamic and reversible (Elliott et al., 2010, Joncker et al., 2010). Further, it has been reported that "education" is linked to rearrangement of the plasma membrane (Guia et al., 2011), yet the exact mechanism of this process remains unresolved. One of the most important consequences of education is the production of different populations of NK cells possessing diverse effector functions against missing self. However, it should be noted that the density of activating ligands at the surface of target cells play an important role in the final decision of NK cells response (Thielens et al., 2012).

1.5 KIRs

1.5.1 KIRs and their gene structure

1.5.1.1. Lineages of KIR

KIRs expanded in primates ~ 40 million years ago, and diversified in a species-specific manner (Martin et al., 2000). Assembly of *KIR* genes in the LRC occurs in a head-to-head manner, and the sets of *KIRs* are inherited as haplotypes. These genes are categorized in four different lineages based on structural characteristics of proteins that they encode for.

The arrangement of the *KIR* genes complexes is common to humans and apes and comprises four phylogenetic ancestries (Lineages I, II, III and IV), classified according to structural differences and the specificity of their interaction with MHC class I molecules (Parham and Moffett, 2013, Vilches and Parham, 2002). Further diversity in KIRs content is produced through unequal crossover of *KIRs* that has led to the formation of hybrid loci and the development of separate haplotypes (Carrillo-Bustamante et al., 2016, Martin et al., 2000, Martin et al., 2003, Vilches and Parham, 2002, Wende et al., 1999, Wilson et al., 2000). The lineage I KIRs (KIR2DL4 and KIR2DL5) are yet to have their ligands conclusively identified, though an interaction between KIR2DL4 and HLA-G has been reported (Rajagopalan, 2010). The lineage II (*KIR3DL1/S1* and *-L2*) recognize HLA-Bs and certain alleles of HLA-A. The lineage III *KIRs* including *KIR2DL1*, *-L2 /3*, *KIR2DS1*, *-S2*, *-S3*, *-S5* and *-S4* recognize HLA-C molecules. The ligands of the lineage IV, comprising KIR3DL3 are still unidentified (Carrillo-Bustamante et al., 2016, Trowsdale et al., 2001, Falco et al., 2013, Hsu et al., 2002, Vilches and Parham, 2002).

KIRs genotypes display significant degrees of diversity as a result of the presence or absence of *KIR* gene loci on dissimilar KIR haplotypes. KIR genes typically encode either activating or inhibitory receptors. The exceptions are *KIR2DL4* and the *KIR3DL1*/S1 allele. The *KIR2DL4* gene encodes for a dual function receptor with both activating and inhibitory potential. The *KIR3DL1*/S1 locus encodes the inhibitory *KIR3DL1* or the activating *KIR3DS1* that segregate as alleles (Figure 1.11) (Middleton

and Gonzelez, 2010, Rajagopalan et al., 2001)

1.5.1.2 KIR haplotypes

The divergence between the centromeric and telomeric regions of the *KIR* loci led to the formation of two distinct KIR haplotypes in humans. Haplotype group A and B differ in both their frequency and their gene content (Carrillo-Bustamante et al., 2016, Gendzekhadze et al., 2009, Hollenbach et al., 2010, Norman et al., 2013, Yawata et al., 2006). Group A haplotypes are defined by the existence of genes encoding for inhibitory KIRs and consist of *KIR2DL1*, *KIR2DL3*, *KIR3DL1*, *KIR2DS4* and the pseudogene *KIR2DP1*. Because of individual allelic polymorphism, diversity in this group exists. Unlike haplotype group A, haplotype B comprises different varieties of activating and inhibitory combinations (Uhrberg et al., 2002, Wilson et al., 2000). Group B haplotypes are defined as possessing at least one of the following genes *KIR2DL2*, *KIR2DL5A*, *KIRDL5B*, *KIR2DS1*, *KIR2DS2*, *KIR2DS3*, *KIR2DS5* or *KIR3DS1* (Uhrberg et al., 1997, Levinson, 2011). It has been postulated that group A and B haplotypes are maintained in humans via balancing selection. It has been proposed that group A haplotypes are linked to enhanced responses related to pathogen infections while group B haplotypes are associated with developed responses related to re-productivity, health, and survival (Falco et al., 2013, Moffett and Loke, 2006, Parham, 2005, Rajagopalan and Long, 2005).

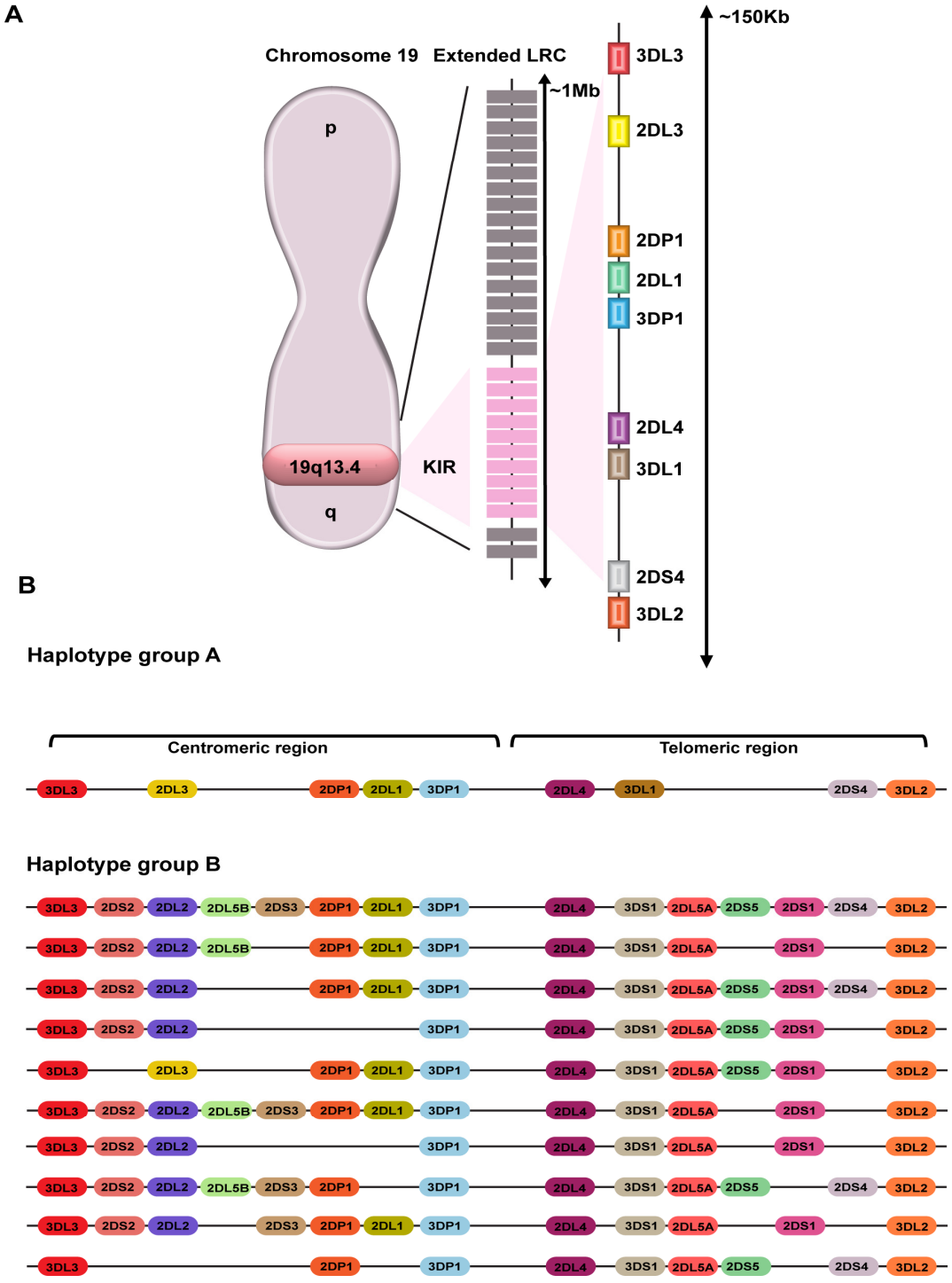

Figure 1.11 KIR genes and their haplotypes.
Genes that encode KIRs are located on chromosome 19 where they occupy 50 kb of the 1 Mb extended LRC. Figure is adapted from (www.ebi.ac.uk.) **B**. KIR haplotypes, A and B. The figure is adapted from (Middleton and Gonzelez, 2010).

1.5.2 Structure of KIRs

KIR proteins are transmembrane glycoproteins with two or three extracellular Ig domains that are located on the surface of NK cells (Borrego et al., 2002). They can be sub-divided further into two groups, inhibitory and activating receptors. KIRs with short cytoplasmic tails are activating receptors, and KIRs with long cytoplasmic tails are inhibitory receptors. The extracellular KIR Ig domains are numbered from the N-terminus. In KIR2Ds, the two domains are named D1 and D2, and in KIR3Ds, the three Ig domains are named D0, D1, and D2 (Vilches and Parham, 2002). However, the exception to this is KIR2DL4 and -L5 that instead of having a D1 domain, they both contain a D0 domain that has high similarity to D0 domain of KIR3Ds (Figure 1.12 and Figure 1.13) (Khakoo et al., 2000, Moesta et al., 2009).

DAP12 associates with lysine in the transmembrane region of activating KIR2DS and KIR3DS (Lanier et al., 1998). By contrast, the transmembrane domain of KIR2DL4 contains an arginine residue that couples the adaptor FcεRI-γ (Miah et al., 2008). Site-directed mutagenesis studies indicated that mutation of these basic residues disrupts the association of KIR2DL4 and KIR2DS2 with FcεRI-γ and DAP12, respectively (Feng et al., 2006, Feng et al., 2005, Miah et al., 2008). Interestingly, KIR2DL4 and KIR2DS can be detected at the surface of NK cells in the absence of FcεRI-γ and DAP12, respectively, although their expression is low (Kikuchi-Maki et al., 2005, Steiner et al., 2008, VandenBussche et al., 2009).

Polymorphism is also found in the cytoplasmic tail of KIR2DL and affects their function via regulation of downstream signal transduction. For example, it has been observed that KIR2DL1*010 displays stronger inhibitory activity compared to that of -L1*004. Interestingly, they just differ in one amino acid located in their cytoplasmic tail. It's been suggested that the existence of arginine at position 245 (as opposed to cysteine) in its cytoplasmic tail results in the stronger capability of KIR2DL1*010 to recruit SHP-2 and β-arrestin (Bari et al., 2009).

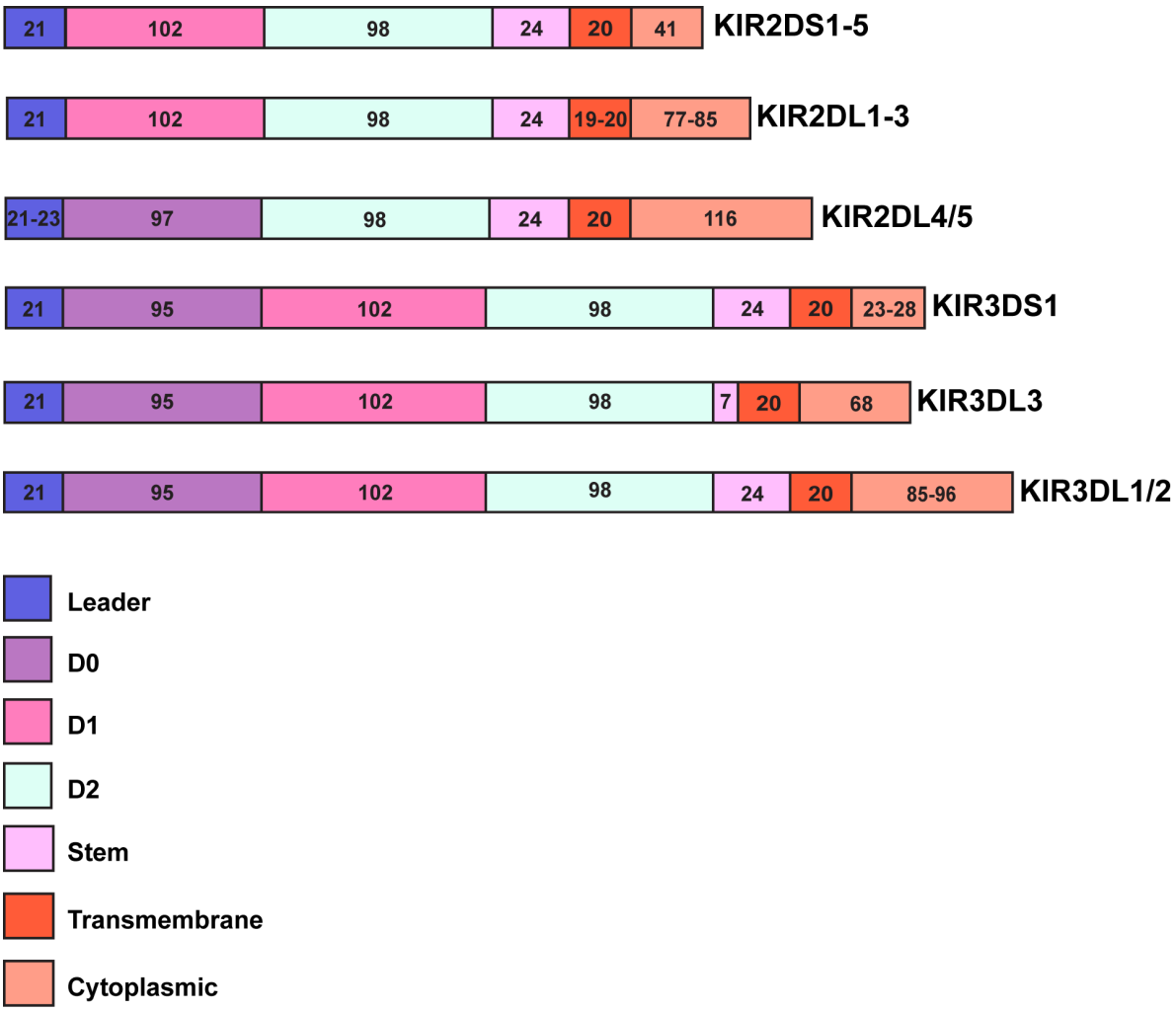

Figure 1.12 KIR domains and their lengths.
The length of each KIR domain is shown. The figure is adapted from (www.ebi.ac.uk.). The length of each domain is shown in numbers within their respective box.

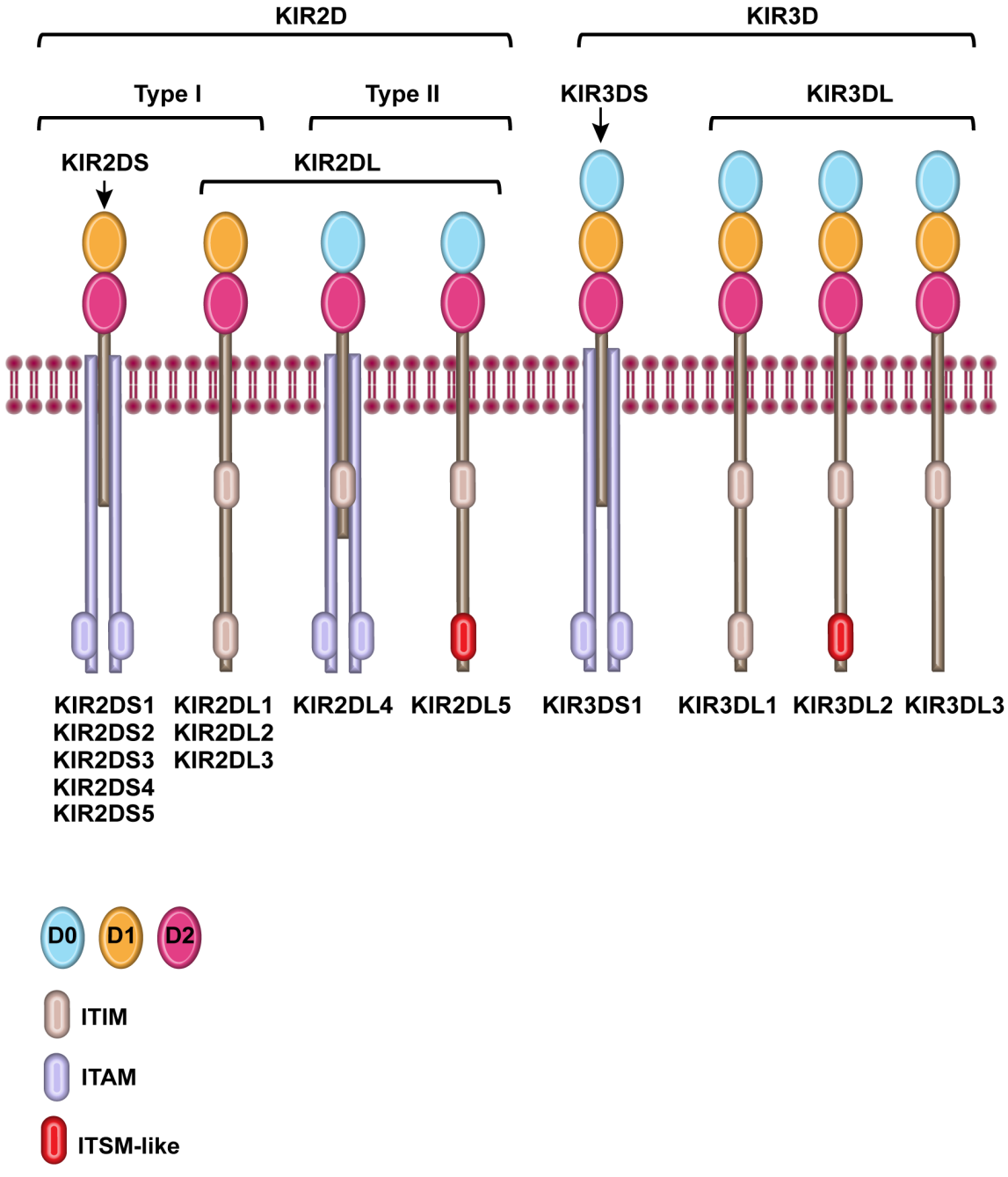

Figure 1.13 Members of KIR family.
The structural arrangement of two and three Ig-like domain KIRs are shown. KIRs are divided into two groups of inhibitory and activating based on the length of their respective cytoplasmic tails. They can further be subdivided based upon the number of Ig domains they possess. The figure is adapted from (www.ebi.ac.uk) and (Saunders et al., 2015b).

1.5.3 KIRs and HLA class I molecules act as a system: lessons from evolution

Based on the phylogenetic evidence, it has been suggested that the development of *KIRs* has mirrored that of their *HLA* ligands (Hao and Nei, 2005). The MHC class I and KIR system of humans differ from that of chimpanzees with respect to differences in their genetics and function of their receptors (Older Aguilar et al., 2010), and are the result of evolution and segregation of humans from chimpanzees ~10 million years ago (Older Aguilar et al., 2010). One of the unique features that humans acquired during evolution in their coevolved *MHC-KIR* system, is the appearance of group A and B haplotypes, and also the profusion of HLA-C in regulation of the NK cells function. For example, it's been reported by Abi-Rached and colleagues that the residues of KIR2DL2/L3 that are responsible for binding to HLA-C1 epitope underwent thorough positive selection during evolution (Older Aguilar et al., 2010). More interestingly, it has been suggested that HLA-C molecules are specialized during evolution to become ligands for KIRs compared to the majority of HLA-A and -B molecules that became specific ligands for TCRs (Older Aguilar et al., 2010). Considering the evidence that the level of cell surface expression of HLA-C molecules is around 10 times lower than that of HLA-A and -B (Zemmour and Parham, 1992, Apps et al., 2015), it's been proposed that this might be due to the specialization of HLA-C for recognition by NK cells and that NK cell receptors can generate efficient and effective responses even with limited expression of HLA-C molecules (Augusto and Petzl-Erler, 2015).

Results obtained from genotyping studies on 1,642 persons from 30 geographically dissimilar populations supports the notion of co-evolution of *KIR* and *HLA* genes (Single et al., 2007), showing significant negative correlation between the existence of activating KIRs and their respective HLA ligands, mainly for *KIR3DS1* and its ligand HLA-B Bw4 (a serological epitope defined by the 5 C-terminal residues on the α1-helix that distinguish it from the Bw6 motif that is present in all other HLA-B alleles). Other groups have reported a strong positive association between the distribution of *KIR2DL3* and its ligand group 1 HLA-C (Hollenbach et al., 2013). Studies on more than 200 individuals from Ghana—where the risk of infection by malaria parasite is

very high—demonstrated that each individual had a unique association of *HLA* class I and *KIR* (Norman et al., 2013), highlighting the existence of balance and selection between *KIRs* and *HLAs* during evolution. The association of *KIR2DL3* and group 1 HLA-C escalates the possibility of cerebral malaria. Therefore, their distribution is very low in this population, which further emphasizes the co-evolution of *KIRs* and *HLAs* in response to pathogens (Hirayasu et al., 2012).

The combination of KIR3D with HLA class I molecules carrying Bw4 epitopes is suggested to be protective against HIV (Hernandez-Ramirez et al., 2015). KIR3D receptors have D0 domain in their extracellular domain which resembles D0 domain of KIR2DL4 and -L5. By characterizing the molecular basis of the interaction between KIR3DL1 and HLA-B*57 in the presence of self-peptide (shown in Figure 1.17), first insights about the importance of D0 domain of KIR3D in complex formation with HLA Bw4 molecules is emerged recently (Vivian et al., 2011). Vivian and colleagues reported that 30% of buried surface area of the complex formation between KIR3DL1 and HLA-B*57 is credited to D0 domain. The existence of D0 is crucial for recognition of loop region of HLA-B*57 covering the residues from 14–18 and 88–92 which display a low degree of polymorphism among alleles of HLA-A and -B (Vivian et al., 2011). It has been suggested that the D0 domain performs as an innate sensor, due to its important role in mediating the interaction of KIR3DL1 with HLA-B*57 by establishing a particular molecular recognition binding site for the limited polymorphic region of HLA-As and -Bs (Vivian et al., 2011).

1.5.3.1 KIR2DL genes and their HLA-C ligands

Genes of *KIR2DL1*, *-L2*, and *-L3* which are positioned in the centromeric part of the KIR locus, encode the receptors which bind to *HLA-C* allotypes. HLA-C allotypes displaying HLA-C2 epitopes are recognized by KIR2DL1 while recognition of HLA-C allotypes presenting HLA-C1 epitopes is performed by *KIR2DL2* and *KIR2DL3* (Biassoni et al., 1995, Colonna, 1997, Falco et al., 2013, Lanier, 1998, Long, 1999, Moesta et al., 2008, Moretta et al., 1994, Pende et al., 2009). For instance, Moesta et al., studied binding of KIR2DL1, -L2 and -L3 against different a panel of HLA-C1 and

HLA-C2 epitopes and their results indicated that KIR2DL1 only binds to HLA-C2 epitopes but KIR2DL2 and -L3, not only displayed interaction with all panels of HLA-C1 epitopes with high affinity of binding, but also exhibited binding to some of the HLA-C2 epitopes, although affinity of binding was lower. While KIR2DL2 and -L3 can interact with the same panel of HLA-Cs, the avidity of binding for KIR2DL2 was shown to be much higher than that of KIR2DL3 (Moesta et al., 2008).

The outcome of studies on the arrangement of KIR haplotypes and sequences of KIR genes indicates that non-reciprocal recombination of *KIR2DL1* with *KIR2DL3* resulted in the development of *KIR2DL2*, suggesting that *KIR2DL2* has evolved from a *KIR2DL3-like* ancestor (Moesta et al., 2008). Site directed mutagenesis experiments have also shown that position 44 of *KIR2DL1*, *-L2*, and *-L3*, located in their D1 domain, creates a dimorphic site and dictates their specificity (Winter and Long, 1997). Accordingly, KIR2DL1/2/3 are highly similar receptors whose function is dictated by a small number of polymorphic residues (Figure 1.14 and Figure 1.15).

A

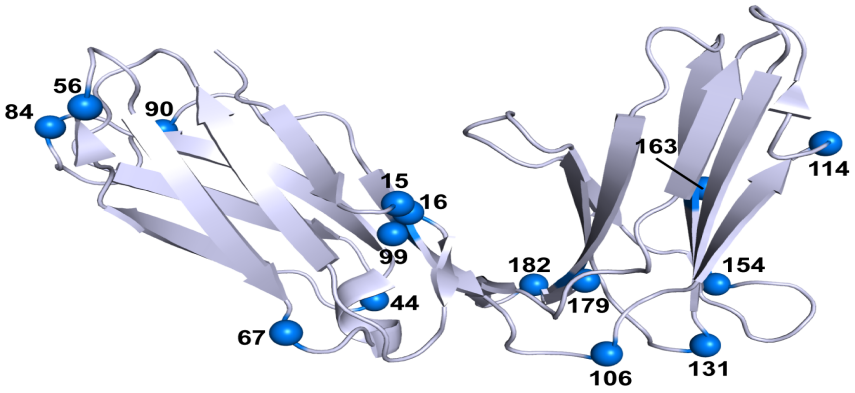

B

	15	16	44	56	67	84	90	99	106	114	131	154	163	179	182
	G	R	M	H	S	T	V	I	E	P	R	P	D	G	H
L1*001	—	P	—	—	—	—	—	—	—	—	—	—	—	—	—
L1*002	—	P	—	—	—	—	—	—	—	—	—	—	—	—	—
L1*003	—	—	—	—	—	—	—	—	—	L	—	—	—	—	—
L1*004	—	—	—	—	—	—	—	—	—	—	—	T	N	—	R
L1*005	—	—	—	—	—	—	—	—	—	L	—	—	—	—	—
L1*007	—	—	—	—	—	—	—	V	—	—	—	T	N	—	R
L1*008	D	P	—	—	—	—	—	—	—	—	—	—	—	—	—
L1*009	—	—	—	—	—	—	—	—	—	L	—	—	—	—	—
L1*010	—	—	—	—	—	—	—	—	—	L	—	T	N	—	R
L1*011	—	—	—	—	—	—	—	—	—	—	—	T	N	—	R
L1*012	—	—	—	—	—	—	—	—	—	—	—	—	—	—	—
L1*014	—	—	—	—	—	—	—	—	—	L	—	—	—	S	—
L1*015	—	—	—	—	—	—	—	—	—	L	—	—	—	—	—
L1*016	—	—	—	—	—	—	—	—	—	L	—	—	—	—	—
L1*017	—	—	—	—	—	—	—	—	—	L	—	—	—	—	—
L1*018	—	—	—	—	—	—	—	—	—	L	—	—	—	—	—
L1*019	—	—	—	—	—	—	—	—	—	—	—	—	—	—	—
L1*020	—	—	—	—	G	—	—	—	—	L	—	—	—	—	—
L1*021	—	P	—	—	—	—	—	—	Q	—	—	—	—	—	—
L1*022	—	P	K	—	—	—	—	—	—	—	—	—	—	—	—
L1*023	—	—	—	—	—	P	L	—	—	L	—	—	—	—	—
L1*024	—	—	—	R	—	—	—	—	—	—	—	T	N	—	R
L1*025	—	—	—	—	—	—	—	—	—	L	W	—	—	—	—

Figure 1.14. Polymorphisms among KIR2DL1 alleles.

Polymorphic residues within alleles of KIR2DL1. Their positions are shown in the crystal structure of KIR2DL1. Blue spheres represent the position of the Cα of polymorphic residues. Involved in polymorphism and digits indicate the number of each residue within KIR2DL1. **B**. Sequence alignment of alleles of KIR2DL1, highlighting the polymorphic residues. PDB ID: 1IM9.

A

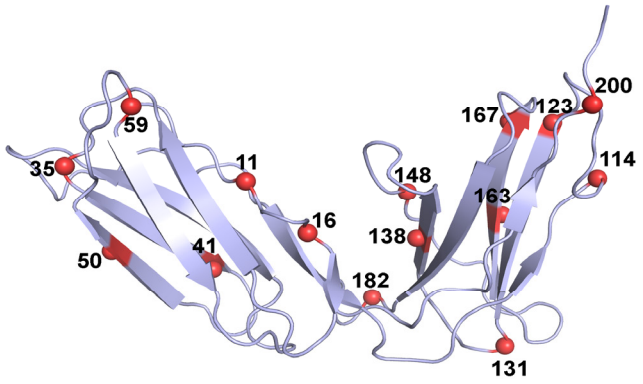

B

	11	16	35	41	50	59	114	123	131	138	148	163	167	182	200
	L	P	E	R	H	V	P	S	R	H	R	D	G	R	T
L2*001	—	R	—	—	—	—	—	—	—	—	C	—	—	—	I
L2*002	—	R	—	—	—	—	—	—	—	—	C	—	—	—	I
L2*003	—	R	—	—	—	—	—	—	—	—	C	—	—	—	—
L2*004	—	—	Q	T	—	—	—	—	—	—	C	—	D	—	—
L2*005	—	R	—	—	—	—	—	—	—	—	C	—	—	—	I
L2*006	—	—	—	—	—	—	—	—	—	—	C	—	—	—	—
L2*007	—	R	—	—	—	—	—	—	—	—	C	—	—	—	I
L2*008	—	R	—	—	—	—	—	—	—	—	C	—	—	—	I
L2*009	—	R	—	—	—	—	—	—	—	—	—	—	—	—	—
L2*010	—	R	—	—	—	—	—	—	—	—	C	—	—	—	I
L2*011	—	—	—	—	—	—	—	—	—	—	C	—	D	—	—
L2*012	—	R	—	—	—	—	—	—	—	—	C	—	—	—	—
L3*001	—	—	Q	—	—	—	—	—	—	—	—	—	—	—	—
L3*002	—	—	Q	—	—	—	—	—	—	—	—	—	—	—	—
L3*003	—	—	Q	—	—	—	—	—	—	—	—	—	—	—	—
L3*004	R	—	—	—	R	—	—	—	—	—	—	—	—	—	—
L3*005	R	—	—	—	R	—	—	—	—	—	—	—	—	—	—
L3*006	—	—	Q	—	—	—	—	—	—	—	—	—	—	—	—
L3*007	—	—	Q	—	—	—	—	—	—	—	—	—	—	—	—
L3*009	—	—	Q	—	—	—	—	—	—	—	P	—	—	—	—
L3*010	R	—	—	—	R	—	—	—	—	—	—	—	—	—	—
L3*011	—	—	Q	—	—	—	L	—	—	—	—	—	—	—	—
L3*012	—	—	Q	—	—	—	—	—	—	—	—	—	—	—	—
L3*013	—	—	Q	—	—	—	—	—	Q	—	—	—	—	—	—
L3*014	—	—	—	—	R	—	—	—	—	—	—	—	—	—	—
L3*015	—	—	—	—	—	—	—	—	—	—	—	—	—	—	—
L3*016	—	—	Q	—	—	—	—	N	—	—	—	—	—	—	—
L3*017	—	—	—	—	R	—	—	—	—	—	—	—	—	—	—
L3*019	—	—	Q	—	—	—	—	—	—	R	—	—	—	—	—
L3*020	—	—	Q	—	—	—	—	—	—	—	—	—	—	H	—
L3*021	—	—	Q	—	—	—	—	—	—	—	—	—	—	—	—
L3*022	—	—	Q	—	—	—	—	—	—	—	—	N	—	—	—
L3*023	—	—	Q	—	—	I	—	—	—	—	—	—	—	—	—
L3*024	—	—	Q	—	—	—	—	—	—	—	—	—	—	—	—

Figure 1.15 Polymorphisms among KIR2DL2 and KIR2DL3 alleles.
Polymorphic residues within the alleles of KIR2DL2 and KIR2DL3. Their positions are shown in the crystal structure of KIR2DL2. Red spheres represent the positions of the Cα of polymorphic residues. **B**. Sequence alignment of alleles of KIR2DL2 and KIR2DL3, highlighting the polymorphic residues. PDB ID: 1EFX.

1.5.3.1.1 KIR2DL4: unique among KIR2DLs

KIR2DL4 is a unique member of the KIR family that differs in many aspects from the other members. Structurally, the extracellular Ig domains of KIR2DL4 comprise a D0 and D2 arrangement, a feature it shares with KIR2DL5. Unlike other KIRs that are expressed on the cell surface of NK cells, KIR2DL4 is mostly localized and signals in the endosome. Unlike other KIRs, expression of KIR2DL4 occurs on CD56high NK cells and interestingly instead of association with DAP12, binds to ITAM-containing FcεRI-γ adaptor, displaying more cytokine production than cytolytic activity (Goodridge et al., 2003, Kikuchi-Maki et al., 2005, Rajagopalan et al., 2001). Therefore, KIR2DL4 engagement results in robust cytokine production including IFN-γ, chemokines, and angiogenic factors (Kikuchi-Maki et al., 2003), and weak cytotoxicity (Rajagopalan et al., 2006).

It has been suggested that KIR2DL4 may play a crucial role during early pregnancy and HLA-G which is expressed by fetal-derived trophoblast cells, may be a ligand for KIR2DL4 (Ponte et al., 1999, Rajagopalan and Long, 1999). However, this remains controversial as others have reported that HLA-G does not bind KIR2DL4 (Le Page et al., 2014). Recombinants of KIR2DL4 have been reported to exhibit binding to different types of cell lines lacking the expression of HLA-G, which suggests the existence of alternative ligand(s) (Brusilovsky et al., 2013). Brusilovsky et al. demonstrated that KIR2DL4 recognition of these yet to be identified ligand(s) is directly regulated by heparan sulfate (HS) glucosamine 3-O-sulfotransferase 3B1 (HS3ST3B1). They reported that KIR2DL4 directly binds to HS/heparin, and the D0 domain of KIR2DL4 is key to this interaction (Brusilovsky et al., 2013).

1.5.3.2 HLA-C and the interplay with KIR2DLs

HLA-Cs can be subdivided into two groups based on dimorphism at position 80. Those having an asparagine at position 80 are C1 epitopes (HLA-C1), and those with lysine at their position 80 generate the C2 group (HLA-C2). Among the 312 HLA-C allotypes that have been identified so far, half of them have HLA-C1, and the other half are HLA-C2. Recent reports have shown that HLA-C has evolved recently from classical HLA molecules and are limited to humans and apes (Adams and Parham, 2001, Kulpa and Collins, 2011, Older Aguilar et al., 2010).

Based on sequence alignment, using sequences of alleles of HLA-C molecules (http://www.ebi.ac.uk/imgt/hla/), there are rare HLA-C alleles that differ from the conventional asparagine and lysine at position 80. For example, HLA-C*07:115 displays aspartic acid, HLA-C*15:60 displays glutamine and HLA-C*05:32 displays arginine (Falco et al., 2013). Different alleles of HLA-C comprising HLA-C1 and HLA-C2 epitopes have been shown to behave differently regarding their affinity of binding to KIR2DL1, -L2, and -L3 (Frazier et al., 2013, Moesta et al., 2008). For instance, it has been observed that the affinity of KIR2DL1 binding to HLA-C*02:02 allele is much higher than the other alleles of HLA-C*02 allotypes (Moesta et al., 2008).

Comparison of activating KIRs has demonstrated that they have limited ligands compared to their inhibitory counterparts. This has led to the suggestion that inhibitory KIRs evolved before activating KIRs (Fauriat et al., 2010a). Furthermore, it has been demonstrated that the expression of KIRs is also affected by the existence of HLA-C molecules. For instance, the number of NK cells expressing genes of *KIR3DL1* and *KIR2DL1* were shown to increase in the presence of their respective ligands, *HLA-B* Bw4 and *HLA-C2* in individuals (Yawata et al., 2006). Studies also indicate that the pattern of gene methylation can affect the expression of KIRs. Furthermore, in some cases, it has been shown that polymorphisms in the coding region of KIR genes can lead to the changes in expression (Pando et al., 2003, VandenBussche et al., 2006, VandenBussche et al., 2009).

1.5.3.3 Recognition of HLA-Cs by KIRs

It is well established that HLA-A, -B, and -C molecules act as ligands for some KIRs. It has been reported that ~ 45% of HLA-A, ~ 36% of HLA-B and 100 % of HLA-C molecules are known KIRs ligands (Parham et al., 2012). Investigations into the interactions of KIRs with their respective ligands indicated that they have a fast association and dissociation rates and their affinity of binding is in the low micro-molar range. The interaction between KIR and HLA-C is driven by shape and charge complementarity that takes place at the surface of contacting sites of both KIRs and HLA-Cs. Figure 1.16 highlights HLA class I molecules that are reported to interact with KIRs and act as their ligands. Briefly, KIR2DL1/S1 and KIR2DL2/3 interact with HLA-C2 and -C1, respectively. KIR3DL1 binds to HLA-Bw4, KIR3DL2 recognizes HLA-A3, -A11. KIR2DS2/S4 interact with HLA-A11, and the ligands for KIR2DL4/L5 and KIR3DS1 are yet to be confirmed.

Before this study, there were two crystal structures of HLA-Cs bound to KIRs. Boyington and his colleagues determined the crystal structure of HLA-C*03:04 bound to KIR2DL2, and one year later, Fan and colleagues revealed the crystal structure of KIR2DL1 in complex with HLA-C*04:03 (Boyington et al., 2000, Fan et al., 2001). The structures from the two studies were highly similar to each other with the D1 and D2 domains of KIR2DL1 and -L2 on top of the α1 and α2 domains of the heavy chain of HLA-C*04 and -C*03, respectively. The crystal structure of KIR2DL2 in complex with HLA-C*03 revealed that lysine 44 of KIR2DL2 interacts with asparagine 80 of HLA-C*03, located on the α1 domain of the heavy chain, as well as a few contacts with the peptide. Interestingly, the crystal structure of KIR2DL1 in complex with HLA-C*04 shows the same pattern of binding with the notable difference that it is a methionine residue at 44 of KIR2DL1 that participates in interactions with Lysine 80 of HLA-C*04 as well as a few contacts with the peptide. As such, the dimorphism at position 44 of KIR2DLs is thought to dictate the specificity of KIR2DLs for HLA-C1 or HLA-C2 epitopes through its interaction with position 80.

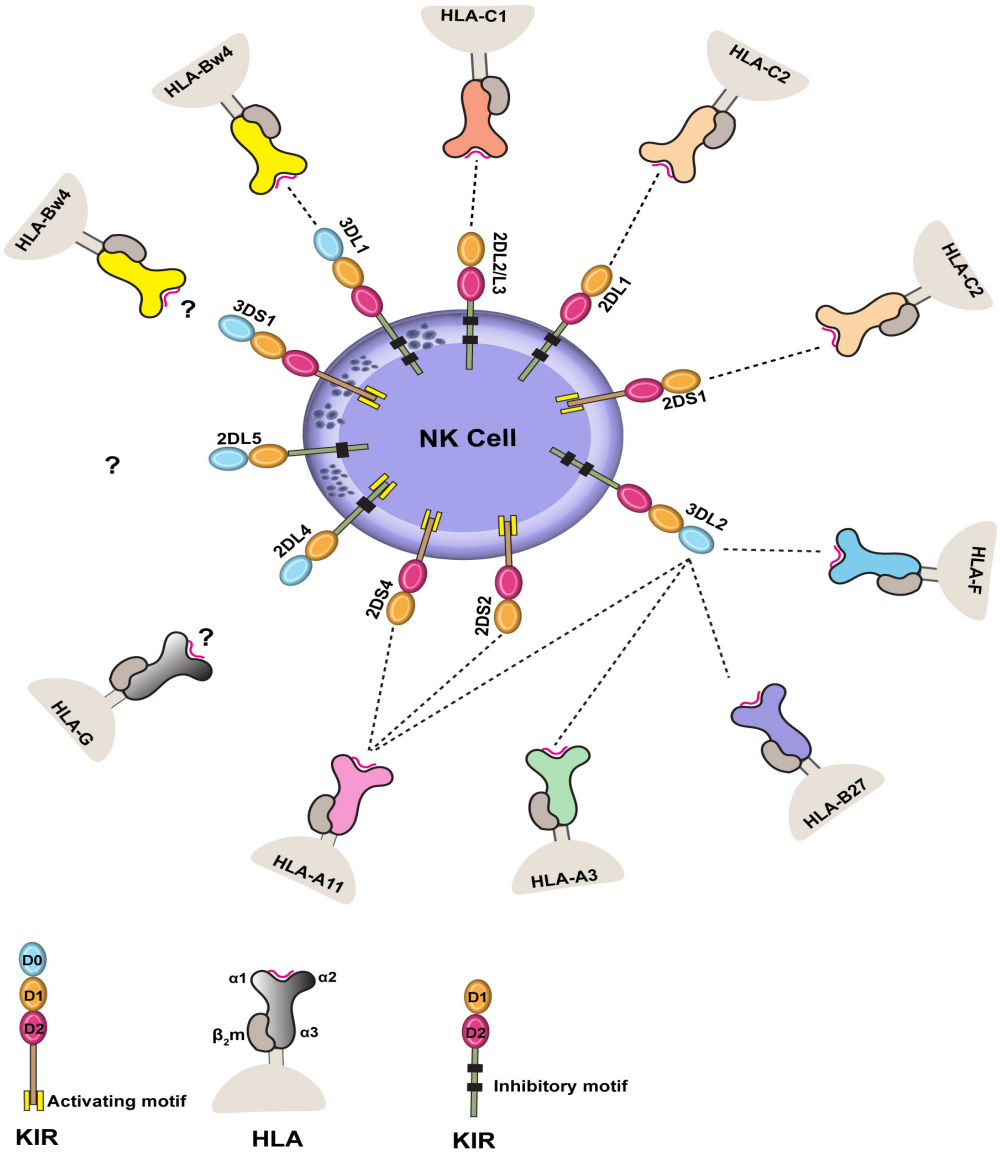

Figure 1.16 HLA class I ligands of KIRs.
Cartoon representation of HLA class I ligands for KIRs. Although the interaction of HLA class I molecule ligands for some KIRs have been established, there remains a lack of data and controversy for some reported ligands for KIR2DL4, KIR2DL5, and KIR3DS1 (specified by question marks). The figure is adapted from (Augusto and Petzl-Erler, 2015, Saunders et al., 2015b).

1.5.3.4 Allotype diversity of KIR2DLs and HLA-Cs recognition

Diversity in the affinity of KIR2DLs for HLA-C1 and HLA-C2 epitopes exist at the gene and allele level, and more recently it has been appreciated that there are differences at the allotypic level. Frazier and his colleagues investigated the impact of allelic diversity of KIR2DL3 on its affinity for HLA-C1 and HLA-C2 alleles. They showed that indeed there were significant differences in recognition of HLA-C alleles with KIR2DL3*005 showing the greatest HLA-C1/C2 cross-reactivity akin to KIR2DL2 (Frazier et al., 2013). To date, the structural details underpinning these allotypic differences, and KIR2DL2 C1/C2 cross-reactivity remain to be elucidated.

1.5.4 Crystal structures of KIR

So far, crystal structures of KIR2DL1, 2DL2, 2DL3, 2DS2, 2DS4, 3DL1, alone or in complex with their cognate HLA class I ligands have been solved (Table 1.4 and Figure 1.17) (Boyington et al., 2000, Fan et al., 2001, Graef et al., 2009, Liu et al., 2014, Maenaka et al., 1999, Moradi et al., 2015, Saulquin et al., 2003, Snyder et al., 1999, Vivian et al., 2011). Common to these complexes is a broad recognition mode characterized by a V-shaped interface at the junction of the D1 and D2 domains that sit on top of the α1 and α2 helices of HLA. There are few contacts at the C-terminal part of the peptide. Crystal structures of different unbound KIR2Ds reveal differences about their D1/D2 hinge angles that suggest a degree of flexibility for the receptors. Further, the hinge angle between these domains changes upon interaction of KIRs with their cognate HLA class I ligands.

The D1 domains of KIRs show the greatest variability in terms of binding to HLA molecules. Comparison of the structure of KIR2DL2-HLA-C*03 with KIR2DL1-HLA-C*04 indicates that the most variable contacts are found in those generated by D1 domain of KIRs with the α1 domain of HLA. This region is believed to define the specificity of the KIRs. Conversely, highly conserved contacts are found in those generated by the D2 domain atop the α2 domain of the cognate HLA ligand, covering the area between residues 145 to 151 of the α2 domain (Boyington et al., 2000, Fan

et al., 2001, Liu et al., 2014, Vivian et al., 2011). The highest degree of conservation is found in Asp 135 of the D2 domain of KIR2D and Asp 230 of KIR3DL1 forming a salt-bridge with Arg 145 on the α2 domain of HLA class I ligand. Arg 145 on the α2 domain of HLA class I is also involved in the formation of a highly conserved hydrogen bond with Ser133 on D2 domains of KIR2D and Ser228 of KIR3DL1 (Boyington et al., 2000, Fan et al., 2001, Liu et al., 2014, Vivian et al., 2011). Accordingly, the D1 domain contacts are more varied and determine the specificity of the interaction while the contacts to the D2 domain are more conserved.

Table 1.4 Crystal structures of KIR2D and 3D, alone or in complex with their ligand.

Structure	PDB ID	Refrences
Isolated		
2DL1	1NKR	(Fan et al., 1997)
2DL2	2DLI, 2DL2	(Snyder et al., 1999)
2DL3	1B6U	(Maenaka et al., 1999)
2DS2	1M4K	(Saulquin et al., 2003)
2DS4	3H8N	(Graef et al., 2009)
In complex		
2DL1/HLA-C*04:01	1IM9	(Fan et al., 2001)
2DL2/HLA-C*03:04	1EFX	(Boyington et al., 2000)
2DS2/HLA-A*11:01	4N8V	(Liu et al., 2014)
3DL1/HLA-B*57:01	5B38, 5B39	(Vivian et al., 2011)

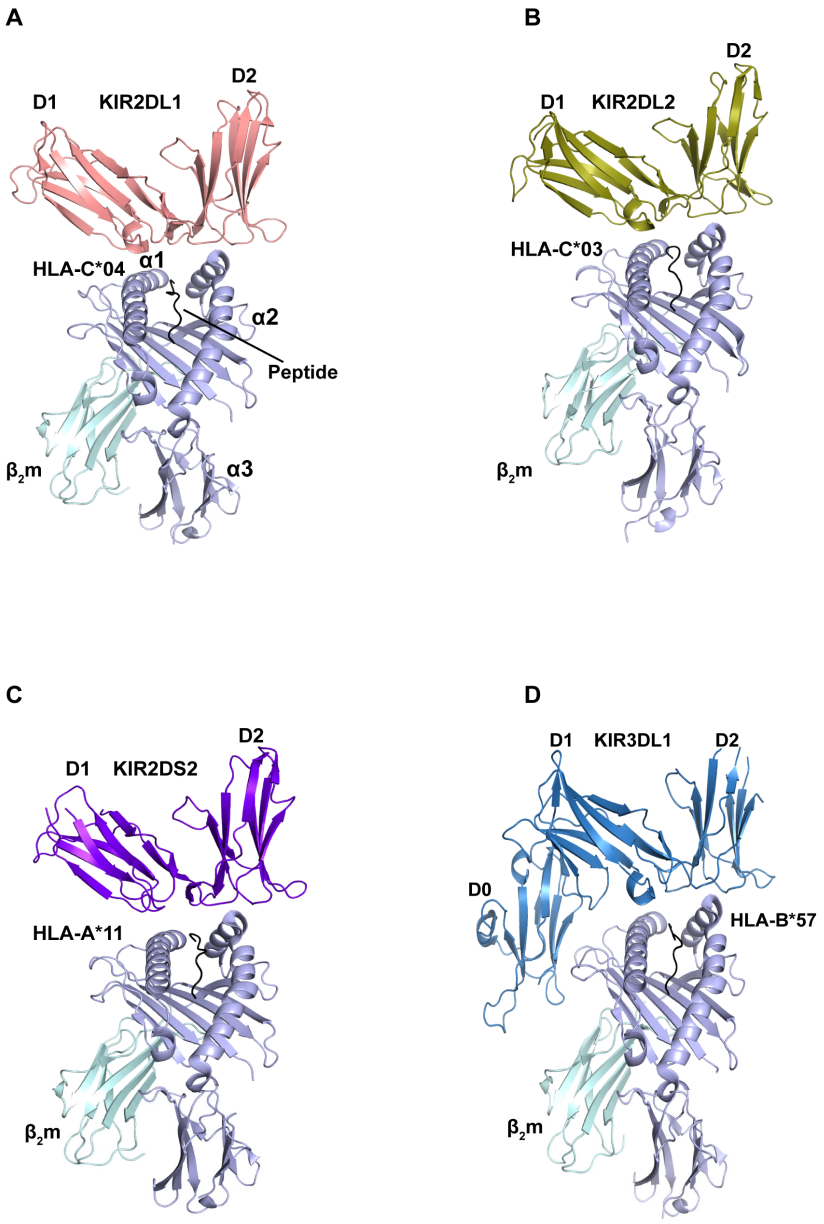

Figure 1.17 Crystal structures of KIR2D and KIR3D in complex with their respective ligands. Crystal structures of KIR2DL1 in complex with HLA-C*04 (PDB ID: 1IM9) (**A**), KIR2DL2 in complex with HLA-C*03 (PDB ID: 1EFX) (**B**), KIR2DS2 in complex with HLA-A*11 (PDB ID: 4N8V) (**C**), and KIR3DL1 in complex with HLA-B*57 (PDB ID: 3VH8) (**D**) are shown. The same pattern of docking of KIR domains typified by a V shape docking of D1 and D2 from KIR2DL1, -L2, -S2, and KIR3DL1 on top of α1 and α2 domains of their HLA class I ligand is observed.

1.5.4.1 The role of peptide in KIRs binding to HLA-Cs

It has been suggested that the sensitivity and selectivity of KIR for HLA might allow NK cells to sense the change of peptides repertoire inside the cells during viral infections. There are several studies specifying the existence of peptide sensitivity and selectivity for binding of KIRs to their HLA class I ligands (Colantonio et al., 2011, Hansasuta et al., 2004, Malnati et al., 1995, Rajagopalan and Long, 1997, Zappacosta et al., 1997). Details obtained from crystal structures of KIR2DL1 and 2DL2 bound to their cognate ligands and also results from direct binding assays highlights the involvement of the interaction between KIRs and position 8 of the peptide and its adjacent position 7 in the formation of these complexes (Boyington et al., 2000, Fan et al., 2001, Rajagopalan and Long, 1997). A closer look at the interface between KIR2DL2 and HLA-C*03:04 reveals that Glutamine 71 of the D1 domain hydrogen bonds with alanine at position 8 of the peptide and leucine 104 which is located in the hinge loop of 2DL2, interacts with leucine 7 of the peptide (Boyington et al., 2000). This interaction is stabilized and restricted further due to extra contacts from lysine 44 from the D1 domain and serine 184 and asparagine 187 from the D2 domain to position 8 of the peptide. As a result, short side chains such as alanine and serine are accommodated at position 8 while larger side chains like tyrosine and lysine attenuate binding of KIR2DL2 to HLA-C*03:04 (Boyington et al., 2000, Fan et al., 2001).

1.5.5 KIRs and infectious diseases

KIRs play an essential role in infectious diseases, auto-inflammatory and auto-immunity since they can activate or inhibit the actions of cells involved in regulation of immune responses. For example, it's been shown that the association of *KIR3DS1* and *HLA-B* results in the delay in development of acquired immune deficiency syndrome (AIDS) (Martin et al., 2002a). Similar studies highlight the impact of *KIR3DL1* association with *HLA-B* in control of HIV infection (Alter et al., 2011, Martin et al., 2007). Interestingly, the finding is similar to other reports indicating that the development of AIDS is slower in patients being infected with HIV type 1, due to their

link with *HLA-Bw4* homozygosity (Flores-Villanueva et al., 2001). Similarly, the progress of rheumatoid vasculitis and psoriatic arthritis are associated with *KIR2DS2* (Martin et al., 2002b, Yen et al., 2001) and *KIR2DS1* (Martin et al., 2002b). Table 1.5 summarizes KIRs associations with disease.

Studies point to the relationship between KIRs and their association with HLA class I molecules and susceptibility to viral infections. For example, it has been reported by Khakoo and colleagues that homozygosity for *KIR2DL3* and its ligand HLA-C1, influences the resolution of low dose HCV infection in individuals. Based on their observations, it was suggested that upon viral infections, KIR2DL3 homozygous NK cells produce stronger activating responses since their activating KIR overcome the relatively weak inhibitory response of *KIR2DL3* (Khakoo et al., 2004).

CMV reactivation is considered a major burden following solid organ transplantation, and genetic approaches to study the importance of the correlation between KIRs and CMV reactivation indicate the association of activating KIRs, *KIR2DS2* and *KIR2DS4* with protection against CMV in donors after hematopoietic cell transplantation (HCT) (Zaia et al., 2009). Similar observations were observed by Chen et al. that highlight the importance and impact of activating KIRs on reactivation of CMV during haematopoietic stem cell transplantation (Chen et al., 2006). Others have discovered that the existence of activating KIRs or the absence the interaction between *KIR2DL1/HLA-C2* or *KIR2DL2/L3* and *HLA-C1* alleles are connected with a reduction in the degree of CMV infection after kidney transplantation (Hadaya et al., 2008). Consistent with this observation Stern et al. showed that an increase in the number of multiple activating KIR genes is associated with a reduction in the level of reactivation for CMV infection during kidney transplantation (Stern et al., 2008).

KIR2DL2 has also been shown to have an influence on HIV infection (Alter et al., 2011). It has been observed that in HIV^{+} individuals, the antiviral cytolytic activity of NK cells bearing *KIR2DL2* were reduced due to the enhancement of the interaction between viral-infected CD4 T cells and *KIR2DL2* (Alter et al., 2011). It's been

revealed by genetic studies that *KIR2DL2* also participates in protection against chronic viral infections such as HCV and human T lymphotropic virus type 1 (HTLV-1) (Seich Al Basatena et al., 2011). It was also shown that the expression of *KIR2DL2* gene improves protection against HTLV-1 and HCV infections (Seich Al Basatena et al., 2011). However, several genetic studies reported by Witt and colleagues highlight that there is no association between non-expressed alleles of KIR2DL4 and several pathologic diseases including asthma (Le Page et al., 2013), pre-eclampsia (Witt et al., 2002), and spontaneous abortion (Witt et al., 2004).

Table 1.5 Association of KIRs and HLA Class I molecules with different diseases.

KIR and *HLA* combination	Disease	Outcome	Reference
2DL1/*C2*	HIV-1	Protective	(Jennes et al., 2013)
2DL1/*C2*	Oral squamous cell carcinoma	Increased risk of susceptibility	(Dutta et al., 2014)
2DL1/*C2*	Diabetes type-1	Protective	(van der Slik et al., 2003)
2DL1/*C2*	Diabetes mellitus type 1	Protective	(Jobim et al., 2010)
2DL2/*L3* and *C2*	HIV-1	More rapid development	(Gaudieri et al., 2005)
2DL2/*L3* and *C2*	Conjunctival scarring in trachoma	Increased risk of susceptibility	(Roberts et al., 2014)
2DL2/*L3* and *C2*/*C2*	Crohn's	Heterozygosity of *L2*/*L3* and homozygosity of *C2* provides protection	(Hollenbach et al., 2009)
2DL2/*L3* and *C1*	Crohn's	Increased risk of susceptibility	(Hollenbach et al., 2009)
2DL2 and *C1*	Leprosy	Increased risk of susceptibility	(Jarduli et al., 2014)
2DL2 and *C2*	Diabetes type-1	Increased risk of susceptibility but their absence is protective	(Shastry et al., 2008)
2DL2 and *C1*	Diabetes mellitus type-1	Increasing risk of susceptibility	(Shastry et al., 2008)
2DL2/*L3* and *C1*	Malignant melanoma	Increased risk of susceptibility	(Naumova et al., 2005)
2DL2/*L3* and *C1*	Myeloid leukaemia	Heterozygosity of *L2*/*L3* increases risk of susceptibility	(Verheyden and Demanet, 2006)
2DL3 and *C1*	Myeloid leukaemia	Homozygosity of *2DL3* confers protection	(Wechsler et al., 2003)
2DL3 and *C1*	Melanoma	Protective	(Campillo et al., 2013)
2DL3 and *C1*	Malaria	Increased risk of susceptibility	(Hirayasu et al., 2012)
2DL3 and *C1*	Dengue	Protective	
2DL3 and *C1*	celiac disease and type 1 diabetes (co-occurrence)	Increased risk of susceptibility	(Smigoc Schweiger et al., 2014)
2DL3 and *C1*	Ulcerative colitis	Protective	(Boyton et al., 2006)
2DS1 and *C1*	Idiopathic bronchiectasis	Increased risk of susceptibility	(Boyton et al., 2006)
2DS1 and *C2*	Lupus	Increased risk of susceptibility	(Hou et al., 2015)
2DS1 and *C2*	Ankylosing spondylitis	Increased risk of susceptibility	(Jiao et al., 2008)
2DS1 and *C2*	Autism	Increased risk of susceptibility	(Torres et al., 2012)
2DS1 and C2	Multiple sclerosis	Protective	(Fusco et al., 2010)
2DS2 and *C1*	Dry eye disease	Increased risk of susceptibility	(Ren et al., 2012)
2DS2 and *C1*	Idiopathic bronchiectasis	Increased risk of susceptibility	(Boyton et al., 2006)
2DS2 and *C1*	Diabetes mellitus type 1	Increased risk of susceptibility	(van der Slik et al., 2003)

Table 1.5 Association of KIRs and HLA Class I molecules with different diseases. (Continued)

KIR and *HLA* combination	Disease	Outcome	Reference
3DL1 and *B57* (*Bw4*)	HIV-1	Delay in development	(Martin et al., 2007)
3DL1 and *Bw4*	Chronic lymphoid leukaemia	Homozygosity of 3DL1 in the absence of *Bw4* confers protection	(Verheyden and Demanet, 2006)
3DL1 and *Bw4*	Chronic lymphoid leukaemia	Homozygosity of 3DL1 in the presence of *Bw4* elevates risk of susceptibility	(Verheyden and Demanet, 2006)
3DL2 and *A3*	Pemphigus foliaceus	Increased risk of susceptibility	(Augusto et al., 2015)
3DL2 and *A11*	Pemphigus foliaceus	Increased risk of susceptibility	(Augusto et al., 2015)
3DS1 and *Bw4*	HCV	Resolution of infection	(Khakoo et al., 2004)
3DS1 and *Bw4*	hepatocellular carcinoma	Protective	(Lopez-Vazquez et al., 2005)
3DS1 and *C2*/*Bw4*	Cervical cancer	In the absence of *C2* or *Bw4*, presence of *3DS1* increases risk of susceptibility	(Carrington et al., 2005)
3DS1 and *Bw4*	Pemphigus foliaceus	Protective	(Augusto et al., 2012)
3DS1 and *Bw4*	Endometriosis	Protective	(Kitawaki et al., 2007)
3DS1 and *Bw4*	HIV-1	Delay in development	(Martin et al., 2002a)
3DS1 and *Bw4*	Autism	Increased risk of susceptibility	(Torres et al., 2012)
3DS1 and *Bw4*	Tuberculosis	Protective	(Shahsavar et al., 2012)
3DS1 and *Bw4*	Diabetes mellitus type 1	Increased risk of susceptibility	(Jobim et al., 2010)

1.5.5.1 KIRs and auto-immunity

To date, several associations between KIR genes and auto-immune diseases have been reported. For example, Luszczek and colleague studied the association of *KIR2DL1* and *KIR2DS1* genes with their cognate ligand, *HLA-C*06* in 116 patients suffering from psoriasis vulgaris infection along with 123 healthy individuals and found that the association of *KIR2DS1* with *HLA-C*06* increases susceptibility (Luszczek et al., 2004). A similar result was observed in a Japanese study (Suzuki et al., 2004). By contrast, *KIR2DS2*$^{+}$ *HLA-C1*$^{+}$ individuals that lack inhibitory *HLA-C2* reactive KIRs had a higher risk of the development of type 1 diabetes (van der Slik et al., 2003). Research on 194 patients suffering from ulcerative colitis disease, an inflammatory disorder of the colonic mucosa, showed that the outcome of a combination of *KIR2DL3* and *HLA-C1* epitope was protective whereas the association of *KIR2DL2* and *KIR2DS2* dramatically elevated the progress of the disease (Boyton et al., 2006). Taken together, association of KIRs and HLAs plays a crucial role in auto-immunity.

1.6 Statement of purpose

1.6.1 Proposed Ph.D. project plan

Although genetic studies indicate that HLA class I molecules are the ligands of KIRs, recent findings have revealed that certain types of KIRs despite sharing high similarity with each other and having the same HLA class I molecule ligands, are obviously associated with different disease outcome. Latest discoveries also point at specific types of KIRs that can recognize and interact with a broader range of HLA class I molecules, despite being very similar to each other in their extracellular domains. However, there is still a lack of data to compare the molecular basis of their differences from the structural point of view. While there are only two crystal structures of KIR in complex with HLA-Cs (Boyington et al., 2000, Fan et al., 2001) — KIR2DL1 with HLAC*04:01 (C2 epitope) and KIR2DL2 with HLA-C*03:04 (C1 epitope) — there remains a lack of data to address the specificity of many KIRs to HLA-C1 and C2 epitopes. Further to this, while other KIR2Ds have D1 and D2 domain arrangements, there is still a lack of structural data for KIR2DL4/L5, which share a D0

and D2 domain organization. Further, the ligands for these KIRs are yet to be conclusively identified. For this reason, my Ph.D. thesis has focused on understanding the molecular basis of the interactions between inhibitory KIRs, typically KIRs with two extracellular Ig domains and their respective HLA class I molecule ligands in order to reveal the structural differences of their ligand recognition.

1.6.2 Specific aims

My Ph.D. project aims to elucidate the structural differences of the HLA class I ligand recognition by KIR2DL. The ligand specificity of certain types of KIRs leads to the change in the outcome of transplantation. The combination of KIRs/HLA class I molecules are also associated with different disease outcome. Elucidating the molecular basis of KIRs and HLA class I molecules will further help for designing new strategies towards curing certain types of disease.

Aim 1: Structural and functional characterisation of KIR2DL1, -L2 and -L3.
- I hypothesized that due to differences in specificity of HLA-C epitopes recognition by KIR2DL1, -L2, and -L3, they differ in the structural pattern of binding upon interaction with the same ligand.

Aim 2: Structural and functional characterisation of KIR2DL4.
- I hypothesized that due to different Ig domain organization, and absence of conventional binding of KIR2DL4 to a panel of HLA class I molecules like other KIRs, KIR2DL4 may have a unique structural feature among members of KIR family.

2 Chapter 2

Chapter 2 covers the first aim of my thesis which is the structural and functional characterisation of KIR2DL1, -L2, and -L3. Although the extracellular domain of KIR2DL1, -L2 and -L3 share high sequence similarity with each other, they show different avidity of binding to a panel of HLA-C1 and -C2 molecules, which consequently leads to diverse function and responses against pathogen infection. I used different techniques including X-ray protein crystallography, surface plasmon resonance (SPR), LUMINEX, and cell assays in order to explore the molecular basis of the interaction between KIR2DL2/-L3 and their cognate ligand HLA-C*07:02. I characterized the crystal structures of KIR2DL2 and KIR2DL3 in complex with HLA-C*07:02 to 3.1 Å and 2.5 Å bound to RYRPGTVAL (RL9) peptide, respectively. The structures revealed that KIR2DL2 and KIR2DL3 differed in the relative juxtaposition of their domains resulting in KIR2DL2 binding more extensively to the α1 helix of HLA-C. This data elucidated the structural basis underlying the functional differences between KIR2DL alleles and between alleles of their HLA-C ligands.

This chapter is prepared and completed as a paper draft with collaboration from Prof. Andrew Brooks laboratory at Melbourne University, Australia in order to be submitted to a top tier journal. The contribution of individuals who have contributed to this work is summarized, and nature of their contribution is stated.

Nature and contribution of individuals in chapter 2

Name	Nature of Contribution	% of contribution and student from Monash University?
Shoeib Moradi	Structural analysis Writing Introduction and Discussion Writing methods	(70%), Yes. (100%) (40%)
Dr. Julian Vivian	Structural analysis Writing methods	(30%), No. (60%)
Dr. Geraldine O'Connor	FACS analysis and detecting the binding of tetramers of KIR2DL1 and KIR2DL2 to HLA-C*03:04 and HLA-C*07:02, expression of HLA-C03:04 Data is shown in Figure 2.13 and 2.14	(100%), No. Prof. Brooks laboratory, Melbourne University
Dr. Phillip Pymm	Performing the LUMINEX assay. Analysis of the experiment Data is shown in Figure 2.17 and 2.18 and Supplementary pictures, S6.6, S6.7, and S6.8	(100%), No. (100%) ***KIR2DL2 is prepared by Shoeib Moradi
Dr. Lucy Sullivan	SPR experiment to measure binding of KIR2DL2 and -L3 to HLA-C*03:04	(100%), No. Prof. Brooks laboratory, Melbourne University
Dr. Geraldine O'Connor	Comparison of KIR2DL2 binding to tetramers Data is shown in Figure 2.16	(100%), No. Prof. Brooks laboratory, Melbourne University
Shoeib Moradi	Solving the crystal structures of KIR2DL2 and --L3 in complex with HLA-C*03:04 and HLA-C*07:02 bound to the RL9	100%, Yes
Shoeib Moradi	SPR experiment to measure binding of KIR2DL2 and -L3 to HLA-C*07:02	100%, Yes
Shoeib Moradi	FACS analysis and detecting the binding of tetramers of KIR2DL3 to HLA-C*03:04 and HLA-C*07:02	100%, Yes

The undersigned hereby certify that the above declaration correctly reflects the nature and extent of the student's and co-authors' contributions to this work. In instances where I am not the responsible author, I have consulted with the responsible author to agree on the respective contributions of the authors.

Signatures and Date: 08 August 2017

Prof. Jamie Rossjohn
Head of laboratory, Monash University

[redacted]

Shoeib Moradi

[redacted]

2.1 Introduction

Natural Killer (NK) cell are the main machinery within the innate immune system, and their cytolytic activity is highly controlled by numbers of receptors, which are expressed on their cell surface. NK cells apply these receptors for detection of their respective ligands on the surface of target cells to distinguish between healthy cells (self) and infected (non-self) cells. Detection of target cells by NK cells is crucial for elimination of pathogens such as viruses (Mishra et al., 2014, Ogbomo et al., 2013).

Killer cell immunoglobulin-like receptors (KIRs) are located on the surface of NK cells and govern the activation and inhibition of NK cells by inhibiting via their interaction with human leukocyte antigen (HLA) class I molecules, which are located on the surface of target cells (Cerwenka and Lanier, 2001, Diefenbach and Raulet, 2001, Kumar and McNerney, 2005). HLA class I molecules include HLA-A, -B and -C molecules, among which 100% of HLA-C molecules can be recognized by KIRs. KIRs can also interact with 45% of HLA-A and 36% of HLA-B molecules (Parham et al., 2012). Recognition of HLA-A*11 and -A*03 molecules by KIR3DL2 and (Hansasuta et al., 2004) and binding of HLA class I molecules bearing Bw4 motif to KIR3DL1 have been reported (Gumperz et al., 1995, Litwin et al., 1994, Vivian et al., 2011, Saunders et al., 2015a, Vivian et al.). KIR2DL1, -L2, and -L3 can recognize and interact with HLA-C molecules including HLA-C1 and -C2 epitopes (Winter et al., 1998, Winter and Long, 1997). It has been shown that species specificity exists among KIR2DL1, -L2, and -L3. HLA-C1 molecules are sensed by KIR2DL2 and -L3, and HLA-C2 molecules can be recognized by KIR2DL1 (Mandelboim et al., 1996), although KIR2DL2 shows cross reactivity and interacts with HLA-C2 molecules (Wilson et al., 2000). Although KIR2DL2 and KIR2DL3 recognize HLA-C1 molecules, the affinity of binding to HLA-C1 molecules is much higher for KIR2DL2 compared to that of KIR2DL3 (Moesta et al., 2008, Frazier et al., 2013, Cassidy et al., 2015).

During evolution, alleles of KIR2DL2 and -L3 segregated from each other, which has led to the formation of different KIR haplotypes. Association of KIR haplotypes with HLA class I molecules results in different disease outcomes. Figure 1.11 shows the distribution of KIR2DL2 and -L3 among KIR haplotypes. That is, KIR2DL2 is found only on haplotypes group B, whereas KIR2DL3 is located on haplotype group A (with one exception which is found in haplotype group B) (Parham, 2005, Uhrberg et al., 2002, Wilson et al., 2000, Levinson, 2011, Uhrberg et al., 1997). Despite sharing high similarity with each other, KIR2DL2 and -L3 are associated with different disease outcomes. For example, in HCV infection, KIR2DL3 in combination with HLA-C1 molecules is protective, but KIR2DL2 is not (Khakoo et al., 2004, Romero et al., 2008). Despite enormous genetic studies to address the differences between KIR2DL2 and -L3, there is still a lack of structural data to elucidate the structural molecular basis of the differences between KIR2DL2 and -L3 in combination with HLA class I molecules.

In order to elucidate the molecular basis of the interaction between KIR2DL2 and KIR2DL3 in complex with HLA class I molecules and investigate their differences, I characterized their crystal structures bound to HLA-C*07:02 in the presence of RL9 peptide. I found that KIR2DL2 and -L3 display different docking mode upon interaction with HLA class I molecules. Further, it was revealed that HLA-C*07:02 is a greater HLA-C ligand for KIR2DL2 and -L3, indicating that it differs from HLA-C*03:04 with respect to their structure and function. My findings are consistent with the fact that KIR2DL2 has a broader range of binding to HLA-C1 and -C2 molecules, as it was revealed that it generates more contacts on the α1 helix of HLA-C*07:02.

2.2 Material and methods

2.2.1 Cloning and expression of KIR2DL1, KIR2DL2, and KIR2DL3

The extracellular D1-D2 domains (residues 1-204) of KIR2DL1*001, KIR2DL2*001, and KIR2DL3*001 were cloned into the expression vector pET-30(b) for expression in *E. coli* BL21 (DE3) (Figure 2.1). The receptors were expressed as inclusion bodies and refolded and purified as described previously (Boyington et al., 2000, Maenaka et al., 1999). Briefly, 100 mg of the KIR2DL1, -L2, and -L3 were refolded by rapid dilution in a buffer containing 100 mM Tris-HCl pH.8.0, 400 mM L-arginine-HCl, 5 mM reduced glutathione, and 0.5 mM oxidized glutathione for 72 h. The refolded receptors were then applied onto a diethylaminoethyl (DEAE) cellulose column followed by size exclusion chromatography using Superdex 200 16/60 column (GE Healthcare). The KIRs were further purified by anion–exchange chromatography using Hi-Trap Q HP 5 ml column (GE Healthcare) (Figures 2.2, 2.3 and 2.4).

2.2.2 Cloning and expression of HLA-C*03:04, -C*06:02, and -C*07:02

The extracellular α1, α2, and α3 domains of HLA-C*03:04 and -C*07:02 (residues 1 – 276) and human β_2-microglobulin (β_2M) (residues 1 – 99) were cloned into the vector pET-30(b) for expression in *E. coli* BL21 (DE3) (Figure 2.1). HLA-C*03:04, -C*06:02, -C*07:02 and β2M were expressed separately into inclusion bodies and refolded in the presence of the GAVDPLLAL (GL9) peptide, which is a self-peptide isolated from Importin α-2 subunit (Zappacosta et al., 1997), the TRATKMQVI (TI9) which is a non self-peptide originated from Human beta herpesvirus 5 (Human cytomegalovirus) (Nastke et al., 2005) and the RYRPGTVAL (RL9) peptide which is a self-peptide isolated from human histone H3 (Falk et al., 1993), respectively. The presence of peptide is crucial for the refolding of HLA class I molecules since it provides their stability by binding to their peptide binding pocket during refolding process. The refolding process is described previously (Boyington et al., 2000, Moradi et al., 2015), (Figures 2.5 and 2.6). The expression and refolding of HLA-C*03:04 was done at Prof. Brooks laboratory.

2.2.3 Surface plasmon resonance

SPR experiments were performed on a BIAcore 3000 (GE Healthcare). Three independent experiments were performed at 25 °C in a buffer containing 10 mM Tris-HCl pH.8.0, 150 mM NaCl and 0.005% surfactant P20 (TBS-P20). The HLA-Class I specific monoclonal antibody W6/32 was coupled to the surface of CM5 Sensorchip flow cells (GE Healthcare) by amine coupling. HLA-C*07:02 was captured by W6/32 to a density of ~600 resonance units. KIR2DL2 and KIR2DL3 were serially diluted in TBS-P20 (0.5–400 mM) and passed over the test and control flow cells surfaces at a flow rate of 10 µl/min, with measurements taken in duplicate. The obtained data were analysed using BIAevaluation software (GE Healthcare) shown in (Figures 2.7 and 2.15).

2.2.4 Crystallization, data collection, structure determination, and refinement

KIR2DL2 and KIR2DL3 were each concentrated to 10 mg/ml and added separately to HLA-C*07:02-RL9 at a 1:1 molar ratio. Crystals were obtained at 20 °C using the hanging-drop vapour-diffusion method. Crystals of the KIR2DL2-HLA-C*07:02-RL9 complex were obtained from a solution consisting 0.2 M Sodium tartrate dibasic dehydrate and 20% w/v PEG 3350 (Figure 2.8). Crystals of the KIR2DL3-HLA-C*07:02-RL9 complex were obtained from a solution containing 0.2 M Ammonium acetate, 0.1 M Tris-HCl pH.8.0, and 25% PEG 3350. Prior to flash-cooling in liquid nitrogen at 100 K, all crystals were equilibrated in a cryo-protectant solution containing their respective crystallisation solution and 35 % PEG 3350 (Figure 2.8). Data sets for the KIR2DL2 and KIR2DL3-HLA-C*07:02-RL9 complexes were collected to a resolution of 3.1 Å and 2.5 Å, respectively at the MX1 beamline (Australian Synchrotron, Victoria). The data were recorded on a Quantum-315 CCD detector and integrated and scaled using the HKL/HKL-2000 program package (Otwinowski and Minor, 1997) (data collection statistics are summarised in Table 2.2). Structural determination proceeded by molecular replacement using PHASER (McCoy et al., 2007) with the previously determined KIR2DL2-HLA-C*03:04 structure utilised as the search model (PDB accession code: 1EFX (Boyington et al., 2000)). Both the KIR2DL2 and 2DL3 crystals comprised two copies of their respective

complexes in the asymmetric unit. Refinement of the complexes progressed with iterative rounds of manual building in COOT (Emsley and Cowtan, 2004) and refinement in PHENIX (Adams et al., 2010) with two-fold non-crystallographic symmetry restraints applied throughout. The final model of the KIR2DL2-HLA-C*07:02-RL9 complex comprises residues 4 to 190. The final model of the KIR2DL3-HLA-C*07:02-RL9 complex comprises residues 6 to 195. The structures were validated with MOLPROBITY (Chen et al., 2010) (refinement statistics are summarised in Table 2.2).

2.2.5 KIR2DL2 and -L3 mutagenesis and transfection

Full-length constructs of KIR2DL2 and KIR2DL3 were cloned into the pEF6 vector with FLAG tag fused to the N-terminus of the constructs. The QuikChange II site-directed mutagenesis kit (Stratagene) was used to generate mutants of KIR2DL2 and -L3, in order to study the contribution of particular amino acids located on their D1-D2 domains in binding to HLA-C*07:02 (Table 2.1). FuGENE 6 transfection reagent (Roche) was used for transfection of the mutant constructs of KIR2DL2 and -L3 into HEK293T cells based on the manufacturer's instructions. Expression and binding of KIR2DL2 and -L3 mutants to HLA-C*07:02 were monitored using flow cytometry after staining with DX9, Z27, and anti-FLAG mAbs. Fluorochrome-conjugated tetramer of HLA-C*07:02 was generated as described previously (O'Connor et al., 2014). HEK293T cell transfectants expressing mutants of KIR2DL2 and -L3 were stained with the optimum amount of HLA-C*07:02 tetramer (0.2 mg with respect to the monomeric component in minimal residual volume) or anti-FLAG (clone M2; Sigma-Aldrich) mAb for 30 min at 4 ˚C. Wild type KIR2DL2 and KIR2DL3 transfectant cell lines were used as a positive control for binding to HLA-C*07:02 tetramer. After two steps of washing cells, their binding was monitored using an LSRFortessa flow cytometer (BD Biosciences). For the control, a secondary PE anti IgG antibody was used to provide fluorescent background for the tetramer. For the tetramer staining, the negative controls are testing the tetramer against a cell line with an irrelevant HLA or lacking HLA expression (e.g. untransfected 221 cells). For a positive control, KIR3DL1 with HLA B*57 transfected cells were used. Tetramers were prepared using

Neutravidin PE conjugate (Thermo Fisher Scientific). Tetramer conjugation was calculated by biotinylation efficiency (estimated by streptavidin pull-down, Appendix). For the heat-map of LUMINEX, the colour is a conditional formatting scheme with red at 100%, blue at 0% and white/grey at 50%, the colouring between those three set points is done according to the value in the cell (e.g. 75% will be halfway between red and white/grey, 25% will be halfway between white/grey and blue). LUMINEX assay was done at Australian Red Cross Blood Service, Melbourne, Australia by Dr. Phillip Pymm.

Table 2.1. KIR2DL2 and -L3 mutants which were used for flow cytometry and LUMINEX

Mutant	Position on KIR
E21A	D1 domain
K44A	D1 domain
F45A	D1 domain
M70A	D1 domain
Q71A	D1 domain
D72A	D1 domain
L104A	Hinge region (interdomain) between D1 and D2 domains
Y105A	Hinge region (interdomain) between D1 and D2 domains
E106A	Hinge region (interdomain) between D1 and D2 domains
S132A	D2 domain
S133A	D2 domain
D135A	D2 domain
F181A	D2 domain
D183A	D2 domain

2.3 Results

2.3.1 Cloning, protein expression, refolding, and purification

KIR2DL1, -L2 and -L3, HLA-C*03:04, -C*06:02, and -C*07:02 were cloned, sequenced, expressed and purified as described in material and methods section. After purifying each particular protein, its functionality was tested via SPR. Binding of HLA-C*03:04, -C*06:02, and -C*07:02 to HLA specific antibody, W6/32 were tested on the surface of the CM5 chip to ensure their proper folding. The affinity of KIR2DL1, -L2, and -L3 binding to HLA-C1 and C2 via SPR were consistent with their level of binding reported in the literature. That is, a higher level of binding for KIR2DL1 against C2 and low level of binding towards C1 epitopes was observed whereas KIR2DL2 and -L3 display higher level of binding against C1 epitope and lower level of binding to C2 epitopes.

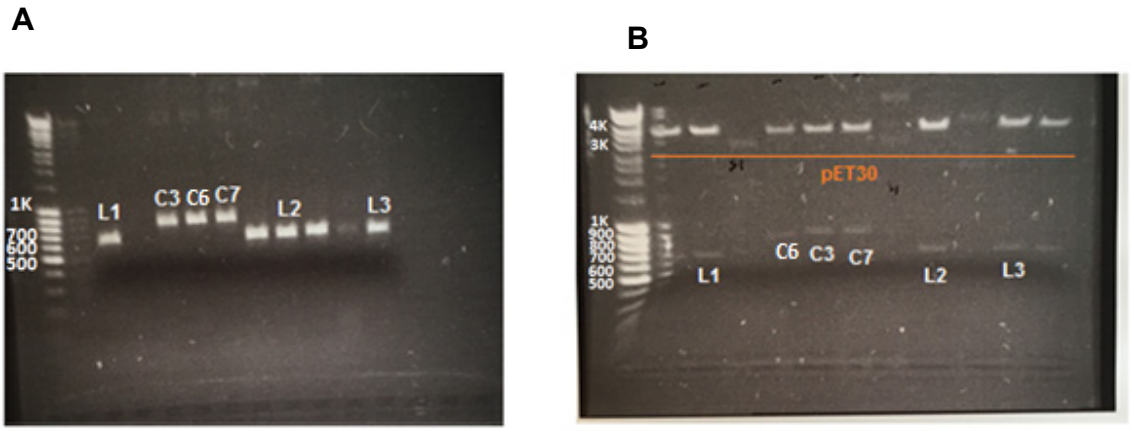

Figure 2.1 Cloning and ligation of KIR2DL1, -L2, -L3 and HLA-C*03:04, -C*06:02, and -C*07:02. A. Amplification of KIR2DL1, -L2, -L3, HLA-C*03:04, -C*06:02 and -C*07:02 via PCR. **B.** Confirmation of ligation by digestion with restriction enzymes NdeI and HindIII. The upper bands represent pET30b, and the lower bands represent the validation of insert products. Done by Shoeib Moradi at Prof. Rossjohn Laboratory, Monash University.

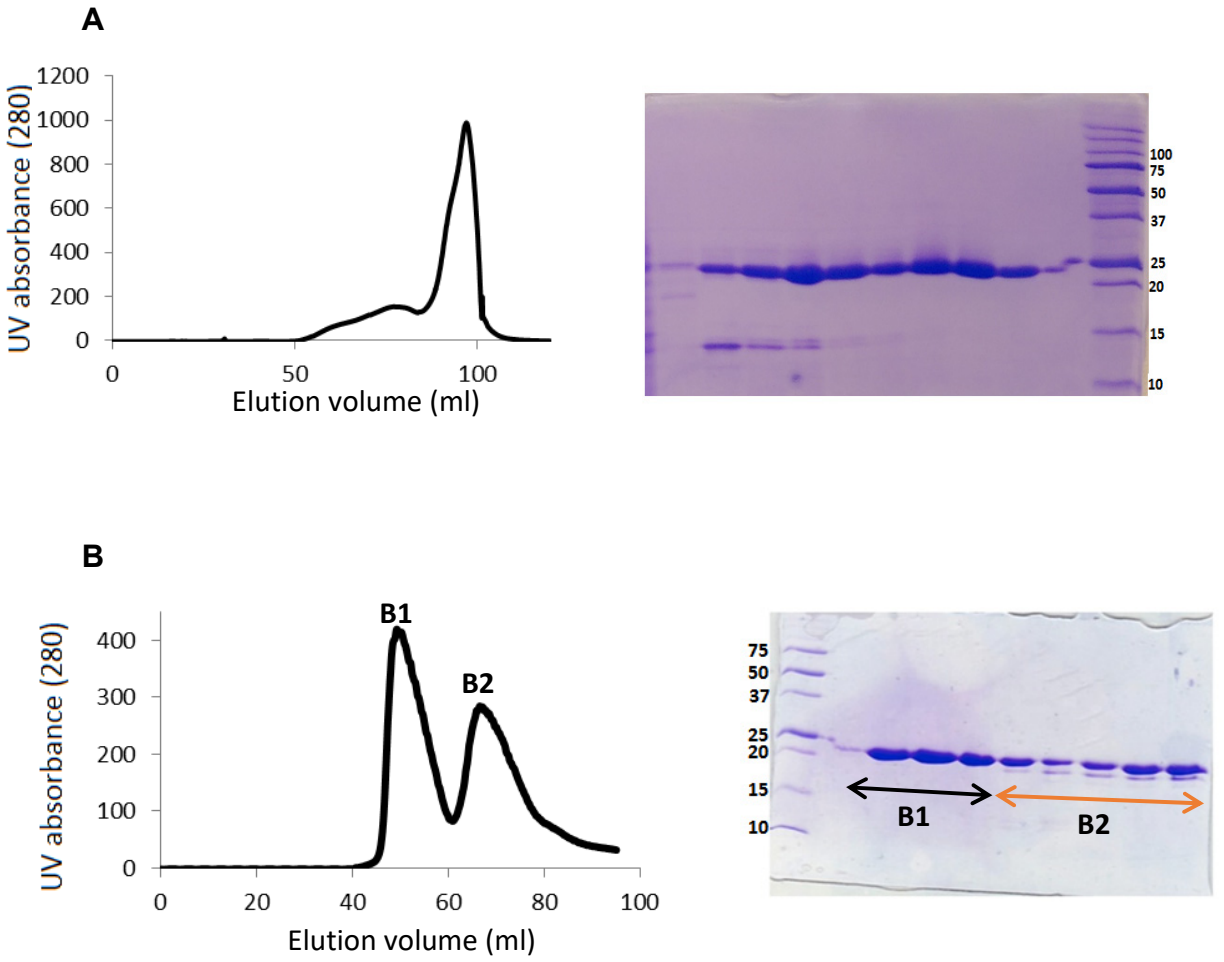

Figure 2.2 Purification of KIR2DL1.
Gel filtration and elution profile of KIR2DL1 from Superdex 200 (16/60) column and the SDS-PAGE representing the eluted fractions consistent with the predicted molecular weight of KIR2DL1. Numbers next to the SDS-PAGE indicate the molecular weight (kDa) of each band. **B.** Anion exchange via Hi-Trap column and the SDS-PAGE indicating the purity of eluted fractions. Only pure fractions (named as **B1** on the Peak and below the black arrow on the SDS-PAGE) were selected for experiments. Done by Shoeib Moradi at Prof. Rossjohn Laboratory, Monash University.

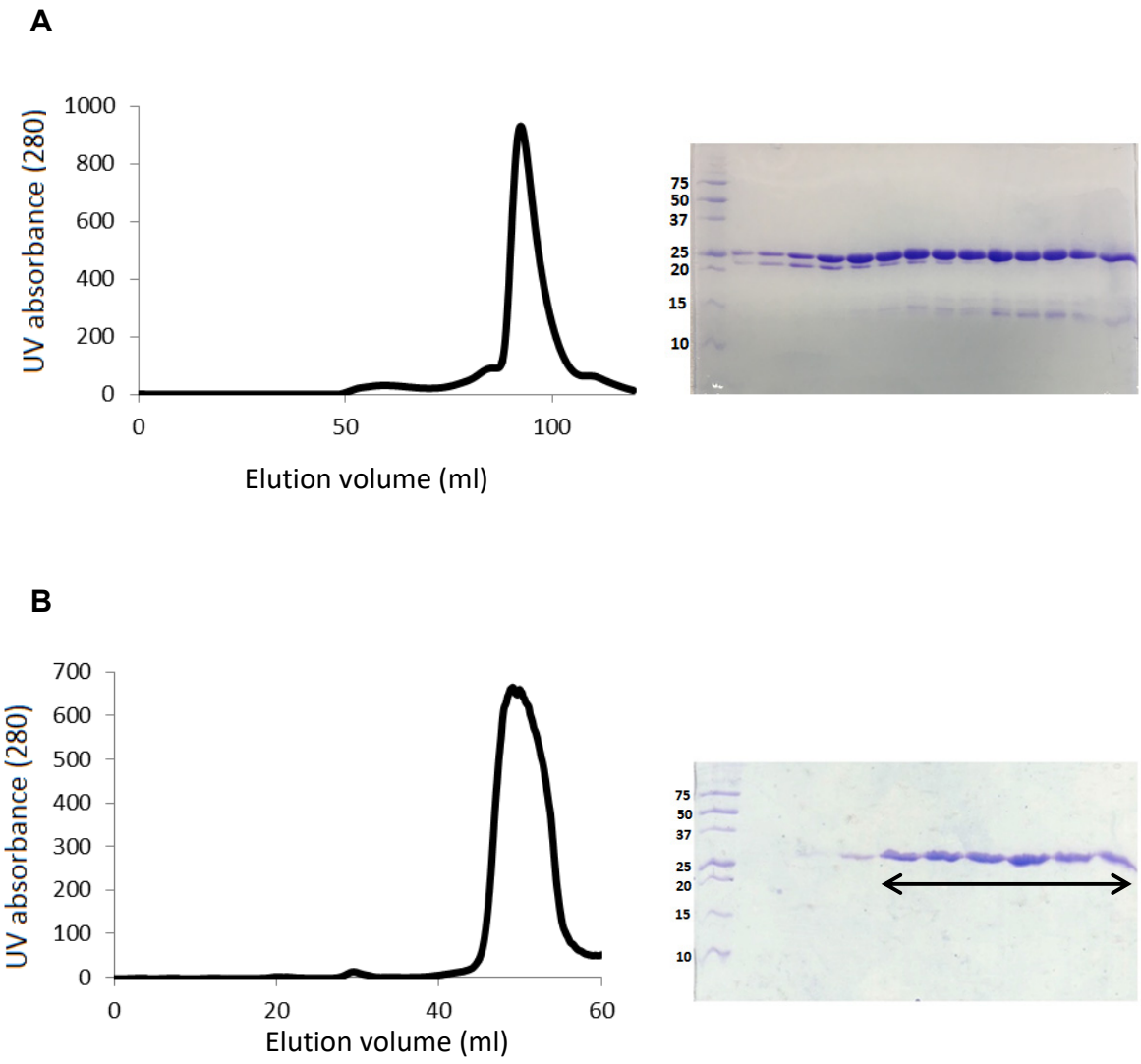

Figure 2.3 Purification of KIR2DL2.
Gel filtration and elution profile of KIR2DL2 from Superdex 200 (16/60) column and the SDS-PAGE representing the eluted fractions consistent with the predicted molecular weight of KIR2DL2. Numbers next to the SDS-PAGE indicate the molecular weight (kDa) of each band. **B.** Anion exchange via Hi-Trap column and the SDS-PAGE indicating the purity of eluted fractions. Only pure fractions highlighted by black arrow on SDS-PAGE were selected for experiments. Done by Shoeib Moradi at Prof. Rossjohn Laboratory, Monash University.

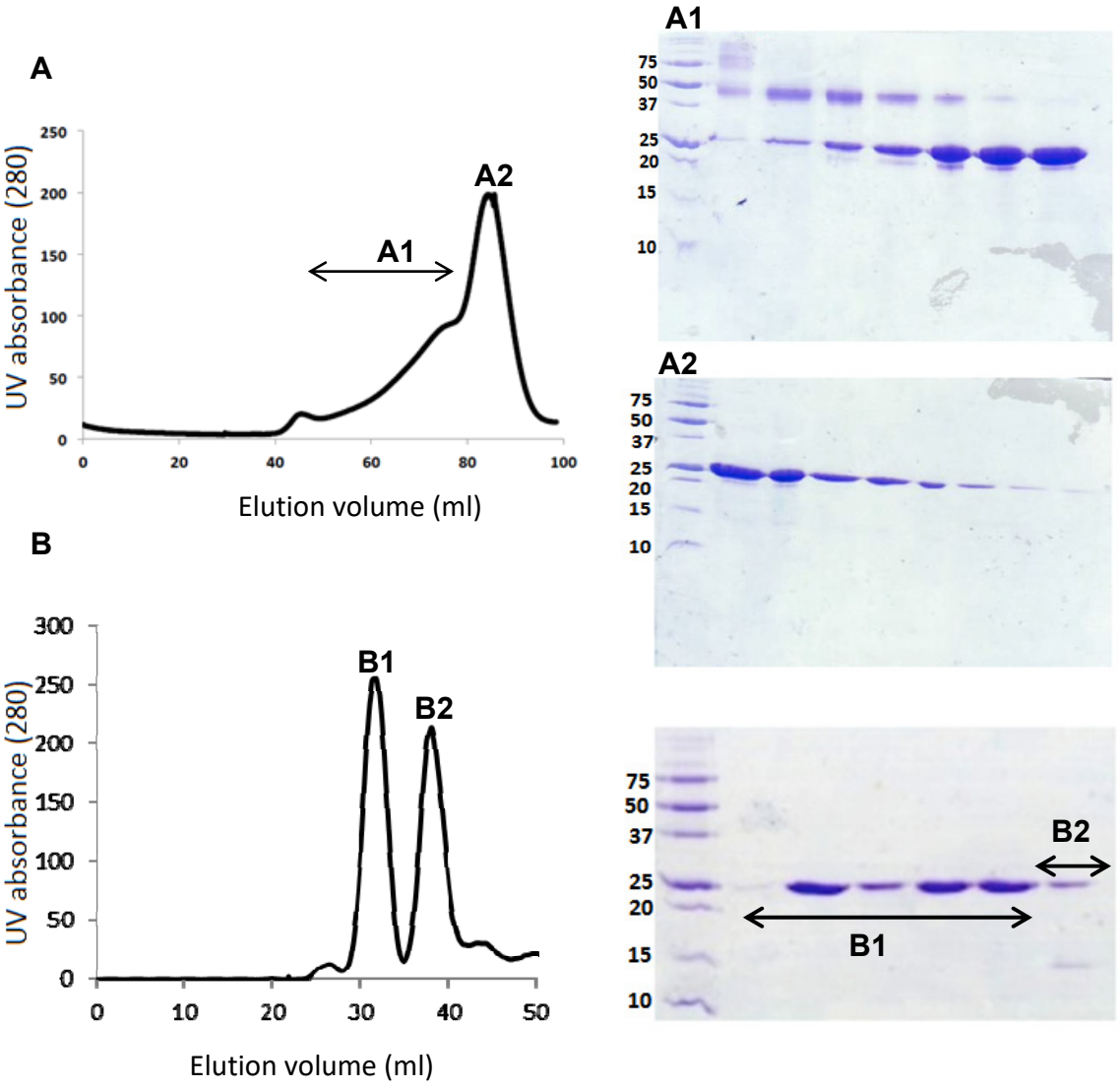

Figure 2.4 Purification of KIR2DL3.
Gel filtration and elution profile of KIR2DL3 from Superdex 200 (16/60) column and the SDS-PAGE representing the eluted fractions (**A1** and **A2**) consistent with the predicted molecular weight of KIR2DL3. **B.** Anion exchange via Hi-Trap column and the SDS-PAGE indicating the purity of eluted fractions. Only pure fractions (named as **B1** on the Peak and below the black arrow on the SDS-PAGE) were selected for experiments as **B2** fractions contain impurities and were discarded. Done by Shoeib Moradi at Prof. Rossjohn Laboratory, Monash University.

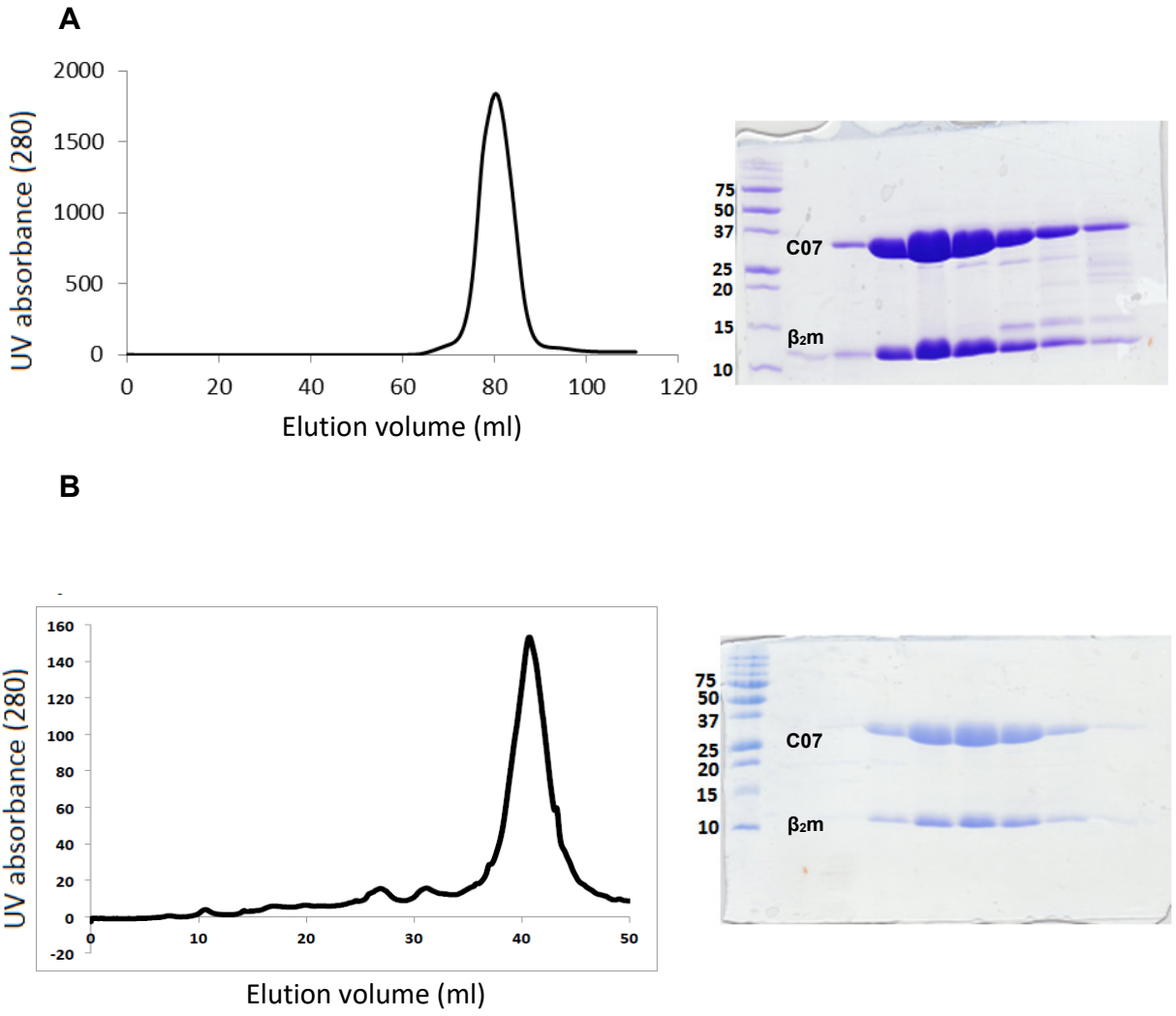

Figure 2.5 Purification of HLA-C*07:02.
Gel filtration and elution profile of HLA-C*07:02 bound to the RL9 peptide from Superdex 200 (16/60) column and the SDS-PAGE representing the eluted fractions consistent with the predicted molecular weight of HLA-C*07:02. **B.** Anion exchange via Hi-Trap column and the SDS-PAGE indicating the purity of eluted fractions. The SDS-PAGE represents the purity of the eluted fractions that I used for my experiments. Done by Shoeib Moradi at Prof. Rossjohn Laboratory, Monash University.

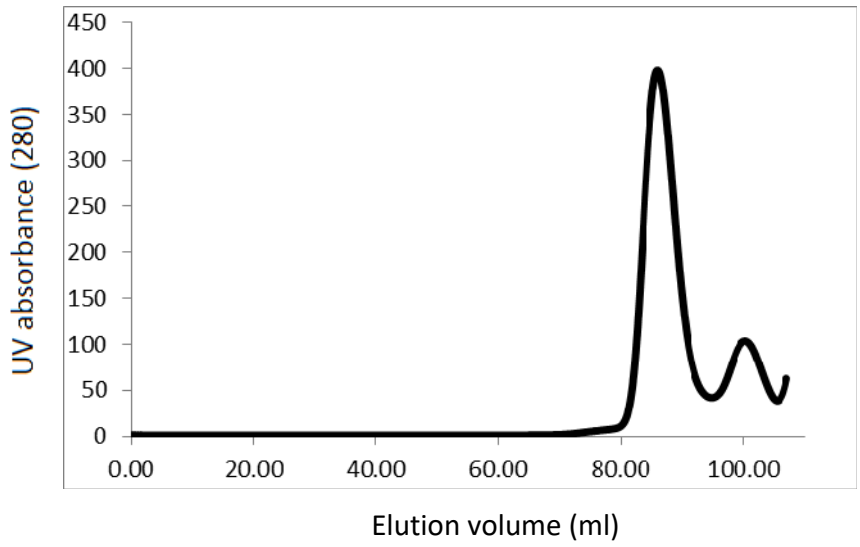

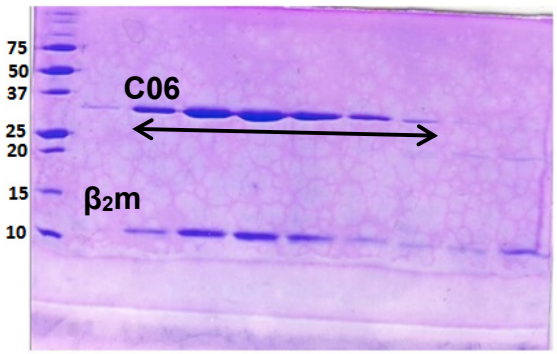

Figure 2.6 Purification of HLA-C*06:02.
Gel filtration and elution profile of HLA-C*06:02 bound to TRATKMQVI peptide from Superdex 200 (16/60) column and the SDS-PAGE representing the eluted fractions consistent with the predicted molecular weight of HLA-C*06:02. Pure fractions which are highlighted by black arrow were used for experiments. Done by Shoeib Moradi at Prof. Rossjohn Laboratory, Monash University.

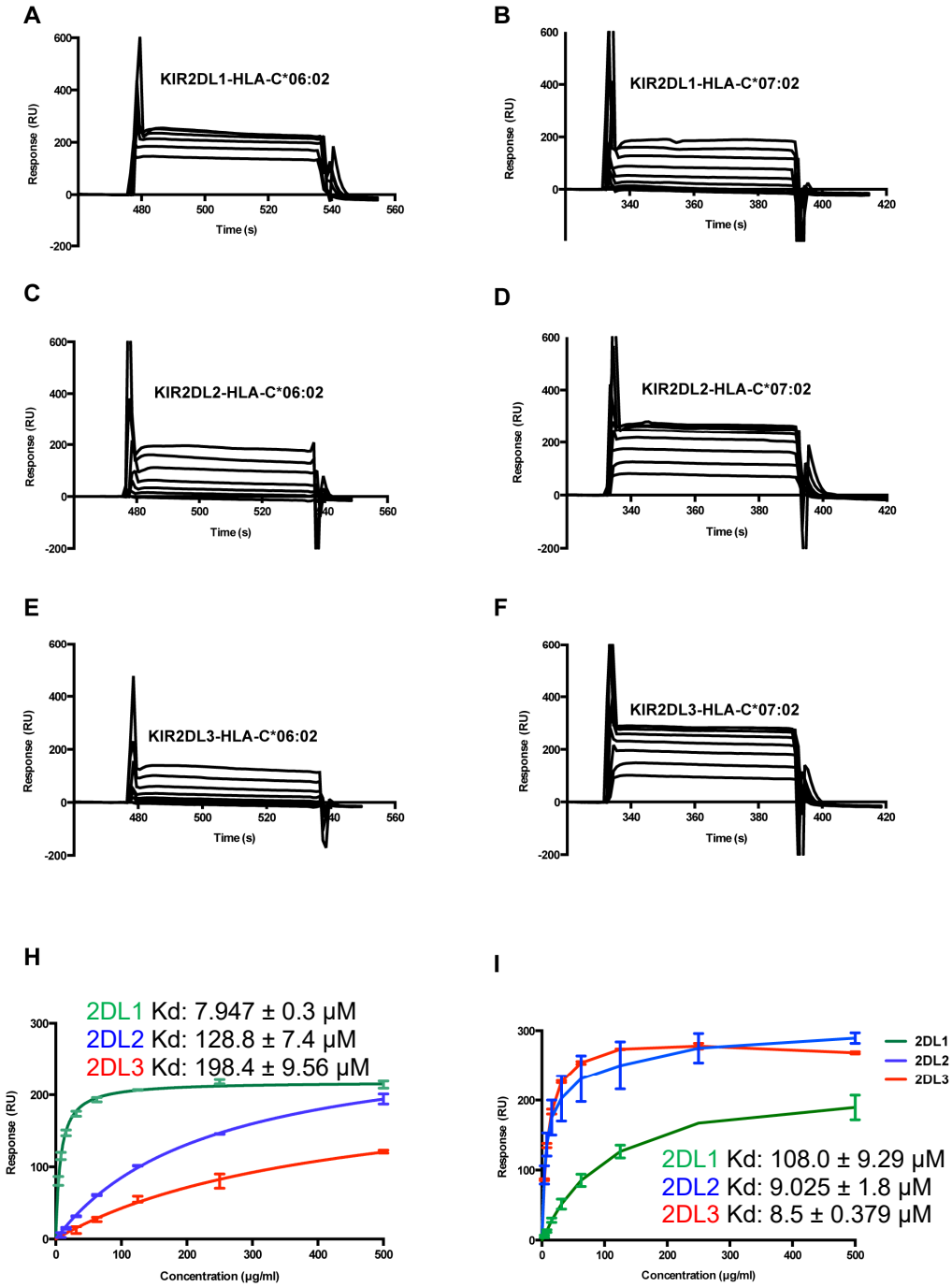

Figure 2.7 Direct binding of KIR2DL1, -L2, and -L3 to HLA-C*07:02 and -C*06:02 molecules. SPR assay is done to check the functionality of purified KIR2DL1, -L2 and -L3 and test their binding against HLA-C1 and -C2 molecules. Purified KIR2DL1 shows significantly higher affinity of binding towards HLA-C*06:02 (C2 epitope) compared to HLA-C*07:02, whereas KIR2DL2 and KIR2DL3 display high affinity of binding against HLA-C*07:02 compared to that of -C*06:02. HLA-C*06:02 and -C*07:02 are captured by HLA class I specific antibody, W6/32 on the surface of the chip to ensure their proper folding. KIR2DL4 was used as a negative control, and binding of KIR3DL1 to HLA-B*57 was monitored as a positive control. Done by Shoeib Moradi at Prof. Rossjohn Laboratory, Monash University.

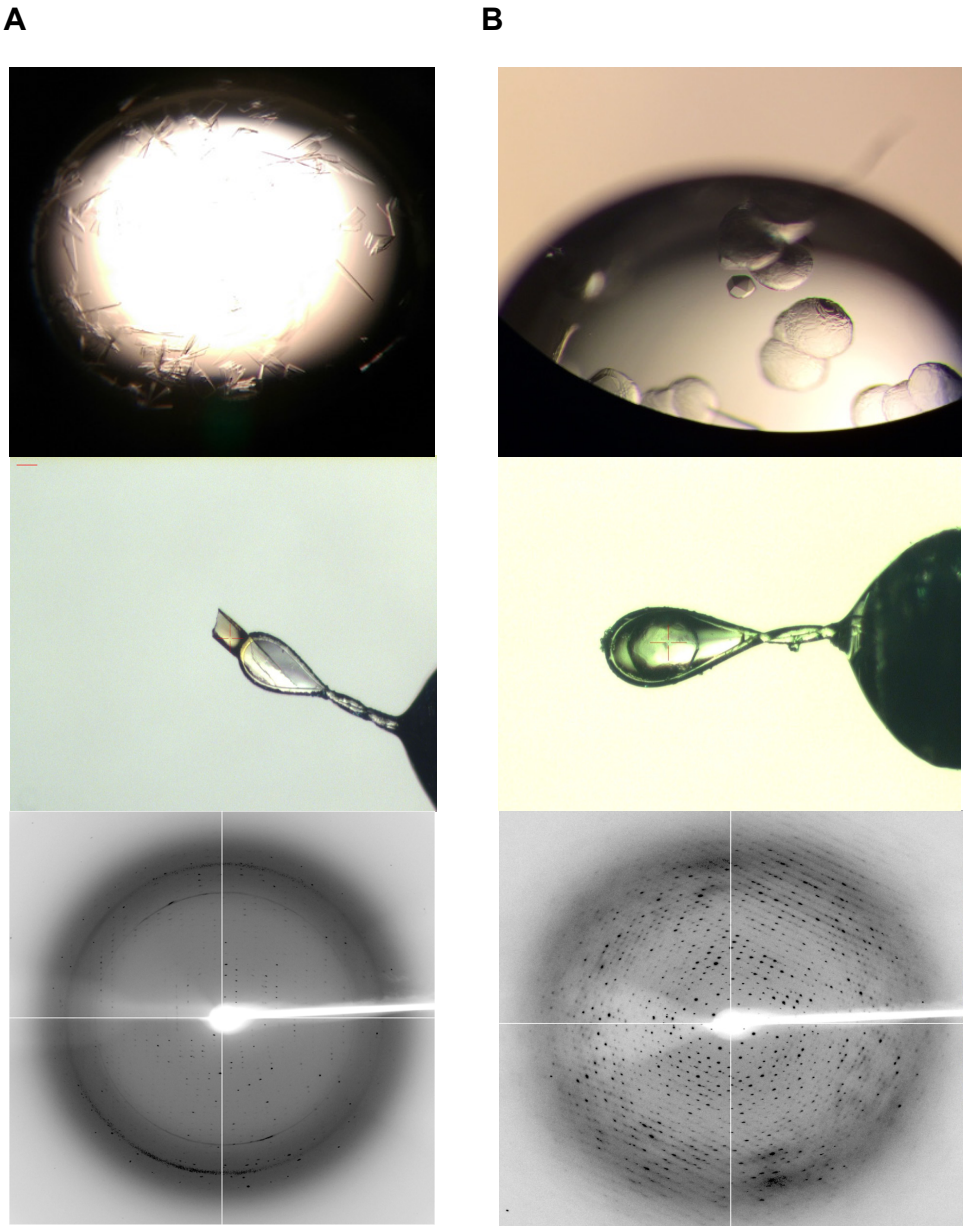

Figure 2.8. Protein crystals and diffraction patterns.
A. Obtained crystals for KIR2DL3/HLA-C*07:02 and its related diffraction pattern.
B. Obtained crystals for KIR2DL2/HLA-C*07:02 and its related diffraction pattern.
(A and B **Top**) Represent the obtained crystals of KIR2DL2 and –L3 in complex with HLA-C*07:02 from in house manual hand tray screens. (A and B **middle**) Represent the obtained crystals used for X-ray data collection. (A and B **bottom**) Represent the diffraction pattern of the KIR2DL2 and –L3 bound to HLA-C*07:02, respectively. Done by Shoeib Moradi at Prof. Rossjohn Laboratory, Monash University.

2.3.2 Overall structure of KIR2DL2 and KIR2DL3 in complex with HLA-C*07:02-RL9.

To assess the structural basis of the binding differences between KIR2DL2 and –L3 and between HLA-C*03:04 and HLA-C*07:02, the extracellular D1-D2 domains of the inhibitory NK receptors, KIR2DL2*001 and KIR2DL3*001, were obtained separately in complex with HLA-C*07:02 loaded with a peptide derived from histone H3 (residues 40-48, RYRPGTVAL (RL9)) (Falk et al., 1993). The KIR2DL2 and -L3 complexes were resolved to 3.1 Å and 2.5 Å resolutions, respectively (Figure 2.9 A and B). The resolution cut-off was chosen as a combination of I/sigma, Rmerge, and completeness. The final R_{work} and R_{free} values for KIR2DL2 in complex with HLA-C*07:02 are 25% and 29%, respectively (Table 2.2). KIR2DL3 in complex with HLA-C*07:02 was refined to final R_{work} and R_{free} values of 22% and 25%, respectively (Table 2.2). In each crystal lattice, 2 copies of the complexes were observed in the asymmetric unit. As these copies were highly similar (root mean square deviation (r.m.s.d.) < 0.4 Å over all Cα positions), only 1 copy of each complex was used for analysis. I used KIR2DL2 crystal structure (PDB ID: 1EFX) to build KIR2DL3 via Coot software. In order to confirm the differences between KIR2DL2 and -L3 structures, I used the unbiased electron density of KIR2DL3 to validate that the electron density fits the residues from KIR2DL3 and not KIR2DL2. KIR2DL2 and -L3 differ in certain residues close to the inter-domain between D1-D2 including residues P16 and R148 shown in Figure 1.15, which can be clearly distinguished in unbiased electron density (Explained and shown in Figure S6.1 A and B).

Overall, the binding of KIR2DL2 and KIR2DL3 to HLA-C*07:02-RL9 was reminiscent of that observed for other KIR2Ds in complex with HLA-C*03:04, HLA-C*04:01, HLA-A*11, HLA-B*57, shown in Figure 1.17 (Fan et al., 2001, Boyington et al., 2000, Liu et al., 2014). That is, the two C-type immunoglobulin domains of the KIR2D, the D1, and D2, bind over the C-terminus of the α1 and N-terminus of the α2 helices of the HLA, respectively (Figures 2.9A and B). Nonetheless, significant differences in the juxtaposition of the D1 and D2 domains of KIR2DL2 and KIR2DL3 relative to the HLA

were observed. These differences likely underlie the different binding characteristics of the receptors.

2.3.3 Comparison of KIR2DL2 in complex with HLA-C*03:02-GL9 and HLA-C*07:02-RL9

Comparison of the structure of KIR2DL2*001 in complex with HLA-C*07:02-RL9 with the previously determined structure of KIR2DL2 in complex with HLA-C*03:02-GL9 (PDB accession code 1EFX (Boyington et al., 2000)), revealed a highly similar hinge angle for the receptor of 76.1° (KIR2DL2-HLA-C*07:02) and 77.7° (KIR2DL2-HLA-C*03:02) (Figures 2.9C and D). Notably, the docking of KIR2DL2 on the two HLA alleles differed about the “twist” of the receptor by a twist of 5.2° for D1 domains and the twist of 9.8° for D2 domains (Figures 2.9C and D). This resulted in the D1 domain of KIR2DL2 receptor sitting more to the C-terminus of the peptide-binding groove of HLA-C*03:02. Consequently, whilst the buried surface area (B.S.A.) of the complexes was maintained (KIR2DL2-HLA-C*03:02 1630 $Å^2$, KIR2DL2-HLA-C*07:02 1690 $Å^2$) the contacts to the α1 and α2 helices, differed at a few key residues (Table 2.3). That is, on the α1 domain of the HLA there were additional contacts to Pro20 by the KIR2DL2 residue Phe45 and to Val76 by the KIR2DL2 residues Lys44 and Glu187 (Figure S6.2). Similarly, there was an additional contact to the HLA-C*03:04 residue Arg75 by Asp72. Extra contacts to the D2 domain of HLA-C*07:02 were observed at positions Lys146 and Ala149 from the KIR2DL2 residues Glu187 and Tyr134, respectively (Figure S6.3). Thus, although the sequence of residues contacted by KIR2DL2 is conserved between HLA-C*03:04 and -C*07:02, distal polymorphisms nonetheless affects the nature of the HLA allele and influences the binding mode of the KIR2DL2 receptor.

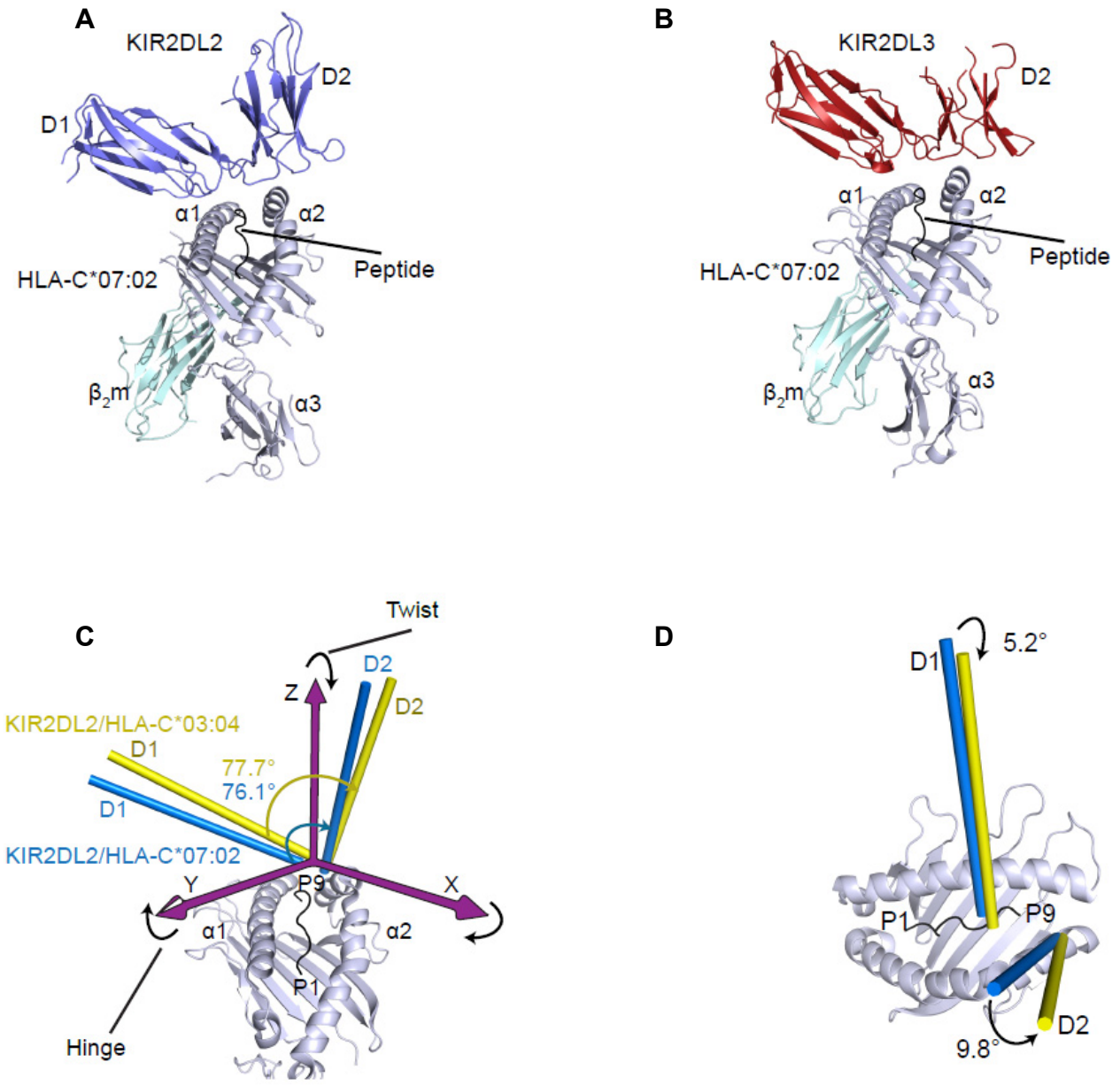

Figure 2.9. Overall structures of KIR2DL2 and -L3 in complex with HLA-C*07:02.
A and B. Comparison of KIR2DL2 binding to HLA-C*03:04 and HLA-C*07:02 and the hinge angle between the D1 and D2 domains. Cylinders represent each domain of KIR2DL2. **C** and **D.** Docking mode of the KIR2DL2 binding to HLA-C*03:04 and HLA-C*07:02 and the twist angle upon switching the HLA-C. Done by Shoeib Moradi at Prof. Rossjohn Laboratory, Monash University.

2.3.4 Comparison of HLA-C*03:02-GL9 and HLA-C*07:02-RL9

To understand the structural variation between HLA-C*03:02-GL9 and HLA-C*07:02-RL9, a comparison of the HLA was performed. Across the peptide-binding domains, the HLA had an r.m.s.d. of 0.90 Å (residues 1-177). The maximum displacement across the α1 and α2 helices was observed at the α2 helix linker (residues 144-153) that deviated ~2.7 Å (Figure 2.10). Indeed, comparison of available HLA-C structures (HLA-C*04:02 PDB codes 1IM9 (Fan et al., 2001) and1QQD (Fan and Wiley, 1999), HLA-C*08:01 PDB code 4NT6 (Choo et al., 2014)), showed that the deviation at the α2 linker was the most pronounced in HLA-C*07:02. In consequence, the peptide-binding cleft was narrower in HLA-C*07:02 than observed in other HLA-C structures. Furthermore, this helical linker is the binding site of the D2 domain of KIR2DL2, with contact to HLA residues 145, 146 and 149-151 (Table 2.3). Thus, the different docking angles of KIR2DL2 on HLA-C*03:02 and HLA-C*07:02 (shown in Figure 2.9) likely reflect an accommodation of the D2 domain of the receptor to a structural variation on the α2 helix of HLA-C.

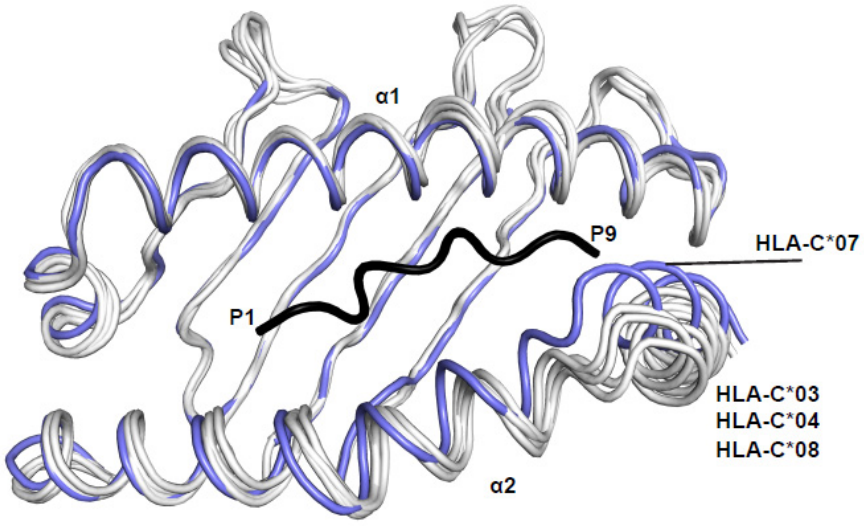

Figure 2.10. Comparison of HLA-Cs α2 helix in complex with KIRs.
Comparison of crystal structures of HLA-C*03:04, HLA-C*04:02, HLA-C*07:02, and HLA-C*08:01 on the α2 helix. Done by Shoeib Moradi at Prof. Rossjohn Laboratory, Monash University.

2.3.5 Comparison of KIR2DL2 and KIR2DL3 in complex with HLA-C*07:02-RL9

The KIR2DL2 and KIR2DL3 receptors adopted a similar conformation upon binding to HLA-C*07:02 with similar hinge angles of 77.7° and 77.1°, respectively. Further, the D1 and D2 domains aligned with an r.m.s.d. values of 0.45 Å (residues 1-102) and 0.61 Å (residues 108-200), respectively. Yet, despite this structural similarity, the "twist" differs between the receptors by 13.3° for the D1 domains and 10.4° for the D2 domains (Figures 2.11A and B). As a result, the KIR2DL3 receptor sits more to C-terminus of the peptide-binding groove of the HLA.

The net result of these differences in binding mode is that KIR2DL2 makes more extensive contacts than KIR2DL3 to the α1 and α2 helices and the peptide of the HLA-C*07:02-RL9 complex. The predominant differences in the D1 domain are at the E-F loop that shifted ~3.4 Å between the complexes (residues 68-73) (Figure S6.4). This enables additional contacts at positions Met70, Gln71 and Asp72 to Gln 72 on the α1 helix and between Gln71 and Asp72 (and Glu187 on the D2) to residue Val76 on the α1 helix in the KIR2DL2 complex (Figure 2.12). There are also additional KIR2DL2 D1 contacts between the C-C' loop residues Lys44 and Phe45 to Val76 and Pro20 respectively. Similarly, across the D1/D2 hinge loop (residues 103 to 107) and the D2 domain, there are additional contacts made by KIR2DL2. For instance, the D1/ D2 hinge residue Glu106 makes an additional contact to Arg151 on the α2 helix. Further, residues Ser184 and Glu187 and Tyr134 on the KIR2DL2 D2 domain make additional contacts to Lys146 and Ala149 on the α2 helix, respectively. Common to the KIR2DL2 and -L3 complexes are peptide contacts to the P7 and P8 positions. However, KIR2DL2 makes an additional contact made between the P7-Leu and Leu104 on the D1/D2 hinge loop (Table 2.3) (Figure 2.12 and Figure S6.5). Accordingly, the B.S.A. of the KIR2DL3 complex (1560 $Å^2$) is less than the KIR2DL2 complex (1690 $Å^2$). This difference in B.S.A. is mostly due to the footprint of the D1 domain that buried ~20 % less surface area in KIR2DL3 than in KIR2DL2 and correlated with the ability of KIR2DL2 to functionally recognise a broader range of HLA-C1/C2 ligands.

The contribution of the D1 domain to the docking of KIR2DL3-HLA-C*07:02 complex more closely resembles that of the previously determined KIR2DL1-HLA-C*04:02 complex (PDB code 1IM9 (Fan et al., 2001)) (Figure 2.11C and D). The KIR2D1 complex had a similar B.S.A. to KIR2DL3 of 1520 $Å^2$ and a relative twist of 3.6 degrees on D1 and 0.8 degrees for D2 domains. This suggested that the C-terminal binding of KIR2DL1 and KIR2DL3 was more characteristic of restricted HLA-C binding whilst the N-terminal docking observed in KIR2DL2 is characteristic of permissive HLA-C binding.

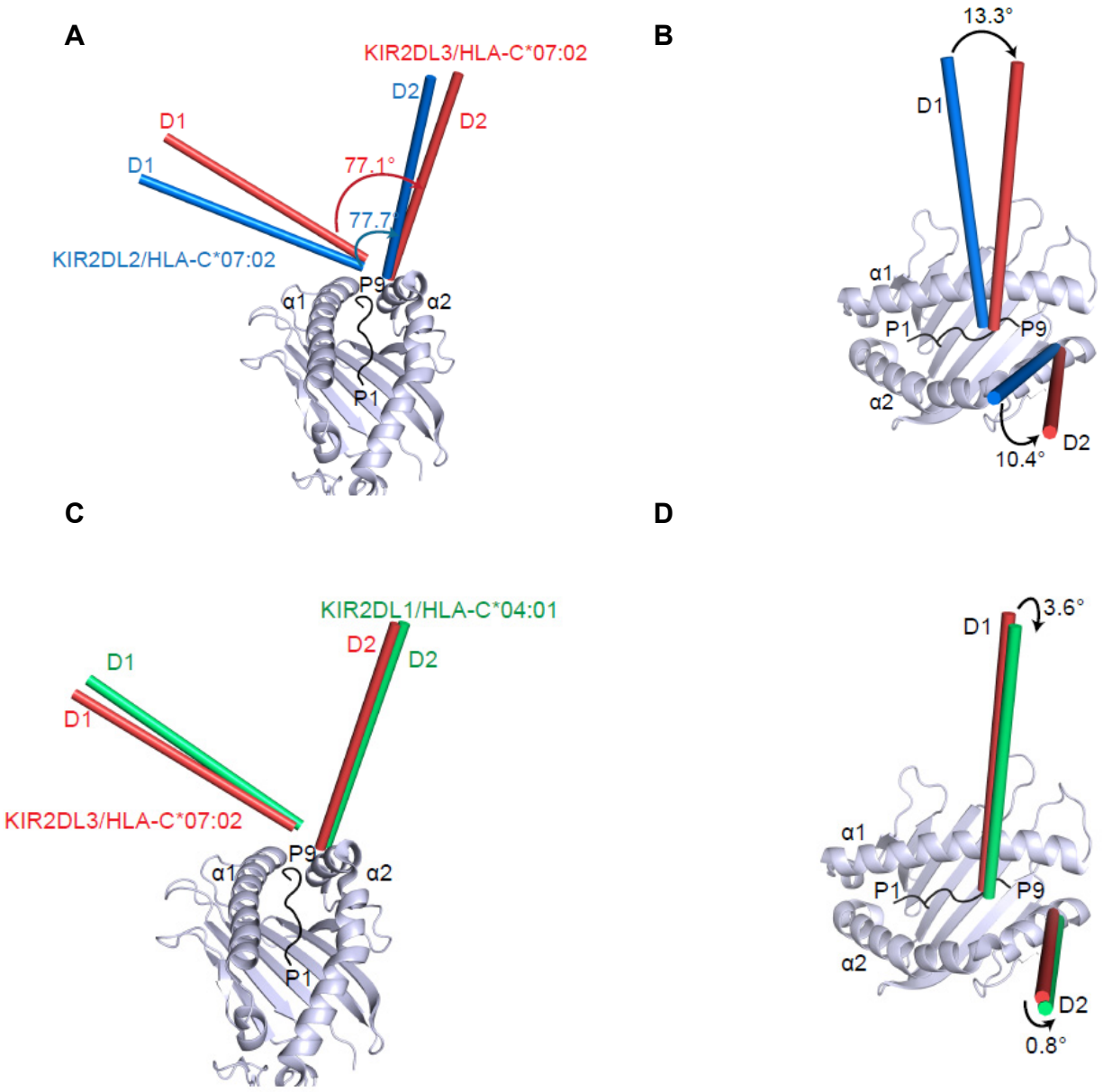

Figure 2.11. Docking mode of KIR2DL1, -L2, and -L3 in complex with HLA-Cs. Comparison of KIR2DL2 and KIR2DL3 bound to HLA-C*07:02 and the hinge angle between D1 and D2 domains. Cylinders represent the D1 and D2 domains. **B**. Docking mode of the KIR2DL2 binding to HLA-C*03:04 and HLA-C*07:02 and the twist angle between their domain upon binding to HLA-C. **C.** Comparison of KIR2DL1 and KIR2DL3 in complex with HLA-C*04:01 and HLA-C*07:02, respectively. Cylinders represent each domain of KIR2DL2. **D.** Docking mode of the KIR2DL1 and KIR2DL3 binding to HLA-C*04:01 and HLA-C*07:02, respectively and the twist angle among their domains. Done by Shoeib Moradi at Prof. Rossjohn Laboratory, Monash University.

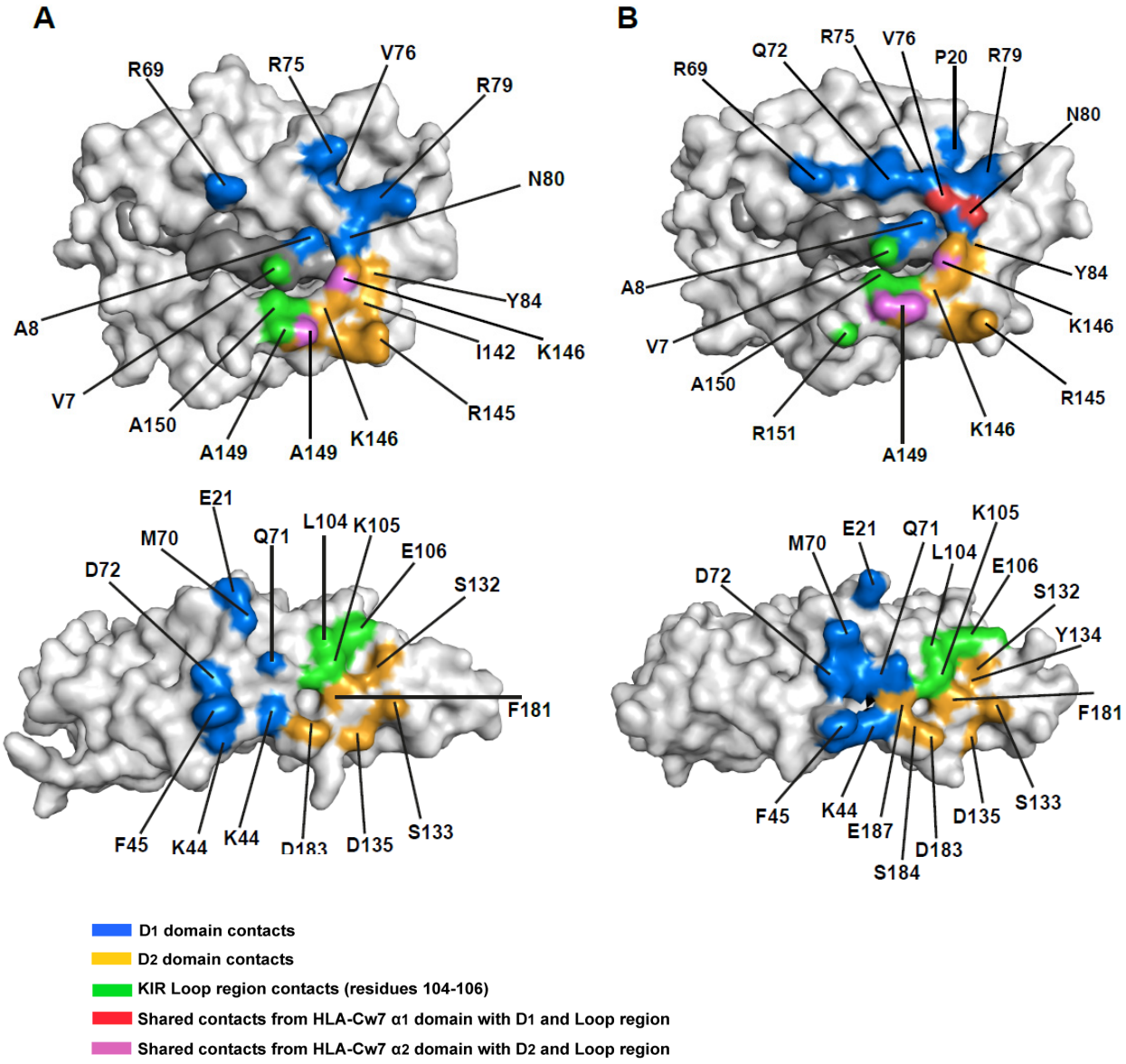

Figure 2.12. Footprints of KIR2DL2 and -L3 contacts on HLA-C*07:02.
Footprints of the interaction generated from KIR2DL3 (**A**) and KIR2DL2 (**B**) at the surface of HLA-C*07:02 (C and D), respectively. Done by Shoeib Moradi at Prof. Rossjohn Laboratory, Monash University.

Table 2.2 Statistics data for KIR2DL2 and KIR2DL3 in complex with HLAC*07:02-RL9

Data collection statistics	KIR2DL2	KIR2DL3
Temperature (K)	100	100
X-ray source	MX1 Australian Synchrotron	MX1 Australian Synchrotron
Space group	*P* 1 2_1 1	*P* 6_4
Cell Dimensions (Å)	*a*=68.565 *b*=82.086 *c*=104.887 α= 90.00º β=90.119º γ=90.00º	*a*=111.855 *b*=111.855 *c*=87.994 α=β=γ=90.00º
Resolution (Å)	32.32 – 3.01 (3.117 – 3.01)	32.57 - 2.501 (2.591 - 2.501)
Total no. observations	90401(8384)	131580(13083)
No. unique observations	20697 (2015)	21403 (2136)
Multiplicity	4.0 (3.8)	3.1 (3.0)
Data completeness (%)	96.66 (90.54)	98.51 (98.75)
I/σI (Average)	4.6 (1.8)	14.2 (6.8)
Rmerge[1] (%)	0.24 (0.88)	0.055 (0.23)
Refinement statistics		
Rfactor[2] (%)	0.2501	0.2263
Rfree (%)	0.2936	0.2565
Non-hydrogen atoms	9022	4517
Macromolecules	9022	4478
Protein residues	1118	553
Water	0	39
r.m.s.d. from ideality		
Bond lengths (Å)	0.004	0.003
Bond angles (°)	0.85	0.65
Ramachandran plot		
Favoured regions (%)	95	96
Allowed regions (%)	4.53	3.906
Outliers regions (%)	0.47	0.93
B-factors (Å^2) (Average)	46.40	67.60

[1] $R_{merge} = \sum_{hkl} \sum_j |I_{hkl,j} - < I_{hkl} > | / \sum_{hkl} \sum_j I_{hkl,j}$. [2] $R_{factor} = \sum_{hkl} ||F_o| - |F_c|| / \sum_{hkl} |F_o|$ for all data excluding the 5% that comprised the R_{free} used for cross-validation. $F_{c,hkl}$ and $F_{o,hkl}$ are the calculated and observed amplitudes of the structure factor *hkl*, respectively. 5% of data was used for the R_{free} calculation. Values in brackets refer to the highest resolution bin. Due to the radiation damage and/or poor quality of the crystals, Rmerge for KIR2Dl2 is relatively high. It also depends on multiplicity, however it evaluate data consistency and not quality of the reduced data (Diederichs and Karplus, 1997).

Table 2. 3 KIR2DLs residue contacts with HLA-C molecules

HLA				KIR			
C3	C4	C7 (L2)	C7 (L3)	2DL2 (C3)	2DL1	2DL2 (C7)	2DL3
		Pro 20				Phe 45	
Arg 69	Arg 69	Arg 69	Arg 69	Glu 21	Arg 68	Glu 21	Glu 21
				Met 70		Met 70	Met 70
Gln 72	Gln 72	Gln 72		Met 70	Arg 68	Met 70	
				Asp 72		Gln 71	
						Asp 72	
Arg 75	Arg 75	Arg 75	Arg 75	Phe 45	Phe 45	Phe 45	Phe 45
				Asp 72			Asp 72
Val 76	Val 76	Val 76	Val 76	Phe 45	Met 44	Lys 44	Phe 45
				Gln 71	Phe 45	Phe 45	
				Asp 72	Asp 72	Gln 71	
						Asp 72	
						Glu 187	
Arg 79	Arg 79	Arg 79	Arg 79	Lys 44	Met 44	Lys 44	Lys 44
				Phe 45	Phe 45	Phe 45	Phe 45
Asn 80	Lys 80	Asn 80	Asn 80	Lys 44	Met 44	Lys 44	Lys 44
				Ser 184	Gln 71	Ser 184	
					Ser184		
					Glu187		
Tyr 84	Tyr 84	Tyr 84	Tyr 84	Asp 183	Asp183	Asp183	Asp 183
			Ile 142				Asp 183
Arg 145	Arg 145	Arg145	Arg 145	Ser 133	Ser133	Ser 133	Ser 133
				Asp 135	Asp135	Asp135	Asp 135
							Phe 181
Lys 146	Lys 146	Lys146	Lys 146	Tyr 105	Tyr 105	Tyr 105	Tyr 105
				Phe 181	Phe181	Phe 181	Phe 181
				Asp 183	Asp183	Asp 183	Asp 183
				Ser 184	Ser184	Ser 184	
						Glu 187	
Ala 149	Ala 149	Ala149	Ala 149	Tyr 105	Tyr 105	Tyr 105	Tyr 105
				Glu 106	Glu106	Glu 106	Glu 106
				Ser 132	Ser132	Ser 132	Ser 132
					Tyr 134	Tyr 134	Phe 181
						Phe 181	
Ala 150	Ala 150	Ala150	Ala 150	Leu 104	Leu104	Leu 104	Leu 104
				Tyr 105		Tyr 105	Tyr 105
Arg 151	Arg 151	Arg151		Glu 106	Glu106	Glu 106	
Peptide							
Leu 7		Val 7	Val 7	Gln 71		Gln 71	Leu 104
				Leu 104		Leu 104	
				Tyr 105			
Ala 8	Lys 8	Ala 8	Ala 8	Gln71	Gln 71	Gln 71	Gln 71

Blue colors indicate salt bridge interactions. *Cut-offs for these interatomic contacts are set at 3.8 Ang

2.3.6 Direct binding studies suggest HLA-C*07:02 is superior to HLA-C*03:04 as a ligand for KIR2DL2 and -L3

The interactions between KIR2DL1, KIR2DL2, and KIR2DL3 and a series of KIR mutants in each (Table 2.1) with their respective HLA-C ligands are evaluated and compared to each other. The HLA-C allotypes chosen were the C1 allotype HLA-C*03:04 and the C2 allotype HLA-C*04:02, for which structural information was available, the canonical C2 allotype HLA-C*06:02 to investigate KIR2DL2 cross-reactivity, and the C1 allotype HLA-C*07:02, a widely distributed allotype across populations and typically found in most cohorts studied to date in frequencies above 0.15. While HLA-C*03:04, HLA-C*04:02, and HLA-C*07:02 tetramers bound to their respective wild type KIR receptors, the patterns of reactivity with transfectants expressing matched levels of mutant varied markedly at a number of positions. Specifically, the binding of KIR2DL1 to HLA-C*04:02, KIR2DL2 to HLA-C*03:04 and -C*07:02 and the binding of KIR2DL3 to HLA-C*07:02 showed similar patterns of contact residue dependence (Figure 2.13, 2.14 and 2.15). Of these, mutation of residues Phe45, Leu104, Asp135, and Asp183 abrogated binding of HLA-C*03:04 tetramers. However, these mutations had much more effect on the binding of HLA-C*07:02 tetramers to KIR2DL2 and -L3. We hypothesized that this altered binding pattern may be attributable to differences in the affinity of the HLA-C*03:04 complex for KIR2DL2 and -L3 relative to that of HLA-C*07:02. Comparisons of tetramer preparations with a similar capacity to bind cells expressing the pan-HLA-I-reactive receptor leukocyte immunoglobulin-like receptor (LILR) B1, showed preferential binding of HLA-C*07:02 (Figure 2.16) and SPR analysis also showed that the interaction of KIR2DL2 with HLA-C*07:02 was considerably stronger than that with HLA-C*03:04 (Unpublished data from Prof. Brooks laboratory, Melbourne University, done by Dr. Lucy Sullivan). While we and others have published that KIRs recognition of HLA-I can be peptide dependent, the differences in both overall reactivity and tolerance of mutations suggested that while both HLA-C*03:04 and HLA-C*07:02 are ligands for KIR2DL2 and -L3, HLA-C*07:02 may be a functionally superior ligand.

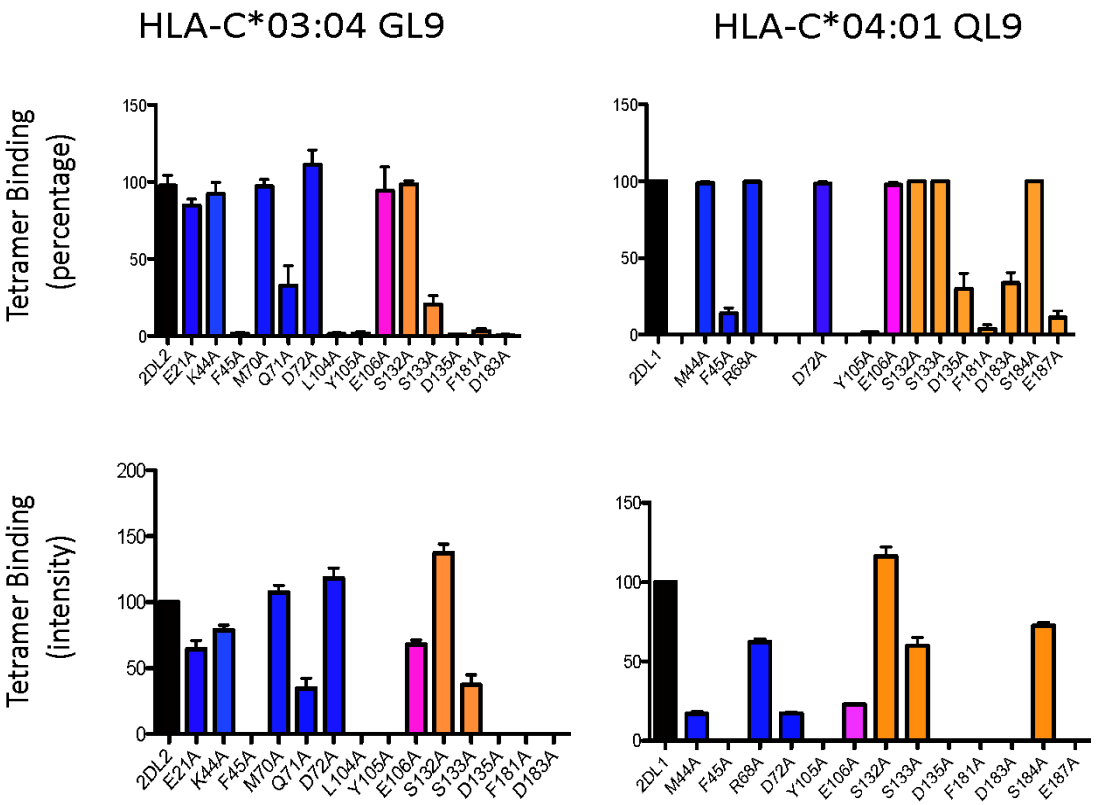

Figure 2.13 Interactions between KIR2DL1 and KIR2DL2 mutants and HLA-C*04:01 and C*03:04. Binding of KIR2DL1 and KIR2DL2 and respective mutants to tetramers of HLA-C*04:01 and C*03:04, respectively. Data was collected and analysed by Dr. Geraldin O' Connor at Prof. Brooks laboratory, Melbourne University. The standard error of the mean (SEM) was used as the assay was three independent experiments. * QL9: QYDDAVYKL.

*Percentage tetramer positive: Of the KIR expressing (FLAG positive) cells, what percentage are tetramer positive. MFI Tetramer positive: Of the KIR expressing (FLAG positive) cells, the mean fluorescent intensity of fluorescence in the tetramer channel.

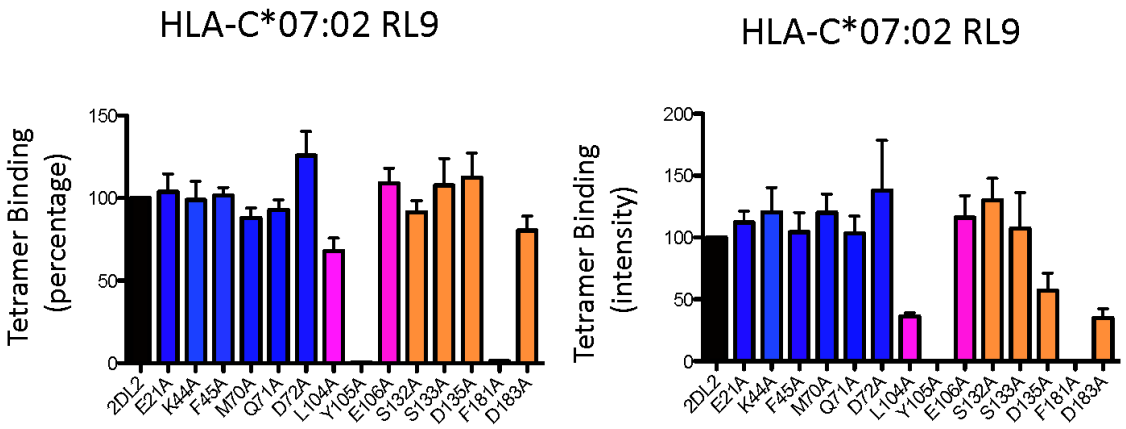

Figure 2.14 Interactions between KIR2DL2 and HLA-C*07:02. Binding of KIR2DL2 and its respective mutants to tetramers of HLA-C*07:02. Data was collected and analysed by Dr. Geraldin O' Connor at Prof. Brooks laboratory, Melbourne University. The standard error of the mean (SEM) was used as the assay was three independent experiments.

*Percentage tetramer positive: Of the KIR expressing (FLAG positive) cells, what percentage are tetramer positive. MFI Tetramer positive: Of the KIR expressing (FLAG positive) cells, the mean fluorescent intensity of fluorescence in the tetramer channel.

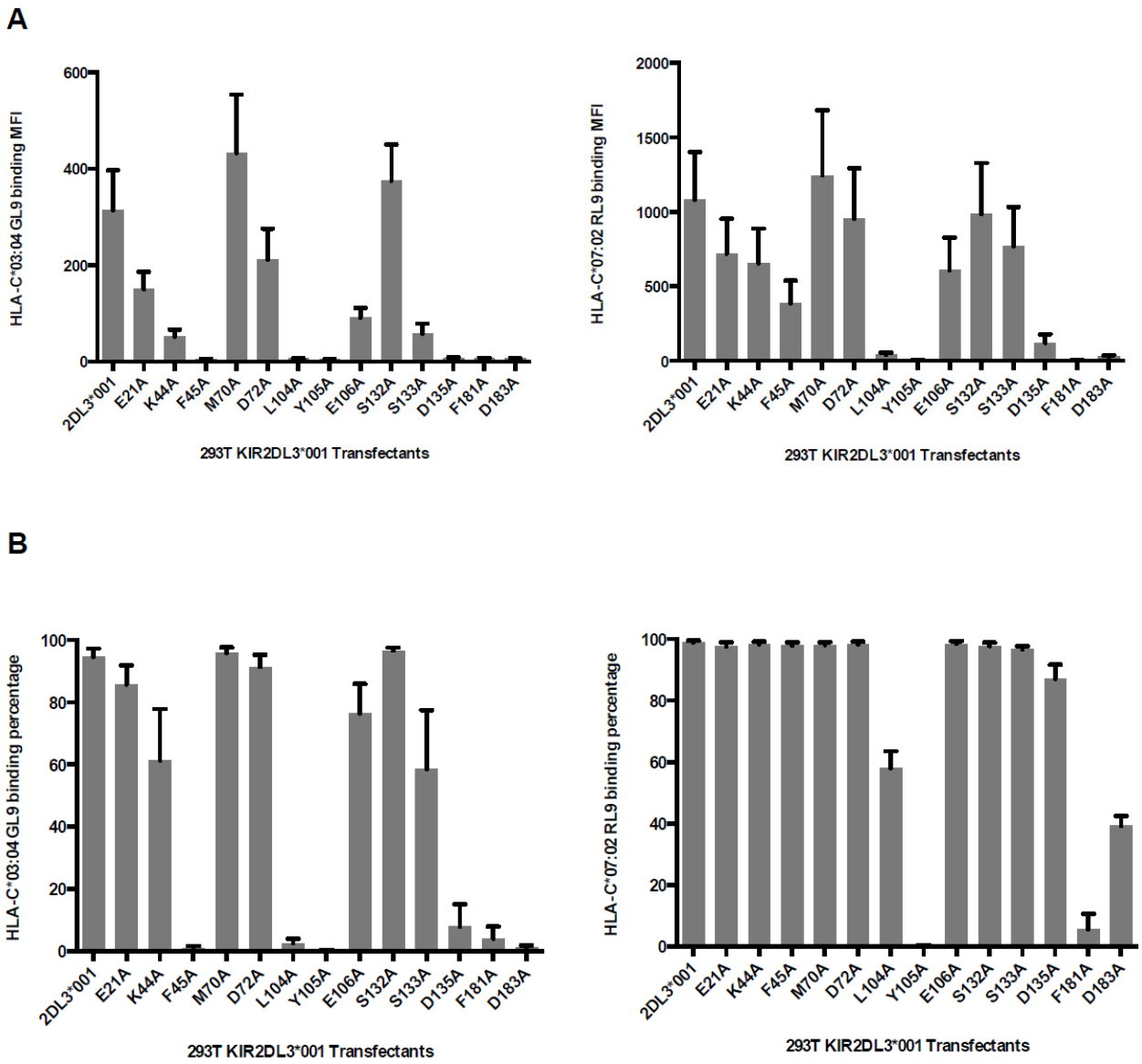

Figure 2.15. Interactions between KIR2DL3 mutants and HLA-C*03:04 and -C*07:02. **A.** Binding of KIR2DL3 and its respective mutants to tetramers of HLA-C*03:04 and HLA-C*07:02. **B.** The percentage of tetramer binding of KIR2DL3 and its mutants to HLA-C*03:04 and HLA-C*07:02. The standard error of the mean (SEM) was used as the assay was three independent experiments. This assay was performed at Prof. Brooks laboratory at Melbourne University by Shoeib Moradi and supervision of Dr. Geraldin O' Connor. Data was analyzed by Shoeib Moradi at Prof. Rossjohn Laboratory, Monash University. *MFI: Mean fluorescence intensity. *Percentage tetramer positive: Of the KIR expressing (FLAG positive) cells, what percentage are tetramer positive. MFI Tetramer positive: Of the KIR expressing (FLAG positive) cells, the mean fluorescent intensity of fluorescence in the tetramer channel.

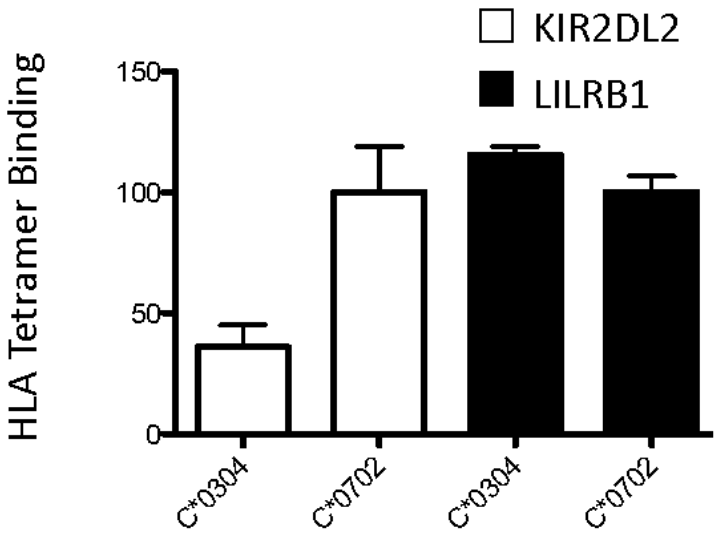

Figure 2.16. Comparison of KIR2DL2 binding to tetramers.

Comparisons of tetramer preparations with a similar capacity to bind cells expressing the pan-HLA-I-reactive receptor leukocyte immunoglobulin-like receptor (LILR) B1, HLA-C*03:04 and HLA-C*07:02. Data was collected and analysed by Dr. Geraldin O' Connor at Prof. Brooks laboratory, Melbourne University. *Percentage tetramer positive: Of the KIR expressing (FLAG positive) cells, what percentage are tetramer positive. MFI Tetramer positive: Of the KIR expressing (FLAG positive) cells, the mean fluorescent intensity of fluorescence in the tetramer channel.

2.3.7 Single-antigen bead binding highlights the distinct characteristics of HLA-C*07:02 recognition by KIR2DL2

To investigate the relative contribution of individual residues of KIR2DL2 on the recognition of HLA-C1 group members, soluble KIR2DL2 mutants were produced and used to create fluorescently labeled tetramers. These KIR2DL2 tetramers were then assessed for their ability to bind a panel of bead-bound HLA-C1 molecules presenting a broad repertoire of peptides. Wild-type KIR2DL2 bound most of the HLA-C1 molecules with similar avidity, with the exception being alleles -C*14:02 and -C*12:03 for which recognition was relatively poor (Figure 2.17). Similarly, Ala mutations of KIR2DL2 consistently attenuated binding across the HLA-C1 alleles with the clear exception of HLA-C*07:02 (Figure 2.17). That is, binding to HLA-C*07:02 was relatively insensitive to a mutation in KIR2DL2, as Ala substitutions at positions Gln71 and Ser133, resulting in increased avidity and substitutions at positions Phe45 and Asp183 exhibiting reduced attenuation (Figure 2.18). Accordingly, as these results are independent of the peptide, the intrinsic differences in the HLA-C1 heavy chains modulate KIR2DL2 recognition with HLA-C*07:02 being the most “robust” ligand. Raw data are shown in Figures 6S.6, 6S.7 and 6S.8.

HLA	Motif	WT	45A	71A	133A	135A	183A
B*73:01	C1	100	60.5	100	100	4.56	31.5
C*03:02	C1	95.8	97.7	91.2	87.4	91.2	100
C*03:03	C1	82.4	22.4	94.2	91.9	17.5	31.1
C*07:02	C1	80.9	100	83.3	78.5	100	53.9
C*16:01	C1	79.2	78.4	85.2	78.6	43.8	63.6
C*03:04	C1	76.4	15.3	88.7	83.7	22.8	29.8
B*46:01	B	68.5	26.5	81.6	75.6	14.6	12.5
C*01:02	C1	57.5	14.7	83.3	70.2	0.04	0.47
C*15:02	C2	55.1	22.1	95.8	60.5	0.00	0.00
C*17:01	C1	54.7	59.6	68.8	48.0	0.37	0.00
C*08:01	C1	53.8	8.99	74.0	65.0	3.98	8.36
C*05:01	C2	47.4	29.8	76.7	45.1	0.00	0.00
C*12:03	C1	42.7	1.92	74.8	71.1	0.30	7.44
C*18:02	C2	33.0	15.1	74.3	38.3	0.00	0.00
C*02:02	C2	29.0	8.18	84.5	32.4	0.06	0.00
C*14:02	C1	14.7	0.67	55.6	28.8	0.06	0.00
C*06:02	C2	11.0	0.46	73.1	20.8	0.00	0.00
A*11:02	A3	9.25	4.21	94.7	0.04	0.00	0.75
C*04:01	C2	4.83	0.59	67.6	4.75	0.02	0.00
B*38:01	B	0.07	0.00	0.24	0.33	0.36	0.00

Figure 2.17. Single-antigen bead binding of KIR2DL2.

Binding of KIR2DL2 and its respective mutants to a panel of HLA class I molecules. The standard error of the mean (SEM) was used as the assay was three independent experiments. This assay was performed by Dr. Phillip Pymm at Prof. Rossjohn Laboratory, Monash University. Data was collected and analysed by Dr. Phillip Pymm. Raw data are shown in Figures S6.6, S6.7, and S6.8).

100-75% Max Binding
75-50% Max Binding
50-25% Max Binding
>25% Max Binding

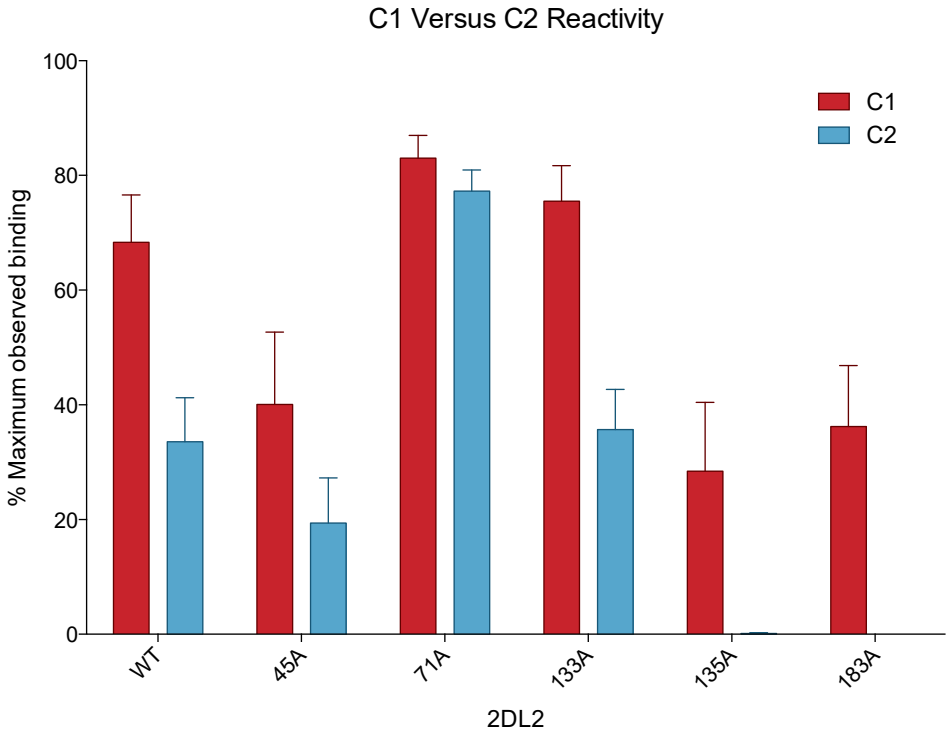

Figure 2.18. Comparison of KIR2DL2 binding to HLA-C1 and -C2 molecules.

Comparison of wildtype KIR2DL2 and mutants which are crucial for the formation of the complex with HLA-C*03:04 and -*C07:02 including F45A, Q71A, S133, D135A, D183A.This assay was performed by Dr. Phillip Pymm from Prof. Rossjohn Laboratory, Monash University. Data was collected and analysed by Dr. Phillip Pymm.

2.4 Discussion

Sensing the HLA class I molecules on the surface of the target cells by receptors, which are located on the surface of NK cells plays a crucial role in immunity. Recognition of HLA class I molecules by KIRs could be considered as one major phase in the “education” of NK cells. During the process of education, by distinguishing the HLA class I molecules, KIRs can introduce a level at which NK cells can be activated. Genes related to the expression of KIR2DL1, -L2 and -L3 are evolutionary segregated from each other, which means that these proteins are highly similar to each other. Still, despite the high degree of similarity, KIR2DL1 only recognizes HLA-C2 and KIR2DL3 senses HLA-C1. Dissimilar from them, KIR2DL2 not only interacts with HLA-C1, but it also recognizes HLA-C2 molecules. Interestingly, among alleles of KIR2DL1, -L2 and -L3, some alleles can disturb the conventional pattern of HLA-C1 and -C2 recognition by KIR2DL1, -L2 and -L3. That is, instead of binding to HLA-C1 they bind to HLA-C2 and vice versa. For example, KIR2DL1*022, instead of binding to HLA-C2 interacts with HLA-C1, and KIR2DL3*007 shows significant affinity of binding to HLA-C2 molecules (Frazier et al., 2013, Moesta et al., 2008, Saunders et al., 2016, Hilton et al., 2015), which may consequently lead to different functional activity. Before characterizing the crystal structures of KIR2DL2 and KIR2DL3 in complex with HLA-C*07:02 bound to RL9 peptide, other groups have suggested that the differences between KIR2DL2 and -L3 in recognition of HLA-C1 and -C2 specificity rises from dissimilarities that they share in the hinge angle among D1 and D2 domain which was concluded based on molecular modelling experiments (Frazier et al., 2013, Saunders et al., 2016). Nevertheless, in the present study, I was able to show that KIR2DL2 and -L3 share same hinge angle and instead they differ in the docking mode of their D1 and D2 domains interaction on HLA-C molecules and may be related to the different species specificity of KIR2DL2 and -L3.

Recognition of HLA class I molecules by KIRs have a critical impact on the outcome of transplantation. Although it is not clear that contribution of what type of KIR/HLA molecule results in an enhanced treatment, recent studies have shown that gene

expression of certain types of KIRs can effect on expression of other KIRs in different haplotypes. For example, it has been shown that in haplotypes of KIR, expression of KIR2DL1 is inhibited in the presence of KIR2DL2 expression. However, in haplotypes of KIR missing the expression of KIR2DL2, the expression of KIR2DL1 and KIR2DL3 remains intact (Schonberg et al., 2011). This may provide clues for designing new strategies for improvement of transplantation treatment, by choosing a right KIR/HLA combination.

By solving the crystal structures of KIR2DL2 and KIR2DL3, in complex with HLA-C*07:02, I revealed that their D1-D2 domains dock differently upon interaction with HAL-C*07:02. I was able to show that α1 domain of HLA-C1 shows the majority of the differences in the docking mode of such interactions. I could also find that the buried surface area for KIR2DL2 bound to HLA-C*07:02 is higher than that of KIR2DL3. My investigations indicate that the D1 domain of KIR2DL2 and KIR2DL3 as well as α1 domain of HLA-C1 and -C2 are involved in dictating the docking mode of the interaction.

3 Chapter 3

Chapter 3 covers the second aim of my thesis, which is the structural and functional characterization of KIR2DL4. KIR2DL4 is different from other KIRs (except KIR2DL5) regarding the extracellular domains arrangement. Instead of having a D1-D2 domain arrangement, it includes D0-D2 domain arrangement and the D0 domain resembles D0 domain of KIR3D. Unlike other KIRs having only inhibitory or activating signalling domain, KIR2DL4 appear to be unique, as it contains both activating and inhibitory signalling domains. Being equipped with inhibitory and activating signalling domains, KIR2DL4 may be able to display unique function(s) compared to other KIRs.

In chapter 3, I present the crystal structure of the D0-D2 domains of KIR2DL4 to the resolution of 2.8 Å. As the crystal lattice showed atypical domain arrangements of KIR2DL4 D0-D2 domains, I further characterized the structure of the extracellular domains of KIR2DL4 by means of analytical gel filtration, analytical ultracentrifugation (AUC), small-angle X-ray scattering (SAXS) and multi angle light scattering (MALS). Complementary experiments indicated that KIR2DL4 oligomerizes via its D0 domain and it resides in the equilibrium of dimer: tetramer. I further found that the oligomerization of KIR2DL4 takes place in a concentration dependent manner. Overall, I found that domain arrangement of KIR2DL4 is unique among KIRs and based on the location of its D0 domain in the tetramer, it is less likely that it binds to HLA molecules in a manner that other KIRs interact. Indeed, I found no direct interaction between KIR2DL4 and HLA molecules via binding experiments including SPR, SAXS, and LUMINEX. My findings suggest that function of KIR2DL4 may not follow the conventional HLA molecules binding of other KIR family and its function might be controlled by the dimer-tetramer self-association property.

THE JOURNAL OF BIOLOGICAL CHEMISTRY VOL. 290, NO. 16, pp. 10460–10471, April 17, 2015

The Structure of the Atypical Killer Cell Immunoglobulin-like Receptor, KIR2DL4*

Received for publication, September 16, 2014, and in revised form, February 10, 2015 Published, JBC Papers in Press, March 10, 2015, DOI 10.1074/jbc.M114.612291

Shoeib Moradi[‡1], Richard Berry[‡§1,2], Phillip Pymm[‡], Corinne Hitchen[‡], Simone A. Beckham[‡], Matthew C. J. Wilce[‡], Nicholas G. Walpole[‡], Craig S. Clements[‡], Hugh H. Reid[‡], Matthew A. Perugini[¶], Andrew G. Brooks[‖], Jamie Rossjohn[‡§3], and Julian P. Vivian[‡§4]**

*From the [‡]Department of Biochemistry and Molecular Biology, School of Biomedical Sciences, and the [§]Australian Research Council Centre of Excellence for Advanced Molecular Imaging, Monash University, Clayton, Victoria 3800, Australia, the [¶]Department of Biochemistry, La Trobe Institute for Molecular Science, La Trobe University, Melbourne Victoria 3086 Australia, the [‖]Department of Microbiology and Immunology, Peter Doherty Institute for Infection and Immunity, University of Melbourne, Parkville, Victoria 3010, Australia, and the **Institute of Infection and Immunity, Cardiff University, School of Medicine, Heath Park, Cardiff CF14 4XN, United Kingdom*

Background: KIR2DL4 is an important natural killer cell receptor with properties distinct from other KIRs.
Results: The D0 domain of KIR2DL4 drove self-association of the receptor.
Conclusion: Among KIRs, the self-association of KIR2DL4 is unique and a result of discrete differences in its D0 domain.
Significance: The self-association of KIR2DL4 has implications for its unique signaling and function.

The engagement of natural killer cell immunoglobulin-like receptors (KIRs) with their target ligands, human leukocyte antigen (HLA) molecules, is a critical component of innate immunity. Structurally, KIRs typically have either two (D1-D2) or three (D0-D1-D2) extracellular immunoglobulin domains, with the D1 and D2 domain recognizing the α1 and α2 helices of HLA, respectively, whereas the D0 domain of the KIR3DLs binds a loop region flanking the α1 helix of the HLA molecule. KIR2DL4 is distinct from other KIRs (except KIR2DL5) in that it does not contain a D1 domain and instead has a D0-D2 arrangement. Functionally, KIR2DL4 is also atypical in that, unlike all other KIRs, KIR2DL4 has both activating and inhibitory signaling domains. Here, we determined the 2.8 Å crystal structure of the extracellular domains of KIR2DL4. Structurally, KIR2DL4 is reminiscent of other KIR2DL receptors, with the D0 and D2 adopting the C2-type immunoglobulin fold arranged with an acute elbow angle. However, KIR2DL4 self-associated via the D0 domain in a concentration-dependent manner and was observed as a tetramer in the crystal lattice by size exclusion chromatography, dynamic light scattering, analytical ultracentrifugation, and small angle x-ray scattering experiments. The assignment of residues in the D0 domain to forming the KIR2DL4 tetramer precludes an interaction with HLA akin to that observed for KIR3DL1. Accordingly, no interaction was observed to HLA by direct binding studies. Our data suggest that the unique functional properties of KIR2DL4 may be mediated by self-association of the receptor.

Natural killer (NK)[5] cells are cytotoxic lymphocytes that are a vital component of the innate immune system. NK cells have been implicated in the control of viral infections, including HIV, herpes viruses, and poxviruses (1), together with malignancies, including acute myeloid leukemia and neuroblastoma (2, 3). Activation of NK cells is determined by the interplay between inhibitory and activating signals transduced from an array of cell surface receptors that include the killer cell immunoglobulin-like receptor (KIR) family in humans.

Classification of KIRs is based on whether they contain two or three extracellular immunoglobulin domains (KIR2D or KIR3D) as well as on the nature of the signaling domains ("L" is inhibitory, and "S" is activating). Previous studies have elucidated the structures of KIR2Ds with a D1-D2 domain arrangement (4–9) and of KIR3DL1 that has a D0-D1-D2 configuration (10). The D1 and D2 domains of KIR2Ds and KIR3DL1 recognize HLA in much the same manner, with the D1 sitting atop the α1 domain and the D2 atop the α2 domain of the HLA molecule. The D0 domain of KIR3DL1 acted as an "innate sensor" contacting the highly conserved loop between the β1 and β2 stands of the peptide-binding groove of the HLA molecule (10–12). The activating KIRs lack cytoplasmic signaling motifs but have a charged lysine residue in the transmembrane region that facilitates pairing with DAP12, a disulfide-linked immunoreceptor tyrosine-based activation motif-containing adaptor protein (13). Inhibitory KIRs have immunoreceptor tyrosine-based inhibition motifs in their cytoplasmic domains that upon engagement with ligand recruit the protein-tyrosine phosphatases SHP-1 and SHP-2 to transduce inhibitory signals (14).

KIR2DL4 is an atypical KIR that differs from the other family members in manner of cellular localization, ligand specificity, signaling, and structure. Structurally, KIR2DL4 is distinct from

* This work was supported by Australian Research Council (ARC) Grant DE130101504 and by National Health and Medical Research Council (NHMRC) of Australia Grant 1046685.
The atomic coordinates and structure factors (code 3WYR) have been deposited in the Protein Data Bank (http://wwpdb.org/).
[1] Both authors contributed equally to this work.
[2] Supported by NHMRC Peter Doherty Fellowship GNT1035636.
[3] Supported by an NHMRC Australia Fellowship. To whom correspondence may be addressed. E-mail: Jamie.rossjohn@monash.edu.
[4] Supported by an ARC DECRA Fellowship. To whom correspondence may be addressed. E-mail: Julian.vivian@monash.edu.

[5] The abbreviations used are: NK, natural killer; KIR, natural killer cell immunoglobulin-like receptor; HSPG, heparan sulfate proteoglycan; SAXS, small angle x-ray scattering; SEC, size-exclusion chromatography; MALS, multi-angle light scattering; r.m.s., root mean square.

other KIR (except KIR2DL5) in that the D1 domain is absent; instead it has a D0-D2 domain architecture (similar to KIR2DL5). Uniquely, KIR2DL4 has both inhibitory and activating signaling domains (15). Namely, KIR2DL4 contains a single cytoplasmic immunoreceptor tyrosine-based inhibition motif domain as well as a basic arginine residue in the transmembrane domain. However, instead of coupling with DAP12, KIR2DL4 recruits the FcεR-γ chain to transduce stimulatory signals (16). Further, unlike other KIRs, which signal from the plasma membrane, KIR2DL4 signals predominantly from endosomes (17).

The confirmed ligands for KIRs are HLA-class Ia molecules. Specifically, KIR2DL1/2/3 recognize HLA-C (18), KIR3DL1 binds HLA-Bw4 (19), and KIR3DL2 binds HLA-A3 and HLA-A11 (20). Despite the high level of sequence identity to their inhibitory counterparts, the ligands for many activating KIRs are unclear. KIR2DL4 is unusual in that it does not appear to interact with HLA class Ia (pHLA-Ia). Instead, cellular assays have indicated an interaction with the HLA class Ib molecule HLA-G, a monomorphic antigen-presenting molecule that resembles HLA-Ia molecules (17, 21, 22). However, whether KIRDL4 binds HLA-G remains unclear (23, 24). Indeed, recent work has suggested that KIR2DL4 can bind heparin and heparanated proteoglycans (HSPG) distinct from HLA-G (25). Further, the binding of HSPG was shown to be modulated by the D0 domain of KIR2DL4 and to affect endosomal uptake of the receptor. However, the physiological significance of this interaction is not well defined.

Here we describe the crystal structure of KIR2DL4. In keeping with its unusual functional characteristics, KIR2DL4 oligomerizes in a concentration-dependent manner, a feature not seen in other members of the KIR family to date. The oligomerization interface was formed by the association of D0 domains via residues that have been previously identified as important for KIR3DL1 binding to HLA. This suggests that the D0 domain of the KIR2DL4 tetramer does not recognize HLA in the same manner as the D0 domain of KIR3Ds. Furthermore, no interaction was observed between KIR2DL4 and a panel of 100 pHLA-Ia by single antigen bead assay nor to HLA-G by surface plasmon resonance. The data herein cast new light on the unique functional properties of KIR2DL4 and the degree to which they may be driven by self-association of the receptor.

EXPERIMENTAL PROCEDURES

Cloning and Expression of KIR2DL4—The extracellular domains of KIR2DL4*001 (residues 1–195) and the mutants F34A, W56A, F77A, and W85A were subcloned into vectors for insect cell and mammalian cell expression. For insect cell expression, the genes were subcloned into a modified baculoviral pFastBac expression vector (Invitrogen) containing a secretion signal peptide sequence and an N-terminal hexahistidine tag (26). For generating tetramers of KIR2DL4, a similar pFastBac construct was generated for the wild-type KIR2DL4 with a secretion signal peptide sequence, an N-terminal hexahistidine tag, and a C-terminal BirA tag. Similarly, for mammalian expression, the residues 1–295 and the mutants F34A, W56A, F77A, and W85A were subcloned into the pHLSec expression vector containing a secretion signal peptide sequence and an N-terminal hexahistidine tag (27). Insect cell expression of KIR2DL4 was performed by baculoviral infection of BTI-TN-5B1–4 cells (Hi-5 cells, Invitrogen). Mammalian expression was performed by transient transfection of HEK293S GnTI$^-$ cells as detailed by Aricescu *et al.* (27). From both cell lines, the KIR2DL4 was secreted into the expression medium and then dialyzed into 10 mM Tris, pH 8.0, 500 mM NaCl (buffer 1). The protein was then purified by binding to nickel-Sepharose resin in buffer 1 with 30 mM imidazole, pH 8.0, washed in buffer 1 with 30 mM imidazole, pH 8.0, and eluted with buffer 1 with 30 mM imidazole, pH 8.0, and 50 mM EDTA. KIR2DL4 was then purified by size exclusion chromatography (S200 16/60 column, GE Healthcare) in buffer 1. The yield of KIR2DL4 from insect cells was 0.5 mg/liter, which was utilized for analytical ultracentrifugation, small angle x-ray scattering, size exclusion, and multiangle light scattering experiments. However, the insect cell material was not amenable to crystallization. The yield of KIR2DL4 expressed in HEK293S GnTI$^-$ cells was 0.02 mg/liter. The material produced in mammalian cells was used in x-ray crystallography studies following overnight incubation at 298 K with 200 units of the deglycosidase endoglycosidase H (New England Biolabs).

Analytical Ultracentrifugation—Sedimentation experiments of KIR2DL4 (0.017–0.15 mg/ml) dissolved in 10 mM Tris, 150 mM NaCl, pH 8.0, were performed using a Beckman model XL-I analytical ultracentrifuge equipped with a photoelectric optical absorbance system. Sample (380 μl) and reference (400 μl) solutions were loaded into a conventional double sector quartz cell and mounted in a Beckman An-60 Ti rotor. The samples were then centrifuged at 40,000 rpm at a temperature of 293 K. Data were collected at a single wavelength (268 nm) in continuous mode without averaging using a step size of 0.003 cm. Solvent density (1.0047 g/ml at 293 K) and viscosity (1.0182 centipoise) as well as estimates of the partial specific volume, $\bar{\nu}$ (0.7208 ml/g at 293 K), were computed using the program SEDNTERP (57). Sedimentation velocity data at multiple time points were fitted to a continuous size distribution model (28–30) using the program SEDFIT (58).

Single HLA-Antigen Bead Assay—HLA class I recognition by KIR2DL4 was assessed through binding of KIR2DL4 tetramers to beads coated with a panel of 100 HLA class I A, B, and C allotypes (LabScreen HLA class I single antigen bead screen (One Lambda, Canoga Park, CA)). 5 μg of phycoerythrin-labeled KIR2DL4 tetramer was incubated with the beads for 30 min at room temperature in the dark in phosphate-buffered 300 mM NaCl (PBS-300) with 5% fetal calf serum (Ausgenex). The beads were then washed three times in PBS-300 with 0.05% Tween 20 and resuspended in PBS-300. Binding was measured on a Luminex platform (LABScan™ 100 (One Lambda)) through identification of the individual HLA allotypes via unique bead labeling and detection of the fluorescent intensity of the tetramer on each bead set. Normalized fluorescent values for analysis were obtained using the HLA Fusion software suite (One Lambda), which subtracted background using the formula,

$$\text{Normalized fluorescent value} = (S\#N - SNC\,bead) - (BG\#N - BGNC\,bead) \quad \text{(Eq. 1)}$$

where *S#N* represents sample-specific fluorescent value (trimmed mean) for bead *#N*, *SNC bead* is the sample-specific fluorescent value for negative control (nude) bead, *BG#n* is the background negative control fluorescent value for bead *#N*, and *BGNC bead* is the background negative control fluorescent value for negative control bead.

Negative control samples were obtained using unconjugated streptavidin PE in place of KIR tetramer. The experiments were performed in triplicate.

Cloning and Expression of HLA—The extracellular domains of HLA-G*01:01 and HLA-B*57:01 (residues 1–275) and β_2-microglobulin were cloned into the pET-30(b) expression vector for overexpression in *E. coli* as described previously (31, 32). The HLA and β_2-microglobulin were expressed into inclusion bodies separately in *E. coli*, refolded, and purified, as described previously (31, 32). Briefly, 60 mg of both the HLA-G and HLA-B*57:01 were refolded by rapid dilution in a solution containing 100 mM Tris-HCl, pH 8.0, 400 mM L-arginine-HCl, 5 mM reduced glutathione, and 0.5 mM oxidized glutathione (and 4 M urea for HLA-B*57:01) in the presence of 20 mg β_2-microglobulin and 10 mg of synthetic peptide. HLA-G was refolded with the RIIPRHLQL and RLPKDFRIL peptides, and HLA-B*57:01 was refolded with the LSSPVTKSF peptide. The refolded peptide·HLA·β_2-microglobulin complexes were purified by anion exchange on a diethylaminoethylcellulose column followed by size exclusion chromatography (S200 16/60 column, GE Healthcare), followed by an additional high resolution anion exchange chromatography step (Mono Q 5/5 column, GE Healthcare).

Surface Plasmon Resonance—The interaction between the extracellular domains of KIR2DL4 and HLA-G and HLA-B*57:01 was analyzed by surface plasmon resonance using a BIAcore 3000 system (GE Healthcare). All experiments were performed at 298 K. Two independent experiments were performed in separate buffers. The buffer comprised either 10 mM HEPES (pH 7.4), 300 mM NaCl, and 0.005% surfactant P20 (HBS-P20) or 10 mM sodium citrate (pH 5.5), 300 mM NaCl, and 0.005% P20 (CBS-P20). The monoclonal anti-His_6 antibody 4D11 (Thermo Scientific) was immobilized on adjacent flow cells of a CM5 Sensorchip (GE Healthcare) by amine coupling to a surface density of ~1000 resonance units. His_6-tagged KIR2DL4 was captured by the immobilized antibody. An adjacent flow cell to which KIR2DL4 was not added was activated and quenched in the same manner and served as a control cell. HLA-G and the negative control HLA-B*57:01 were serially diluted in either HBS-P20 or CBS-P20 (0.5–300 μM) and injected simultaneously over the test and control surfaces at a flow rate of 5 μl/min, with measurements taken in duplicate. The experiment was also conducted in reverse. Here, the monoclonal anti-HLA antibody W6/32 was immobilized as above, and HLA-G and the negative control HLA-B57:01 were captured on the surface. The KIR2DL4 was serially diluted as above, and the experiment was performed as above. The integrity of the analytes was confirmed by the binding of the monoclonal antibodies W6/32 to HLA by surface plasmon resonance (33) and mAb 33 to KIR2DL4 by an enzyme-linked immunosorbent assay (ELISA) (34).

Enzyme-linked Immunosorbent Assay—Direct ELISA screening of mAb 33 (34) binding to KIR2DL4 and the negative control KIR2DL2 was performed by the standard protocol (35) on Maxisorb Nunc Immunoplates (Nunc, Roskilde, Denmark). The plates were coated with 2.5 μg/well of recombinant KIR2DL4 or KIR2DL2 diluted in phosphate-buffered saline.

Small Angle X-ray Scattering—For SAXS data collection, KIR2DL4 (0.3–5 mg/ml) and KIR2DL2 (0.35–1.5 mg/ml) were prepared in 10 mM citrate, pH 5.5, plus 0.3 M NaCl. To prevent the formation of disulfide-linked dimers, a low concentration of DTT (1 mM) was added to KIR2DL4 samples. This did not adversely impact the fold (as judged by circular dichroism spectroscopy) or the ability of KIR to oligomerize (data not shown). SAXS data were collected at the SAXS/WAXS beamline of the Australian synchrotron using a 1 M Pilatus detector. Samples and matching buffer solutions were loaded into 96-well plates, and multiple 1-s exposures were collected and compared with each other to assess for radiation damage. Data were collected to cover momentum transfer intervals of $0.0097\ \text{Å}^{-1} < q < 0.6\ \text{Å}^{-1}$ for KIR2DL4 and $0.0044\ \text{Å}^{-1} < q < 0.26\ \text{Å}^{-1}$ for KIR2DL2. The modulus of the momentum transfer is defined as $q = 4\pi\sin(\theta/\lambda)$, where 2θ is the scattering angle and λ is the wavelength. Scattering images were integrated, averaged, and calibrated against water using beamline-specific software. Scattering from the buffer and empty capillaries was subtracted after scaling scattering intensities to correspond to incident beam intensities. Molecular mass was calculated by extrapolating scattering intensity at zero angle, $I(0)$, following calibration using water. Data quality was assessed on the basis of the linearity of Guinier plots, and the R_g and the pairwise intraparticle distance distribution function were determined using GNOM (36). *Ab initio* models were generated using DAMMIF (37) using *P2* symmetry. At least 10 independent DAMMIF runs were aligned, combined, and filtered to generate a final model that retained the most consistent features using the DAMAVER package. The normalized spatial discrepancies between individual models were 0.673–0.996 (dimer) and 0.512–0.871 (tetramer). High resolution models of KIR2DL2 and 2DL4 were fitted within *ab initio* models using DAMAVER.

Size Exclusion-coupled Multiangle Light Scattering (SEC-MALS)—SEC-MALS was used to estimate the molecular masses of the KIR2DL4 samples. KIR2DL4 was prepared to a final concentration of 3, 5, and 10 mg/ml. 100 μl of each sample was subjected to SEC-MALS at a flow rate of 0.5 ml/min using a WTC030s5 column in 10 mM sodium citrate, pH 5.5, 300 mM NaCl. The system comprised a Shimadzu DGU-$20A_5$ degasser, LC-20AD liquid chromatograph, SIL-$20A_{HT}$ autosampler, CBM-20A communications bus module, SPD-20A UV-visible detector, and CTO-20AC column oven, coupled to a Wyatt Technology Corp. DAWN HELEOS-II light scattering detector and an Optilab T-rEX refractive index detector. A WyattQELS detector had been installed in the DAWN HELEOS-II at a 90° angle, replacing detector number 12. Normalization was performed against bovine serum albumin, and data collection and analysis were performed with ASTRA6 (Wyatt Technology Corp.).

Crystallization, Data Collection, Structure Determination, and Refinement—KIR2DL4 expressed in mammalian HEK 293S cells was concentrated to 4 mg/ml and crystallized at 294 K by the hanging drop vapor diffusion method from a solution comprising 10–16% PEG 3350, 4% tacsimate, pH 6.0. The crystals typically grew as plates with dimensions 0.1 × 0.1 × 0.02 mm in 7 days. Before data collection, the crystals were equilibrated in crystallization solution with 35% PEG 3350 added as a cryoprotectant and then flash-cooled in a stream of liquid nitrogen at 100 K. A 2.8 Å resolution data set was collected at the MX2 beamline (Australian Synchrotron, Victoria). The data were recorded on a Quantum-315 CCD detector and were integrated and scaled using MOSFLM and SCALA from the CCP4 program suite (38–40). Details of the data processing statistics are summarized in Table 1. The crystal structure was solved by molecular replacement, as implemented in PHASER (41), with KIR2DS4 used as the search model (Protein Data Bank accession number 3H8N (6)). The asymmetric unit contained two copies of KIR2DL4. Refinement of the model proceeded with iterative rounds of manual building in COOT (42) and refinement in PHENIX (43), with strict 2-fold non-crystallographic symmetry applied. The final model comprised residues 7–195 and an *N*-acetylglucosamine group at Asn^{118}. The sugar groups at position 152 could not be accurately modeled and were therefore excluded from the final model. The structure was validated with MOLPROBITY (44). Refinement statistics are summarized in Table 1. Coordinates and structure factors were deposited in the PDB under accession 3WYR.

TABLE 1
Data collection and refinement statistics

Parameter	Value
Data collection statistics	
Temperature (K)	100
X-ray source	MX2 Australian synchrotron
Space group	$P42_12$
Cell dimensions (Å)	$a = 87.8$, $b = 87.8$, $c = 106.0$
Resolution (Å)	50-2.8 (2.90-2.80)[a]
Total no. of observations	21,500 (2068)
No. of unique observations	10,753 (1034)
Multiplicity	2.0 (2.0)
Data completeness (%)	100 (100)
$1/\sigma_I$	10.8 (2.2)
R_{merge}[b]	0.059 (0.333)
Refinement statistics	
Non-hydrogen atoms	
Protein	2943
ligands	67
R_{factor}^2	0.211
R_{free}^2	0.243
r.m.s. deviation from ideality	
Bond lengths (Å)	0.003
Bond angles (degrees)	0.72
Ramachandran plot	
Favored regions (%)	94.0
Allowed regions (%)	6.0
B-Factors (Å^2)	
Wilson	49.1
Average protein	53.4
Average ligand	66.2

[a] Values shown in parentheses are for the highest resolution shell.
[b] $R_{merge} = \Sigma_{hkl} \Sigma_i |I_{hkli} - \langle I_{hkl} \rangle| / \Sigma_{hkl} \Sigma_i I_{hkli}$.
[c] $R_{factor} = \Sigma_{hkl} ||F_o| - |F_c|| / \Sigma_{hkl} |F_o|$ for all data excluding the 5% that comprised the R_{free} used for cross-validation.

RESULTS

Overall Structure of KIR2DL4

The structure of the extracellular domain of KIR2DL4, comprising residues 7–195, was resolved to 2.8 Å and refined to final R_{work} and R_{free} values of 21.1 and 24.3%, respectively (Table 1 and Fig. 1*A*). The asymmetric unit of the crystal contained two copies of KIR2DL4, each comprising two C2-type immunoglobulin (Ig) domains, the D0 domain and the D2 domain, arranged with an acute elbow angle (Fig. 1*A*).

The D0 Ig domain contained eight β-strands, with a three-stranded β-sheet comprising strands A, B, and E sandwiched against the five-stranded β-sheet comprising strands A′, C, C′, F, and G. The D0 domain had two 3_{10} helices, one connecting the C and C′ strands and the other connecting the E and F strands (Fig. 1*A*). The D2 Ig domain contained 10 β-strands and differed from the D0 domain topology with an additional short D strand. Further, linking the D0 and D2 domains was an additional F′ strand on the D2 domain that formed a sheet with the F strand of the D0 domain (Fig. 1*A*) (45).

The D2 domains within the asymmetric unit were highly similar, aligning with an r.m.s. deviation of 0.5 Å (over Cα positions 101–195). By contrast, the D0 domains aligned with an r.m.s. deviation of 1.2 Å (over Cα positions 7–97) with a notable deviation in the conformation of the loop between the C and C′ strands (5.6 Å) (Fig. 1*B*). These structural differences within the D0 domains were concomitant with a 1.2° difference in the interdomain angle between the D0 and D2 domains, with an angle of 82.3° in copy 1 and 83.5° in copy 2 (Fig. 1*B*).

KIR2DL4 had two glycosylation sites, at positions Asn^{118} and Asn^{152}, both located on the D2 domain (Fig. 1*A*). The glycosylation at Asn^{152} was conserved across KIR genes, whereas the Asn^{118} was only partially conserved and is absent from KIR3DL1 (Fig. 1*C*).

KIR2DL4 has an unusual disulfide pairing in the D0 domain. The canonical disulfide bond between residues Cys^{28} and Cys^{74} (linking the B and F strands), present in the structure of KIR3DL1 and conserved in the sequences of all other D0-containing KIRs, was absent in the crystal structure of KIR2DL4 (Fig. 1*C*). This disulfide bond is replaced by a disulfide bond linking the A and B strands between Cys^{10} and Cys^{28} (Fig. 2*A*). The tripartite arrangement of Cys^{10}, Cys^{28}, and Cys^{74} could conceivably form three separate disulfide bond configurations. However, only one configuration was observed. Among KIRs, the presence of a Cys at position 10 is unique to KIR2DL4 (Leu^{10} in other KIRs) and is conserved in KIR2DL4 sequences across primate species. This correlation suggests that Cys^{10} may play an important role in the conformation of the D0 domain. Indeed, comparison with KIR3DL1 revealed that the shift in Cys^{28} upon binding to Cys^{10} was coincident with conformational movements of Phe^{37} and Phe^{55} that directly impacted the conformation of the B, C, and C′ strands (Fig. 2*B*).

The Tetramer Interface

Unlike all known KIR structures, the oligomeric assembly of KIR2DL4 observed in the crystal lattice was tetrameric. The tetramer was generated through crystallographic symmetry (Fig. 2, *C* and *D*). The tetramer comprised two dimers, the translational dimer as observed in the asymmetric unit and the rotational dimer generated by crystallographic symmetry (Fig.

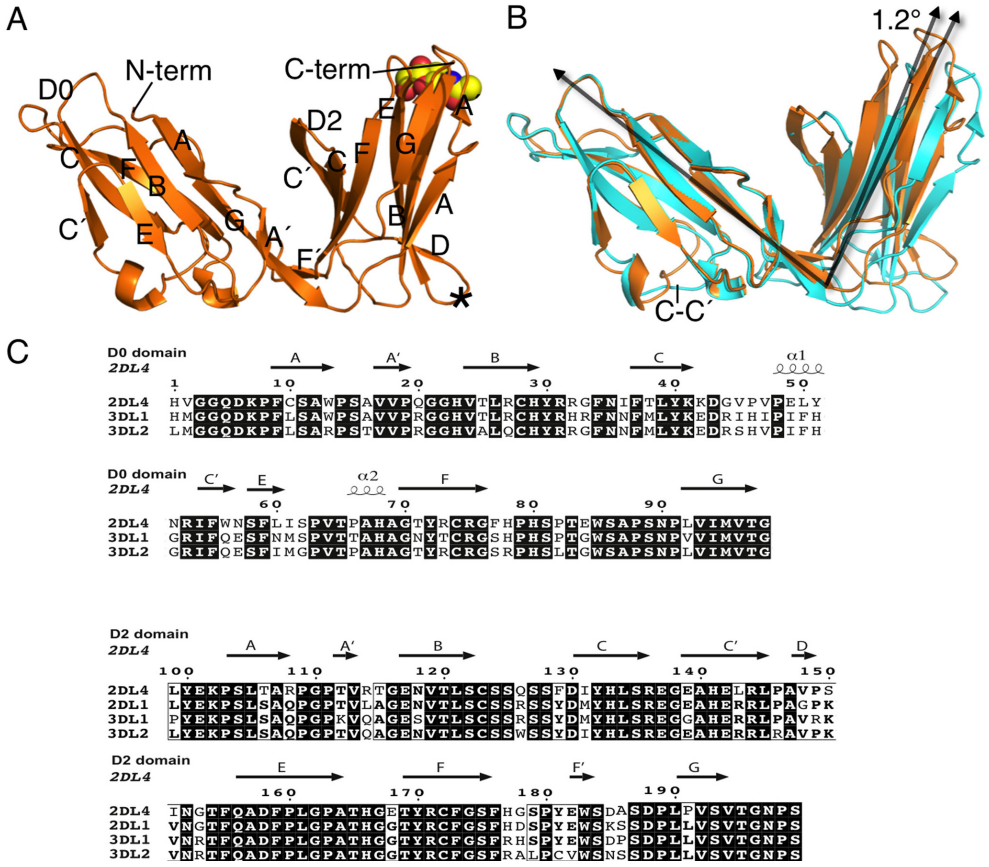

FIGURE 1. **Overall structure of KIR2DL4.** *A*, schematic representation of the monomeric KIR2DL4. The secondary structure elements are *labeled*. The position of the *N*-acetylglucosamine at position 118 is indicated as a *space-filling model*. The unmodeled *N*-acetylglucosamine at position 152 is indicated with an *asterisk*. *B*, superposition of the two copies of KIR2DL4 in the asymmetric unit (*orange* and *cyan*). The two copies deviate by 1.2° about the hinge angle of the domains. *C*, sequence alignment of the D0 and D2 domains of KIR2DL4 with KIR2DL1, KIR3DL1, and KIR3DL2.

2, *C* and *D*). The interface of the tetramer was dominated by residues in the D0 domain.

The translational dimer buried a total surface area of ~1400 Å^2, of which ~1080 Å^2 (77%) is contributed by the D0 domain (Fig. 2*D*). The D0 domains were arranged head-to-tail with the A and A′ strands and their interconnecting loop of one D0 domain packing against the C strand and the F-G loop of the other D0 domain (Fig. 3*A*). Interestingly, the A strand residues Phe^9, Ser^{11}, and Trp^{13} that were previously shown to be important in KIR3DL1 binding to HLA-B*57:01 (10) were integral to this interface, clustering with Thr^{38}, Tyr^{40}, Pro^{82}, Thr^{83}, and Trp^{85} on the opposing protomer's C strand (Fig. 3*A*). There were three hydrogen bonds at this interface, two between the D0 domains (Tyr^{51} Oη–Ser^{62} Oη and Arg^{75} Nϵ–Pro^{14} O) and one between the D2 domains (Tyr^{181} Oη–Arg^{171} Nη2) as well as a salt bridge linking the D0 and D2 domains, Arg^{73}–Glu^{137} (Fig. 3*A*). Accordingly, this interface was predominantly formed through VDW contacts. Similarly, the rotational dimer buried a total surface area of ~1110 Å^2 entirely contributed by the D0 domains. This interface contained no hydrogen bonds and was formed through a symmetric clustering of hydrophobic residues (Fig. 3*B*). Specifically, Phe^{34}, Ile^{36}, Arg^{53}, Ile^{54}, Phe^{77}, and Pro^{79} spanning the B-C, C-C′, C′-E, and F-G loops formed a large hydrophobic cluster with their symmetry counterparts (Fig. 3*B*). Flanking this central core were Phe^{77} and Trp^{85} on the interconnecting loop between the F and G strands that packed against Trp^{56} on the C′-E loop (Fig. 3*B*). Together, the tetramer interface was extensive, burying a total surface area of 4550 Å^2 and displayed good shape complementarity of 0.6 (46). Mutational experiments at the tetramer interface (F34A, W56A, F77A, and W85A) resulted in aggregated protein (data not shown). This suggests that residues at the interface and the self-association of KIR2LD4 are important to the stability of the protein.

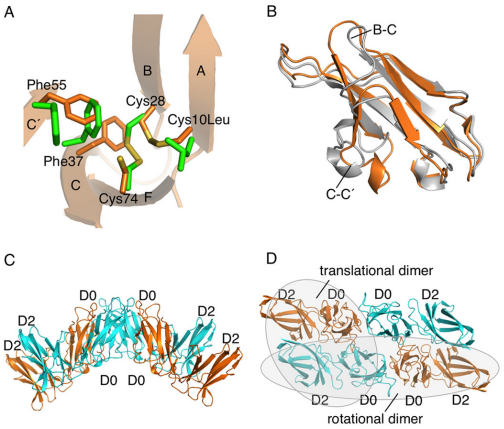

FIGURE 2. **Comparison of D0 domains from KIR2DL4 and KIR3DL1.** *A*, the trio of cysteines in KIR2DL4 D0 domain (*orange*) overlaid with the equivalent position in KIR3DL1 (*green*). The effect of the disulfide exchange on the residues Phe^{37} and Phe^{55} on the C and C′ strands is shown. *B*, superposition of the D0 from KIR2DL4 (*orange*) with that from KIR3DL1 (*gray*). *Labeled* are the major points of deviation at the B-C and C-C′ loops. *C*, KIR2DL4 tetramer formed by crystallographic symmetry. *D*, decomposition of the KIR2DL4 tetramer into rotational and translational dimers.

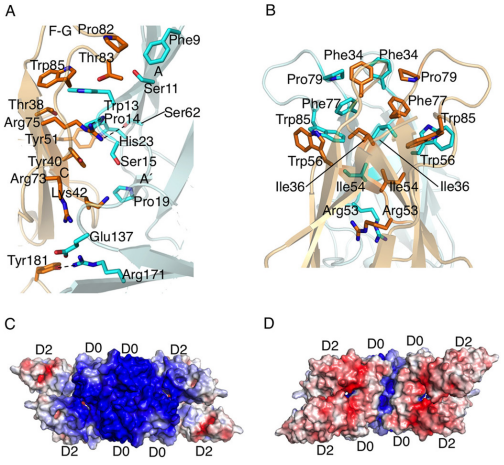

FIGURE 3. **Residues at the interface of the tetramer and mapping of electrostatic potential to the surface of KIR2DL4.** *A*, residues at the translational dimer interface. Residues on each subunit of the dimer are *colored orange* and *cyan*, respectively. *B*, residues at the rotational dimer interface. Residues on each subunit of the dimer are *colored orange* and *cyan*, respectively. *C*, the membrane proximal surface potential is predominantly electropositive (*blue*) due to the charge on the D0 domains. *D*, the membrane distal surface potential is predominantly electronegative (*red*) due to the charge on the D2 domains.

In order to determine whether the recombinant KIR2DL4 tetramer was comparable with physiological KIR2DL4, we measured binding to mAb 33 by ELISA. mAb 33 has been previously shown to recognize KIR2DL4 *in vivo* (34). The mAb 33 bound KIR2DL4 in a concentration-dependent manner and did not bind to the control KIR2DL2 (data not shown). Thus, this antibody that recognizes intracellular KIR2DL4 also recognizes our recombinantly produced KIR2DL4, which we observe to be predominantly in tetrameric form.

The tetramerization of KIR2DL4 resulted in the grouping of charged regions to form continuous, large, charged patches on the surface of the protein (Fig. 3, *C* and *D*). The charge distribution on KIR2DL4 was dipolar, with the D0 domain carrying a large positive charge on the membrane proximal face, whereas the D2 domain displayed a negative charge on the membrane distal face (Fig. 3, *C* and *D*). This large electropositive patch is a feature of the D0 domain and is absent in other KIR2DL structures solved to data. Further, relative to the membrane, the orientation of the positively charged region on KIR2DL4 is the converse to that observed in KIR3DL1. Thus, the distribution and orientation of the charged regions are unique to KIR2DL4.

Comparison with KIR2DLs and KIR3DL1 Structures

The D0 domain of KIR2DL4 shared ~81, 83, and 85% sequence similarity with the D0 domains from KIR3DL1, KIR3DL2, and KIR2DL5, respectively. The predominant area of sequence divergence corresponded to the C-C′ loop (Figs. 1*C* and 2*B*) that was associated with the tetramer interface. Compounding this difference were substitutions at Cys^{10} (discussed above) and Trp^{56} (Gln) and Phe^{77} (Ser) that were integral to the hydrophobic core of the oligomerization interface (Figs. 1*C* and 3*B*). These deviations at the C-C′ loop and at positions 10, 56, and 77 were conserved across primate species and are probably key determinants of the self-association. By contrast, the D2 domain shared between 88 and 90% sequence similarity across the KIR family and lacked continuous regions that were unique in sequence to KIR2DL4. Accordingly, the unique self-association of KIR2DL4 was probably a result of discrete structural alterations in the D0 domain.

The interdomain angle in KIR2DL4 more closely resembled that of the D0-D1 angle in KIR3DL1 (82.4°) than the D1-D2 angles observed in other KIR structures. Typically, the equivalent D1-D2 arrangement is more acute (ranging from 66° for KIR2DL1 to 81° for KIR2DL2). Notwithstanding the differences in the interdomain angle, the structure of the D2 domain in KIR2DL4 was conserved with that of other KIR structures (r.m.s. deviation ranging from 0.75 Å for KIR2DS4 to 0.90 Å for KIR2DL1). Interestingly, D2 residues that formed HLA contacts in KIR2DL1/2 and KIR3DL1, including the critical residues Tyr^{100}, Phe^{176}, and Glu^{182} are conserved in KIR2DL4 (Fig. 1*C*).

By contrast, the structure of the D0 domain deviates significantly (r.m.s. deviation of 3.5 Å) from that of KIR3DL1. The major deviations occur at the B-C (7 Å) and C-C′ loops (12 Å). These regions are directly impacted upon by the Cys^{10}–Cys^{28} disulfide bond and are involved at the interface of the tetramer (Fig. 2, *A* and *B*). Furthermore, the residues on the D0 domain important for KIR3DL1 binding to HLA are instead contributing to the tetramer interface in KIR2DL4. Namely, the A strand residues Phe^{9}, Ser^{11}, and Trp^{13} were shown in KIR3DL1 to bind to the β1-β2 loop of HLA, whereas in KIR2DL4 they interact with the F-G loop (residues 82–85) at the tetramer interface (Fig. 3*A*). Further-

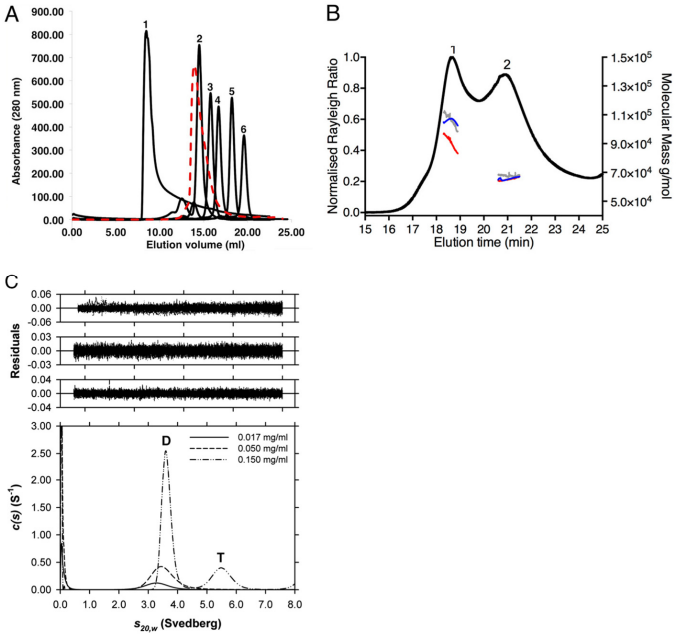

FIGURE 4. **Biophysical characterization of KIR2DL4.** *A*, size exclusion profile of purified KIR2DL4 (*red dashed line*) run on a S200 10/30 column compared with known analytical standards. Standards are as follows: BDX (2000 kDa) (*1*), conalbumin (75 kDa) (*2*), ovalbumin (44 kDa) (*3*), carbonic anhydrase (29 kDa) (*4*), ribonuclease A (13.7 kDa) (*5*), and aprotinin (6.5 kDa) (*6*). *B*, molecular mass estimations by SEC-MALS. The light scattering (at 90°) from 10 mg/ml KIR2DL4 is shown in *black*. The molecular mass estimations from three different KIR2DL4 concentrations are shown (3 mg/ml in *red*, 5 mg/ml in *gray*, and 10 mg/ml in *blue*). *C*, sedimentation velocity analysis of KIR2DL4. The continuous sedimentation coefficient ($c(s)$) distribution is plotted as a function of the standardized sedimentation coefficient for KIR2DL4 at 0.017 mg/ml (*solid line*), 0.05 mg/ml (*dashed line*), and 0.15 mg/ml (*dashed and dotted line*). The KIR2DL4 dimer and tetramer are indicated with *D* and *T*, respectively. Sedimentation velocity experiments were conducted in a Beckman model XL-I analytical ultracentrifuge as described under "Experimental Procedures." Continuous size distribution analysis was performed using the program SEDFIT at a resolution of 200, with s_{min} = 0 S, s_{max} = 8 S, and p = 0.95 (28–30).

more, Phe[34] that similarly binds the β1-β2 loop of HLA in KIR3DL1 was observed to have shifted 7.4 Å in KIR2DL4 to form an integral part of the tetramer interface (Figs. 2*B* and 3B). Clearly, by reassigning residues to forming the tetramer interface, the D0 domain of the KIR2DL4 multimer cannot engage HLA analogously to KIR3DL1.

KIR2DL4 Tetramers Do Not Interact with pHLA-Ia or HLA-G in Direct Binding Studies

To probe the interaction between KIR2DL4 and pHLA-Ia, a panel of 100 pHLA-Ia comprising HLA-A, -B, and -C was screened via a single HLA-antigen bead assay. For each of the HLAs, no binding was observed above the background level determined by the negative control (data not shown). Further, binding to HLA-G (with the peptides RIIPRHLQL and RLPKDFRIL) was assessed by surface plasmon resonance. The experiment was performed in two orientations (*i.e.* with either HLA-G (and the control HLA-B*57:01) coupled to the chip via the monoclonal antibody W6/32 or by KIR2DL4 coupled to the chip with the anti-His_6 monoclonal antibody 4D11). No interaction between KIR2DL4 and HLA-G was observed regardless of orientation (data not shown).

Biophysical Characterization of the Oligomeric State of KIR2DL4

Size Exclusion Chromatography and Dynamic Light Scattering—The tetrameric assembly observed in the crystal lattice of KIR2DL4 prompted further investigation by a number of biophysical techniques, first by analytical size exclusion chromatography performed on a Superdex S200 10/30 column equilibrated in either a buffer solution comprising 10 mM Tris, pH 8.0, and 150 mM NaCl or in a buffer comprising 10 mM citrate, pH 5.5, and 150 mM NaCl. In both running buffers, KIR2DL4 was observed to elute predominantly at a molecular weight consistent with a 100-kDa protein (14.8 ml), with a trailing edge to the elution peak consistent with a 50-kDa protein (15.2 ml) when compared with a set of known standards (Fig. 4*A*). This corresponded to protein species with molecular weights consistent with tetramers and dimers of KIR2DL4 in solution.

The molecular mass of KIR2DL4 was further analyzed using SEC-MALS. Signals from the MALS were normalized using BSA. Three different concentrations of KIR2DL4 (3, 5, and 10 mg/ml) were injected onto the column with a pore size of ~300 Å, with all three concentrations resulting in identical light scat-

tering profiles (Fig. 6). Two major peaks were observed with retention times of 18.57 and 20.80 min (Fig. 4*B*). The MALS estimated molecular mass for peak 1 at 10, 5, and 3 mg was 107.1 kDa ± 2.73%, 107.3 kDa ± 1.84%, and 97.2 kDa ± 3.34%, respectively. The MALS estimated molecular mass for peak 2 at 10, 5, and 3 mg was 64.5 kDa ± 3.33%, 67.7 kDa ± 2.27%, and 64.5 kDa ± 4.12%, respectively (Fig. 6). These molecular masses are consistent with peak 1 representing a tetramer and peak 2 representing a dimer of KIR2DL4 in solution.

Analytical Ultracentrifugation—To determine the quaternary structure of KIR2DL4 in aqueous solution, sedimentation velocity studies were performed using analytical ultracentrifugation (Table 2). Data at multiple time points generated at a rotor speed of 40,000 rpm were fitted to a continuous size distribution model (28–30). The resulting $c(s)$ distributions at initial concentrations of 0.017, 0.05, and 0.15 mg/ml are compared in Fig. 4*C*, which shows that KIR2DL4 undergoes concentration-dependent self-association. At low protein concentrations of 0.017 and 0.05 mg/ml, the protein exists as a single peak spanning a sedimentation coefficient range of 2.5–4.5 S. This suggests that KIR2DL4 exists in a rapid monomer-dimer equilibrium at low protein concentrations. However, at the higher protein concentration of 0.15 mg/ml, KIR2DL4 forms dimers (s = 3.5 S) and tetramers (s = 5.5 S). The hydrodynamic properties of the KIR2DL4 dimer and tetramer are reported in Table 2.

Small Angle X-ray Scattering—To further probe KIR2DL4 oligomerization, we performed small angle x-ray scattering analysis at a range of protein concentrations (Fig. 5, *A–C*). KIR2DL4 was observed to undergo a concentration-dependent increase in molecular mass, radius of gyration, and maximal particle dimension, indicating that the molecule has a propensity to oligomerize in solution (Table 3). These effects were not due to the presence of nonspecific protein aggregation, as judged by the linearity of Guinier plots (Fig. 5). At low protein concentrations (0.3 mg/ml), KIR2DL4 had a molecular mass of 49 kDa, suggesting that the predominant species present at this

TABLE 2
Hydrodynamic properties of KIR2DL4 oligomers

Oligomeric species	$s^0_{20,w}$ [a]	f/f_0 [b]
	S	
Dimer	3.6	1.3
Tetramer	5.5	1.4

[a] Standardized sedimentation coefficient obtained from the ordinate maxima of the $c(s)$ distribution peaks calculated at a KIR2DL4 concentration of 0.15 mg/ml (Fig. 1).
[b] Frictional ratio calculated using the $\bar{\nu}$ method (57).

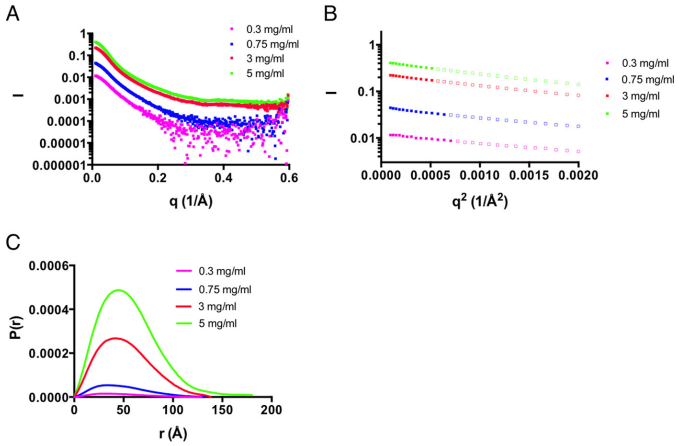

FIGURE 5. **KIR2DL4 SAXS data analysis.** *A*, raw SAXS scattering curves for KIR2DL4 recorded at a range of protein concentrations. *B*, the low angle region of the SAXS curves are represented as Guinier plots, which, for well behaving samples are linear for values of $q \leq 1/R_g$ (*filled squares*). *C*, distance distribution function. The distributions of interatomic spacings are represented as $p(r)$ plots.

TABLE 3
Summary of SAXS measurements

The radius of gyration (R_g) calculated by Guinier analysis and the indirect transfer program GNOM, the maximal particle dimension (D_{max}), molecular mass (MM) and oligomeric status of KIR2DL4 and KIR2DL2 were determined by SAXS at a range of protein concentrations. The oligomeric status was calculated by dividing the observed molecular mass by that calculated from the amino acid sequence.

Sample	Concentration	R_g, Guinier	R_g, GNOM	D_{max}	MM	Oligomeric status	$I(0)$
	mg/ml	*Å*	*Å*	*Å*	*kDa*		
KIR2DL4	0.35	36.9	37.7	129.0	49.0	1.9	0.0120
	0.75	38.8	39.1	132.3	87.0	3.3	0.044
	3	40.9	41.2	138.3	113.0	4.3	0.230
	5	42.5	45.8	159.1	125.0	4.8	0.420
KIR2DL2	0.35	29.3	22.4	71.8	25.1	1.0	0.006
	0.7	23.3	23.8	79.8	27.2	1.1	0.013
	1.4	24.3	25.2	85.4	28.3	1.2	0.027

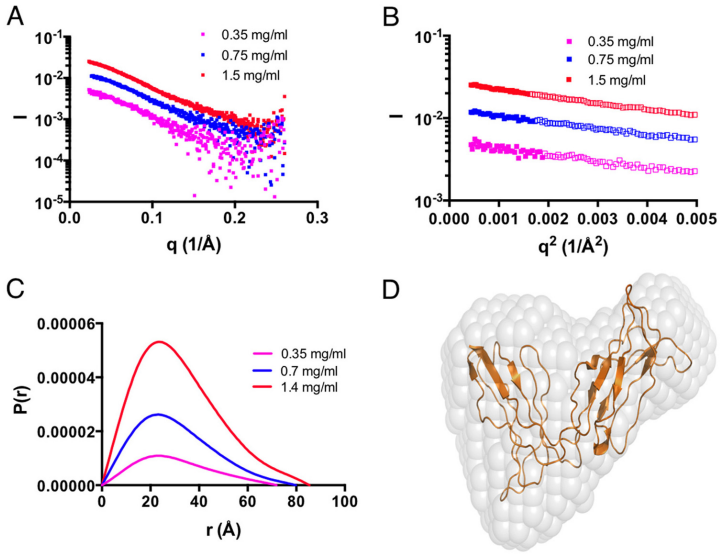

FIGURE 6. **KIR2DL2 SAXS data analysis.** *A*, raw SAXS scattering curves for KIR2DL2 recorded at a range of protein concentrations. *B*, the low angle region of the SAXS curves are represented as Guinier plots, which, for well behaving samples are linear for values of $q \leq 1/R_g$ (*filled squares*). *C*, distance distribution function. The distributions of interatomic spacings are represented as $p(r)$ plots. *D*, DAMMIF *ab initio* model overlaid with the structure of KIR2DL2.

concentration is a dimer. At the highest concentration tested (5 mg/ml), KIR2DL4 had a molecular mass of 125 kDa, which corresponds to an oligomeric status of 4.8. Accordingly, KIR2DL4 has the capacity to form tetramers and potentially even higher order oligomers. In contrast, KIR2DL2, another two-domain KIR with a D1-D2 arrangement, has a mass (25.1–28.3 kDa) that was consistent with that predicted for a monomer (23 kDa) and did not change appreciably with increasing protein concentrations (Table 3) (Fig. 6, *A–C*). The *ab initio* SAXS model derived from this data overlaid well with the structure of KIR2DL2 (Fig. 6*D*), further supporting the conclusion that KIR2DL2 is monomeric in solution. Thus, our data suggest that the ability to oligomerize is not a general feature of KIRs.

To gain an insight into the shape of KIR2DL4 in solution, we performed *ab initio* modeling using the SAXS data that best correspond to the KIR2DL4 dimer (0.35 mg/ml, oligomeric status 1.9) and tetramer (3 mg/ml, oligomeric status 4.3). At 0.35 mg/ml, KIR2DL4 has a butterfly-like appearance with approximate dimensions 130 × 55 × 40 Å that overlaid well with the extended head-to-head dimer (Fig. 7*A*) but not the more compact side-by-side dimer (Fig. 7*B*). At 3 mg/ml, the KIR2DL4 SAXS envelope retains the appearance of a flattened particle but is markedly wider, with approximate dimensions of 140 × 80 × 35 Å. The 3 mg/ml SAXS model overlays reasonably well with the KIR2DL4 tetramer observed within the crystal lattice (Fig. 7*C*). Overall, our SAXS data indicate that KIR2DL4 dimerizes via D0-mediated head-to-head interactions and that tetramers and potentially larger order oligomers can be formed from the stepwise lateral association of further KIR2DL4 molecules (Fig. 7*D*).

DISCUSSION

KIR2DL4 is atypical and in comparison with other KIRs differs in manner of cellular localization, candidate ligand preference, and structure. The expression of HLA-G, a proposed ligand for KIR2DL4 (47), at the maternal-fetal interface has led to the suggestion that KIR2DL4 is involved in the maintenance of pregnancy. It is postulated that this interaction leads to the activation of NK cells and the secretion of factors that promote vascular remodeling in the uterus (48, 49). To this end, some groups have reported an interaction with HLA-G, whereas other investigations suggest that it does not (23, 24). Hence, to further understand this enigmatic molecule, we studied KIR2DL4 structurally and by a number of biophysical techniques.

We showed that, unlike other KIR receptors, KIR2DL4 oligomerizes in a concentration-dependent manner. KIR2DL4 was observed as a tetramer in the crystal lattice and in a dimer-tetramer equilibrium by SEC-MALS, SAXS, and analytical ultracentrifugation. By SAXS, the architecture of the dimer was observed to be more consistent with the crystallographic rotational dimer, raising the possibility that oligomerization may proceed by the lateral addition of rotationally related molecules in a stepwise fashion. This is driven by the association of the D0 domains.

The oligomerization is probably facilitated by key residues in the D0 domain of KIR2LD4. The unique Cys^{10}–Cys^{28} disulfide bond pairing was shown to impact the B-C and C-C′ loops at the interface of the tetramer, giving the D0 domain of KIR2DL4 a conformation that is distinct from that of KIR3DL1. Fur-

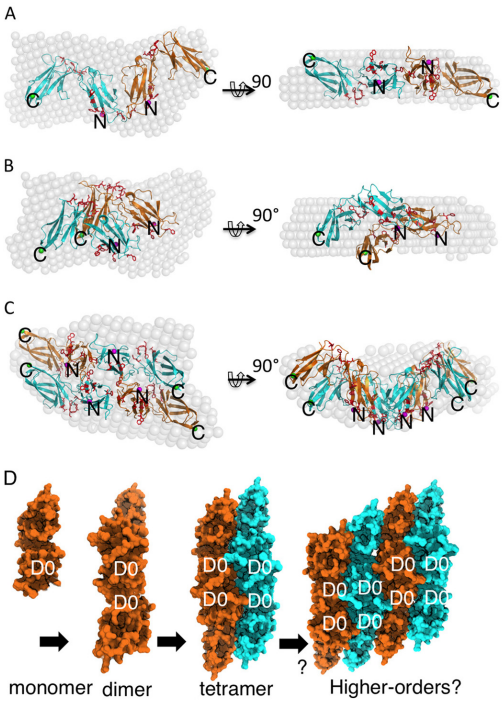

FIGURE 7. **KIR2LD4 SAXS modeling and schematic representation of oligomerization.** *A–C*, DAMMIF *ab initio* models were generated for KIR2DL4. At a concentration of 0.3 mg/ml, the KIR2DL4 oligomeric status is 1.9 (dimer), and at 3 mg/ml, the oligomeric status is 4.3 (tetramer). For *A–C*, the N termini are represented by *magenta spheres* and the letter *N*, and the C termini are shown by *green spheres* and the letter *C*. Residues that contact HLA-B*57:01 in KIR3DL1 are shown by *red sticks*. *A*, fitting the rotational dimer model at 0.3 mg/ml; *B*, fitting the translational dimer model at 0.3 mg/ml; *C*, fitting the tetramer model at 3 mg/ml; *D*, schematic representation of the oligomeric assembly of KIR2DL4. The dimer is assembled by the head-to-head association of KIR2DL4 D0 domains. The stepwise association of dimers assembles the tetramer and higher order oligomers via the D0 domains.

ther, unlike in KIR3DL1, the D0 domain of KIR2DL4 was not glycosylated. The KIR2DL4 residue (Thr^{71}) that is equivalent to the glycosylated residue on the D0 domain of KIR3DL1 (Asn^{71}) abuts the tetramerization interface such that glycosylation at this position would prevent oligomerization of the receptor.

The contribution of conserved residues that are critical to HLA binding in KIR3DL1 to forming the oligomerization interface in KIR2DL4 indicates that the D0 domain of the KIR2DL4 multimer does not bind HLA analogously to the D0-D1 arrangement in KIR3DL1. Whether the KIR2DL4 dimer or tetramer is capable of binding HLA similarly to the D1-D2 arrangement observed for KIR3DL1 and KIR2Ds remains uncertain, although modeling suggests that the docking mode would need to be distinctly different to accommodate the KIR2DL4 tetramer (data not shown). Indeed, we were unable to detect an interaction between KIR2DL4 and a panel of 100 pHLA-Ia by single HLA-antigen bead assay. Further, we were unable to detect an interaction between KIR2DL4 and HLA-G by surface plasmon resonance. Thus, as judged by direct binding investigations, KIR2DL4 does not appear to bind pHLA-I with an appreciable affinity. Certainly, further work is required to elucidate the ligand preference for the receptor. In this vein, the details of the oligomerization of the receptor will provide a base to explore the importance of self-association in regulating ligand binding.

Clues as to potential KIR2DL4 ligands may be seen in the distribution of charge across the molecule. KIR2DL4 has a dipolar charge distribution with the D0 domain carrying an overall electropositive net charge such that the association of these domains in the tetramer forms a large positively charged patch. This is in keeping with the KIR2DL4 D0 domain being the proposed binding site for the negatively charged HSPG (25). The report of HSPG binding to KIR2LD4 is in line with similar studies on the natural cytotoxicity receptors NKp30, NKp44, and NKp46 (50, 51). Similar to this, the positive charge on the KIR3DL2, KIR3DL1/S1, and KIR2DL4 D0 domains has been proposed to act as a pattern recognition motif in the binding of CpG oligodeoxynucleotide (52). Presumably, the role of the D0 domain in these interactions is to provide charge complementarity with the ligands. However, the specificity of the interactions and the role of the other KIR domains are not yet clear. It remains to be substantiated whether HSPG is a functional KIR2LD4 ligand and how specificity for the interaction is achieved.

Oligomerization of KIR2DL4 may be an important mechanism for regulating signal transduction. KIR2DL4 possesses both activating and inhibitory signaling domains. The cytoplasmic immunoreceptor tyrosine-based inhibition motif domain has been reported to elicit functional inhibitory signals (15, 53). However, intracellular KIR2DL4 signaling appears to be predominantly activating, via recruitment of the FcϵR-γ adaptor, resulting in a proinflammatory response characterized by IFN-γ secretion and minimal cytotoxicity (34, 54, 55). Indeed, it has been suggested that vascular remodeling in the uterus during early pregnancy is a result of NK cell senescence from prolonged activatory signaling through KIR2DL4 (49). Whether inhibitory signaling through KIR2DL4 is physiologically significant and whether there is a balance between activating and inhibitory signaling remains unknown. However, oligomerization of the receptor may provide an important means for regulating signal output, by either sequestering or concentrating local regions for adaptor protein and signaling protein binding. Further, the ability of KIR2DL4 to recruit signaling proteins to the endosome may provide a scaffold to regulate NK cell signal transduction in isolation from the cell surface (56). Whether KIR2DL4 functions as an immunoregulatory scaffold protein and the role of self-association in coordinating signaling are questions that remain to be answered.

Acknowledgments—Crystallization experiments were performed at the Monash Macromolecular Crystallization Facility (Monash University, Victoria, Australia). This research was undertaken in part on the MX2 and SAXS/WAXS beamlines at the Australian Synchrotron (Victoria, Australia).

REFERENCES

1. Jost, S., and Altfeld, M. (2013) Control of human viral infections by natural killer cells. *Annu. Rev. Immunol.* **31,** 163–194
2. Costello, R. T., Sivori, S., Marcenaro, E., Lafage-Pochitaloff, M., Mozziconacci, M. J., Reviron, D., Gastaut, J. A., Pende, D., Olive, D., and Moretta, A. (2002) Defective expression and function of natural killer cell-triggering receptors in patients with acute myeloid leukemia. *Blood* **99,** 3661–3667
3. Raffaghello, L., Prigione, I., Airoldi, I., Camoriano, M., Levreri, I., Gambini, C., Pende, D., Steinle, A., Ferrone, S., and Pistoia, V. (2004) Downregulation and/or release of NKG2D ligands as immune evasion strategy of human neuroblastoma. *Neoplasia* **6,** 558–568
4. Liu, J., Xiao, Z., Ko, H. L., Shen, M., and Ren, E. C. (2014) Activating killer cell immunoglobulin-like receptor 2DS2 binds to HLA-A*11. *Proc. Natl. Acad. Sci. U.S.A.* **111,** 2662–2667
5. Saulquin, X., Gastinel, L. N., and Vivier, E. (2003) Crystal structure of the human natural killer cell activating receptor KIR2DS2 (CD158j). *J. Exp. Med.* **197,** 933–938
6. Graef, T., Moesta, A. K., Norman, P. J., Abi-Rached, L., Vago, L., Older Aguilar, A. M., Gleimer, M., Hammond, J. A., Guethlein, L. A., Bushnell, D. A., Robinson, P. J., and Parham, P. (2009) KIR2DS4 is a product of gene conversion with KIR3DL2 that introduced specificity for HLA-A*11 while diminishing avidity for HLA-C. *J. Exp. Med.* **206,** 2557–2572
7. Maenaka, K., Juji, T., Stuart, D. I., and Jones, E. Y. (1999) Crystal structure of the human p58 killer cell inhibitory receptor (KIR2DL3) specific for HLA-Cw3-related MHC class I. *Structure* **7,** 391–398
8. Boyington, J. C., Motyka, S. A., Schuck, P., Brooks, A. G., and Sun, P. D. (2000) Crystal structure of an NK cell immunoglobulin-like receptor in complex with its class I MHC ligand. *Nature* **405,** 537–543
9. Fan, Q. R., Long, E. O., and Wiley, D. C. (2001) Crystal structure of the human natural killer cell inhibitory receptor KIR2DL1-HLA-Cw4 complex. *Nat. Immunol.* **2,** 452–460
10. Vivian, J. P., Duncan, R. C., Berry, R., O'Connor, G. M., Reid, H. H., Beddoe, T., Gras, S., Saunders, P. M., Olshina, M. A., Widjaja, J. M., Harpur, C. M., Lin, J., Maloveste, S. M., Price, D. A., Lafont, B. A., McVicar, D. W., Clements, C. S., Brooks, A. G., and Rossjohn, J. (2011) Killer cell immunoglobulin-like receptor 3DL1-mediated recognition of human leukocyte antigen B. *Nature* **479,** 401–405
11. Finton, K. A., and Strong, R. K. (2012) Structural insights into activation of antiviral NK cell responses. *Immunol. Rev.* **250,** 239–257
12. O'Connor, G. M., Vivian, J. P., Widjaja, J. M., Bridgeman, J. S., Gostick, E., Lafont, B. A., Anderson, S. K., Price, D. A., Brooks, A. G., Rossjohn, J., and McVicar, D. W. (2014) Mutational and structural analysis of KIR3DL1 reveals a lineage-defining allotypic dimorphism that impacts both HLA and peptide sensitivity. *J. Immunol.* **192,** 2875–2884
13. McVicar, D. W., and Burshtyn, D. N. (2001) Intracellular signaling by the killer immunoglobulin-like receptors and Ly49. *Sci. STKE* **2001,** re1
14. Burshtyn, D. N., Scharenberg, A. M., Wagtmann, N., Rajagopalan, S., Berrada, K., Yi, T., Kinet, J. P., and Long, E. O. (1996) Recruitment of tyrosine phosphatase HCP by the killer cell inhibitor receptor. *Immunity* **4,** 77–85
15. Faure, M., and Long, E. O. (2002) KIR2DL4 (CD158d), an NK cell-activating receptor with inhibitory potential. *J. Immunol.* **168,** 6208–6214
16. Kikuchi-Maki, A., Catina, T. L., and Campbell, K. S. (2005) Cutting edge: KIR2DL4 transduces signals into human NK cells through association with the Fc receptor γ protein. *J. Immunol.* **174,** 3859–3863
17. Rajagopalan, S. (2010) Endosomal signaling and a novel pathway defined by the natural killer receptor KIR2DL4 (CD158d). *Traffic* **11,** 1381–1390
18. Moesta, A. K., Norman, P. J., Yawata, M., Yawata, N., Gleimer, M., and Parham, P. (2008) Synergistic polymorphism at two positions distal to the ligand-binding site makes KIR2DL2 a stronger receptor for HLA-C than KIR2DL3. *J. Immunol.* **180,** 3969–3979
19. Gumperz, J. E., Barber, L. D., Valiante, N. M., Percival, L., Phillips, J. H., Lanier, L. L., and Parham, P. (1997) Conserved and variable residues within the Bw4 motif of HLA-B make separable contributions to recognition by the NKB1 killer cell-inhibitory receptor. *J. Immunol.* **158,** 5237–5241
20. Hansasuta, P., Dong, T., Thananchai, H., Weekes, M., Willberg, C., Aldemir, H., Rowland-Jones, S., and Braud, V. M. (2004) Recognition of HLA-A3 and HLA-A11 by KIR3DL2 is peptide-specific. *Eur. J. Immunol.* **34,** 1673–1679
21. Rajagopalan, S., Bryceson, Y. T., Kuppusamy, S. P., Geraghty, D. E., van der Meer, A., Joosten, I., and Long, E. O. (2006) Activation of NK cells by an endocytosed receptor for soluble HLA-G. *PLoS Biol.* **4,** e9
22. Clements, C. S., Kjer-Nielsen, L., Kostenko, L., Hoare, H. L., Dunstone, M. A., Moses, E., Freed, K., Brooks, A. G., Rossjohn, J., and McCluskey, J. (2005) Crystal structure of HLA-G: a nonclassical MHC class I molecule expressed at the fetal-maternal interface. *Proc. Natl. Acad. Sci. U.S.A.* **102,** 3360–3365
23. Boyson, J. E., Erskine, R., Whitman, M. C., Chiu, M., Lau, J. M., Koopman, L. A., Valter, M. M., Angelisova, P., Horejsi, V., and Strominger, J. L. (2002) Disulfide bond-mediated dimerization of HLA-G on the cell surface. *Proc. Natl. Acad. Sci. U.S.A.* **99,** 16180–16185
24. Le Page, M. E., Goodridge, J. P., John, E., Christiansen, F. T., and Witt, C. S. (2014) Killer Ig-like receptor 2DL4 does not mediate NK cell IFN-γ responses to soluble HLA-G preparations. *J. Immunol.* **192,** 732–740
25. Brusilovsky, M., Cordoba, M., Rosental, B., Hershkovitz, O., Andrake, M. D., Pecherskaya, A., Einarson, M. B., Zhou, Y., Braiman, A., Campbell, K. S., and Porgador, A. (2013) Genome-wide siRNA screen reveals a new cellular partner of NK cell receptor KIR2DL4: heparan sulfate directly modulates KIR2DL4-mediated responses. *J. Immunol.* **191,** 5256–5267
26. Stifter, S. A., Gould, J. A., Mangan, N. E., Reid, H. H., Rossjohn, J., Hertzog, P. J., and de Weerd, N. A. (2014) Purification and biological characterization of soluble, recombinant mouse IFNβ expressed in insect cells. *Protein Expr. Purif.* **94,** 7–14
27. Aricescu, A. R., Lu, W., and Jones, E. Y. (2006) A time- and cost-efficient system for high-level protein production in mammalian cells. *Acta Crystallogr. D Biol. Crystallogr.* **62,** 1243–1250
28. Perugini, M. A., Schuck, P., and Howlett, G. J. (2000) Self-association of human apolipoprotein E3 and E4 in the presence and absence of phospholipid. *J. Biol. Chem.* **275,** 36758–36765
29. Schuck, P. (2000) Size-distribution analysis of macromolecules by sedimentation velocity ultracentrifugation and Lamm equation modeling. *Biophys. J.* **78,** 1606–1619
30. Schuck, P., Perugini, M. A., Gonzales, N. R., Howlett, G. J., and Schubert, D. (2002) Size-distribution analysis of proteins by analytical ultracentrifugation: strategies and application to model systems. *Biophys. J.* **82,** 1096–1111
31. Clements, C. S., Kjer-Nielsen, L., Kostenko, L., McCluskey, J., and Rossjohn, J. (2006) The production, purification and crystallization of a soluble form of the nonclassical MHC HLA-G: the essential role of cobalt. *Acta Crystallogr. Sect. F Struct. Biol. Cryst. Commun.* **62,** 70–73
32. Saunders, P. M., Vivian, J. P., Baschuk, N., Beddoe, T., Widjaja, J., O'Connor, G. M., Hitchen, C., Pymm, P., Andrews, D. M., Gras, S., McVicar, D. W., Rossjohn, J., and Brooks, A. G. (2015) The interaction of KIR3DL1*001 with HLA class I molecules is dependent upon molecular microarchitecture within the Bw4 epitope. *J. Immunol.* **194,** 781–789
33. Parham, P., Barnstable, C. J., and Bodmer, W. F. (1979) Use of a monoclonal antibody (W6/32) in structural studies of HLA-A,B,C, antigens. *J. Immunol.* **123,** 342–349
34. Rajagopalan, S., Fu, J., and Long, E. O. (2001) Cutting edge: induction of IFN-γ production but not cytotoxicity by the killer cell Ig-like receptor KIR2DL4 (CD158d) in resting NK cells. *J. Immunol.* **167,** 1877–1881
35. Goding, J. W. (1996) *Monoclonal Antibodies: Principles and Practice*, Chapter 10, pp. 234–326, Elsevier Science, Amsterdam
36. Semenyuk, A. V., and Svergun, D. I. (1991) GNOM: a program package for small-angle scattering data processing. *J. Appl. Crystallogr.* **24,** 537–540
37. Franke, D., and Svergun, D. I. (2009) DAMMIF, a program for rapid *ab-initio* shape determination in small-angle scattering. *J. Appl. Crystallogr.* **42,** 342–346
38. Collaborative Computational Project, Number 4 (1994) The CCP4 suite: programs for protein crystallography. *Acta Crystallogr. D Biol. Crystallogr.* **50,** 760–763
39. Evans, P. (2006) Scaling and assessment of data quality. *Acta Crystallogr. D Biol. Crystallogr.* **62,** 72–82
40. Leslie, A. G. W. (1992) Recent changes to the MOSFLM package for process-

ing film and image plate data. *Joint CCP4 + ESF-EAMCB Newsletter on Protein Crystallography*, Number 26, Daresbury Laboratory, Warrington, UK
41. McCoy, A. J., Grosse-Kunstleve, R. W., Adams, P. D., Winn, M. D., Storoni, L. C., and Read, R. J. (2007) Phaser crystallographic software. *J. Appl. Crystallogr.* **40,** 658–674
42. Emsley, P., and Cowtan, K. (2004) Coot: model-building tools for molecular graphics. *Acta Crystallogr. D Biol. Crystallogr.* **60,** 2126–2132
43. Adams, P. D., Afonine, P. V., Bunkóczi, G., Chen, V. B., Davis, I. W., Echols, N., Headd, J. J., Hung, L. W., Kapral, G. J., Grosse-Kunstleve, R. W., McCoy, A. J., Moriarty, N. W., Oeffner, R., Read, R. J., Richardson, D. C., Richardson, J. S., Terwilliger, T. C., and Zwart, P. H. (2010) PHENIX: a comprehensive Python-based system for macromolecular structure solution. *Acta Crystallogr. D Biol. Crystallogr.* **66,** 213–221
44. Chen, V. B., Arendall, W. B., 3rd, Headd, J. J., Keedy, D. A., Immormino, R. M., Kapral, G. J., Murray, L. W., Richardson, J. S., and Richardson, D. C. (2010) MolProbity: all-atom structure validation for macromolecular crystallography. *Acta Crystallogr. D Biol. Crystallogr.* **66,** 12–21
45. Halaby, D. M., Poupon, A., and Mornon, J. (1999) The immunoglobulin fold family: sequence analysis and 3D structure comparisons. *Protein Eng.* **12,** 563–571
46. Lawrence, M. C., and Colman, P. M. (1993) Shape complementarity at protein/protein interfaces. *J. Mol. Biol.* **234,** 946–950
47. Rajagopalan, S., and Long, E. O. (2012) KIR2DL4 (CD158d): An activation receptor for HLA-G. *Front. Immunol.* **3,** 258
48. Rajagopalan, S. (2014) HLA-G-mediated NK cell senescence promotes vascular remodeling: implications for reproduction. *Cell. Mol. Immunol.* **11,** 460–466
49. Rajagopalan, S., and Long, E. O. (2012) Cellular senescence induced by CD158d reprograms natural killer cells to promote vascular remodeling. *Proc. Natl. Acad. Sci. U.S.A.* **109,** 20596–20601
50. Bloushtain, N., Qimron, U., Bar-Ilan, A., Hershkovitz, O., Gazit, R., Fima, E., Korc, M., Vlodavsky, I., Bovin, N. V., and Porgador, A. (2004) Membrane-associated heparan sulfate proteoglycans are involved in the recognition of cellular targets by NKp30 and NKp46. *J. Immunol.* **173,** 2392–2401
51. Hecht, M. L., Rosental, B., Horlacher, T., Hershkovitz, O., De Paz, J. L., Noti, C., Schauer, S., Porgador, A., and Seeberger, P. H. (2009) Natural cytotoxicity receptors NKp30, NKp44 and NKp46 bind to different heparan sulfate/heparin sequences. *J. Proteome Res.* **8,** 712–720
52. Sivori, S., Falco, M., Carlomagno, S., Romeo, E., Soldani, C., Bensussan, A., Viola, A., Moretta, L., and Moretta, A. (2010) A novel KIR-associated function: evidence that CpG DNA uptake and shuttling to early endosomes is mediated by KIR3DL2. *Blood* **116,** 1637–1647
53. Cantoni, C., Verdiani, S., Falco, M., Pessino, A., Cilli, M., Conte, R., Pende, D., Ponte, M., Mikaelsson, M. S., Moretta, L., and Biassoni, R. (1998) p49, a putative HLA class I-specific inhibitory NK receptor belonging to the immunoglobulin superfamily. *Eur. J. Immunol.* **28,** 1980–1990
54. Kikuchi-Maki, A., Yusa, S., Catina, T. L., and Campbell, K. S. (2003) KIR2DL4 is an IL-2-regulated NK cell receptor that exhibits limited expression in humans but triggers strong IFN-γ production. *J. Immunol.* **171,** 3415–3425
55. Goodridge, J. P., Witt, C. S., Christiansen, F. T., and Warren, H. S. (2003) KIR2DL4 (CD158d) genotype influences expression and function in NK cells. *J. Immunol.* **171,** 1768–1774
56. Shaw, A. S., and Filbert, E. L. (2009) Scaffold proteins and immune-cell signalling. *Nat. Rev. Immunol.* **9,** 47–56
57. Laue, T. M., Shah, B. D., Ridgeway, T. M., Pelletier, S. L. (1991) in *Analytical Ultracentrifugation in Biochemistry and Polymer Science*, pp. 90–125, Royal Society of Chemistry, London
58. Brown, P. H., Balbo, A., and Schuck, P. (2007). Using prior knowledge in the determination of macromolecular size distributions by analytical ultracentrifugation. *Biomacromolecules* **8,** 2011–2024

4 Chapter 4: Discussion

4.1 Overview of discussion:

4.1.1 KIR2DL1, -L2, and -L3: the devil is in the details

Despite the sequence similarity between KIR2DL1, -L2, and -L3 they nonetheless differ in many aspects. For example, KIR2DL1 is reported to be specific for HLA-C2, KIR2DL3 specifically interacts with HLA-C1, and KIR2DL2 that has evolved as a recombinant of KIR2DL1 and -L3, associated predominantly with HLA-C1 but shows functional cross-reactivity with HLA-C2. Further to this, their signaling capacity differs with KIR2DL1 stronger than KIR2DL2 that in turn is stronger than KIR2DL3. Accordingly, there is a hierarchy of specificity KIR2DL1>KIR2DL3>KIR2DL2 and functional output KIR2DL1>KIR2DL2>KIR2DL3. The structural bases of these differences were unresolved.

In determining the crystal structures of KIR2DL2 and -L3, in complex with HLA-C*07:02, I demonstrated that the docking of KIR2DL2 and KIR2DL3 is different. These differences mapped to the α1 domain of HLA-C1. My findings indicate that the buried surface area of the interaction for KIR2DL2 is higher than that of KIR2DL3. I also found that the D1 domain of KIR2DL2 and -L3, as well as the α1 domain of HLA-C1 and -C2 determine the docking mode of the interaction. This observation correlates with the cross-reactivity of KIR2DL2 and goes some way to explaining the functional differences observed between KIR2DL receptors.

4.1.2 KIRDL4: an unusual KIR receptor

KIR2DL4 is a member of KIR2DL subgroup, yet does not comprise a D1-D2 domain arrangement, but instead, has a D0-D2 domain arrangement. Investigations into identifying the ligand for KIR2DL4 led to the suggestion that KIR2DL4 interacts with HLA-G. However, in this study, and from reports from other groups, there was no evidence by direct binding methods of interaction with HLA-G. By characterizing the structural features of KIR2DL4, I showed that KIR2DL4 is an atypical member of the KIR2DL family and unlike other members of this family, it oligomerizes and exists in an equilibrium between dimeric and tetrameric states. This unique feature of KIR2DL4

indicates that in solution its structure is significantly different from other members of KIR family and it does not follow the conventional pattern of KIRs binding to HLA class I molecules.

4.2 Structural basis of the allelic differences between KIR2DL2 and KIR2DL3 and its impact on recognition of HLA-C07:02

4.2.1 Link between KIRs and diseases

Numerous studies on NK cells and their involvement in protection against viral infections and diseases such as HIV (Khakoo et al., 2004), and HSCT (Ruggeri et al., 2002) highlight the key role of KIRs and their reactive HLA class I ligands in immunity and the health of human beings (reviewed in (Moesta and Parham, 2012)). It has been shown that homozygosity or heterozygosity for KIRs haplotype A or B is linked to different diseases such as HIV infection, hepatitis C, auto-immune diseases, preeclampsia and miscarriage (Boyton and Altmann, 2007, Rajagopalan and Long, 2005, Trowsdale and Moffett, 2008, Vivier and Romagne, 2007). Despite this link, the mechanistic details underpinning these associations and different disease outcomes remain to be fully elucidated. For instance, genetic studies demonstrate that, despite their high degree of similarity, KIR2DL2 and KIR2DL3 are associated with different disease outcomes. That is, the expression of KIR2DL3 against HLA-C1 allelic background has been observed to be protective in the context of HCV infection, yet KIR2DL2 expression was not protective (Khakoo et al., 2004, Romero et al., 2008). Similarly, KIR2DL3 was observed to be protective in chronic hepatitis B infection (Gao et al., 2010).

4.2.2 KIR2DL2 and KIR2DL3 dock differently to HLA-C7

In determining the crystal structures of KIR2DL2 and KIR2DL3 in complex with the same HLA class I ligand, HLA-C*07:02, I was able to provide a structural perspective to understand the disparate functional activity of KIR2DL2 and KIR2DL3. Previous reports had speculated that the differences in binding affinity of KIR2DL2/L3 to group 1 HLA-C was due to differences in their D1-D2 hinge angle (Frazier et al., 2013).

Contrary to this, my data revealed that KIR2DL2 and -L3 display the same hinge angle in complex with HLA-C*07:02. The predominant structural difference was instead the “twist” of the receptor upon the HLA, indicating that they differ in the binding of the D1 domain to the α1 domain of HLA-C*07:02. As a result, there were more contacts from residues in the D1 domain of KIR2DL2 with the α1 domain of HLA-C*07:02. I speculate that due to the existence of more contacts made by KIR2DL2 on top of HLA-C*07:02 compared to that of KIR2DL3, KIR2DL2/ HLA-C*07:02 association results in the production of stronger inhibitory signal compared to the association of KIR2DL3/ HLA-C*07:02. This speculation could be tested for other alleles of HLA-C in the presence of KIR2DL2 and -L3, to monitor the level of inhibitory signal that they produce. Further investigation on the molecular basis of the interaction between KIR2DL2 and -L3 and a panel of other alleles of HLA-C molecules at the structural level will help to further compare between their structural differences and the biological function of their association.

4.2.3 KIR2DL3 is more sensitive to alteration of peptide content compared to KIR2DL2

Individuals with different KIRs genotypes have dissimilar responses against alterations in the peptide repertoire bound to HLA class I. Variations in response to the peptide content of HLA class I might be a clue to the protective effects of dissimilar KIR genes against pathogen infection and their related disease (Cassidy et al., 2015). For example, functional studies by Khakoo et al. revealed that NK cells with homozygosity of KIR2DL3 were more sensitive to alteration in HLA class I peptide repertoire than KIR2DL2.

Indeed, in the complexes between KIR2DL2/L3 and HLA-C*07:02, I showed that KIR2DL2 generates more contacts with the RL9 peptide derived from histone H3 (residues 40-48, RYRPGTVAL), bound to HLA-C*07:02. Accordingly, I speculate that the functional differences that have been observed for peptide repertoire are due to the differences in the docking between the KIR2DL2 and KIR2DL3 receptors which may consequently result in the production of weak or stronger inhibitory signals.

4.2.4 KIR2DL2 and –L3, show similar binding affinity to HLA-C*07:02-RL9

In order to monitor the avidity of binding for KIR2DL2 and -L3 against HLA-C*07:02, I conducted SPR experiments. Interestingly, I observed that via this setup, KIR2DL2 and -L3 have a similar binding affinity to HLA-C*07:02 loaded with the RL9 peptide. Others have reported differences in binding avidity between KIR2DL2 and -L3 with HLA-C1 ligands (Frazier et al., 2013). This may be due to the limited scope of my study that focused on one allele of group 1 HLA-C, as well as using only one peptide.

4.2.5 Impact of residue at position 70 of D1 on docking and avidity of KIR2DL1, -L2 and -L3 to HLA-*C*

Residue 44 of KIR2DL1, -L2 and -L3, located on the D1 domain, determines the specificity of binding to HLA-C1 and HLA-C2. However, there are other residues within KIR2DL1, -L2 and -L3 that are crucial for binding to their cognate HLA-C ligands. It has been reported that the main residue involved in increasing the affinity of binding for KIR2DL3 and KIR2DL1 to HLA-C molecules is residue 70; methionine 70 for KIR2DL3 and threonine 70 for KIR2DL1. A notable difference between KIR2DL2 and KIR2DL1 in complex with HLA-C is the formation of a hydrophobic bond between methionine 70 of KIR2DL2 and arginine 69 of HLA-C*03:04. This direct contact does not form between threonine 70 of KIR2DL1 and HLA-C*04:01 (Boyington et al., 2000, Fan et al., 2001). Methionine 70 of KIR2DL2 also generates contacts with glutamine 72 of HLA-C*03:04, yet the equivalent contact to threonine 70 of KIR2DL1 is not formed (Boyington et al., 2000, Fan et al., 2001). I observed in the crystal structure of KIR2DL3 in complex with HLA-07:02 that methionine 70 of KIR2DL3 forms no contact with glutamine 72 of HLA-C*07:02, yet retains binding to arginine 69 of HLA-C*07:02. I speculate that the differences in the contacts produced by methionine 70 for KIR2DL2 and -L3 are linked to the selection of their docking mode upon interaction with HLA-C ligands. Indeed, the docking of KIR2DL3 more closely resembles that of KIR2DL1.

4.2.6 Different docking of KIR2DL2 and -L3 to HLA-A molecules

Changes in the residues located at position 44 for KIR2DL2 or at position 71 and 131 of KIR2DL3 results in their binding to HLA-A*03 and HLA-A*11. Hilton et al. showed that replacement of glutamine 71 with proline or mutation of arginine 131 to glutamine confers reactivity of KIR2DL3 to HLA-A*11:02 (Hilton et al., 2012). Others have also reported very weak inhibition of KIR3DL2 with HLA-A*03 and HLA-A*11 (Valiante et al., 1997), although it has been shown that this binding does not provide any "education" of NK cells (Andersson et al., 2009, Yawata et al., 2008).

4.3 A structural view of the impact of allelic KIR2DL polymorphism on recognition of HLA-C1 and -C2

4.3.1 KIR2DL3*005 is similar to KIR2DL2 alleles

Binding studies via single-antigen bead array (Luminex) indicate that unlike other alleles of KIR2DL3, KIR2DL3*005 resembles other alleles of KIR2DL2 (Frazier et al., 2013). This data was supported by other functional data including inhibition of INF-γ production. Although based on molecular modeling, it was suggested that this difference arises from differences in the hinge angles for KIR2DL3 allotypes; however, my structural determination for KIR2DL2 and -L3 bound to HLA-C1 indicates that they have similar hinge angles and in fact differ in their "twist". I speculate that the docking of KIR2DL3*005 on HLA-C1 and -C2 is similar to KIR2DL2. That is, KIR2DL3*005 has the same hinge-angle as other KIR2DL2 and -L3 but the "twist" of KIR2DL2. This hypothesis requires the crystal structures of KIR2DL3*005 complex bound to HLA-C1 and -C2 ligands for further support. Figure 1.15.A shows the location of polymorphic sites of KIR2DL3*005 at positions 11 and 50, which are distal from its binding interface area and may be involved in the alteration of the docking of the D1 domain of KIR2DL3*005. This, likely affects the dynamics of the D1 domain and mimics the docking of the D1 domain of KIR2DL2.

4.3.2 KIR2DL3*005 and -L3*015 are different from other alleles of KIR2DL3

Observations by Falco et al. further emphasize the evidence of structural differences among alleles of KIR2DL3. They reported that two alleles of KIR2DL3, KIR2DL3*005 and -L3*015 have no binding to ECm41, a mono-clonal antibody specifically raised against KIR2DL3. Interestingly, they detected binding of KIR2DL3*005 and -L3*015 to EB6B and 11PB6, mono-clonal antibodies specific for binding to KIR2DL1 and KIR2DS1 (Falco et al., 2010). It was revealed that glutamic acid 35/arginine 50, and glutamine 35 are crucial for binding of KIR2DL3*005 to EB6B/11PB6 and ECM41 mAb, respectively (Falco et al., 2010). In summary, the structural differences among KIR2DL alleles correlate with their functional differences. Beyond this, differences at the allotypic level need to be further explored and cross-referenced with NK cell repertoire and functional definitions of KIR subsets to further understand the role of allotype variation in disease outcome.

4.3.3 Impact of HLA-C1 and -C2 on the docking of KIR2DLs

4.3.3.1 KIR2DL2 docks differently on top of HLA-C*07 and -C*03

By comparing the crystal structure of KIR2DL2 bound to HLA-C*07:02 with the previously reported structure of KIR2DL2 in complex with HLA-C*03:02, the degree to which the differences in KIR2DL2 docking were due to the structural variation between their respective HLA-C1 ligands, was observed. Structural analysis revealed the existence of different docking angles of KIR2DL2 on HLA-C*03:02 and HLA-C*07:02 which indicated the effect of different HLA-C1 alleles to the accommodation of the D1 and D2 domains.

4.3.3.2 Alleles of HLA-C show different sensitivity of binding to KIR2DL2 and -L3.

Functional *in vivo* studies of mutants of KIR2DL2 and KIR2DL3 binding HLA-C*03:02 and HLA-C*07:02 highlights the impact of different HLA-C alleles on the binding. I showed that mutation of lysine 44 which has been shown to determine the specificity of KIR2DL3 binding to HLA-C molecules, did not prevent binding of KIR2DL3 to HLA-

C*07:02 or HLA-C*03:04. However, the result of a mutation in position 45 of KIR2DL3 to binding HLA-C*07:02 and HLA-C*03:04 was significantly different. Differences were also detected by mutating leucine 104 to alanine that is located at hinge loop of KIR2DL3. No binding was observed for HLA-C*03:04 to KIR2DL3 L104A but binding of HLA-C*07:02 to KIR2DL3 L104A was detected. Taken together, these data indicate that different alleles of HLA-C respond differently to alteration in the sequence of KIR2DL3 and that binding to HLA-C*03:04 is more sensitive to substitution than binding to HLA-C*07:02. This can be explored further by monitoring the interaction of KIR2DL2 and -L3 and their respective mutants to a broader panel of other alleles of HLA-C. The result will further help to understand if KIR2DL2 and -L3 receive different responses from the entire alleles of HLA-C or there are only limited number of HLA-C alleles which are sensitive to alteration in the sequence of KIR2DL2 and -L3. As a result, new strategies can be applied to engineer new NK cell lines in order to overcome the transplantation rejection and curing infectious diseases.

4.4 KIR haplotypes and their impact on recognition of HLA-C by KIR2DLs

4.4.1 KIR2DL2 expression suppresses the expression of *KIR2DL1*

Genetic diversity of KIR haplotypes is an important element that affects the function of HLA-C-specific NK cell repertoires. Recently, it has been shown that in haplotype group B of KIRs, the function and frequency of expression of *KIR2DL1* is suppressed as a result of the expression of *KIR2DL2* (Schonberg et al., 2011). This is in contrast to *KIR2DL1* expression in haplotype A where the presence of *KIR2DL3* does not affect the level of expression of *KIR2DL1*. It was also shown that the expression of *KIR2DL2* does not interfere with expression of *KIR2DS1*. These observations potentially explain why homozygosity and heterozygosity of either *KIR2DL2* or *KIR2DL3* are associated with different disease outcome.

4.4.2 KIR2DL2 may have evolved to supplement -L1 and -L3 under pressure from pathogens

KIR2DL1 and *KIR2DL3* are highly restricted for binding to *HLA-C2* and *-C1*, respectively, whereas *KIR2DL2* is less specific and interacts with both *HLA-C1* and *-C2*. This may explain why the majority of haplotype B include *KIR2DL2*, instead of *KIR2DL3* and suppress the expression of KIR2DL1. I speculate that during evolution, *KIR2DL2* has emerged to produce overlapping yet different responses against pathogens via interaction with both *HLA-C1* and *-C2*.

4.5 KIR2DL4: different from other two domain KIRs

Unlike other KIR2D receptors that have D1 and D2 domain arrangement, KIR2DL4 consist of a D0 and D2 domain. The D0 domain is similar to that of the lineage II KIRs (KIR3Ds). I found that the D0 domain served as the oligomerization site of KIR2DL4. I showed that the structure of KIR2DL4 is markedly different from other members of KIR2Ds. Although the monomeric structure of KIR2DL4 resembles other members of KIR2D family, I revealed that KIR2DL4 oligomerizes in a concentration-dependent manner. In the crystal lattice, KIR2DL4 exists as a tetramer and this oligomerization state was confirmed by SAXS, MALS, and analytical ultracentrifugation.

4.5.1 Other KIRs with D0 domain show no oligomerization

The structure of the KIR3DL1 in complex with HLA-B*57 revealed that its D0 domain is involved in making key conserved contacts with HLA-B*57, that are crucial for the formation of the complex (Vivian et al., 2011) and not in the oligomerization of the receptor. This observation suggested that HLA may be a ligand for KIR2DL4. Indeed, it has been reported that HLA-G acts as a ligand for KIR2DL4 (Rajagopalan et al., 2006, Rajagopalan and Long, 1999, Rajagopalan, 2010). Whether HLA-G is, in fact, a ligand for KIR2DL4 is disputed in the literature with cellular assays using confocal microscopy and flow cytometry techniques reporting an interaction (Rajagopalan et al., 2006, Rajagopalan and Long, 1999), whilst direct binding techniques such as SPR, ELISA, and flow cytometry observing no interaction (Boyson et al., 2002, Le Page et al., 2014). Certainly, my studies using SPR, SAXS and single-antigen bead

binding techniques, were unable to detect any interaction between KIR2DL4 and HLA-G or any other HLA molecule tested. (Boyson et al., 2002, Le Page et al., 2014). Modelling of the potential KIR2DL4-HLA complexes suggests that due to the oligomerization of KIR2DL4, the D0 domain is no longer accessible for interaction with HLA in a manner like that observed for the D0 domain of KIR3DL1 or the D1 domain of KIR2DL1/2/3 (Boyington et al., 2000, Fan et al., 2001, Vivian et al., 2011). The caveats of this model are: (i) KIR2DL4 may be a functional monomer and/or dimer *in vivo.* (ii) KIR2DL4 may bind HLA in a manner not previously observed for KIR receptors. (iii) The interaction of KIR2DL4 and HLA may require the presence of other factors such as adaptor proteins which were missing in my experiments. (iv) The affinity of the interaction may be too weak to be detectable by the methods I employed.

4.5.2 Other examples of oligomeric proteins

Like other multimeric proteins that signal through their oligomerization state, the oligomerization of KIR2DL4 may be related to its signal transduction, and the tetramer/dimer status of KIR2DL4 might act as on/off switch for its function. It is possible that KIR2DL4 is active as a dimer and could interact with its unknown ligand in this state, whereas the tetramer of KIR2DL4 is its inactive form or *vice versa*. At lower concentrations, KIR2DL4 is detected to be in its monomeric state. Thus, it is possible that at low concentration at the cell surface, KIR2DL4 is monomeric, and oligomerizes when it is relocated to the endosome or bound to its unknown ligand (Rajagopalan, 2010).

KIR2DL4 oligomerization might be related to its activation/inhibition or association/disassociation with yet to be identified ligand, like what is observed for Src homology 2-B (SH2-B) protein (Qian and Ginty, 2001). It has been reported that SH2-B multimerization is crucial for nerve growth factor signaling (Qian and Ginty, 2001). Others have shown that formation of Hedgehog multimeric protein complex is a prerequisite for activation of its signaling and has a key role in embryonic development (Chen et al., 2004). Whether KIR2DL4 signaling is controlled via its

oligomerization is a question that remains unanswered, and further investigation is required. Regarding further investigation, I suggest designing mutants of KIR2DL4 lacking to form a tetrameric state. By site direct mutagenesis and alteration in amino acid residues crucial for tetramerization of KIR2DL4 in order to establish mutants of KIR2DL4 which can only form monomer and/or dimer. These mutants would help further to investigate if KIR2DL4 may interact with its unknown ligand as monomer/dimer. Investigation on cell signaling of KIR2DL4 mutants unable of oligomerization will help to address if KIR2DL4 oligomerization has a direct impact on its signaling. It should also be noted that the exact physiological function and signaling of KIR2DL4 cannot be precisely investigated unless its exact ligand(s) is discovered.

It was reported that the KIR2DL4 mediated responses are modulated by heparin sulfate and positively charged patch of the D0 domain of KIR2DL4 interacts with the negatively charged heparin sulfate (Brusilovsky et al., 2013). Further investigations are required to address whether KIR2DL4/heparin sulfate interaction may have influence on the oligomerization state of KIR2DL4. Whether heparin sulfate acts as an intermediate to facilitate access of potential ligand(s) of KIR2DL4 to its binding site needs to be investigated further (Brusilovsky et al., 2014).

4.6 Conclusion

In summary, I reported for the first time, the crystal structure of KIR2DL2 and KIR2DL3 bound to HLA-C*07:02. I showed that the binding surface area of their interaction is different and D1 domain of KIR2DL2 generates more contacts with the α1 domain of HLA-C*07:02, compared to that of KIR2DL3. Contacts made by D1 domain are less conserved, and this may play a crucial role in flexibility and specificity determination of KIR2DL2 and -L3 which further results in different docking mode on top of α1 domain of HLA-C. Whereas contacts made by D2 domain are highly conserved and may act as a platform in order to maintain the same hinge angle between D1-D2 domain. Further, I showed that HLA molecules play an important role in docking of KIRs and are involved in dictating the docking mode of KIR bound to

their cognate ligand. Further, I showed that KIR2DL4 is an atypical receptor among KIR family and unlike other members of this family it oligomerizes via its D0 domain and its structure in solution is markedly different from other members of the KIR family. By examining the molecular basis of ligand recognition by KIRs using biochemical and structural approaches, I obtained data that provides a molecular basis to understand why certain types of KIRs have a broader range of HLA class I ligands.

5 References

ADAMS, E. J. & PARHAM, P. 2001. Species-specific evolution of MHC class I genes in the higher primates. *Immunol Rev,* 183**,** 41-64.

ADAMS, P. D., AFONINE, P. V., BUNKOCZI, G., CHEN, V. B., DAVIS, I. W., ECHOLS, N., HEADD, J. J., HUNG, L. W., KAPRAL, G. J., GROSSE-KUNSTLEVE, R. W., MCCOY, A. J., MORIARTY, N. W., OEFFNER, R., READ, R. J., RICHARDSON, D. C., RICHARDSON, J. S., TERWILLIGER, T. C. & ZWART, P. H. 2010. PHENIX: a comprehensive Python-based system for macromolecular structure solution. *Acta Crystallogr D Biol Crystallogr,* 66**,** 213-21.

AKIRA, S. & TAKEDA, K. 2004. Toll-like receptor signalling. *Nat Rev Immunol,* 4**,** 499-511.

AKIRA, S., UEMATSU, S. & TAKEUCHI, O. 2006. Pathogen recognition and innate immunity. *Cell,* 124**,** 783-801.

ALTER, G., HECKERMAN, D., SCHNEIDEWIND, A., FADDA, L., KADIE, C. M., CARLSON, J. M., ONIANGUE-NDZA, C., MARTIN, M., LI, B., KHAKOO, S. I., CARRINGTON, M., ALLEN, T. M. & ALTFELD, M. 2011. HIV-1 adaptation to NK-cell-mediated immune pressure. *Nature,* 476**,** 96-100.

ANDERSSON, S., FAURIAT, C., MALMBERG, J. A., LJUNGGREN, H. G. & MALMBERG, K. J. 2009. KIR acquisition probabilities are independent of self-HLA class I ligands and increase with cellular KIR expression. *Blood,* 114**,** 95-104.

ANDREWS, D. M., SCALZO, A. A., YOKOYAMA, W. M., SMYTH, M. J. & DEGLI-ESPOSTI, M. A. 2003. Functional interactions between dendritic cells and NK cells during viral infection. *Nat Immunol,* 4**,** 175-81.

ANDROLEWICZ, M. J., ANDERSON, K. S. & CRESSWELL, P. 1993. Evidence that transporters associated with antigen processing translocate a major histocompatibility complex class I-binding peptide into the endoplasmic reticulum in an ATP-dependent manner. *Proc Natl Acad Sci U S A,* 90**,** 9130-4.

APPS, R., MENG, Z., DEL PRETE, G. Q., LIFSON, J. D., ZHOU, M. & CARRINGTON, M. 2015. Relative expression levels of the HLA class-I proteins in normal and HIV-infected cells. *J Immunol,* 194**,** 3594-600.

ARCHBOLD, J. K., ELY, L. K., KJER-NIELSEN, L., BURROWS, S. R., ROSSJOHN, J., MCCLUSKEY, J. & MACDONALD, W. A. 2008. T cell allorecognition and MHC restriction--A case of Jekyll and Hyde? *Mol Immunol,* 45**,** 583-98.

ARTYOMOV, M. N., LIS, M., DEVADAS, S., DAVIS, M. M. & CHAKRABORTY, A. K. 2010. CD4 and CD8 binding to MHC molecules primarily acts to enhance Lck delivery. *Proc Natl Acad Sci U S A,* 107**,** 16916-21.

ASHKAR, A. A., DI SANTO, J. P. & CROY, B. A. 2000. Interferon gamma contributes to initiation of uterine vascular modification, decidual integrity, and uterine natural killer cell maturation during normal murine pregnancy. *J Exp Med,* 192**,** 259-70.

AUGUSTO, D. G., LOBO-ALVES, S. C., MELO, M. F., PEREIRA, N. F. & PETZL-ERLER, M. L. 2012. Activating KIR and HLA Bw4 ligands are associated to decreased susceptibility to pemphigus foliaceus, an autoimmune blistering skin disease. *PLoS One,* 7**,** e39991.

AUGUSTO, D. G., O'CONNOR, G. M., LOBO-ALVES, S. C., BASS, S., MARTIN, M. P., CARRINGTON, M., MCVICAR, D. W. & PETZL-ERLER, M. L. 2015. Pemphigus is

associated with KIR3DL2 expression levels and provides evidence that KIR3DL2 may bind HLA-A3 and A11 in vivo. *Eur J Immunol,* 45**,** 2052-60.

AUGUSTO, D. G. & PETZL-ERLER, M. L. 2015. KIR and HLA under pressure: evidences of coevolution across worldwide populations. *Hum Genet,* 134**,** 929-40.

BALLAS, Z. K., TURNER, J. M., TURNER, D. A., GOETZMAN, E. A. & KEMP, J. D. 1990. A patient with simultaneous absence of "classical" natural killer cells (CD3-, CD16+, and NKH1+) and expansion of CD3+, CD4-, CD8-, NKH1+ subset. *J Allergy Clin Immunol,* 85**,** 453-9.

BANCROFT, G. J., SCHREIBER, R. D., BOSMA, G. C., BOSMA, M. J. & UNANUE, E. R. 1987. A T cell-independent mechanism of macrophage activation by interferon-gamma. *J Immunol,* 139**,** 1104-7.

BARBER, E. M. & POLLARD, J. W. 2003. The uterine NK cell population requires IL-15 but these cells are not required for pregnancy nor the resolution of a Listeria monocytogenes infection. *J Immunol,* 171**,** 37-46.

BARI, R., BELL, T., LEUNG, W. H., VONG, Q. P., CHAN, W. K., DAS GUPTA, N., HOLLADAY, M., ROONEY, B. & LEUNG, W. 2009. Significant functional heterogeneity among KIR2DL1 alleles and a pivotal role of arginine 245. *Blood,* 114**,** 5182-90.

BENICHOU, G., YAMADA, Y., AOYAMA, A. & MADSEN, J. C. 2011. Natural killer cells in rejection and tolerance of solid organ allografts. *Curr Opin Organ Transplant,* 16**,** 47-53.

BEUTLER, B. 2004. Innate immunity: an overview. *Mol Immunol,* 40**,** 845-59.

BIASSONI, R., FALCO, M., CAMBIAGGI, A., COSTA, P., VERDIANI, S., PENDE, D., CONTE, R., DI DONATO, C., PARHAM, P. & MORETTA, L. 1995. Amino acid substitutions can influence the natural killer (NK)-mediated recognition of HLA-C molecules. Role of serine-77 and lysine-80 in the target cell protection from lysis mediated by "group 2" or "group 1" NK clones. *J Exp Med,* 182**,** 605-9.

BIRKINSHAW, R. W., PELLICCI, D. G., CHENG, T. Y., KELLER, A. N., SANDOVAL-ROMERO, M., GRAS, S., DE JONG, A., ULDRICH, A. P., MOODY, D. B., GODFREY, D. I. & ROSSJOHN, J. 2015. alphabeta T cell antigen receptor recognition of CD1a presenting self lipid ligands. *Nat Immunol,* 16**,** 258-66.

BIRON, C. A., BYRON, K. S. & SULLIVAN, J. L. 1989. Severe herpesvirus infections in an adolescent without natural killer cells. *N Engl J Med,* 320**,** 1731-5.

BLANCHARD, N., KANASEKI, T., ESCOBAR, H., DELEBECQUE, F., NAGARAJAN, N. A., REYES-VARGAS, E., CROCKETT, D. K., RAULET, D. H., DELGADO, J. C. & SHASTRI, N. 2010. Endoplasmic reticulum aminopeptidase associated with antigen processing defines the composition and structure of MHC class I peptide repertoire in normal and virus-infected cells. *J Immunol,* 184**,** 3033-42.

BLERY, M., OLCESE, L. & VIVIER, E. 2000. Early signaling via inhibitory and activating NK receptors. *Hum Immunol,* 61**,** 51-64.

BLUM, J. S., WEARSCH, P. A. & CRESSWELL, P. 2013. Pathways of antigen processing. *Annu Rev Immunol,* 31**,** 443-73.

BOEHM, T., MCCURLEY, N., SUTOH, Y., SCHORPP, M., KASAHARA, M. & COOPER, M. D. 2012. VLR-based adaptive immunity. *Annu Rev Immunol,* 30**,** 203-20.

BOOG, C. J., KAST, W. M., TIMMERS, H. T., BOES, J., DE WAAL, L. P. & MELIEF, C. J. 1985. Abolition of specific immune response defect by immunization with dendritic cells. *Nature,* 318**,** 59-62.

BORREGO, F., KABAT, J., KIM, D. K., LIETO, L., MAASHO, K., PENA, J., SOLANA, R. & COLIGAN, J. E. 2002. Structure and function of major histocompatibility complex (MHC) class I specific receptors expressed on human natural killer (NK) cells. *Mol Immunol,* 38**,** 637-60.

BOYINGTON, J. C., MOTYKA, S. A., SCHUCK, P., BROOKS, A. G. & SUN, P. D. 2000. Crystal structure of an NK cell immunoglobulin-like receptor in complex with its class I MHC ligand. *Nature,* 405**,** 537-43.

BOYSON, J. E., ERSKINE, R., WHITMAN, M. C., CHIU, M., LAU, J. M., KOOPMAN, L. A., VALTER, M. M., ANGELISOVA, P., HOREJSI, V. & STROMINGER, J. L. 2002. Disulfide bond-mediated dimerization of HLA-G on the cell surface. *Proc Natl Acad Sci U S A,* 99**,** 16180-5.

BOYTON, R. J. & ALTMANN, D. M. 2007. Natural killer cells, killer immunoglobulin-like receptors and human leucocyte antigen class I in disease. *Clin Exp Immunol,* 149**,** 1-8.

BOYTON, R. J., SMITH, J., WARD, R., JONES, M., OZEROVITCH, L., WILSON, R., ROSE, M., TROWSDALE, J. & ALTMANN, D. M. 2006. HLA-C and killer cell immunoglobulin-like receptor genes in idiopathic bronchiectasis. *Am J Respir Crit Care Med,* 173**,** 327-33.

BROSENS, I., PIJNENBORG, R., VERCRUYSSE, L. & ROMERO, R. 2011. The "Great Obstetrical Syndromes" are associated with disorders of deep placentation. *Am J Obstet Gynecol,* 204**,** 193-201.

BROWNLIE, R. J. & ZAMOYSKA, R. 2013. T cell receptor signalling networks: branched, diversified and bounded. *Nat Rev Immunol,* 13**,** 257-69.

BRUHNS, P., MARCHETTI, P., FRIDMAN, W. H., VIVIER, E. & DAERON, M. 1999. Differential roles of N- and C-terminal immunoreceptor tyrosine-based inhibition motifs during inhibition of cell activation by killer cell inhibitory receptors. *J Immunol,* 162**,** 3168-75.

BRUSILOVSKY, M., CORDOBA, M., ROSENTAL, B., HERSHKOVITZ, O., ANDRAKE, M. D., PECHERSKAYA, A., EINARSON, M. B., ZHOU, Y., BRAIMAN, A., CAMPBELL, K. S. & PORGADOR, A. 2013. Genome-wide siRNA screen reveals a new cellular partner of NK cell receptor KIR2DL4: heparan sulfate directly modulates KIR2DL4-mediated responses. *J Immunol,* 191**,** 5256-67.

BRUSILOVSKY, M., RADINSKY, O., YOSSEF, R., CAMPBELL, K. S. & PORGADOR, A. 2014. Carbohydrate-mediated modulation of NK cell receptor function: structural and functional influences of heparan sulfate moieties expressed on NK cell surface. *Front Oncol,* 4**,** 185.

BRYCESON, Y. T., MARCH, M. E., LJUNGGREN, H. G. & LONG, E. O. 2006. Synergy among receptors on resting NK cells for the activation of natural cytotoxicity and cytokine secretion. *Blood,* 107**,** 159-66.

BURNET, F. M. F. 1959. *The Clonal Selection Theory of Acquired Immunity*, University Press.

BURSHTYN, D. N., LAM, A. S., WESTON, M., GUPTA, N., WARMERDAM, P. A. & LONG, E. O. 1999. Conserved residues amino-terminal of cytoplasmic tyrosines contribute to the SHP-1-mediated inhibitory function of killer cell Ig-like receptors. *J Immunol,* 162**,** 897-902.

BURSHTYN, D. N., SCHARENBERG, A. M., WAGTMANN, N., RAJAGOPALAN, S., BERRADA, K., YI, T., KINET, J. P. & LONG, E. O. 1996. Recruitment of tyrosine phosphatase HCP by the killer cell inhibitor receptor. *Immunity,* 4**,** 77-85.

CALIGIURI, M. A. 2008. Human natural killer cells. *Blood,* 112**,** 461-9.

CAMPBELL, K. S., DESSING, M., LOPEZ-BOTET, M., CELLA, M. & COLONNA, M. 1996. Tyrosine phosphorylation of a human killer inhibitory receptor recruits protein tyrosine phosphatase 1C. *J Exp Med,* 184**,** 93-100.

CAMPBELL, K. S. & HASEGAWA, J. 2013. Natural killer cell biology: an update and future directions. *J Allergy Clin Immunol,* 132**,** 536-44.

CAMPILLO, J. A., LEGAZ, I., LOPEZ-ALVAREZ, M. R., BOLARIN, J. M., LAS HERAS, B., MURO, M., MINGUELA, A., MOYA-QUILES, M. R., BLANCO-GARCIA, R., MARTINEZ-BANACLOCHA, H., GARCIA-ALONSO, A. M., ALVAREZ-LOPEZ, M. R. & MARTINEZ-ESCRIBANO, J. A. 2013. KIR gene variability in cutaneous malignant melanoma: influence of KIR2D/HLA-C pairings on disease susceptibility and prognosis. *Immunogenetics,* 65**,** 333-43.

CARRILLO-BUSTAMANTE, P., KESMIR, C. & DE BOER, R. J. 2016. The evolution of natural killer cell receptors. *Immunogenetics,* 68**,** 3-18.

CARRINGTON, M., WANG, S., MARTIN, M. P., GAO, X., SCHIFFMAN, M., CHENG, J., HERRERO, R., RODRIGUEZ, A. C., KURMAN, R., MORTEL, R., SCHWARTZ, P., GLASS, A. & HILDESHEIM, A. 2005. Hierarchy of resistance to cervical neoplasia mediated by combinations of killer immunoglobulin-like receptor and human leukocyte antigen loci. *J Exp Med,* 201**,** 1069-75.

CARSON, R. T., VIGNALI, K. M., WOODLAND, D. L. & VIGNALI, D. A. 1997. T cell receptor recognition of MHC class II-bound peptide flanking residues enhances immunogenicity and results in altered TCR V region usage. *Immunity,* 7**,** 387-99.

CASSIDY, S., MUKHERJEE, S., MYINT, T. M., MBIRIBINDI, B., NORTH, H., TRAHERNE, J., MULDER, A., CLAAS, F. H., PURBHOO, M. A., DAS, J. & KHAKOO, S. I. 2015. Peptide selectivity discriminates NK cells from KIR2DL2- and KIR2DL3-positive individuals. *Eur J Immunol,* 45**,** 492-500.

CERWENKA, A. & LANIER, L. L. 2001. Ligands for natural killer cell receptors: redundancy or specificity. *Immunol Rev,* 181**,** 158-69.

CHAN, C. J., SMYTH, M. J. & MARTINET, L. 2014. Molecular mechanisms of natural killer cell activation in response to cellular stress. *Cell Death Differ,* 21**,** 5-14.

CHEN, C., BUSSON, M., ROCHA, V., APPERT, M. L., LEPAGE, V., DULPHY, N., HAAS, P., SOCIE, G., TOUBERT, A., CHARRON, D. & LOISEAU, P. 2006. Activating KIR genes are associated with CMV reactivation and survival after non-T-cell depleted HLA-identical sibling bone marrow transplantation for malignant disorders. *Bone Marrow Transplant,* 38**,** 437-44.

CHEN, M. H., LI, Y. J., KAWAKAMI, T., XU, S. M. & CHUANG, P. T. 2004. Palmitoylation is required for the production of a soluble multimeric Hedgehog protein complex and long-range signaling in vertebrates. *Genes Dev,* 18**,** 641-59.

CHEN, V. B., ARENDALL, W. B., 3RD, HEADD, J. J., KEEDY, D. A., IMMORMINO, R. M., KAPRAL, G. J., MURRAY, L. W., RICHARDSON, J. S. & RICHARDSON, D. C. 2010. MolProbity: all-atom structure validation for macromolecular crystallography. *Acta Crystallogr D Biol Crystallogr,* 66**,** 12-21.

CHOO, J. A., LIU, J., TOH, X., GROTENBREG, G. M. & REN, E. C. 2014. The immunodominant influenza A virus M158-66 cytotoxic T lymphocyte epitope exhibits degenerate class I major histocompatibility complex restriction in humans. *J Virol,* 88**,** 10613-23.

CICCIA, F., ACCARDO-PALUMBO, A., ALESSANDRO, R., RIZZO, A., PRINCIPE, S., PERALTA, S., RAIATA, F., GIARDINA, A., DE LEO, G. & TRIOLO, G. 2012. Interleukin-22 and interleukin-22-producing NKp44+ natural killer cells in subclinical gut inflammation in ankylosing spondylitis. *Arthritis Rheum,* 64**,** 1869-78.

COLANTONIO, A. D., BIMBER, B. N., NEIDERMYER, W. J., JR., REEVES, R. K., ALTER, G., ALTFELD, M., JOHNSON, R. P., CARRINGTON, M., O'CONNOR, D. H. & EVANS, D. T. 2011. KIR polymorphisms modulate peptide-dependent binding to an MHC class I ligand with a Bw6 motif. *PLoS Pathog,* 7**,** e1001316.

COLONNA, M. 1997. Specificity and function of immunoglobulin superfamily NK cell inhibitory and stimulatory receptors. *Immunol Rev,* 155**,** 127-33.

COLONNA, M. & SAMARIDIS, J. 1995. Cloning of immunoglobulin-superfamily members associated with HLA-C and HLA-B recognition by human natural killer cells. *Science,* 268**,** 405-8.

COLUCCI, F., DI SANTO, J. P. & LEIBSON, P. J. 2002. Natural killer cell activation in mice and men: different triggers for similar weapons? *Nat Immunol,* 3**,** 807-13.

COOPER, M. A., ELLIOTT, J. M., KEYEL, P. A., YANG, L., CARRERO, J. A. & YOKOYAMA, W. M. 2009. Cytokine-induced memory-like natural killer cells. *Proc Natl Acad Sci U S A,* 106**,** 1915-9.

COOPER, M. A., FEHNIGER, T. A., TURNER, S. C., CHEN, K. S., GHAHERI, B. A., GHAYUR, T., CARSON, W. E. & CALIGIURI, M. A. 2001. Human natural killer cells: a unique innate immunoregulatory role for the CD56(bright) subset. *Blood,* 97**,** 3146-51.

COOPER, M. D. & ALDER, M. N. 2006. The evolution of adaptive immune systems. *Cell,* 124**,** 815-22.

COOPER, M. D., RAYMOND, D. A., PETERSON, R. D., SOUTH, M. A. & GOOD, R. A. 1966. The functions of the thymus system and the bursa system in the chicken. *J Exp Med,* 123**,** 75-102.

CRESSWELL, P., BANGIA, N., DICK, T. & DIEDRICH, G. 1999. The nature of the MHC class I peptide loading complex. *Immunol Rev,* 172**,** 21-8.

CUTURI, M. C., ANEGON, I., SHERMAN, F., LOUDON, R., CLARK, S. C., PERUSSIA, B. & TRINCHIERI, G. 1989. Production of hematopoietic colony-stimulating factors by human natural killer cells. *J Exp Med,* 169**,** 569-83.

DANILOVA, N. 2006. The evolution of immune mechanisms. *J Exp Zool B Mol Dev Evol,* 306**,** 496-520.

DEGLIANTONI, G., MURPHY, M., KOBAYASHI, M., FRANCIS, M. K., PERUSSIA, B. & TRINCHIERI, G. 1985. Natural killer (NK) cell-derived hematopoietic colony-inhibiting activity and NK cytotoxic factor. Relationship with tumor necrosis factor and synergism with immune interferon. *J Exp Med,* 162**,** 1512-30.

DEN HAAN, J. M., ARENS, R. & VAN ZELM, M. C. 2014. The activation of the adaptive immune system: cross-talk between antigen-presenting cells, T cells and B cells. *Immunol Lett,* 162**,** 103-12.

DENIZ, G., VAN DE VEEN, W. & AKDIS, M. 2013. Natural killer cells in patients with allergic diseases. *J Allergy Clin Immunol,* 132**,** 527-35.
DENKERS, E. Y., GAZZINELLI, R. T., MARTIN, D. & SHER, A. 1993. Emergence of NK1.1+ cells as effectors of IFN-gamma dependent immunity to Toxoplasma gondii in MHC class I-deficient mice. *J Exp Med,* 178**,** 1465-72.
DI SANTO, J. P. 2006. Natural killer cell developmental pathways: a question of balance. *Annu Rev Immunol,* 24**,** 257-86.
DI SANTO, J. P. 2008. Natural killer cells: diversity in search of a niche. *Nat Immunol,* 9**,** 473-5.
DIEDERICHS, K. & KARPLUS, P. A. 1997. Improved R-factors for diffraction data analysis in macromolecular crystallography. *Nat Struct Biol,* 4**,** 269-75.
DIEFENBACH, A. & RAULET, D. H. 2001. Strategies for target cell recognition by natural killer cells. *Immunol Rev,* 181**,** 170-84.
DOHRING, C. & COLONNA, M. 1997. Major histocompatibility complex (MHC) class I recognition by natural killer cells. *Crit Rev Immunol,* 17**,** 285-99.
DOOLAN, D. L. & HOFFMAN, S. L. 1999. IL-12 and NK cells are required for antigen-specific adaptive immunity against malaria initiated by CD8+ T cells in the Plasmodium yoelii model. *J Immunol,* 163**,** 884-92.
DRANOFF, G. 2004. Cytokines in cancer pathogenesis and cancer therapy. *Nat Rev Cancer,* 4**,** 11-22.
DULPHY, N., CHRETIEN, A. S., KHAZNADAR, Z., FAURIAT, C., NANBAKHSH, A., CAIGNARD, A., CHOUAIB, S., OLIVE, D. & TOUBERT, A. 2016. Underground Adaptation to a Hostile Environment: Acute Myeloid Leukemia vs. Natural Killer Cells. *Front Immunol,* 7**,** 94.
DUTTA, A., SAIKIA, N., PHOOKAN, J., BARUAH, M. N. & BARUAH, S. 2014. Association of killer cell immunoglobulin-like receptor gene 2DL1 and its HLA-C2 ligand with family history of cancer in oral squamous cell carcinoma. *Immunogenetics,* 66**,** 439-48.
ELLIOTT, J. M., WAHLE, J. A. & YOKOYAMA, W. M. 2010. MHC class I-deficient natural killer cells acquire a licensed phenotype after transfer into an MHC class I-sufficient environment. *J Exp Med,* 207**,** 2073-9.
EMSLEY, P. & COWTAN, K. 2004. Coot: model-building tools for molecular graphics. *Acta Crystallogr D Biol Crystallogr,* 60**,** 2126-32.
FALCO, M., MORETTA, L., MORETTA, A. & BOTTINO, C. 2013. KIR and KIR ligand polymorphism: a new area for clinical applications? *Tissue Antigens,* 82**,** 363-73.
FALCO, M., ROMEO, E., MARCENARO, S., MARTINI, S., VITALE, M., BOTTINO, C., MINGARI, M. C., MORETTA, L., MORETTA, A. & PENDE, D. 2010. Combined genotypic and phenotypic killer cell Ig-like receptor analyses reveal KIR2DL3 alleles displaying unexpected monoclonal antibody reactivity: identification of the amino acid residues critical for staining. *J Immunol,* 185**,** 433-41.
FALK, K., ROTZSCHKE, O., GRAHOVAC, B., SCHENDEL, D., STEVANOVIC, S., GNAU, V., JUNG, G., STROMINGER, J. L. & RAMMENSEE, H. G. 1993. Allele-specific peptide ligand motifs of HLA-C molecules. *Proc Natl Acad Sci U S A,* 90**,** 12005-9.
FAN, Q. R., GARBOCZI, D. N., WINTER, C. C., WAGTMANN, N., LONG, E. O. & WILEY, D. C. 1996. Direct binding of a soluble natural killer cell inhibitory receptor to a soluble human leukocyte antigen-Cw4 class I major histocompatibility complex molecule. *Proc Natl Acad Sci U S A,* 93**,** 7178-83.

FAN, Q. R., LONG, E. O. & WILEY, D. C. 2001. Crystal structure of the human natural killer cell inhibitory receptor KIR2DL1-HLA-Cw4 complex. *Nat Immunol,* 2**,** 452-60.

FAN, Q. R., MOSYAK, L., WINTER, C. C., WAGTMANN, N., LONG, E. O. & WILEY, D. C. 1997. Structure of the inhibitory receptor for human natural killer cells resembles haematopoietic receptors. *Nature,* 389**,** 96-100.

FAN, Q. R. & WILEY, D. C. 1999. Structure of human histocompatibility leukocyte antigen (HLA)-Cw4, a ligand for the KIR2D natural killer cell inhibitory receptor. *J Exp Med,* 190**,** 113-23.

FAURIAT, C., IVARSSON, M. A., LJUNGGREN, H. G., MALMBERG, K. J. & MICHAELSSON, J. 2010a. Education of human natural killer cells by activating killer cell immunoglobulin-like receptors. *Blood,* 115**,** 1166-74.

FAURIAT, C., LONG, E. O., LJUNGGREN, H. G. & BRYCESON, Y. T. 2010b. Regulation of human NK-cell cytokine and chemokine production by target cell recognition. *Blood,* 115**,** 2167-76.

FEHNIGER, T. A., COOPER, M. A., NUOVO, G. J., CELLA, M., FACCHETTI, F., COLONNA, M. & CALIGIURI, M. A. 2003. CD56bright natural killer cells are present in human lymph nodes and are activated by T cell-derived IL-2: a potential new link between adaptive and innate immunity. *Blood,* 101**,** 3052-7.

FENG, J., CALL, M. E. & WUCHERPFENNIG, K. W. 2006. The assembly of diverse immune receptors is focused on a polar membrane-embedded interaction site. *PLoS Biol,* 4**,** e142.

FENG, J., GARRITY, D., CALL, M. E., MOFFETT, H. & WUCHERPFENNIG, K. W. 2005. Convergence on a distinctive assembly mechanism by unrelated families of activating immune receptors. *Immunity,* 22**,** 427-38.

FLAJNIK, M. F. 2002. Comparative analyses of immunoglobulin genes: surprises and portents. *Nat Rev Immunol,* 2**,** 688-98.

FLAJNIK, M. F. & KASAHARA, M. 2010. Origin and evolution of the adaptive immune system: genetic events and selective pressures. *Nat Rev Genet,* 11**,** 47-59.

FLODSTROM-TULLBERG, M., BRYCESON, Y. T., SHI, F. D., HOGLUND, P. & LJUNGGREN, H. G. 2009. Natural killer cells in human autoimmunity. *Curr Opin Immunol,* 21**,** 634-40.

FLORES-VILLANUEVA, P. O., YUNIS, E. J., DELGADO, J. C., VITTINGHOFF, E., BUCHBINDER, S., LEUNG, J. Y., UGLIALORO, A. M., CLAVIJO, O. P., ROSENBERG, E. S., KALAMS, S. A., BRAUN, J. D., BOSWELL, S. L., WALKER, B. D. & GOLDFELD, A. E. 2001. Control of HIV-1 viremia and protection from AIDS are associated with HLA-Bw4 homozygosity. *Proc Natl Acad Sci U S A,* 98**,** 5140-5.

FOLEY, B., COOLEY, S., VERNERIS, M. R., CURTSINGER, J., LUO, X., WALLER, E. K., ANASETTI, C., WEISDORF, D. & MILLER, J. S. 2012. Human cytomegalovirus (CMV)-induced memory-like NKG2C(+) NK cells are transplantable and expand in vivo in response to recipient CMV antigen. *J Immunol,* 189**,** 5082-8.

FRAZIER, W. R., STEINER, N., HOU, L., DAKSHANAMURTHY, S. & HURLEY, C. K. 2013. Allelic variation in KIR2DL3 generates a KIR2DL2-like receptor with increased binding to its HLA-C ligand. *J Immunol,* 190**,** 6198-208.

FREUD, A. G. & CALIGIURI, M. A. 2006. Human natural killer cell development. *Immunol Rev,* 214**,** 56-72.

FUSCO, C., GUERINI, F. R., NOCERA, G., VENTRELLA, G., CAPUTO, D., VALENTINO, M. A., AGLIARDI, C., GALLOTTI, J., MORRA, V. B., FLORIO, C., CLERICI, M. & LOMBARDI, M. L. 2010. KIRs and their HLA ligands in remitting-relapsing multiple sclerosis. *J Neuroimmunol,* 229**,** 232-7.

GANZ, T. & LEHRER, R. I. 1998. Antimicrobial peptides of vertebrates. *Curr Opin Immunol,* 10**,** 41-4.

GAO, X., JIAO, Y., WANG, L., LIU, X., SUN, W., CUI, B., CHEN, Z. & ZHAO, Y. 2010. Inhibitory KIR and specific HLA-C gene combinations confer susceptibility to or protection against chronic hepatitis B. *Clin Immunol,* 137**,** 139-46.

GAUDIERI, S., DESANTIS, D., MCKINNON, E., MOORE, C., NOLAN, D., WITT, C. S., MALLAL, S. A. & CHRISTIANSEN, F. T. 2005. Killer immunoglobulin-like receptors and HLA act both independently and synergistically to modify HIV disease progression. *Genes Immun,* 6**,** 683-90.

GENDZEKHADZE, K., NORMAN, P. J., ABI-RACHED, L., GRAEF, T., MOESTA, A. K., LAYRISSE, Z. & PARHAM, P. 2009. Co-evolution of KIR2DL3 with HLA-C in a human population retaining minimal essential diversity of KIR and HLA class I ligands. *Proc Natl Acad Sci U S A,* 106**,** 18692-7.

GEORGE, T., YU, Y. Y., LIU, J., DAVENPORT, C., LEMIEUX, S., STONEMAN, E., MATHEW, P. A., KUMAR, V. & BENNETT, M. 1997. Allorecognition by murine natural killer cells: lysis of T-lymphoblasts and rejection of bone-marrow grafts. *Immunol Rev,* 155**,** 29-40.

GODFREY, D. I., ULDRICH, A. P., MCCLUSKEY, J., ROSSJOHN, J. & MOODY, D. B. 2015. The burgeoning family of unconventional T cells. *Nat Immunol,* 16**,** 1114-23.

GOLUBOVSKAYA, V. & WU, L. 2016. Different Subsets of T Cells, Memory, Effector Functions, and CAR-T Immunotherapy. *Cancers (Basel),* 8.

GOODRIDGE, J. P., WITT, C. S., CHRISTIANSEN, F. T. & WARREN, H. S. 2003. KIR2DL4 (CD158d) genotype influences expression and function in NK cells. *J Immunol,* 171**,** 1768-74.

GRAEF, T., MOESTA, A. K., NORMAN, P. J., ABI-RACHED, L., VAGO, L., OLDER AGUILAR, A. M., GLEIMER, M., HAMMOND, J. A., GUETHLEIN, L. A., BUSHNELL, D. A., ROBINSON, P. J. & PARHAM, P. 2009. KIR2DS4 is a product of gene conversion with KIR3DL2 that introduced specificity for HLA-A*11 while diminishing avidity for HLA-C. *J Exp Med,* 206**,** 2557-72.

GRAS, S., VAN RHIJN, I., SHAHINE, A., CHENG, T. Y., BHATI, M., TAN, L. L., HALIM, H., TUTTLE, K. D., GAPIN, L., LE NOURS, J., MOODY, D. B. & ROSSJOHN, J. 2016. T cell receptor recognition of CD1b presenting a mycobacterial glycolipid. *Nat Commun,* 7**,** 13257.

GRAY, J. D., HIROKAWA, M. & HORWITZ, D. A. 1994. The role of transforming growth factor beta in the generation of suppression: an interaction between CD8+ T and NK cells. *J Exp Med,* 180**,** 1937-42.

GREAVES, M. F., ROITT, I. M. & ROSE, M. E. 1968. Effect of bursectomy and thymectomy on the responses of chicken peripheral blood lymphocytes to phytohaemagglutinin. *Nature,* 220**,** 293-5.

GREGOIRE, C., CHASSON, L., LUCI, C., TOMASELLO, E., GEISSMANN, F., VIVIER, E. & WALZER, T. 2007. The trafficking of natural killer cells. *Immunol Rev,* 220**,** 169-82.

GUIA, S., JAEGER, B. N., PIATEK, S., MAILFERT, S., TROMBIK, T., FENIS, A., CHEVRIER, N., WALZER, T., KERDILES, Y. M., MARGUET, D., VIVIER, E. & UGOLINI, S. 2011.

Confinement of activating receptors at the plasma membrane controls natural killer cell tolerance. *Sci Signal,* 4**,** ra21.

GUMPERZ, J. E., LITWIN, V., PHILLIPS, J. H., LANIER, L. L. & PARHAM, P. 1995. The Bw4 public epitope of HLA-B molecules confers reactivity with natural killer cell clones that express NKB1, a putative HLA receptor. *J Exp Med,* 181**,** 1133-44.

GUNTHER, E. & WALTER, L. 2000. Comparative genomic aspects of rat, mouse and human MHC class I gene regions. *Cytogenet Cell Genet,* 91**,** 107-12.

HADAYA, K., DE RHAM, C., BANDELIER, C., BANDELIER, C., FERRARI-LACRAZ, S., JENDLY, S., BERNEY, T., BUHLER, L., KAISER, L., SEEBACH, J. D., TIERCY, J. M., MARTIN, P. Y. & VILLARD, J. 2008. Natural killer cell receptor repertoire and their ligands, and the risk of CMV infection after kidney transplantation. *Am J Transplant,* 8**,** 2674-83.

HANDA, K., SUZUKI, R., MATSUI, H., SHIMIZU, Y. & KUMAGAI, K. 1983. Natural killer (NK) cells as a responder to interleukin 2 (IL 2). II. IL 2-induced interferon gamma production. *J Immunol,* 130**,** 988-92.

HANNA, J., GOLDMAN-WOHL, D., HAMANI, Y., AVRAHAM, I., GREENFIELD, C., NATANSON-YARON, S., PRUS, D., COHEN-DANIEL, L., ARNON, T. I., MANASTER, I., GAZIT, R., YUTKIN, V., BENHARROCH, D., PORGADOR, A., KESHET, E., YAGEL, S. & MANDELBOIM, O. 2006. Decidual NK cells regulate key developmental processes at the human fetal-maternal interface. *Nat Med,* 12**,** 1065-74.

HANSASUTA, P., DONG, T., THANANCHAI, H., WEEKES, M., WILLBERG, C., ALDEMIR, H., ROWLAND-JONES, S. & BRAUD, V. M. 2004. Recognition of HLA-A3 and HLA-A11 by KIR3DL2 is peptide-specific. *Eur J Immunol,* 34**,** 1673-9.

HAO, L. & NEI, M. 2005. Rapid expansion of killer cell immunoglobulin-like receptor genes in primates and their coevolution with MHC Class I genes. *Gene,* 347**,** 149-59.

HEARN, A., YORK, I. A. & ROCK, K. L. 2009. The specificity of trimming of MHC class I-presented peptides in the endoplasmic reticulum. *J Immunol,* 183**,** 5526-36.

HERBERMAN, R. B., NUNN, M. E. & LAVRIN, D. H. 1975. Natural cytotoxic reactivity of mouse lymphoid cells against syngeneic acid allogeneic tumors. I. Distribution of reactivity and specificity. *Int J Cancer,* 16**,** 216-29.

HERNANDEZ-RAMIREZ, D., ESPARZA-PEREZ, M. A., RAMIREZ-GARCIALUNA, J. L., ARGUELLO, J. R., MANDEVILLE, P. B., NOYOLA, D. E. & GARCIA-SEPULVEDA, C. A. 2015. Association of KIR3DL1/S1 and HLA-Bw4 with CD4 T cell counts in HIV-infected Mexican mestizos. *Immunogenetics,* 67**,** 413-24.

HILTON, H. G., NORMAN, P. J., NEMAT-GORGANI, N., GOYOS, A., HOLLENBACH, J. A., HENN, B. M., GIGNOUX, C. R., GUETHLEIN, L. A. & PARHAM, P. 2015. Loss and Gain of Natural Killer Cell Receptor Function in an African Hunter-Gatherer Population. *PLoS Genet,* 11**,** e1005439.

HILTON, H. G., VAGO, L., OLDER AGUILAR, A. M., MOESTA, A. K., GRAEF, T., ABI-RACHED, L., NORMAN, P. J., GUETHLEIN, L. A., FLEISCHHAUER, K. & PARHAM, P. 2012. Mutation at positively selected positions in the binding site for HLA-C shows that KIR2DL1 is a more refined but less adaptable NK cell receptor than KIR2DL3. *J Immunol,* 189**,** 1418-30.

HIRANO, M. 2015. Evolution of vertebrate adaptive immunity: immune cells and tissues, and AID/APOBEC cytidine deaminases. *Bioessays,* 37**,** 877-87.

HIRANO, M., DAS, S., GUO, P. & COOPER, M. D. 2011. The evolution of adaptive immunity in vertebrates. *Adv Immunol,* 109**,** 125-57.

HIRAYASU, K., OHASHI, J., KASHIWASE, K., HANANANTACHAI, H., NAKA, I., OGAWA, A., TAKANASHI, M., SATAKE, M., NAKAJIMA, K., PARHAM, P., ARASE, H., TOKUNAGA, K., PATARAPOTIKUL, J. & YABE, T. 2012. Significant association of KIR2DL3-HLA-C1 combination with cerebral malaria and implications for co-evolution of KIR and HLA. *PLoS Pathog,* 8**,** e1002565.

HOFFMANN, J. A. 2003. The immune response of Drosophila. *Nature,* 426**,** 33-8.

HOLLENBACH, J. A., AUGUSTO, D. G., ALAEZ, C., BUBNOVA, L., FAE, I., FISCHER, G., GONZALEZ-GALARZA, F. F., GORODEZKY, C., KARABON, L., KUSNIERCZYK, P., NOBLE, J., RICKARDS, O., ROBERTS, C., SCHAFFER, M., SHI, L., TAVOULARIS, S., TRACHTENBERG, E., YAO, Y. & MIDDLETON, D. 2013. 16(th) IHIW: population global distribution of killer immunoglobulin-like receptor (KIR) and ligands. *Int J Immunogenet,* 40**,** 39-45.

HOLLENBACH, J. A., LADNER, M. B., SAETEURN, K., TAYLOR, K. D., MEI, L., HARITUNIANS, T., MCGOVERN, D. P., ERLICH, H. A., ROTTER, J. I. & TRACHTENBERG, E. A. 2009. Susceptibility to Crohn's disease is mediated by KIR2DL2/KIR2DL3 heterozygosity and the HLA-C ligand. *Immunogenetics,* 61**,** 663-71.

HOLLENBACH, J. A., MEENAGH, A., SLEATOR, C., ALAEZ, C., BENGOCHE, M., CANOSSI, A., CONTRERAS, G., CREARY, L., EVSEEVA, I., GORODEZKY, C., HARDIE, R. A., KARLSEN, T. H., LIE, B., LUO, M., MARTINETTI, M., NAVARETTE, C., DE OLIVEIRA, D. C., OZZELLA, G., PASI, A., PAVLOVA, E., PINTO, S., PORTO, L. C., SANTOS, P., SLAVCEV, A., SRINAK, D., TAVOULARIS, S., TONKS, S., TRACHTENBERG, E., VEJBAESYA, S. & MIDDLETON, D. 2010. Report from the killer immunoglobulin-like receptor (KIR) anthropology component of the 15th International Histocompatibility Workshop: worldwide variation in the KIR loci and further evidence for the co-evolution of KIR and HLA. *Tissue Antigens,* 76**,** 9-17.

HOSHINO, T., WINKLER-PICKETT, R. T., MASON, A. T., ORTALDO, J. R. & YOUNG, H. A. 1999. IL-13 production by NK cells: IL-13-producing NK and T cells are present in vivo in the absence of IFN-gamma. *J Immunol,* 162**,** 51-9.

HOU, Y., ZHANG, C., XU, D. & SUN, H. 2015. Association of killer cell immunoglobulin-like receptor and human leucocyte antigen-Cw gene combinations with systemic lupus erythematosus. *Clin Exp Immunol,* 180**,** 250-4.

HSU, K. C., CHIDA, S., GERAGHTY, D. E. & DUPONT, B. 2002. The killer cell immunoglobulin-like receptor (KIR) genomic region: gene-order, haplotypes and allelic polymorphism. *Immunol Rev,* 190**,** 40-52.

HUARTE, E., RYNDA-APPLE, A., RICCARDI, C., SKYBERG, J. A., GOLDEN, S., ROLLINS, M. F., RAMSTEAD, A. G., JACKIW, L. O., MADDALONI, M. & PASCUAL, D. W. 2011. Tolerogen-induced interferon-producing killer dendritic cells (IKDCs) protect against EAE. *J Autoimmun,* 37**,** 328-41.

HUNTINGTON, N. D., VOSSHENRICH, C. A. & DI SANTO, J. P. 2007. Developmental pathways that generate natural-killer-cell diversity in mice and humans. *Nat Rev Immunol,* 7**,** 703-14.

ISAKOV, N. 1997. ITIMs and ITAMs. The Yin and Yang of antigen and Fc receptor-linked signaling machinery. *Immunol Res,* 16**,** 85-100.

JANEWAY, C. A. 2001. *Immunobiology: The Immune System in Health and Disease*, Churchill Livingstone.

JANEWAY, C. A., JR. & MEDZHITOV, R. 2002. Innate immune recognition. *Annu Rev Immunol,* 20**,** 197-216.

JARDULI, L. R., ALVES, H. V., DE SOUZA-SANTANA, F. C., MARCOS, E. V., PEREIRA, A. C., DIAS-BAPTISTA, I. M., FAVA, V. M., MIRA, M. T., MORAES, M. O., VIRMOND MDA, C. & VISENTAINER, J. E. 2014. Influence of KIR genes and their HLA ligands in the pathogenesis of leprosy in a hyperendemic population of Rondonopolis, Southern Brazil. *BMC Infect Dis,* 14**,** 438.

JENKINS, M. R., KEDZIERSKA, K., DOHERTY, P. C. & TURNER, S. J. 2007. Heterogeneity of effector phenotype for acute phase and memory influenza A virus-specific CTL. *J Immunol,* 179**,** 64-70.

JENNES, W., VERHEYDEN, S., MERTENS, J. W., CAMARA, M., SEYDI, M., DIEYE, T. N., MBOUP, S., DEMANET, C. & KESTENS, L. 2013. Inhibitory KIR/HLA incompatibility between sexual partners confers protection against HIV-1 transmission. *Blood,* 121**,** 1157-64.

JIANG, W., CHAI, N. R., MARIC, D. & BIELEKOVA, B. 2011. Unexpected role for granzyme K in CD56bright NK cell-mediated immunoregulation of multiple sclerosis. *J Immunol,* 187**,** 781-90.

JIAO, Y. L., MA, C. Y., WANG, L. C., CUI, B., ZHANG, J., YOU, L., CHEN, Z. J., LI, J. F. & ZHAO, Y. R. 2008. Polymorphisms of KIRs gene and HLA-C alleles in patients with ankylosing spondylitis: possible association with susceptibility to the disease. *J Clin Immunol,* 28**,** 343-9.

JOBIM, M., CHAGASTELLES, P., SALIM, P. H., PORTELA, P., WILSON, T. J., CURTI, A. G., JOBIM, M. R., JOAO, D. A., NARDI, N. B., TSCHIEDEL, B., JOBIM, L. F., ROESLER, R. & SCHWARTSMANN, G. 2010. Association of killer cell immunoglobulin-like receptors and human leukocyte antigen-C genotypes in South Brazilian with type 1 diabetes. *Hum Immunol,* 71**,** 799-803.

JONCAS, J., MONCZAK, Y., GHIBU, F., ALFIERI, C., BONIN, A., AHRONHEIM, G. & RIVARD, G. 1989. Brief report: killer cell defect and persistent immunological abnormalities in two patients with chronic active Epstein-Barr virus infection. *J Med Virol,* 28**,** 110-7.

JONCKER, N. T. & RAULET, D. H. 2008. Regulation of NK cell responsiveness to achieve self-tolerance and maximal responses to diseased target cells. *Immunol Rev,* 224**,** 85-97.

JONCKER, N. T., SHIFRIN, N., DELEBECQUE, F. & RAULET, D. H. 2010. Mature natural killer cells reset their responsiveness when exposed to an altered MHC environment. *J Exp Med,* 207**,** 2065-72.

JUDICE, C. C., BOURGARD, C., KAYANO, A. C., ALBRECHT, L. & COSTA, F. T. 2016. MicroRNAs in the Host-Apicomplexan Parasites Interactions: A Review of Immunopathological Aspects. *Front Cell Infect Microbiol,* 6**,** 5.

JUNG, S., UNUTMAZ, D., WONG, P., SANO, G., DE LOS SANTOS, K., SPARWASSER, T., WU, S., VUTHOORI, S., KO, K., ZAVALA, F., PAMER, E. G., LITTMAN, D. R. & LANG, R. A. 2002. In vivo depletion of CD11c+ dendritic cells abrogates priming of CD8+ T cells by exogenous cell-associated antigens. *Immunity,* 17**,** 211-20.

KAGI, D., LEDERMANN, B., BURKI, K., SEILER, P., ODERMATT, B., OLSEN, K. J., PODACK, E. R., ZINKERNAGEL, R. M. & HENGARTNER, H. 1994. Cytotoxicity mediated by T cells and natural killer cells is greatly impaired in perforin-deficient mice. *Nature,* 369**,** 31-7.

KARLHOFER, F. M., RIBAUDO, R. K. & YOKOYAMA, W. M. 1992. MHC class I alloantigen specificity of Ly-49+ IL-2-activated natural killer cells. *Nature,* 358**,** 66-70.

KARRE, K., LJUNGGREN, H. G., PIONTEK, G. & KIESSLING, R. 1986. Selective rejection of H-2-deficient lymphoma variants suggests alternative immune defence strategy. *Nature,* 319**,** 675-8.

KASAHARA, M., SUZUKI, T. & PASQUIER, L. D. 2004. On the origins of the adaptive immune system: novel insights from invertebrates and cold-blooded vertebrates. *Trends Immunol,* 25**,** 105-11.

KELLER, A. N., ECKLE, S. B., XU, W., LIU, L., HUGHES, V. A., MAK, J. Y., MEEHAN, B. S., PEDIONGCO, T., BIRKINSHAW, R. W., CHEN, Z., WANG, H., D'SOUZA, C., KJER-NIELSEN, L., GHERARDIN, N. A., GODFREY, D. I., KOSTENKO, L., CORBETT, A. J., PURCELL, A. W., FAIRLIE, D. P., MCCLUSKEY, J. & ROSSJOHN, J. 2017. Drugs and drug-like molecules can modulate the function of mucosal-associated invariant T cells. *Nat Immunol,* 18**,** 402-411.

KHAKOO, S. I., RAJALINGAM, R., SHUM, B. P., WEIDENBACH, K., FLODIN, L., MUIR, D. G., CANAVEZ, F., COOPER, S. L., VALIANTE, N. M., LANIER, L. L. & PARHAM, P. 2000. Rapid evolution of NK cell receptor systems demonstrated by comparison of chimpanzees and humans. *Immunity,* 12**,** 687-98.

KHAKOO, S. I., THIO, C. L., MARTIN, M. P., BROOKS, C. R., GAO, X., ASTEMBORSKI, J., CHENG, J., GOEDERT, J. J., VLAHOV, D., HILGARTNER, M., COX, S., LITTLE, A. M., ALEXANDER, G. J., CRAMP, M. E., O'BRIEN, S. J., ROSENBERG, W. M., THOMAS, D. L. & CARRINGTON, M. 2004. HLA and NK cell inhibitory receptor genes in resolving hepatitis C virus infection. *Science,* 305**,** 872-4.

KIESSLING, R., HOCHMAN, P. S., HALLER, O., SHEARER, G. M., WIGZELL, H. & CUDKOWICZ, G. 1977. Evidence for a similar or common mechanism for natural killer cell activity and resistance to hemopoietic grafts. *Eur J Immunol,* 7**,** 655-63.

KIESSLING, R., KLEIN, E. & WIGZELL, H. 1975. "Natural" killer cells in the mouse. I. Cytotoxic cells with specificity for mouse Moloney leukemia cells. Specificity and distribution according to genotype. *Eur J Immunol,* 5**,** 112-7.

KIKUCHI-MAKI, A., CATINA, T. L. & CAMPBELL, K. S. 2005. Cutting edge: KIR2DL4 transduces signals into human NK cells through association with the Fc receptor gamma protein. *J Immunol,* 174**,** 3859-63.

KIKUCHI-MAKI, A., YUSA, S., CATINA, T. L. & CAMPBELL, K. S. 2003. KIR2DL4 is an IL-2-regulated NK cell receptor that exhibits limited expression in humans but triggers strong IFN-gamma production. *J Immunol,* 171**,** 3415-25.

KILLIG, M., GLATZER, T. & ROMAGNANI, C. 2014. Recognition strategies of group 3 innate lymphoid cells. *Front Immunol,* 5**,** 142.

KING, A., BALENDRAN, N., WOODING, P., CARTER, N. P. & LOKE, Y. W. 1991. CD3- leukocytes present in the human uterus during early placentation: phenotypic and morphologic characterization of the CD56++ population. *Dev Immunol,* 1**,** 169-90.

KING, A., BURROWS, T., VERMA, S., HIBY, S. & LOKE, Y. W. 1998. Human uterine lymphocytes. *Hum Reprod Update,* 4**,** 480-5.

KIRWAN, S. E. & BURSHTYN, D. N. 2007. Regulation of natural killer cell activity. *Curr Opin Immunol,* 19**,** 46-54.

KITAWAKI, J., XU, B., ISHIHARA, H., FUKUI, M., HASEGAWA, G., NAKAMURA, N., MIZUNO, S., OHTA, M., OBAYASHI, H. & HONJO, H. 2007. Association of killer cell immunoglobulin-like receptor genotypes with susceptibility to endometriosis. *Am J Reprod Immunol,* 58**,** 481-6.

KOOPMAN, L. A., KOPCOW, H. D., RYBALOV, B., BOYSON, J. E., ORANGE, J. S., SCHATZ, F., MASCH, R., LOCKWOOD, C. J., SCHACHTER, A. D., PARK, P. J. & STROMINGER, J. L. 2003. Human decidual natural killer cells are a unique NK cell subset with immunomodulatory potential. *J Exp Med,* 198**,** 1201-12.

KULPA, D. A. & COLLINS, K. L. 2011. The emerging role of HLA-C in HIV-1 infection. *Immunology,* 134**,** 116-22.

KUMAR, V., BEN-EZRA, J., BENNETT, M. & SONNENFELD, G. 1979. Natural killer cells in mice treated with 89strontium: normal target-binding cell numbers but inability to kill even after interferon administration. *J Immunol,* 123**,** 1832-8.

KUMAR, V. & MCNERNEY, M. E. 2005. A new self: MHC-class-I-independent natural-killer-cell self-tolerance. *Nat Rev Immunol,* 5**,** 363-74.

LA GRUTA, N. L., TURNER, S. J. & DOHERTY, P. C. 2004. Hierarchies in cytokine expression profiles for acute and resolving influenza virus-specific CD8+ T cell responses: correlation of cytokine profile and TCR avidity. *J Immunol,* 172**,** 5553-60.

LANIER, L. L. 1998. NK cell receptors. *Annu Rev Immunol,* 16**,** 359-93.

LANIER, L. L. 2008. Up on the tightrope: natural killer cell activation and inhibition. *Nat Immunol,* 9**,** 495-502.

LANIER, L. L., CORLISS, B. C., WU, J., LEONG, C. & PHILLIPS, J. H. 1998. Immunoreceptor DAP12 bearing a tyrosine-based activation motif is involved in activating NK cells. *Nature,* 391**,** 703-7.

LASKAY, T., ROLLINGHOFF, M. & SOLBACH, W. 1993. Natural killer cells participate in the early defense against Leishmania major infection in mice. *Eur J Immunol,* 23**,** 2237-41.

LE PAGE, M. E., GOODRIDGE, J. P., JOHN, E., CHRISTIANSEN, F. T. & WITT, C. S. 2014. Killer Ig-like receptor 2DL4 does not mediate NK cell IFN-gamma responses to soluble HLA-G preparations. *J Immunol,* 192**,** 732-40.

LE PAGE, M. E., GOODRIDGE, J. P., ZHANG, G., HOLT, P. G., SLY, P. & WITT, C. S. 2013. Genetic polymorphism of KIR2DL4 (CD158d), a putative NK cell receptor for HLA-G, does not influence susceptibility to asthma. *Tissue Antigens,* 82**,** 276-9.

LECHLER, R. I. & BATCHELOR, J. R. 1982. Restoration of immunogenicity to passenger cell-depleted kidney allografts by the addition of donor strain dendritic cells. *J Exp Med,* 155**,** 31-41.

LEHRER, R. I. & GANZ, T. 2002. Cathelicidins: a family of endogenous antimicrobial peptides. *Curr Opin Hematol,* 9**,** 18-22.

LEMAITRE, B., NICOLAS, E., MICHAUT, L., REICHHART, J. M. & HOFFMANN, J. A. 1996. The dorsoventral regulatory gene cassette spatzle/Toll/cactus controls the potent antifungal response in Drosophila adults. *Cell,* 86**,** 973-83.

LEVINSON, R. D. 2011. Killer immunoglobulin-like receptor genes in uveitis. *Ocul Immunol Inflamm,* 19**,** 192-201.
LIEBERMAN, J. & FAN, Z. 2003. Nuclear war: the granzyme A-bomb. *Curr Opin Immunol,* 15**,** 553-9.
LINEHAN, E. & FITZGERALD, D. C. 2015. Ageing and the immune system: focus on macrophages. *Eur J Microbiol Immunol (Bp),* 5**,** 14-24.
LITMAN, G. W., RAST, J. P. & FUGMANN, S. D. 2010. The origins of vertebrate adaptive immunity. *Nat Rev Immunol,* 10**,** 543-53.
LITWIN, V., GUMPERZ, J., PARHAM, P., PHILLIPS, J. H. & LANIER, L. L. 1994. NKB1: a natural killer cell receptor involved in the recognition of polymorphic HLA-B molecules. *J Exp Med,* 180**,** 537-43.
LIU, J., XIAO, Z., KO, H. L., SHEN, M. & REN, E. C. 2014. Activating killer cell immunoglobulin-like receptor 2DS2 binds to HLA-A*11. *Proc Natl Acad Sci U S A,* 111**,** 2662-7.
LIU, W. R., KIM, J., NWANKWO, C., ASHWORTH, L. K. & ARM, J. P. 2000. Genomic organization of the human leukocyte immunoglobulin-like receptors within the leukocyte receptor complex on chromosome 19q13.4. *Immunogenetics,* 51**,** 659-69.
LONG, E. O. 1999. Regulation of immune responses through inhibitory receptors. *Annu Rev Immunol,* 17**,** 875-904.
LONG, E. O. 2008. Negative signaling by inhibitory receptors: the NK cell paradigm. *Immunol Rev,* 224**,** 70-84.
LOPEZ-VAZQUEZ, A., RODRIGO, L., MARTINEZ-BORRA, J., PEREZ, R., RODRIGUEZ, M., FDEZ-MORERA, J. L., FUENTES, D., RODRIGUEZ-RODERO, S., GONZAEZ, S. & LOPEZ-LARREA, C. 2005. Protective effect of the HLA-Bw4I80 epitope and the killer cell immunoglobulin-like receptor 3DS1 gene against the development of hepatocellular carcinoma in patients with hepatitis C virus infection. *J Infect Dis,* 192**,** 162-5.
LOTZE, M. T., CUSTER, M. C., BOLTON, E. S., WIEBKE, E. A., KAWAKAMI, Y. & ROSENBERG, S. A. 1990. Mechanisms of immunologic antitumor therapy: lessons from the laboratory and clinical applications. *Hum Immunol,* 28**,** 198-207.
LU, X., GIBBS, J. S., HICKMAN, H. D., DAVID, A., DOLAN, B. P., JIN, Y., KRANZ, D. M., BENNINK, J. R., YEWDELL, J. W. & VARMA, R. 2012. Endogenous viral antigen processing generates peptide-specific MHC class I cell-surface clusters. *Proc Natl Acad Sci U S A,* 109**,** 15407-12.
LUCI, C. & TOMASELLO, E. 2008. Natural killer cells: detectors of stress. *Int J Biochem Cell Biol,* 40**,** 2335-40.
LUSZCZEK, W., MANCZAK, M., CISLO, M., NOCKOWSKI, P., WISNIEWSKI, A., JASEK, M. & KUSNIERCZYK, P. 2004. Gene for the activating natural killer cell receptor, KIR2DS1, is associated with susceptibility to psoriasis vulgaris. *Hum Immunol,* 65**,** 758-66.
MAENAKA, K., JUJI, T., STUART, D. I. & JONES, E. Y. 1999. Crystal structure of the human p58 killer cell inhibitory receptor (KIR2DL3) specific for HLA-Cw3-related MHC class I. *Structure,* 7**,** 391-8.
MAGHAZACHI, A. A. 2003. G protein-coupled receptors in natural killer cells. *J Leukoc Biol,* 74**,** 16-24.
MAGHAZACHI, A. A. 2010. Role of chemokines in the biology of natural killer cells. *Curr Top Microbiol Immunol,* 341**,** 37-58.

MALNATI, M. S., PERUZZI, M., PARKER, K. C., BIDDISON, W. E., CICCONE, E., MORETTA, A. & LONG, E. O. 1995. Peptide specificity in the recognition of MHC class I by natural killer cell clones. *Science,* 267**,** 1016-8.

MALONE, D. F. G., LUNEMANN, S., HENGST, J., LJUNGGREN, H. G., MANNS, M. P., SANDBERG, J. K., CORNBERG, M., WEDEMEYER, H. & BJORKSTROM, N. K. 2017. Cytomegalovirus-Driven Adaptive-Like Natural Killer Cell Expansions Are Unaffected by Concurrent Chronic Hepatitis Virus Infections. *Front Immunol,* 8**,** 525.

MANDELBOIM, O., REYBURN, H. T., VALES-GOMEZ, M., PAZMANY, L., COLONNA, M., BORSELLINO, G. & STROMINGER, J. L. 1996. Protection from lysis by natural killer cells of group 1 and 2 specificity is mediated by residue 80 in human histocompatibility leukocyte antigen C alleles and also occurs with empty major histocompatibility complex molecules. *J Exp Med,* 184**,** 913-22.

MARTIN, A. M., FREITAS, E. M., WITT, C. S. & CHRISTIANSEN, F. T. 2000. The genomic organization and evolution of the natural killer immunoglobulin-like receptor (KIR) gene cluster. *Immunogenetics,* 51**,** 268-80.

MARTIN, M. P., BASHIROVA, A., TRAHERNE, J., TROWSDALE, J. & CARRINGTON, M. 2003. Cutting edge: expansion of the KIR locus by unequal crossing over. *J Immunol,* 171**,** 2192-5.

MARTIN, M. P., GAO, X., LEE, J. H., NELSON, G. W., DETELS, R., GOEDERT, J. J., BUCHBINDER, S., HOOTS, K., VLAHOV, D., TROWSDALE, J., WILSON, M., O'BRIEN, S. J. & CARRINGTON, M. 2002a. Epistatic interaction between KIR3DS1 and HLA-B delays the progression to AIDS. *Nat Genet,* 31**,** 429-34.

MARTIN, M. P., NELSON, G., LEE, J. H., PELLETT, F., GAO, X., WADE, J., WILSON, M. J., TROWSDALE, J., GLADMAN, D. & CARRINGTON, M. 2002b. Cutting edge: susceptibility to psoriatic arthritis: influence of activating killer Ig-like receptor genes in the absence of specific HLA-C alleles. *J Immunol,* 169**,** 2818-22.

MARTIN, M. P., QI, Y., GAO, X., YAMADA, E., MARTIN, J. N., PEREYRA, F., COLOMBO, S., BROWN, E. E., SHUPERT, W. L., PHAIR, J., GOEDERT, J. J., BUCHBINDER, S., KIRK, G. D., TELENTI, A., CONNORS, M., O'BRIEN, S. J., WALKER, B. D., PARHAM, P., DEEKS, S. G., MCVICAR, D. W. & CARRINGTON, M. 2007. Innate partnership of HLA-B and KIR3DL1 subtypes against HIV-1. *Nat Genet,* 39**,** 733-40.

MATSUMURA, M., FREMONT, D. H., PETERSON, P. A. & WILSON, I. A. 1992. Emerging principles for the recognition of peptide antigens by MHC class I molecules. *Science,* 257**,** 927-34.

MATSUSHITA, M., ENDO, Y. & FUJITA, T. 1998. MASP1 (MBL-associated serine protease 1). *Immunobiology,* 199**,** 340-7.

MATSUSHITA, M. & FUJITA, T. 1992. Activation of the classical complement pathway by mannose-binding protein in association with a novel C1s-like serine protease. *J Exp Med,* 176**,** 1497-502.

MATSUSHITA, M. & FUJITA, T. 1995. Cleavage of the third component of complement (C3) by mannose-binding protein-associated serine protease (MASP) with subsequent complement activation. *Immunobiology,* 194**,** 443-48.

MCCOY, A. J., GROSSE-KUNSTLEVE, R. W., ADAMS, P. D., WINN, M. D., STORONI, L. C. & READ, R. J. 2007. Phaser crystallographic software. *J Appl Crystallogr,* 40**,** 658-674.

MEHROTRA, P. T., DONNELLY, R. P., WONG, S., KANEGANE, H., GEREMEW, A., MOSTOWSKI, H. S., FURUKE, K., SIEGEL, J. P. & BLOOM, E. T. 1998. Production of IL-10 by human natural killer cells stimulated with IL-2 and/or IL-12. *J Immunol,* 160**,** 2637-44.

MIAH, S. M., HUGHES, T. L. & CAMPBELL, K. S. 2008. KIR2DL4 differentially signals downstream functions in human NK cells through distinct structural modules. *J Immunol,* 180**,** 2922-32.

MIDDLETON, D., CURRAN, M. & MAXWELL, L. 2002. Natural killer cells and their receptors. *Transpl Immunol,* 10**,** 147-64.

MIDDLETON, D. & GONZELEZ, F. 2010. The extensive polymorphism of KIR genes. *Immunology,* 129**,** 8-19.

MISHRA, R., WELSH, R. & SZOMOLANYI-TSUDA, E. 2014. NK cells and virus-related cancers. *Crit Rev Oncog,* 19**,** 107-19.

MOESTA, A. K., ABI-RACHED, L., NORMAN, P. J. & PARHAM, P. 2009. Chimpanzees use more varied receptors and ligands than humans for inhibitory killer cell Ig-like receptor recognition of the MHC-C1 and MHC-C2 epitopes. *J Immunol,* 182**,** 3628-37.

MOESTA, A. K., NORMAN, P. J., YAWATA, M., YAWATA, N., GLEIMER, M. & PARHAM, P. 2008. Synergistic polymorphism at two positions distal to the ligand-binding site makes KIR2DL2 a stronger receptor for HLA-C than KIR2DL3. *J Immunol,* 180**,** 3969-79.

MOESTA, A. K. & PARHAM, P. 2012. Diverse functionality among human NK cell receptors for the C1 epitope of HLA-C: KIR2DS2, KIR2DL2, and KIR2DL3. *Front Immunol,* 3**,** 336.

MOFFAT, J. M., GEBHARDT, T., DOHERTY, P. C., TURNER, S. J. & MINTERN, J. D. 2009. Granzyme A expression reveals distinct cytolytic CTL subsets following influenza A virus infection. *Eur J Immunol,* 39**,** 1203-10.

MOFFETT-KING, A. 2002. Natural killer cells and pregnancy. *Nat Rev Immunol,* 2**,** 656-63.

MOFFETT, A. & COLUCCI, F. 2014. Uterine NK cells: active regulators at the maternal-fetal interface. *J Clin Invest,* 124**,** 1872-9.

MOFFETT, A. & LOKE, C. 2006. Immunology of placentation in eutherian mammals. *Nat Rev Immunol,* 6**,** 584-94.

MOHAMMED, F., COBBOLD, M., ZARLING, A. L., SALIM, M., BARRETT-WILT, G. A., SHABANOWITZ, J., HUNT, D. F., ENGELHARD, V. H. & WILLCOX, B. E. 2008. Phosphorylation-dependent interaction between antigenic peptides and MHC class I: a molecular basis for the presentation of transformed self. *Nat Immunol,* 9**,** 1236-43.

MORADI, S., BERRY, R., PYMM, P., HITCHEN, C., BECKHAM, S. A., WILCE, M. C., WALPOLE, N. G., CLEMENTS, C. S., REID, H. H., PERUGINI, M. A., BROOKS, A. G., ROSSJOHN, J. & VIVIAN, J. P. 2015. The structure of the atypical killer cell immunoglobulin-like receptor, KIR2DL4. *J Biol Chem,* 290**,** 10460-71.

MORETTA, A., BOTTINO, C., MINGARI, M. C., BIASSONI, R. & MORETTA, L. 2002. What is a natural killer cell? *Nat Immunol,* 3**,** 6-8.

MORETTA, L., CICCONE, E., MINGARI, M. C., BIASSONI, R. & MORETTA, A. 1994. Human natural killer cells: origin, clonality, specificity, and receptors. *Adv Immunol,* 55**,** 341-80.

MORTELLARO, A. & RICCIARDI-CASTAGNOLI, P. 2011. From vaccine practice to vaccine science: the contribution of human immunology to the prevention of infectious disease. *Immunol Cell Biol,* 89**,** 332-9.

MOSAAD, Y. M. 2015. Clinical Role of Human Leukocyte Antigen in Health and Disease. *Scand J Immunol,* 82**,** 283-306.

MUENCH, M. O., HUMEAU, L., PAEK, B., OHKUBO, T., LANIER, L. L., ALBANESE, C. T. & BARCENA, A. 2000. Differential effects of interleukin-3, interleukin-7, interleukin 15, and granulocyte-macrophage colony-stimulating factor in the generation of natural killer and B cells from primitive human fetal liver progenitors. *Exp Hematol,* 28**,** 961-73.

NAKAMURA, M. C., NIEMI, E. C., FISHER, M. J., SHULTZ, L. D., SEAMAN, W. E. & RYAN, J. C. 1997. Mouse Ly-49A interrupts early signaling events in natural killer cell cytotoxicity and functionally associates with the SHP-1 tyrosine phosphatase. *J Exp Med,* 185**,** 673-84.

NASTKE, M. D., HERRGEN, L., WALTER, S., WERNET, D., RAMMENSEE, H. G. & STEVANOVIC, S. 2005. Major contribution of codominant CD8 and CD4 T cell epitopes to the human cytomegalovirus-specific T cell repertoire. *Cell Mol Life Sci,* 62**,** 77-86.

NAUMOVA, E., MIHAYLOVA, A., STOITCHKOV, K., IVANOVA, M., QUIN, L. & TONEVA, M. 2005. Genetic polymorphism of NK receptors and their ligands in melanoma patients: prevalence of inhibitory over activating signals. *Cancer Immunol Immunother,* 54**,** 172-8.

NEEFJES, J., JONGSMA, M. L., PAUL, P. & BAKKE, O. 2011. Towards a systems understanding of MHC class I and MHC class II antigen presentation. *Nat Rev Immunol,* 11**,** 823-36.

NEIPP, M., GAMMIE, J. S., EXNER, B. G., LI, S., CHAMBERS, W. H., PHAM, S. M. & ILDSTAD, S. T. 1999. A partial conditioning approach to achieve mixed chimerism in the rat: depletion of host natural killer cells significantly reduces the amount of total body irradiation required for engraftment. *Transplantation,* 68**,** 369-78.

NORMAN, P. J., HOLLENBACH, J. A., NEMAT-GORGANI, N., GUETHLEIN, L. A., HILTON, H. G., PANDO, M. J., KORAM, K. A., RILEY, E. M., ABI-RACHED, L. & PARHAM, P. 2013. Co-evolution of human leukocyte antigen (HLA) class I ligands with killer-cell immunoglobulin-like receptors (KIR) in a genetically diverse population of sub-Saharan Africans. *PLoS Genet,* 9**,** e1003938.

O'CONNOR, G. M., VIVIAN, J. P., WIDJAJA, J. M., BRIDGEMAN, J. S., GOSTICK, E., LAFONT, B. A., ANDERSON, S. K., PRICE, D. A., BROOKS, A. G., ROSSJOHN, J. & MCVICAR, D. W. 2014. Mutational and structural analysis of KIR3DL1 reveals a lineage-defining allotypic dimorphism that impacts both HLA and peptide sensitivity. *J Immunol,* 192**,** 2875-84.

O'LEARY, J. G., GOODARZI, M., DRAYTON, D. L. & VON ANDRIAN, U. H. 2006. T cell- and B cell-independent adaptive immunity mediated by natural killer cells. *Nat Immunol,* 7**,** 507-16.

O'SHEA, J. J., MA, A. & LIPSKY, P. 2002. Cytokines and autoimmunity. *Nat Rev Immunol,* 2**,** 37-45.

OGBOMO, H., ZEMP, F. J., LUN, X., ZHANG, J., STACK, D., RAHMAN, M. M., MCFADDEN, G., MODY, C. H. & FORSYTH, P. A. 2013. Myxoma virus infection promotes NK lysis of malignant gliomas in vitro and in vivo. *PLoS One,* 8**,** e66825.

OLCESE, L., LANG, P., VELY, F., CAMBIAGGI, A., MARGUET, D., BLERY, M., HIPPEN, K. L., BIASSONI, R., MORETTA, A., MORETTA, L., CAMBIER, J. C. & VIVIER, E. 1996. Human

and mouse killer-cell inhibitory receptors recruit PTP1C and PTP1D protein tyrosine phosphatases. *J Immunol,* 156**,** 4531-4.

OLDER AGUILAR, A. M., GUETHLEIN, L. A., ADAMS, E. J., ABI-RACHED, L., MOESTA, A. K. & PARHAM, P. 2010. Coevolution of killer cell Ig-like receptors with HLA-C to become the major variable regulators of human NK cells. *J Immunol,* 185**,** 4238-51.

ORANGE, J. S. 2008. Formation and function of the lytic NK-cell immunological synapse. *Nat Rev Immunol,* 8**,** 713-25.

ORTMANN, B., ANDROLEWICZ, M. J. & CRESSWELL, P. 1994. MHC class I/beta 2-microglobulin complexes associate with TAP transporters before peptide binding. *Nature,* 368**,** 864-7.

ORTMANN, B., COPEMAN, J., LEHNER, P. J., SADASIVAN, B., HERBERG, J. A., GRANDEA, A. G., RIDDELL, S. R., TAMPE, R., SPIES, T., TROWSDALE, J. & CRESSWELL, P. 1997. A critical role for tapasin in the assembly and function of multimeric MHC class I-TAP complexes. *Science,* 277**,** 1306-9.

OTWINOWSKI, Z. & MINOR, W. 1997. [20] Processing of X-ray diffraction data collected in oscillation mode. *Methods in Enzymology.* Academic Press.

PALACIOS, E. H. & WEISS, A. 2004. Function of the Src-family kinases, Lck and Fyn, in T-cell development and activation. *Oncogene,* 23**,** 7990-8000.

PANDO, M. J., GARDINER, C. M., GLEIMER, M., MCQUEEN, K. L. & PARHAM, P. 2003. The protein made from a common allele of KIR3DL1 (3DL1*004) is poorly expressed at cell surfaces due to substitution at positions 86 in Ig domain 0 and 182 in Ig domain 1. *J Immunol,* 171**,** 6640-9.

PARCEJ, D. & TAMPE, R. 2010. ABC proteins in antigen translocation and viral inhibition. *Nat Chem Biol,* 6**,** 572-80.

PARHAM, P. 2005. MHC class I molecules and KIRs in human history, health and survival. *Nat Rev Immunol,* 5**,** 201-14.

PARHAM, P. & MOFFETT, A. 2013. Variable NK cell receptors and their MHC class I ligands in immunity, reproduction and human evolution. *Nat Rev Immunol,* 13**,** 133-44.

PARHAM, P., NORMAN, P. J., ABI-RACHED, L. & GUETHLEIN, L. A. 2012. Human-specific evolution of killer cell immunoglobulin-like receptor recognition of major histocompatibility complex class I molecules. *Philos Trans R Soc Lond B Biol Sci,* 367**,** 800-11.

PARSONS, S. J. & PARSONS, J. T. 2004. Src family kinases, key regulators of signal transduction. *Oncogene,* 23**,** 7906-9.

PAUST, S., GILL, H. S., WANG, B. Z., FLYNN, M. P., MOSEMAN, E. A., SENMAN, B., SZCZEPANIK, M., TELENTI, A., ASKENASE, P. W., COMPANS, R. W. & VON ANDRIAN, U. H. 2010. Critical role for the chemokine receptor CXCR6 in NK cell-mediated antigen-specific memory of haptens and viruses. *Nat Immunol,* 11**,** 1127-35.

PAUST, S. & VON ANDRIAN, U. H. 2011. Natural killer cell memory. *Nat Immunol,* 12**,** 500-8.

PEIXOTO, A., EVARISTO, C., MUNITIC, I., MONTEIRO, M., CHARBIT, A., ROCHA, B. & VEIGA-FERNANDES, H. 2007. CD8 single-cell gene coexpression reveals three different effector types present at distinct phases of the immune response. *J Exp Med,* 204**,** 1193-205.

PENDE, D., MARCENARO, S., FALCO, M., MARTINI, S., BERNARDO, M. E., MONTAGNA, D., ROMEO, E., COGNET, C., MARTINETTI, M., MACCARIO, R., MINGARI, M. C., VIVIER, E., MORETTA, L., LOCATELLI, F. & MORETTA, A. 2009. Anti-leukemia activity of alloreactive NK cells in KIR ligand-mismatched haploidentical HSCT for pediatric patients: evaluation of the functional role of activating KIR and redefinition of inhibitory KIR specificity. *Blood,* 113**,** 3119-29.

PENG, H. & TIAN, Z. 2014. NK cell trafficking in health and autoimmunity:a comprehensive review. *Clin Rev Allergy Immunol,* 47**,** 119-27.

PIONTEK, G. E., TANIGUCHI, K., LJUNGGREN, H. G., GRONBERG, A., KIESSLING, R., KLEIN, G. & KARRE, K. 1985. YAC-1 MHC class I variants reveal an association between decreased NK sensitivity and increased H-2 expression after interferon treatment or in vivo passage. *J Immunol,* 135**,** 4281-8.

PODACK, E. R. 1995. Perforin, killer cells and gene transfer immunotherapy for cancer. *Curr Top Microbiol Immunol,* 198**,** 121-30.

POGGI, A. & ZOCCHI, M. R. 2014. NK cell autoreactivity and autoimmune diseases. *Front Immunol,* 5**,** 27.

PONTE, M., CANTONI, C., BIASSONI, R., TRADORI-CAPPAI, A., BENTIVOGLIO, G., VITALE, C., BERTONE, S., MORETTA, A., MORETTA, L. & MINGARI, M. C. 1999. Inhibitory receptors sensing HLA-G1 molecules in pregnancy: decidua-associated natural killer cells express LIR-1 and CD94/NKG2A and acquire p49, an HLA-G1-specific receptor. *Proc Natl Acad Sci U S A,* 96**,** 5674-9.

QIAN, X. & GINTY, D. D. 2001. SH2-B and APS are multimeric adapters that augment TrkA signaling. *Mol Cell Biol,* 21**,** 1613-20.

RAJAGOPALAN, S. 2010. Endosomal signaling and a novel pathway defined by the natural killer receptor KIR2DL4 (CD158d). *Traffic,* 11**,** 1381-90.

RAJAGOPALAN, S., BRYCESON, Y. T., KUPPUSAMY, S. P., GERAGHTY, D. E., VAN DER MEER, A., JOOSTEN, I. & LONG, E. O. 2006. Activation of NK cells by an endocytosed receptor for soluble HLA-G. *PLoS Biol,* 4**,** e9.

RAJAGOPALAN, S., FU, J. & LONG, E. O. 2001. Cutting edge: induction of IFN-gamma production but not cytotoxicity by the killer cell Ig-like receptor KIR2DL4 (CD158d) in resting NK cells. *J Immunol,* 167**,** 1877-81.

RAJAGOPALAN, S. & LONG, E. O. 1997. The direct binding of a p58 killer cell inhibitory receptor to human histocompatibility leukocyte antigen (HLA)-Cw4 exhibits peptide selectivity. *J Exp Med,* 185**,** 1523-8.

RAJAGOPALAN, S. & LONG, E. O. 1999. A human histocompatibility leukocyte antigen (HLA)-G-specific receptor expressed on all natural killer cells. *J Exp Med,* 189**,** 1093-100.

RAJAGOPALAN, S. & LONG, E. O. 2005. Understanding how combinations of HLA and KIR genes influence disease. *J Exp Med,* 201**,** 1025-9.

RAPHAEL, I., NALAWADE, S., EAGAR, T. N. & FORSTHUBER, T. G. 2015. T cell subsets and their signature cytokines in autoimmune and inflammatory diseases. *Cytokine,* 74**,** 5-17.

RAVETCH, J. V. & LANIER, L. L. 2000. Immune inhibitory receptors. *Science,* 290**,** 84-9.

REN, G., SHAO, T., ZHUANG, Y., HU, H., ZHANG, X., HUANG, J., LIU, Y. & LIU, D. 2012. Association of killer cell immunoglobulin-like receptor and human leukocyte antigen-C

genotype with dry eye disease in a Chinese Han population. *Genet Test Mol Biomarkers,* 16**,** 910-4.
ROBERTS, C. H., MOLINA, S., MAKALO, P., JOOF, H., HARDING-ESCH, E. M., BURR, S. E., MABEY, D. C., BAILEY, R. L., BURTON, M. J. & HOLLAND, M. J. 2014. Conjunctival scarring in trachoma is associated with the HLA-C ligand of KIR and is exacerbated by heterozygosity at KIR2DL2/KIR2DL3. *PLoS Negl Trop Dis,* 8**,** e2744.
ROBERTS, K., LOTZE, M. T. & ROSENBERG, S. A. 1987. Separation and functional studies of the human lymphokine-activated killer cell. *Cancer Res,* 47**,** 4366-71.
ROBERTSON, M. J. 2002. Role of chemokines in the biology of natural killer cells. *J Leukoc Biol,* 71**,** 173-83.
ROCK, K. L., GRAMM, C., ROTHSTEIN, L., CLARK, K., STEIN, R., DICK, L., HWANG, D. & GOLDBERG, A. L. 1994. Inhibitors of the proteasome block the degradation of most cell proteins and the generation of peptides presented on MHC class I molecules. *Cell,* 78**,** 761-71.
ROCK, K. L., YORK, I. A., SARIC, T. & GOLDBERG, A. L. 2002. Protein degradation and the generation of MHC class I-presented peptides. *Adv Immunol,* 80**,** 1-70.
RODGERS, J. R. & COOK, R. G. 2005. MHC class Ib molecules bridge innate and acquired immunity. *Nat Rev Immunol,* 5**,** 459-71.
ROJO, S., WAGTMANN, N. & LONG, E. O. 1997. Binding of a soluble p70 killer cell inhibitory receptor to HLA-B*5101: requirement for all three p70 immunoglobulin domains. *Eur J Immunol,* 27**,** 568-71.
ROLSTAD, B., FOSSUM, S., BAZIN, H., KIMBER, I., MARSHALL, J., SPARSHOTT, S. M. & FORD, W. L. 1985. The rapid rejection of allogeneic lymphocytes by a non-adaptive, cell-mediated mechanism (NK activity). *Immunology,* 54**,** 127-38.
ROMEE, R., SCHNEIDER, S. E., LEONG, J. W., CHASE, J. M., KEPPEL, C. R., SULLIVAN, R. P., COOPER, M. A. & FEHNIGER, T. A. 2012. Cytokine activation induces human memory-like NK cells. *Blood,* 120**,** 4751-60.
ROMERO, V., AZOCAR, J., ZUNIGA, J., CLAVIJO, O. P., TERREROS, D., GU, X., HUSAIN, Z., CHUNG, R. T., AMOS, C. & YUNIS, E. J. 2008. Interaction of NK inhibitory receptor genes with HLA-C and MHC class II alleles in Hepatitis C virus infection outcome. *Mol Immunol,* 45**,** 2429-36.
ROSENBLUM, M. D., WAY, S. S. & ABBAS, A. K. 2016. Regulatory T cell memory. *Nat Rev Immunol,* 16**,** 90-101.
RUGGERI, L., CAPANNI, M., URBANI, E., PERRUCCIO, K., SHLOMCHIK, W. D., TOSTI, A., POSATI, S., ROGAIA, D., FRASSONI, F., AVERSA, F., MARTELLI, M. F. & VELARDI, A. 2002. Effectiveness of donor natural killer cell alloreactivity in mismatched hematopoietic transplants. *Science,* 295**,** 2097-100.
RUPPERT, J., SIDNEY, J., CELIS, E., KUBO, R. T., GREY, H. M. & SETTE, A. 1993. Prominent role of secondary anchor residues in peptide binding to HLA-A2.1 molecules. *Cell,* 74**,** 929-37.
RUSS, B. E., PRIER, J. E., RAO, S. & TURNER, S. J. 2013. T cell immunity as a tool for studying epigenetic regulation of cellular differentiation. *Front Genet,* 4**,** 218.
RYAN, J. C. & SEAMAN, W. E. 1997. Divergent functions of lectin-like receptors on NK cells. *Immunol Rev,* 155**,** 79-89.

SAITO, S., NAKASHIMA, A., MYOJO-HIGUMA, S. & SHIOZAKI, A. 2008. The balance between cytotoxic NK cells and regulatory NK cells in human pregnancy. *J Reprod Immunol,* 77**,** 14-22.

SALAZAR-MATHER, T. P., ORANGE, J. S. & BIRON, C. A. 1998. Early murine cytomegalovirus (MCMV) infection induces liver natural killer (NK) cell inflammation and protection through macrophage inflammatory protein 1alpha (MIP-1alpha)-dependent pathways. *J Exp Med,* 187**,** 1-14.

SALMOND, R. J., FILBY, A., QURESHI, I., CASERTA, S. & ZAMOYSKA, R. 2009. T-cell receptor proximal signaling via the Src-family kinases, Lck and Fyn, influences T-cell activation, differentiation, and tolerance. *Immunol Rev,* 228**,** 9-22.

SAPER, M. A., BJORKMAN, P. J. & WILEY, D. C. 1991. Refined structure of the human histocompatibility antigen HLA-A2 at 2.6 A resolution. *J Mol Biol,* 219**,** 277-319.

SAULQUIN, X., GASTINEL, L. N. & VIVIER, E. 2003. Crystal structure of the human natural killer cell activating receptor KIR2DS2 (CD158j). *J Exp Med,* 197**,** 933-8.

SAUNDERS, P. M., PYMM, P., PIETRA, G., HUGHES, V. A., HITCHEN, C., O'CONNOR, G. M., LOIACONO, F., WIDJAJA, J., PRICE, D. A., FALCO, M., MINGARI, M. C., MORETTA, L., MCVICAR, D. W., ROSSJOHN, J., BROOKS, A. G. & VIVIAN, J. P. 2016. Killer cell immunoglobulin-like receptor 3DL1 polymorphism defines distinct hierarchies of HLA class I recognition. *J Exp Med*.

SAUNDERS, P. M., VIVIAN, J. P., BASCHUK, N., BEDDOE, T., WIDJAJA, J., O'CONNOR, G. M., HITCHEN, C., PYMM, P., ANDREWS, D. M., GRAS, S., MCVICAR, D. W., ROSSJOHN, J. & BROOKS, A. G. 2015a. The interaction of KIR3DL1*001 with HLA class I molecules is dependent upon molecular microarchitecture within the Bw4 epitope. *J Immunol,* 194**,** 781-9.

SAUNDERS, P. M., VIVIAN, J. P., O'CONNOR, G. M., SULLIVAN, L. C., PYMM, P., ROSSJOHN, J. & BROOKS, A. G. 2015b. A bird's eye view of NK cell receptor interactions with their MHC class I ligands. *Immunol Rev,* 267**,** 148-66.

SCHENK, A., BLOCH, W. & ZIMMER, P. 2016. Natural Killer Cells--An Epigenetic Perspective of Development and Regulation. *Int J Mol Sci,* 17**,** 326.

SCHONBERG, K., SRIBAR, M., ENCZMANN, J., FISCHER, J. C. & UHRBERG, M. 2011. Analyses of HLA-C-specific KIR repertoires in donors with group A and B haplotypes suggest a ligand-instructed model of NK cell receptor acquisition. *Blood,* 117**,** 98-107.

SEAMAN, W. E. 2000. Natural killer cells and natural killer T cells. *Arthritis Rheum,* 43**,** 1204-17.

SEAMAN, W. E., BLACKMAN, M. A., GINDHART, T. D., ROUBINIAN, J. R., LOEB, J. M. & TALAL, N. 1978. beta-Estradiol reduces natural killer cells in mice. *J Immunol,* 121**,** 2193-8.

SEAMAN, W. E., SLEISENGER, M., ERIKSSON, E. & KOO, G. C. 1987. Depletion of natural killer cells in mice by monoclonal antibody to NK-1.1. Reduction in host defense against malignancy without loss of cellular or humoral immunity. *J Immunol,* 138**,** 4539-44.

SEICH AL BASATENA, N. K., MACNAMARA, A., VINE, A. M., THIO, C. L., ASTEMBORSKI, J., USUKU, K., OSAME, M., KIRK, G. D., DONFIELD, S. M., GOEDERT, J. J., BANGHAM, C. R., CARRINGTON, M., KHAKOO, S. I. & ASQUITH, B. 2011. KIR2DL2 enhances protective and detrimental HLA class I-mediated immunity in chronic viral infection. *PLoS Pathog,* 7**,** e1002270.

SHAHSAVAR, F., MOUSAVI, T., AZARGON, A. & ENTEZAMI, K. 2012. Association of KIR3DS1+HLA-B Bw4Ile80 combination with susceptibility to tuberculosis in Lur population of Iran. *Iran J Immunol,* 9**,** 39-47.

SHARPE, M. & MOUNT, N. 2015. Genetically modified T cells in cancer therapy: opportunities and challenges. *Dis Model Mech,* 8**,** 337-50.

SHASTRI, N., SCHWAB, S. & SERWOLD, T. 2002. Producing nature's gene-chips: the generation of peptides for display by MHC class I molecules. *Annu Rev Immunol,* 20**,** 463-93.

SHASTRY, A., SEDIMBI, S. K., RAJALINGAM, R., NIKITINA-ZAKE, L., RUMBA, I., WIGZELL, H. & SANJEEVI, C. B. 2008. Combination of KIR 2DL2 and HLA-C1 (Asn 80) confers susceptibility to type 1 diabetes in Latvians. *Int J Immunogenet,* 35**,** 439-46.

SHEN, X. Z., BILLET, S., LIN, C., OKWAN-DUODU, D., CHEN, X., LUKACHER, A. E. & BERNSTEIN, K. E. 2011. The carboxypeptidase ACE shapes the MHC class I peptide repertoire. *Nat Immunol,* 12**,** 1078-85.

SHER, A., OSWALD, I. P., HIENY, S. & GAZZINELLI, R. T. 1993. Toxoplasma gondii induces a T-independent IFN-gamma response in natural killer cells that requires both adherent accessory cells and tumor necrosis factor-alpha. *J Immunol,* 150**,** 3982-9.

SHI, F. D., LJUNGGREN, H. G., LA CAVA, A. & VAN KAER, L. 2011. Organ-specific features of natural killer cells. *Nat Rev Immunol,* 11**,** 658-71.

SHIMIZU, Y. & DEMARS, R. 1989. Demonstration by class I gene transfer that reduced susceptibility of human cells to natural killer cell-mediated lysis is inversely correlated with HLA class I antigen expression. *Eur J Immunol,* 19**,** 447-51.

SIMON, M. M., HAUSMANN, M., TRAN, T., EBNET, K., TSCHOPP, J., THAHLA, R. & MULLBACHER, A. 1997. In vitro- and ex vivo-derived cytolytic leukocytes from granzyme A x B double knockout mice are defective in granule-mediated apoptosis but not lysis of target cells. *J Exp Med,* 186**,** 1781-6.

SINGLE, R. M., MARTIN, M. P., GAO, X., MEYER, D., YEAGER, M., KIDD, J. R., KIDD, K. K. & CARRINGTON, M. 2007. Global diversity and evidence for coevolution of KIR and HLA. *Nat Genet,* 39**,** 1114-9.

SMIGOC SCHWEIGER, D., MENDEZ, A., KUNILO JAMNIK, S., BRATANIC, N., BRATINA, N., BATTELINO, T., BRECELJ, J. & VIDAN-JERAS, B. 2014. Genetic risk for co-occurrence of type 1 diabetes and celiac disease is modified by HLA-C and killer immunoglobulin-like receptors. *Tissue Antigens,* 84**,** 471-8.

SMITH, H. R., KARLHOFER, F. M. & YOKOYAMA, W. M. 1994. Ly-49 multigene family expressed by IL-2-activated NK cells. *J Immunol,* 153**,** 1068-79.

SNYDER, G. A., BROOKS, A. G. & SUN, P. D. 1999. Crystal structure of the HLA-Cw3 allotype-specific killer cell inhibitory receptor KIR2DL2. *Proc Natl Acad Sci U S A,* 96**,** 3864-9.

SPITS, H., ARTIS, D., COLONNA, M., DIEFENBACH, A., DI SANTO, J. P., EBERL, G., KOYASU, S., LOCKSLEY, R. M., MCKENZIE, A. N., MEBIUS, R. E., POWRIE, F. & VIVIER, E. 2013. Innate lymphoid cells--a proposal for uniform nomenclature. *Nat Rev Immunol,* 13**,** 145-9.

STARKEY, P. M. 1991. Expression on cells of early human pregnancy decidua, of the p75, IL-2 and p145, IL-4 receptor proteins. *Immunology,* 73**,** 64-70.

STEINER, N. K., DAKSHANAMURTHY, S., VANDENBUSSCHE, C. J. & HURLEY, C. K. 2008. Extracellular domain alterations impact surface expression of stimulatory natural killer cell receptor KIR2DS5. *Immunogenetics,* 60**,** 655-67.

STERN, M., ELSASSER, H., HONGER, G., STEIGER, J., SCHAUB, S. & HESS, C. 2008. The number of activating KIR genes inversely correlates with the rate of CMV infection/reactivation in kidney transplant recipients. *Am J Transplant,* 8**,** 1312-7.

STORKUS, W. J., ALEXANDER, J., PAYNE, J. A., DAWSON, J. R. & CRESSWELL, P. 1989. Reversal of natural killing susceptibility in target cells expressing transfected class I HLA genes. *Proc Natl Acad Sci U S A,* 86**,** 2361-4.

SU, H. C., ISHIKAWA, R. & BIRON, C. A. 1993. Transforming growth factor-beta expression and natural killer cell responses during virus infection of normal, nude, and SCID mice. *J Immunol,* 151**,** 4874-90.

SUN, J. C., BEILKE, J. N. & LANIER, L. L. 2009. Adaptive immune features of natural killer cells. *Nature,* 457**,** 557-61.

SUN, J. C. & LANIER, L. L. 2011. NK cell development, homeostasis and function: parallels with CD8(+) T cells. *Nat Rev Immunol,* 11**,** 645-57.

SUTTON, V. R. & TRAPANI, J. A. 2010. Proteases in lymphocyte killer function: redundancy, polymorphism and questions remaining. *Biol Chem,* 391**,** 873-9.

SUZUKI, Y., HAMAMOTO, Y., OGASAWARA, Y., ISHIKAWA, K., YOSHIKAWA, Y., SASAZUKI, T. & MUTO, M. 2004. Genetic polymorphisms of killer cell immunoglobulin-like receptors are associated with susceptibility to psoriasis vulgaris. *J Invest Dermatol,* 122**,** 1133-6.

SZABO, S. J., SULLIVAN, B. M., PENG, S. L. & GLIMCHER, L. H. 2003. Molecular mechanisms regulating Th1 immune responses. *Annu Rev Immunol,* 21**,** 713-58.

TAKAYAMA, T., KAMADA, N., CHINEN, H., OKAMOTO, S., KITAZUME, M. T., CHANG, J., MATUZAKI, Y., SUZUKI, S., SUGITA, A., KOGANEI, K., HISAMATSU, T., KANAI, T. & HIBI, T. 2010. Imbalance of NKp44(+)NKp46(-) and NKp44(-)NKp46(+) natural killer cells in the intestinal mucosa of patients with Crohn's disease. *Gastroenterology,* 139**,** 882-92, 892 e1-3.

TERAI, I., KOBAYASHI, K., MATSUSHITA, M. & FUJITA, T. 1997. Human serum mannose-binding lectin (MBL)-associated serine protease-1 (MASP-1): determination of levels in body fluids and identification of two forms in serum. *Clin Exp Immunol,* 110**,** 317-23.

THIEL, S., VORUP-JENSEN, T., STOVER, C. M., SCHWAEBLE, W., LAURSEN, S. B., POULSEN, K., WILLIS, A. C., EGGLETON, P., HANSEN, S., HOLMSKOV, U., REID, K. B. & JENSENIUS, J. C. 1997. A second serine protease associated with mannan-binding lectin that activates complement. *Nature,* 386**,** 506-10.

THIELENS, A., VIVIER, E. & ROMAGNE, F. 2012. NK cell MHC class I specific receptors (KIR): from biology to clinical intervention. *Curr Opin Immunol,* 24**,** 239-45.

TIAN, Z., GERSHWIN, M. E. & ZHANG, C. 2012. Regulatory NK cells in autoimmune disease. *J Autoimmun,* 39**,** 206-15.

TORRES, A. R., WESTOVER, J. B., GIBBONS, C., JOHNSON, R. C. & WARD, D. C. 2012. Activating killer-cell immunoglobulin-like receptors (KIR) and their cognate HLA ligands are significantly increased in autism. *Brain Behav Immun,* 26**,** 1122-7.

TROWSDALE, J. 2001. Genetic and functional relationships between MHC and NK receptor genes. *Immunity,* 15**,** 363-74.

TROWSDALE, J., BARTEN, R., HAUDE, A., STEWART, C. A., BECK, S. & WILSON, M. J. 2001. The genomic context of natural killer receptor extended gene families. *Immunol Rev,* 181**,** 20-38.

TROWSDALE, J. & MOFFETT, A. 2008. NK receptor interactions with MHC class I molecules in pregnancy. *Semin Immunol,* 20**,** 317-20.

TSCHAN-PLESSL, A., STERN, M., SCHMIED, L., RETIERE, C., HIRSCH, H. H., GARZONI, C., VAN DELDEN, C., BOGGIAN, K., MUELLER, N. J., BERGER, C., VILLARD, J., MANUEL, O., MEYLAN, P. & TERSZOWSKI, G. 2016. Human Cytomegalovirus Infection Enhances NK Cell Activity In Vitro. *Transplant Direct,* 2**,** e89.

UHRBERG, M., PARHAM, P. & WERNET, P. 2002. Definition of gene content for nine common group B haplotypes of the Caucasoid population: KIR haplotypes contain between seven and eleven KIR genes. *Immunogenetics,* 54**,** 221-9.

UHRBERG, M., VALIANTE, N. M., SHUM, B. P., SHILLING, H. G., LIENERT-WEIDENBACH, K., CORLISS, B., TYAN, D., LANIER, L. L. & PARHAM, P. 1997. Human diversity in killer cell inhibitory receptor genes. *Immunity,* 7**,** 753-63.

UNANUE, E. R. 1997. Inter-relationship among macrophages, natural killer cells and neutrophils in early stages of Listeria resistance. *Curr Opin Immunol,* 9**,** 35-43.

VALIANTE, N. M., UHRBERG, M., SHILLING, H. G., LIENERT-WEIDENBACH, K., ARNETT, K. L., D'ANDREA, A., PHILLIPS, J. H., LANIER, L. L. & PARHAM, P. 1997. Functionally and structurally distinct NK cell receptor repertoires in the peripheral blood of two human donors. *Immunity,* 7**,** 739-51.

VAN DEN BERG, T. K., YODER, J. A. & LITMAN, G. W. 2004. On the origins of adaptive immunity: innate immune receptors join the tale. *Trends Immunol,* 25**,** 11-6.

VAN DER SLIK, A. R., KOELEMAN, B. P., VERDUIJN, W., BRUINING, G. J., ROEP, B. O. & GIPHART, M. J. 2003. KIR in type 1 diabetes: disparate distribution of activating and inhibitory natural killer cell receptors in patients versus HLA-matched control subjects. *Diabetes,* 52**,** 2639-42.

VAN ENDERT, P. 2011. Post-proteasomal and proteasome-independent generation of MHC class I ligands. *Cell Mol Life Sci,* 68**,** 1553-67.

VANDENBUSSCHE, C. J., DAKSHANAMURTHY, S., POSCH, P. E. & HURLEY, C. K. 2006. A single polymorphism disrupts the killer Ig-like receptor 2DL2/2DL3 D1 domain. *J Immunol,* 177**,** 5347-57.

VANDENBUSSCHE, C. J., MULROONEY, T. J., FRAZIER, W. R., DAKSHANAMURTHY, S. & HURLEY, C. K. 2009. Dramatically reduced surface expression of NK cell receptor KIR2DS3 is attributed to multiple residues throughout the molecule. *Genes Immun,* 10**,** 162-73.

VEILLETTE, A., BOOKMAN, M. A., HORAK, E. M. & BOLEN, J. B. 1988. The CD4 and CD8 T cell surface antigens are associated with the internal membrane tyrosine-protein kinase p56lck. *Cell,* 55**,** 301-8.

VERHEYDEN, S. & DEMANET, C. 2006. Susceptibility to myeloid and lymphoid leukemia is mediated by distinct inhibitory KIR-HLA ligand interactions. *Leukemia,* 20**,** 1437-8.

VIGNERON, N., PEAPER, D. R., LEONHARDT, R. M. & CRESSWELL, P. 2009. Functional significance of tapasin membrane association and disulfide linkage to ERp57 in MHC class I presentation. *Eur J Immunol,* 39**,** 2371-6.

VILCHES, C. & PARHAM, P. 2002. KIR: diverse, rapidly evolving receptors of innate and adaptive immunity. *Annu Rev Immunol,* 20**,** 217-51.

VIVIAN, J. P., DUNCAN, R. C., BERRY, R., O'CONNOR, G. M., REID, H. H., BEDDOE, T., GRAS, S., SAUNDERS, P. M., OLSHINA, M. A., WIDJAJA, J. M., HARPUR, C. M., LIN, J., MALOVESTE, S. M., PRICE, D. A., LAFONT, B. A., MCVICAR, D. W., CLEMENTS, C. S., BROOKS, A. G. & ROSSJOHN, J. Killer cell immunoglobulin-like receptor 3DL1-mediated recognition of human leukocyte antigen B. *Nature,* 479**,** 401-5.

VIVIAN, J. P., DUNCAN, R. C., BERRY, R., O'CONNOR, G. M., REID, H. H., BEDDOE, T., GRAS, S., SAUNDERS, P. M., OLSHINA, M. A., WIDJAJA, J. M., HARPUR, C. M., LIN, J., MALOVESTE, S. M., PRICE, D. A., LAFONT, B. A., MCVICAR, D. W., CLEMENTS, C. S., BROOKS, A. G. & ROSSJOHN, J. 2011. Killer cell immunoglobulin-like receptor 3DL1-mediated recognition of human leukocyte antigen B. *Nature,* 479**,** 401-5.

VIVIER, E. & ROMAGNE, F. 2007. Good news, bad news for missing-self recognition by NK cells: autoimmune control but viral evasion. *Immunity,* 26**,** 549-51.

VIVIER, E., TOMASELLO, E., BARATIN, M., WALZER, T. & UGOLINI, S. 2008. Functions of natural killer cells. *Nat Immunol,* 9**,** 503-10.

VOSKOBOINIK, I., WHISSTOCK, J. C. & TRAPANI, J. A. 2015. Perforin and granzymes: function, dysfunction and human pathology. *Nat Rev Immunol,* 15**,** 388-400.

VOSSHENRICH, C. A., GARCIA-OJEDA, M. E., SAMSON-VILLEGER, S. I., PASQUALETTO, V., ENAULT, L., RICHARD-LE GOFF, O., CORCUFF, E., GUY-GRAND, D., ROCHA, B., CUMANO, A., ROGGE, L., EZINE, S. & DI SANTO, J. P. 2006. A thymic pathway of mouse natural killer cell development characterized by expression of GATA-3 and CD127. *Nat Immunol,* 7**,** 1217-24.

WAGTMANN, N., BIASSONI, R., CANTONI, C., VERDIANI, S., MALNATI, M. S., VITALE, M., BOTTINO, C., MORETTA, L., MORETTA, A. & LONG, E. O. 1995a. Molecular clones of the p58 NK cell receptor reveal immunoglobulin-related molecules with diversity in both the extra- and intracellular domains. *Immunity,* 2**,** 439-49.

WAGTMANN, N., RAJAGOPALAN, S., WINTER, C. C., PERUZZI, M. & LONG, E. O. 1995b. Killer cell inhibitory receptors specific for HLA-C and HLA-B identified by direct binding and by functional transfer. *Immunity,* 3**,** 801-9.

WALZER, T., JAEGER, S., CHAIX, J. & VIVIER, E. 2007. Natural killer cells: from CD3(-)NKp46(+) to post-genomics meta-analyses. *Curr Opin Immunol,* 19**,** 365-72.

WARREN, H. S., KINNEAR, B. F., PHILLIPS, J. H. & LANIER, L. L. 1995. Production of IL-5 by human NK cells and regulation of IL-5 secretion by IL-4, IL-10, and IL-12. *J Immunol,* 154**,** 5144-52.

WECHSLER, J., BAGOT, M., NIKOLOVA, M., PAROLINI, S., MARTIN-GARCIA, N., BOUMSELL, L., MORETTA, A. & BENSUSSAN, A. 2003. Killer cell immunoglobulin-like receptor expression delineates in situ Sezary syndrome lymphocytes. *J Pathol,* 199**,** 77-83.

WEI, H., ZHENG, X., LOU, D., ZHANG, L., ZHANG, R., SUN, R. & TIAN, Z. 2005. Tumor-induced suppression of interferon-gamma production and enhancement of interleukin-10

production by natural killer (NK) cells: paralleled to CD4+ T cells. *Mol Immunol,* 42**,** 1023-31.

WELSH, R. M., BRUBAKER, J. O., VARGAS-CORTES, M. & O'DONNELL, C. L. 1991. Natural killer (NK) cell response to virus infections in mice with severe combined immunodeficiency. The stimulation of NK cells and the NK cell-dependent control of virus infections occur independently of T and B cell function. *J Exp Med,* 173**,** 1053-63.

WENDE, H., COLONNA, M., ZIEGLER, A. & VOLZ, A. 1999. Organization of the leukocyte receptor cluster (LRC) on human chromosome 19q13.4. *Mamm Genome,* 10**,** 154-60.

WEST, W. H., CANNON, G. B., KAY, H. D., BONNARD, G. D. & HERBERMAN, R. B. 1977. Natural cytotoxic reactivity of human lymphocytes against a myeloid cell line: characterization of effector cells. *J Immunol,* 118**,** 355-61.

WHERRY, J. C., SCHREIBER, R. D. & UNANUE, E. R. 1991. Regulation of gamma interferon production by natural killer cells in scid mice: roles of tumor necrosis factor and bacterial stimuli. *Infect Immun,* 59**,** 1709-15.

WILLIAMS, N. S., KLEM, J., PUZANOV, I. J., SIVAKUMAR, P. V., BENNETT, M. & KUMAR, V. 1999. Differentiation of NK1.1+, Ly49+ NK cells from flt3+ multipotent marrow progenitor cells. *J Immunol,* 163**,** 2648-56.

WILSON, M. J., TORKAR, M., HAUDE, A., MILNE, S., JONES, T., SHEER, D., BECK, S. & TROWSDALE, J. 2000. Plasticity in the organization and sequences of human KIR/ILT gene families. *Proc Natl Acad Sci U S A,* 97**,** 4778-83.

WINTER, C. C., GUMPERZ, J. E., PARHAM, P., LONG, E. O. & WAGTMANN, N. 1998. Direct binding and functional transfer of NK cell inhibitory receptors reveal novel patterns of HLA-C allotype recognition. *J Immunol,* 161**,** 571-7.

WINTER, C. C. & LONG, E. O. 1997. A single amino acid in the p58 killer cell inhibitory receptor controls the ability of natural killer cells to discriminate between the two groups of HLA-C allotypes. *J Immunol,* 158**,** 4026-8.

WITT, C. S., GOODRIDGE, J., GERBASE-DELIMA, M. G., DAHER, S. & CHRISTIANSEN, F. T. 2004. Maternal KIR repertoire is not associated with recurrent spontaneous abortion. *Hum Reprod,* 19**,** 2653-7.

WITT, C. S., WHITEWAY, J. M., WARREN, H. S., BARDEN, A., ROGERS, M., MARTIN, A., BEILIN, L. & CHRISTIANSEN, F. T. 2002. Alleles of the KIR2DL4 receptor and their lack of association with pre-eclampsia. *Eur J Immunol,* 32**,** 18-29.

WOOLDRIDGE, L., EKERUCHE-MAKINDE, J., VAN DEN BERG, H. A., SKOWERA, A., MILES, J. J., TAN, M. P., DOLTON, G., CLEMENT, M., LLEWELLYN-LACEY, S., PRICE, D. A., PEAKMAN, M. & SEWELL, A. K. 2012. A single autoimmune T cell receptor recognizes more than a million different peptides. *J Biol Chem,* 287**,** 1168-77.

YANG, J. & RETH, M. 2016. Receptor Dissociation and B-Cell Activation. *Curr Top Microbiol Immunol,* 393**,** 27-43.

YAWATA, M., YAWATA, N., DRAGHI, M., LITTLE, A. M., PARTHENIOU, F. & PARHAM, P. 2006. Roles for HLA and KIR polymorphisms in natural killer cell repertoire selection and modulation of effector function. *J Exp Med,* 203**,** 633-45.

YAWATA, M., YAWATA, N., DRAGHI, M., PARTHENIOU, F., LITTLE, A. M. & PARHAM, P. 2008. MHC class I-specific inhibitory receptors and their ligands structure diverse human NK-cell repertoires toward a balance of missing self-response. *Blood,* 112**,** 2369-80.

YEN, J. H., MOORE, B. E., NAKAJIMA, T., SCHOLL, D., SCHAID, D. J., WEYAND, C. M. & GORONZY, J. J. 2001. Major histocompatibility complex class I-recognizing receptors are disease risk genes in rheumatoid arthritis. *J Exp Med,* 193**,** 1159-67.

YEWDELL, J. W., REITS, E. & NEEFJES, J. 2003. Making sense of mass destruction: quantitating MHC class I antigen presentation. *Nat Rev Immunol,* 3**,** 952-61.

YOKOYAMA, W. M., JACOBS, L. B., KANAGAWA, O., SHEVACH, E. M. & COHEN, D. I. 1989. A murine T lymphocyte antigen belongs to a supergene family of type II integral membrane proteins. *J Immunol,* 143**,** 1379-86.

YU, G., XU, X., VU, M. D., KILPATRICK, E. D. & LI, X. C. 2006. NK cells promote transplant tolerance by killing donor antigen-presenting cells. *J Exp Med,* 203**,** 1851-8.

YU, H., FEHNIGER, T. A., FUCHSHUBER, P., THIEL, K. S., VIVIER, E., CARSON, W. E. & CALIGIURI, M. A. 1998. Flt3 ligand promotes the generation of a distinct CD34(+) human natural killer cell progenitor that responds to interleukin-15. *Blood,* 92**,** 3647-57.

ZAIA, J. A., SUN, J. Y., GALLEZ-HAWKINS, G. M., THAO, L., OKI, A., LACEY, S. F., DAGIS, A., PALMER, J., DIAMOND, D. J., FORMAN, S. J. & SENITZER, D. 2009. The effect of single and combined activating killer immunoglobulin-like receptor genotypes on cytomegalovirus infection and immunity after hematopoietic cell transplantation. *Biol Blood Marrow Transplant,* 15**,** 315-25.

ZAPPACOSTA, F., BORREGO, F., BROOKS, A. G., PARKER, K. C. & COLIGAN, J. E. 1997. Peptides isolated from HLA-Cw*0304 confer different degrees of protection from natural killer cell-mediated lysis. *Proc Natl Acad Sci U S A,* 94**,** 6313-8.

ZEMMOUR, J. & PARHAM, P. 1992. Distinctive polymorphism at the HLA-C locus: implications for the expression of HLA-C. *J Exp Med,* 176**,** 937-50.

6 Supplementary Figures

A

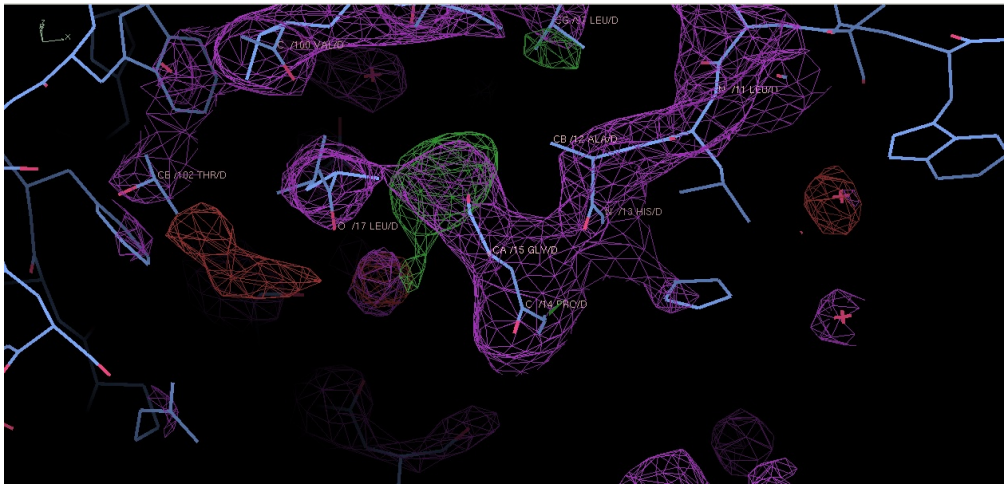

B

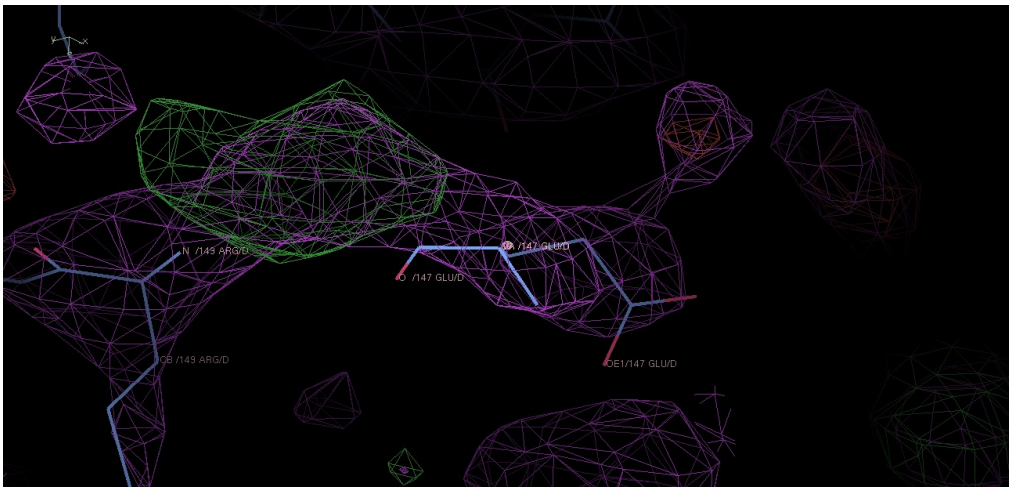

Figure S6.1 Unbiased electron density of refined KIR2DL3.
Unbiased electron density of (**A**) KIR2DL3 P16 (shown in green colour). KIR2DL2 and –L3 amino acid residues differ at positon 16, and instead of P16, KIR2DL2 possess R16. By deleting P16 from KIR2DL3 (built by Coot software via KIR2DL2 as a PDB template) and repeating the refinement process (via PHENIX software), the electron density related to the deleted residue will re-appear which fits with Pro from KIR2DL3 and not Arg from KIR2DL2. (**B**) Unbiased electron density of KIR2DL3 R148 (shown in green colour). The refined electron density map fits Arg located on the D2 domain of KIR2DL3 instead of C148 located on KIR2DL2.

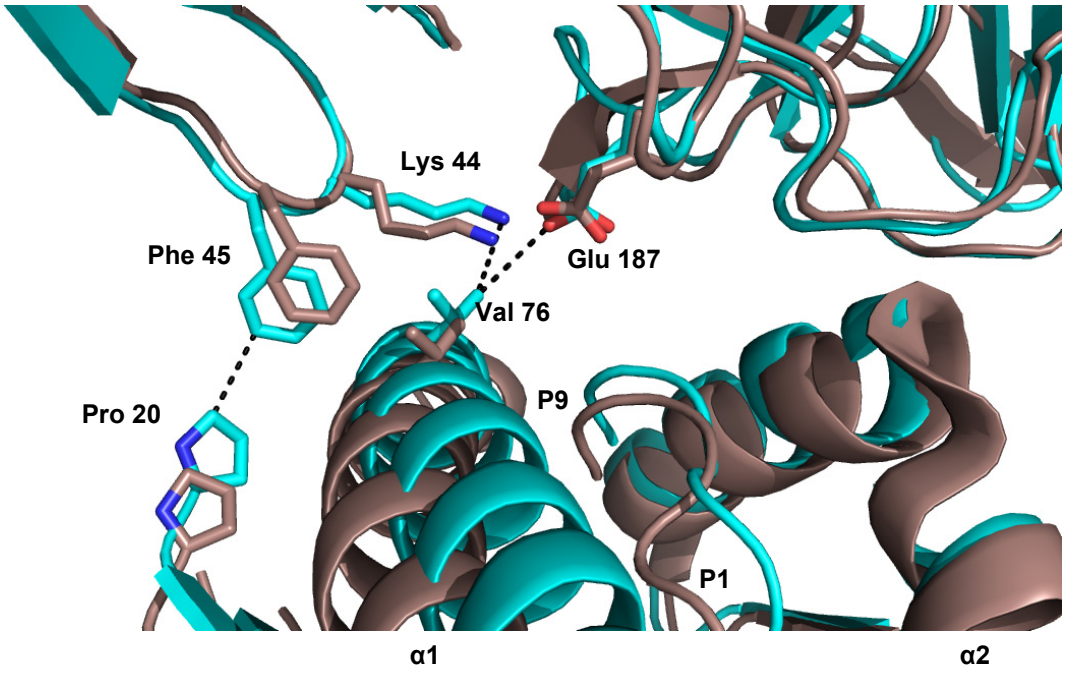

Figure S6.2 Exclusive contacts between KIR2DL2 and HLA-C*07:02.
Additional contacts between the D1 domain of KIR2DL2/HLA-C*07:2 (cyan) compared to that of KIR2DL2/HLA-C*03:04 (deep salmon). The D1 domain of KIR2DL2 contacts with Pro20 and Val76 of the α1 domain of the HLA-C*07:02 via Phe 45 and Lys 44 residues (indicated by black dash lines). (PDB ID 1EFX). Glu187 of KIR2DL2, located on the D2 domain creates additional contacts with Val76 of HLA-C*07:02, which is absent in the complex among KIR2DL2 and HLA-C*03:04.

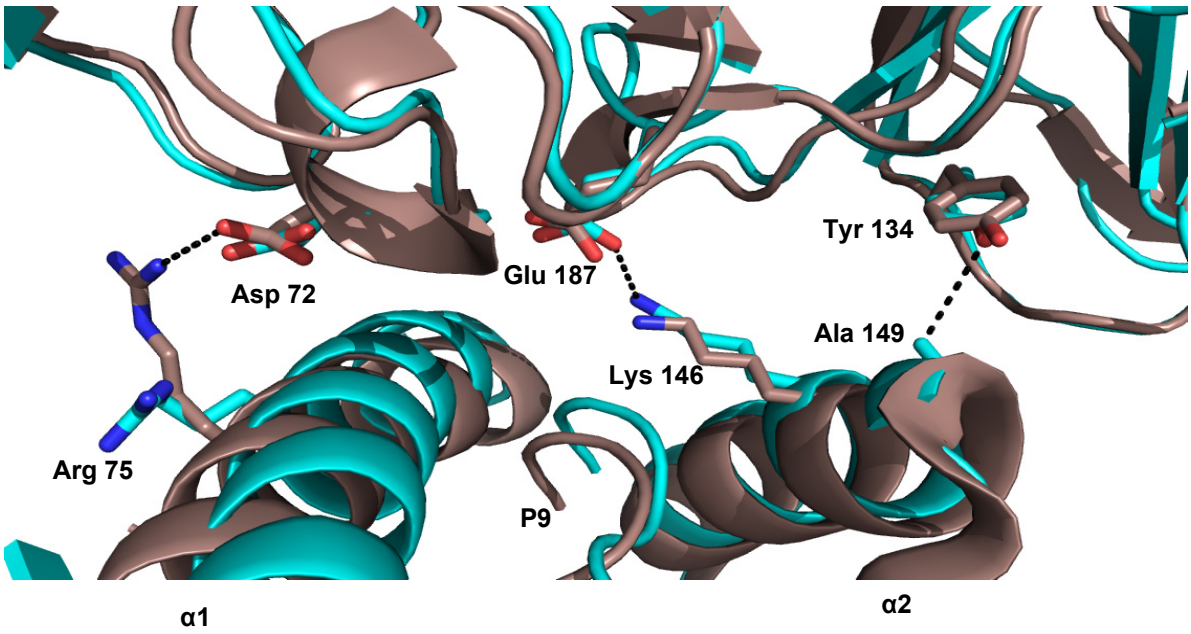

Figure S6.3 Different contacts between KIR2DL2 bound to HLA-C03:04 and -C*07:02. Asp 72 of KIR2DL2 has additional contact with α1 domain Arg 75 of HLA-C*03:04 (cyan) whereas -C*07:02 (deep salmon) cannot establish the same contact with KIR2DL2. KIR2DL2 residues Glu187 and Tyr134, located on the D2 domain, display additional contacts to the α2 domain of HLA-C*07:02 were observed at positions Lys146 and Ala149.

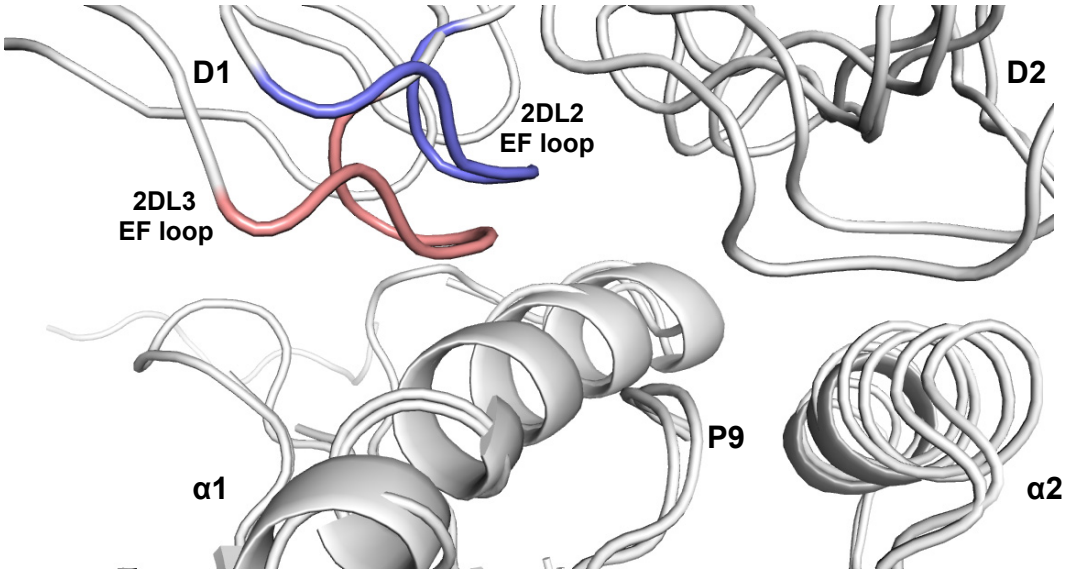

Figure S6.4 Different docking mode of KIR2DL2 and -L3 bound to HLA-C*07:02. Differences in binding mode of KIR2DL2 (light blue) and -L3 (light pink) in complex with HLA-C*07:02 leads to the shift of E-F loop about 3.4 Å between the complexes (residues 68-73). As a result, KIR2DL2 has more extensive contacts than KIR2DL3 to the α1 and α2 helices and the peptide of the HLA-C*07:02-RL9 complex.

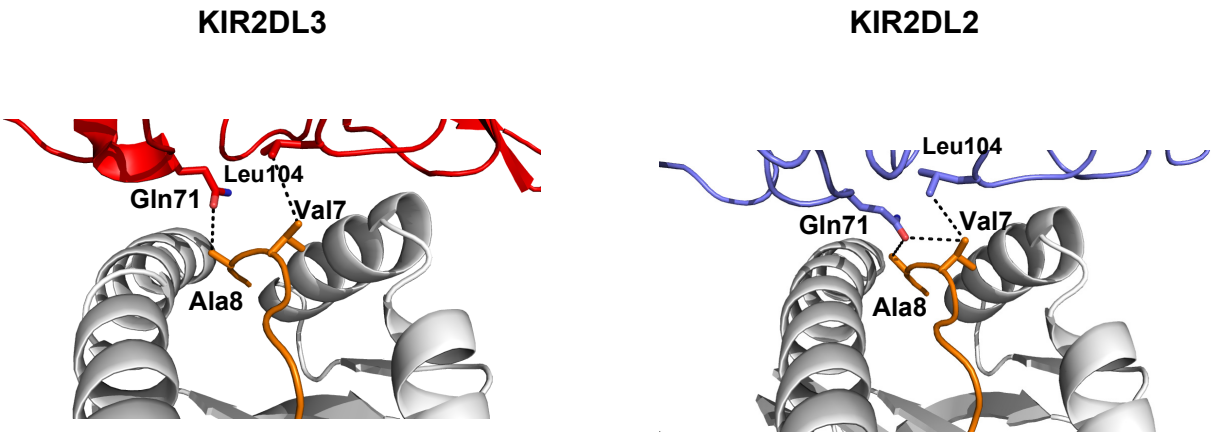

Figure S6.5 Interactions of KIR2DL2 and -L3 with RL9.
Differences in interactions of KIR2DL2 and -L3 with RL9. Gln71 on the D1 domain of KIR2DL2 has additional contact with Val7 of RL9 compared to KIR2DL3.

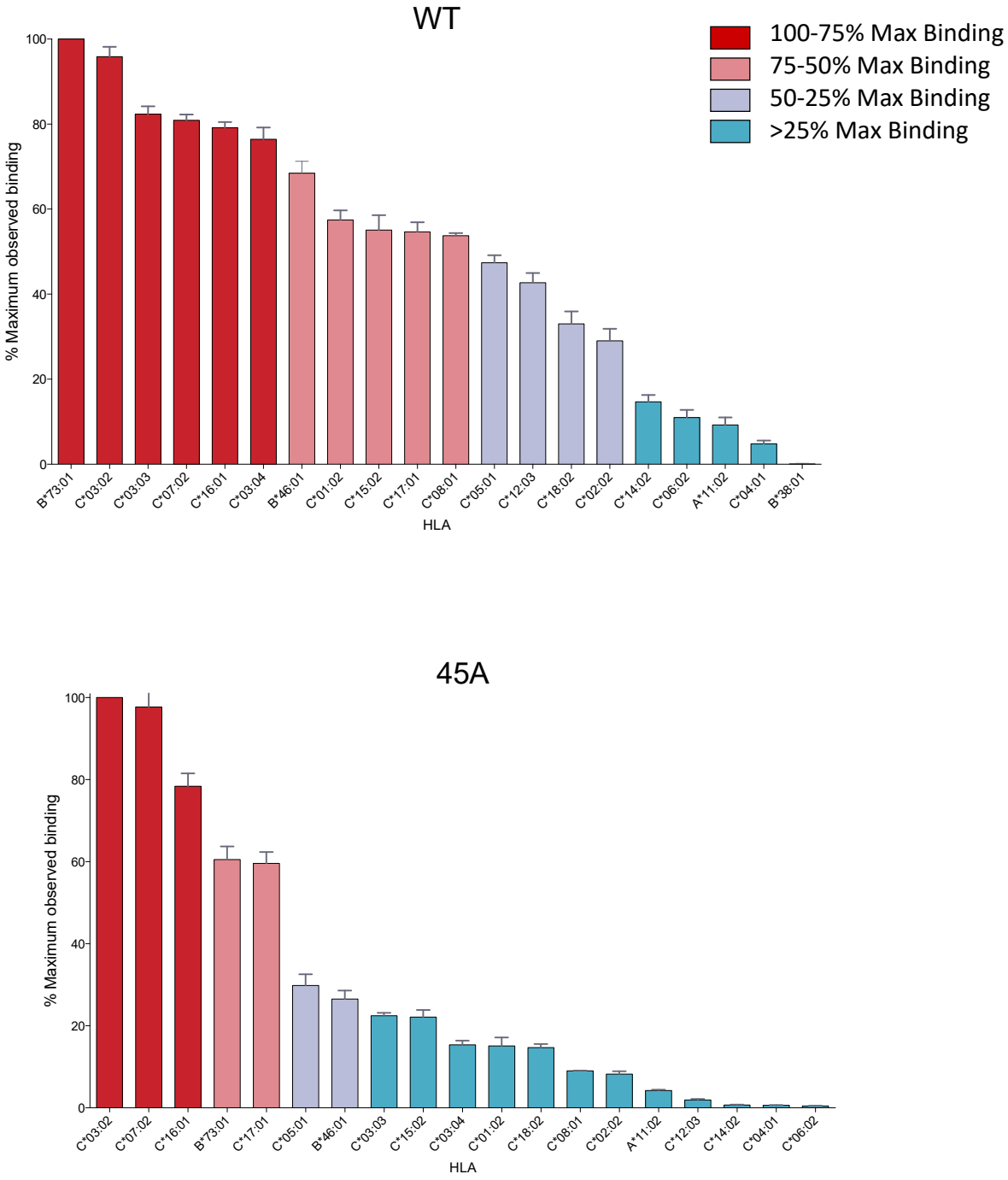

Figure S6.6 Binding of KIR2DL2 WT and F45A to a panel of HLA class I molecules. LUMINEX assay raw data shows the interaction of wild type (top figure) and F45A KIR2DL2 to a panel of HLA class I molecules. This assay was performed by Dr. Phillip Pymm from Prof. Rossjohn Laboratory, Monash University. Data was collected and analysed by Dr. Phillip Pymm.

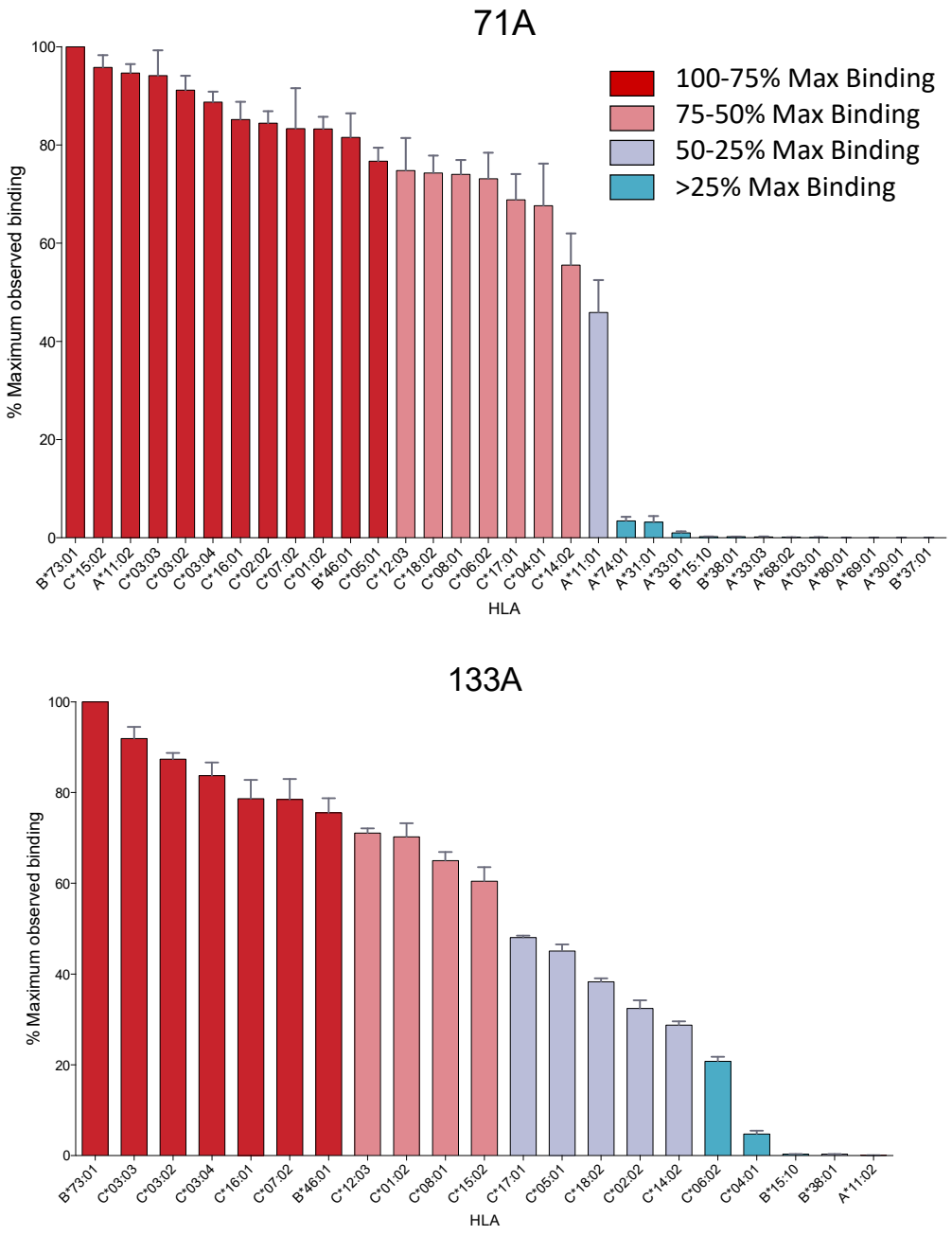

Figure S6.7 Binding of KIR2DL2 Q71A and S133A to a panel of HLA class I molecules. LUMINEX assay raw data shows the interaction of Q71A (top figure) and S133A KIR2DL2 to a panel of HLA class I molecules. This assay was performed by Dr. Phillip Pymm from Prof. Rossjohn Laboratory, Monash University. Data was collected and analysed by Dr. Phillip Pymm.

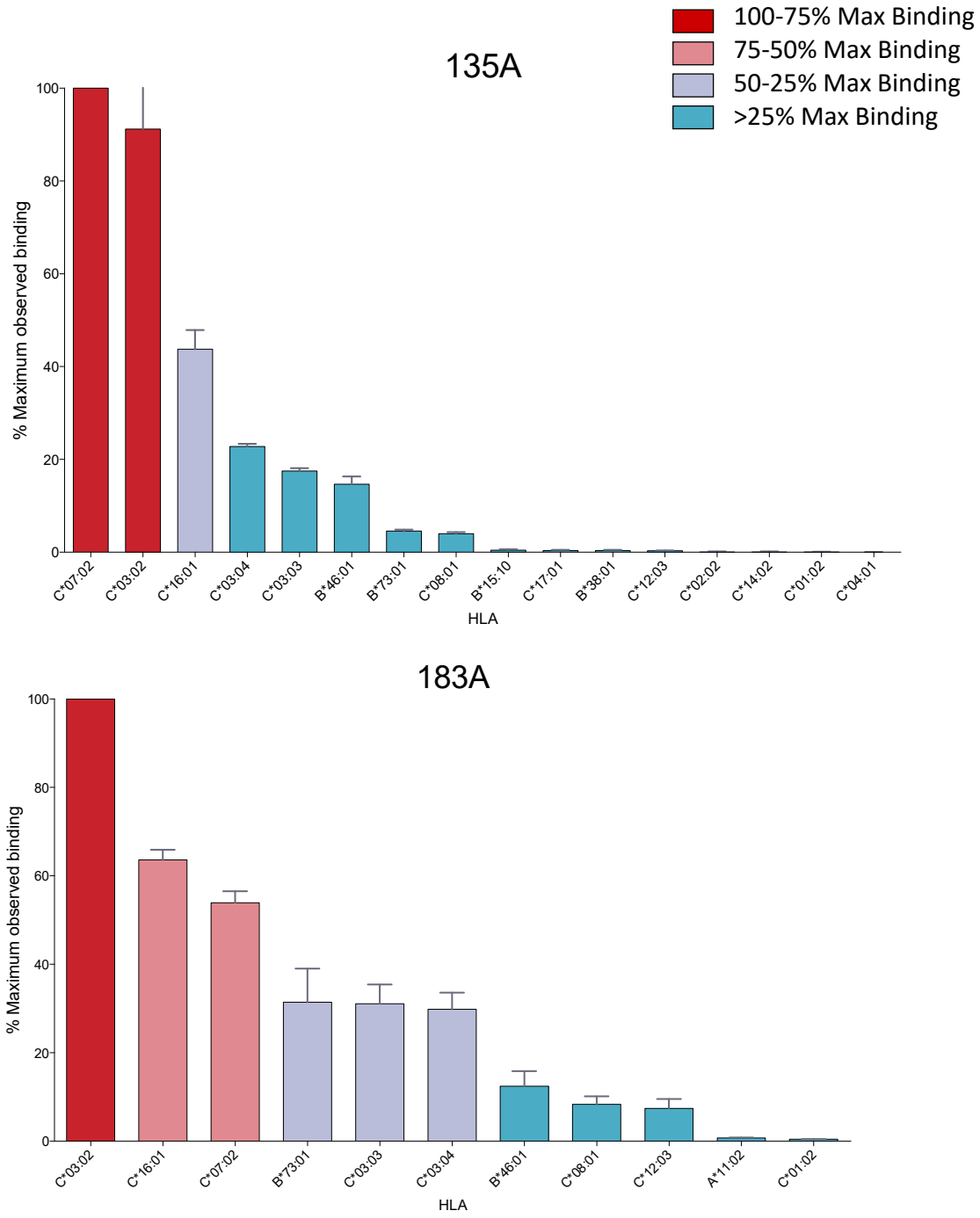

Figure S6.8 Binding of KIR2DL2 D135A and D183A to a panel of HLA class I molecules. LUMINEX assay raw data shows the interaction of D135A (top figure) and D183A KIR2DL2 to a panel of HLA class I molecules. This assay was performed by Dr. Phillip Pymm from Prof. Rossjohn Laboratory, Monash University. Data was collected and analysed by Dr. Phillip Pymm.

7 Appendix

7.1 Streptavidin pulldown protocol

1. Concentrate biotinylated desalted protein to an approximately 1 mg/ml.
2. For each sample add 20µl streptavidin coated Sepharose beads to an Eppendorf tube.
3. Add 180 µl buffer (e.g. TBS, matched to protein buffer) to beads.
4. Spin beads at 1000G for 2-3 minutes to pellet beads.
5. Remove buffer carefully and repeat wash.
6. Add 10 µg protein sample to beads with buffer removed and incubate 10-30 minutes, room temperature.
7. Add 180 µl buffer and mix briefly.
8. Spin at 1000G 2-3 minutes as before.
9. Remove buffer and save in a new tube marked “wash 1”.
10. Add 180 µl buffer, mix briefly and spin.
11. Repeat three times, saving buffer from each wash in separate tubes marked washes 2-4.
12. Take 1 µl of beads (after removal of final wash buffer) and save for gel.
13. To remaining beads add 180 µl buffer, mix and take 10 µl from this mix to run on SDS-PAGE.
14. Take 10 µl of saved wash buffers to run on SDS-PAGE.
15. Samples 1 and 2 containing the streptavidin beads should be prepared for a reducing SDS-PAGE and incubated on a heat block at 90 °C for 30 minutes to remove attached protein from the beads.
16. Remaining samples should be prepared for a reducing SDS-PAGE and heated at 90 °C for 5 minutes as normal.
17. Run bead and wash samples on SDS-PAGE. Run the 10 µl bead sample adjacent to the wash samples to compare the ratio of biotinylated to unbiotinylated protein easily.